MASS SPECTROMETRY STRATEGIES FOR COMPREHENSIVE LIPIDOME ANALYSIS OF COLORECTAL CANCER CELLS AND THEIR SECRETED EXOSOMES

Ву

Cassie J. Fhaner

A DISSERTATION

Submitted to
Michigan State University
in partial fulfillment of the requirements
for the degree of

Chemistry – Doctor of Philosophy

2014

ABSTRACT

MASS SPECTROMETRY STRATEGIES FOR COMPREHENSIVE LIPIDOME ANALYSIS OF COLORECTAL CANCER CELLS AND THEIR SECRETED EXOSOMES

By

Cassie J. Fhaner

Lipids are essential for numerous cellular functions and disruption of lipid metabolism or signaling has been demonstrated to be associated with the onset and progression of diseases, including cancer. Therefore, further investigation into the details of lipid alterations and metabolism in cancer may be beneficial in biomarker and cancer metabolic discovery. Exosomes, 40-100nm vesicles secreted from many cells, have been implicated in cellular communication and progression and metastasis of cancer. However, characterization of exosome lipidomes and their potential roles in cancer progression have had little exploration. Several methods for lipid analysis have been developed such as gas chromatography (GC) and liquid chromatography (LC); however, many of these methods are time consuming and offer limited information on individual lipid structural identity. Mass spectrometry has proven to be beneficial as both a sensitive detector following separation by GC or LC and as a standalone strategy for lipid analysis without previous separation. Recent developments in high resolution mass spectrometry enhance the ability for mass spectrometry to be utilized for unambiguous identification of lipid species.

In this dissertation, a 'shotgun' lipidomics strategy consisting of sequential functional group selective chemical modification reactions coupled with high-resolution/accurate mass spectrometry analysis, and 'targeted' tandem mass spectrometry (MS/MS), has been developed and applied toward the comprehensive

identification, characterization and quantitative analysis of changes in relative abundances of greater than 1500 individual glycerophospholipid, glycerolipid, sphingolipid and sterol lipids between a primary colon adenocarcinoma cell line, SW480, its metastasized derivative, SW620, and their secreted exosomes. Selective chemical derivatization of phosphatidylethanolamine and phosphatidylserine lipids charge' d₆-S,S'using а 'fixed sulfonium ion containing reagent. ¹³C₁-DMBNHS, dimethylthiobutanoylhydroxysuccinimide ester (d₆-DMBNHS) eliminates the possibility of isobaric mass overlap of these species with the precursor ions of all other lipids in crude lipid extracts. Subsequent selective mild acid hydrolysis of plasmenyl-ether containing lipids using formic acid or, alternatively, a method involving the use of plasmenyl-ether selective derivatization with iodine and methanol enables these species to be differentiated from isobaric mass plasmanyl-ether containing lipids. Using this approach, statistically significant differences in the abundances of numerous lipid species previously identified as being associated with cancer development, or that play known roles as mediators in a range of physiological and pathological processes were observed among the cells and exosomes. In the cells, increases in several ether-containing glycerophospholipids, triglyceride and cholesterol ester lipid levels in the SW620 metastatic colon cell line lipid extracts were observed compared to the SW480 cells. Increases in ether phospholipids were also observed in the exosomes compared to their respective cell lines as well as overall glycerophosphoethanolamine, glycerophosphoserine and sphingomyelin levels. The information provided by these analysis techniques is expected to lead to a broader knowledge of the role of lipid metabolism and cancer progression.

ACKNOWLEDGEMENTS

This graduate school journey would not have been possible without the help and support of several people and I owe them my genuine gratitude. First, I'd like to thank my advisor, Dr. Gavin Reid. His knowledge and passion for science is inspirational. He accepted me not only once, but twice, into his group and has guided me throughout my research. My guidance committee, Dr. Gary Blanchard, Dr. Julia Busik and Dr. Dana Spence, has also been very helpful with guiding my research and sometimes just lending an ear and encouragement when needed. I would like to thank Dr. Richard Simpson and Dr. Hong Ji at La Trobe University in Melbourne, Australia for supplying exosomes for my research.

I would also like to thank previous and current members of the Reid Lab. Dr. Todd Lydic, Abduselam Salih and Sichang Liu helped train me in all the glory that is lipid analysis by mass spectrometry. I would also like to sincerely thank Li Cui, Shuai Nie and many other previous Reid Lab members. A special appreciation is also given to the members of Dr. Busik's group, especially Svetlana Bozak and Todd, who helped train me with cell culture and many other biological techniques. Additionally, I'd like to thank Dr. Sarah Roosa from Dr. Andrea Amalfitano's lab, Dr. Sophia Lunt and Inez Yuwanita from Dr. Eran Andrechek's lab, Dr. Nara Parameswaran, Dr. Suzanne Mohr and their group members for training me and allowing me the use of their equipment.

Furthermore, I would like to add my family and friends to the list of thanks. I would like to thank my parents for all the love and support they have shown me throughout this process and always. My mother and mothers-in-law have helped an

extreme amount with watching Connor and Rori when needed, allowing me to put in long hours in the lab and writing. Thank you to my large extended family for all the support and understanding when I was unable to attend family functions due to work. I have gained some fantastic friends, including Team Special, while in graduate school that have been a great source of personal and academic support. I could not have done all of this without all of you. Finally, I would like to thank my husband, Dr. Matthew Fhaner, and my children, Connor Groff and Rori Fhaner, for all your support and patience. My husband's calm voice and understanding (most of the time) kept me from losing my mind when life became overwhelming.

TABLE OF CONTENTS

LIST OF TABLES		x
LIST OF FIGURES		XV
LIST OF SCHEMES	S	xxiii
Chapter 1: An Ov	verview of Analytical Strategies for Lipidome Analysis	1
1.1	Introduction to Lipid Structure and Function	
1.1.1	Structure and Nomenclature of Lipid Classes	
1.1.2	Lipid Function in Mammalian Cells	
1.1.2.1	Lipids as Structural Components	8
1.1.2.2	Cellular Signaling Roles of Lipids	
1.1.2.3	Lipids as Fuel and Energy Storage Molecules	
1.1.3.	The Role of Lipids in Disease	
1.1.3.1	Lipid Alterations in Various Disease States	11
1.1.3.2	Lipid Alterations in Cancer	
1.1.3.3	Lipids in Secreted Cancer Exosomes	15
1.2	Lipid Extraction	
1.3	Strategies for Lipidome Analysis	19
1.3.1	Thin Layer Chromatography (TLC)	
1.3.1.1	Methodologies for TLC Analysis	19
1.3.1.2	Benefits and Drawbacks of TLC	20
1.3.2	Gas Chromatography (GC)	21
1.3.2.1	Methodologies, Including Derivatization, for GC Analysis	22
1.3.2.2	Drawbacks and Benefits of GC	23
1.3.3	Liquid Chromatography (LC)	23
1.3.3.1	Normal and Reverse Phase LC	24
1.3.3.2	Drawbacks and Benefits of LC	
1.3.4	Nuclear Magnetic Resonance (NMR)	25
1.3.4.1	Methodologies for NMR	
1.3.4.2	Drawbacks and Benefits of NMR	27
1.3.5	Mass Spectrometry (MS) Based Lipid Analysis	27
1.3.5.1	Sample Introduction Methods for MS	28
1.3.5.2	Tandem Mass Spectrometry (MS/MS)	31
1.3.5.2.1	Traditional Instrumentation and Methods of CID-MS/MS	31
	Lipid Class Identification by Characteristic Head Group	
	Fragmentation Behaviors upon CID-MS/MS	34
1.3.5.2.3	Fatty Acyl Substituent Identification by CID-MS/MS	
	Derivatization Techniques for MS Based Lipid Identification	
1.3.5.3	High Resolution MS (HRMS)	
1.3.5.3.1	Instrumentation for HRMS	
1.3.5.3.2	Differential Extraction for HRMS	55

1.3.5.3.3	High Resolution MS/MS	55
1.3.5.4	Lipid Quantification and Data Analysis	56
	Internal Standard Methods	
1.3.5.4.2	Derivatization Strategies	57
1.3.5.4.3	Software for MS Lipid Data Analysis	58
Resol	opment of a Sequential Derivatization Strategy for High ution MS Based Comprehensive Lipidome Analysis	60
2.1	Introduction	60
2.2	Selective Derivatization of Aminophospholipids with d ₆ -S,S'-	
	Dimethylthiobutanoylhydroxysuccinimide Ester (d ₆ -	
	DMBNHS) and ¹³ C ₁ -DMBNHS	66
2.2.1	Characterization of the Reactivity and Specificity of Aminophospholipids with DMBNHS	
2.2.2	Sensitivity Enhancement of DMBNHS Derivatized	
	Aminophospholipids	
2.3	Derivatization and Selective Differentiation of Ether Lipids	
2.3.1	Identification of Plasmalogen Lipids by Acid Hydrolysis	73
2.3.2	Identification of Plasmalogen Lipids via Derivatization with	75
2.3.3	Iodine and Methanol	/5
2.3.3	Characterization of the Fragmentation Behavior of DMBNHS Derivatized Lipids	78
2.3.3.1	Characterization of the Fragmentation Behavior of	
	Iodine/Methanol Derivatized Plasmalogen PC Lipids	79
2.3.3.2	Characterization of the Fragmentation Behavior of	
0.4	Iodine/Methanol Derivatized Plasmalogen PE Lipids	
2.4	Sequential Modification of Aminophospholipid and	
	Plasmalogen Lipids	
2.4.1	d ₆ -DMBNHS and Acid Hydrolysis	86
2.4.2	¹³ C ₁ -DMBNHS and Iodine/Methanol	87
2.4.2.1	Characteristic Fragmentation of Sequentially ¹³ C ₁ -DMBNHS	
	and Iodine/Methanol Derivatized Plasmalogen PE	89
2.5	Conclusions	
Chantar 2: Cama	robonoivo Linidomo Profiling of Jacqueia Primary and	
-	rehensive Lipidome Profiling of Isogenic Primary and static Colon Adenocarcinoma Cell Lines	95
3.1	Introduction	
3.2	High Resolution MS Based Lipidomic Analysis of SW480	
	and SW620 Cellular Extracts	
3.2.1	Sample Preparation for MS Analysis	97
3.2.2	High Resolution MS Analysis of SW480 and SW620 Cellular	
	Extracts	
3.2.2.1	High Resolution MS of Underivatized Cellular Extracts	98

Chapt	er 5: Experi	imental Methods	162
4.6		Conclusions and Future Directions	
4.5).ქ	Comparison of Fatty Acyl Distributions Among SW480 and SW620 Cells and Exosomes	.150
4.5		Negative Ionization Mode HCD-MS/MS	.146
4.5		Positive Ionization Mode HCD-MS/MS	
_		HRMS Identified Lipids	.143
4.5		HCD-MS/MS Analysis for Molecular Lipid Characterization of	
T.T		Extracts	.143
4.4	.4	Sterol Lipids of SW480 and SW620 Cell and Exosome	. 140
4.4	⊦.ડ	Glycerolipids of SW480 and SW620 Cell and Exosome Extracts	140
A A	2	Extracts	.138
4.4	.2	Sphingolipids of SW480 and SW620 Cell and Exosome	
•••	· · ·	Exosome Extracts	.130
4.4	.1	Glycerophospholipids of SW480 and SW620 Cell and	. 130
4.4		Comparison of Lipid Sum Composition Alterations Among SW480 and SW620 Cells and Exosomes	130
1 1		and Exosome Lipid Extracts	.127
4.3		Comparison of Total Lipids from SW480 and SW620 Cell	
		¹³ C ₁ -DMBNHS and Iodine/Methanol	.123
4.2	2.2	HRMS of Cell and Exosome Lipid Extracts Derivatized with	
		Exosomes	.122
4.2	2.1	Isolation, Extraction and Derivatization of Cells and Crude	— '
1.4		Exosomes	.121
4.1		HRMS Lipidomic Analysis of SW480 and SW620 Cells and	. 120
4.1	EXUSU	Introduction	
Chapt	•	me Analysis of Colorectal Cancer Cells and their Secreted	120
0 1 ·			
3.5		Conclusions	
J		Characterization	.115
3.4	·. ·	High Resolution MS/MS Data Analysis for Molecular Lipid	. 1 10
3.3 3.3		Sphingolipid AlterationsSterol Lipid Alterations	
3.3		Glycerolipid Alterations	
3.3		Glycerophospholipid Alterations	
		Changes Identified	
3.3		Implications in Colon Cancer Metastasis from Lipidomic	
	3.2.2.4	MS Data Analysis for Relative Quantification	.104
		DMBNHS and Acid Hydrolyzed	.102
	3.2.2.3	High Resolution MS of Cellular Extracts Derivatized with d ₆ -	
	0.2.2.2	DMBNHS	
	3.2.2.2	High Resolution MS of Cellular Extracts Derivatized with d ₆ -	

5.1	Materials	.162
5.2	Cell Culture Conditions and Protocols	.162
5.2.1	Cell Counting	.163
5.2.2	Exosome Isolation	
5.3	Modified Folch Lipid Extraction	.164
5.4	High Resolution MS (HRMS) Analysis	
5.4.1	Aminophospholipid Derivatization with DMBNHS	.166
5.4.2	Acid Hydrolysis of Plasmalogen Lipids	.167
5.4.3	Iodine and Methanol Derivatization of Plasmalogen Lipids	.167
5.5	HRMS and MS/MS Data Analysis Strategies	.168
5.5.1	HRMS Data Analysis Using LIMSA	.168
5.5.2	MS/MS Molecular Lipid Identification and Relative	
	Quantification	.170
APPENDICES		.172
APPENDIX A: S	upplemental Figures for Chapter 3	.173
	ables for Characterization of Lipids Using MS and MS/MS	
	supplemental Figures for Chapter 4	
BIBLIOGRAPHY		.266

LIST OF TABLES

Table 1.1	Examples of level of identification, symbol and structures of the glycerolipids, $TG_{(16:0/18:1, n-9/16:0)}$, $TG_{(O-16:0/18:1, n-9/16:0)}$ and $TG_{(P-16:0/18:1, n-9/16:0)}$.
Table 1.2	Summary of the characteristic fragments for PC lipid ions in positive and negative ionization mode with various common adducts35
Table 1.3	Summary of the characteristic fragments for PE lipid ions in positive and negative ionization mode with various common adducts37
Table 1.4	Summary of the characteristic fragments for PS lipid ions in positive and negative ionization mode with various common adducts38
Table 1.5	Summary of the characteristic fragments for PI lipid ions in positive and negative ionization mode with various common adducts40
Table 1.6	Summary of the characteristic fragments for PG lipid ions in positive and negative ionization mode with various common adducts
Table 1.7	Summary of the characteristic fragments for PA lipid ions in positive and negative ionization mode with various common adducts41
Table 1.8	Summary of the characteristic fragments for SM lipid ions in positive and negative ionization mode with various common adducts
Table 1.9	Characteristic fragment for ammoniated Chol Ester in positive ionization mode
Table 3.1	Summary of the number of assigned lipid ions, identified lipids, and total lipid species from crude lipid extracts derived from the SW480 and SW620 cell lines
Table 4.1	Summary of the number of assigned sum compositions (Sum Comp), identified lipids (ID Lipids), and total lipid species (Total) from crude lipid extracts from SW480 and SW620 colorectal cancer cell lines and secreted exosomes
Table B.1	Base structures for lipid building blocks: Symbol used in the "code" tables, Molecular structure of the base and formula of the base to be used when summing the parts of each lipid of the code

Table B.2	R-group structures for lipid building blocks labeled with R ₁ : Symbol used in the "code" tables, Molecular structure of the R-group and formula of the R-group to be used when summing the parts of each lipid of the code. (Note: F = number of Carbons and T = number of double bonds)
Table B.3	R-group structures for lipid building blocks labeled with R ₂ : Symbol used in the "code" tables, Molecular structure of the R-group and formula of the R-group to be used when summing the parts of each lipid of the code. (Note: F = number of Carbons and U = number of double bonds)
Table B.4	R-group structures for lipid building blocks labeled with R ₃ : Symbol used in the "code" tables, Molecular structure of the R-group and formula of the R-group to be used when summing the parts of each lipid of the code. (Note: G = number of Carbons and V = number of double bonds)
Table B.5	Additional alteration structures for lipid building blocks: Symbol used in the "code" tables, Molecular structure of the alteration and formula of the additional block to be used when summing the parts of each lipid of the code
Table B.6	Codes and Lipid Sum Composition readout for positive ionization mode MS analysis. (Note: E, F, G and X = number of C where E + $F + G = X$. T, U, V and Y = number of double bonds where T + U + $V = Y$)
Table B.7	Codes and Lipid Sum Composition readout for negative ionization mode MS analysis. (Note: E, F, G and X = number of C where E + $F + G = X$. T, U, V and Y = number of double bonds where T + U + $V = Y$)
Table B.8	Codes and Readout for the confirmation and acyl/alkyl/alkenyl chain identification of PC lipids via MS/MS analysis. (Note: E, F and $X = \text{number of C where E} + F = X$. T, U and $Y = \text{number of double}$ bonds where T + U = Y)
Table B.9	Codes and Readout for the confirmation and acyl/alkyl/alkenyl chain identification of PE lipids via MS/MS analysis. (Note: E, F and $X = \text{number of C}$ where $E + F = X$. T, U and $Y = \text{number of double}$ bonds where $T + U = Y$)

Table B.10	Codes and Readout for the confirmation and acyl/alkyl/alkenyl chain identification of PS lipids via MS/MS analysis. (Note: E, F and $X = \text{number of C where E} + F = X$. T, U and $Y = \text{number of double}$ bonds where T + U = Y))5
Table B.11	Codes and Readout for the confirmation and acyl/alkyl/alkenyl chain identification of PI lipids via MS/MS analysis. (Note: E, F and $X = \text{number of C where E} + F = X$. T, U and $Y = \text{number of double}$ bonds where T + U = Y)) 7
Table B.12	Codes and Readout for the confirmation and acyl/alkyl/alkenyl chain identification of PG lipids via MS/MS analysis. (Note: E, F and $X = \text{number of C where E} + F = X$. T, U and $Y = \text{number of double}$ bonds where T + U = Y)	9
Table B.13	Codes and Readout for the confirmation and acyl/alkyl/alkenyl chain identification of PA lipids via MS/MS analysis. (Note: E, F and $X = \text{number of C}$ where E + F = X. T, U and Y = number of double bonds where T + U = Y)	00
Table B.14	Codes and Readout for the confirmation and acyl chain identification of TG lipids via MS/MS analysis. (Note: E, F and X = number of C where E + F = X. T, U and Y = number of double bonds where T + U = Y))1
Table B.15	Codes and Readout for the confirmation and acyl chain identification of SM lipids via MS/MS analysis. (Note: E, F and X = number of C where E + F = X. T, U and Y = number of double bonds where T + U = Y))1
Table B.16	Codes and Readout for the confirmation and acyl chain identification of Cer lipids via MS/MS analysis. (Note: E, F and X = number of C where E + F = X. T, U and Y = number of double bonds where $T + U = Y$))1
Table C.1	PE sum compositions, their positive ionization mode m/z for MS analysis and molecular lipids identified for SW480 cells, SW620 cells, SW480 exosomes and SW620 exosomes)8
Table C.2	LPE sum compositions, their positive ionization mode m/z for MS analysis and molecular lipids identified for SW480 cells, SW620 cells, SW480 exosomes and SW620 exosomes	8
Table C.3	PC sum compositions, their positive ionization mode m/z for MS analysis and molecular lipids identified for SW480 cells, SW620 cells, SW480 exosomes and SW620 exosomes	19

Table C.4	LPC sum compositions, their positive ionization mode m/z for MS analysis and molecular lipids identified for SW480 cells, SW620 cells, SW480 exosomes and SW620 exosomes
Table C.5	PS sum compositions, their positive ionization mode m/z for MS analysis and molecular lipids identified for SW480 cells, SW620 cells, SW480 exosomes and SW620 exosomes
Table C.6	LPS sum compositions, their positive ionization mode m/z for MS analysis and molecular lipids identified for SW480 cells, SW620 cells, SW480 exosomes and SW620 exosomes
Table C.7	PG sum compositions, their positive ionization mode m/z for MS analysis and molecular lipids identified for SW480 cells, SW620 cells, SW480 exosomes and SW620 exosomes
Table C.8	LPG sum compositions, their positive ionization mode m/z for MS analysis and molecular lipids identified for SW480 cells, SW620 cells, SW480 exosomes and SW620 exosomes
Table C.9	PI sum compositions, their positive ionization mode m/z for MS analysis and molecular lipids identified for SW480 cells, SW620 cells, SW480 exosomes and SW620 exosomes
Table C.10	SM sum compositions, their positive ionization mode m/z for MS analysis and molecular lipids identified for SW480 cells, SW620 cells, SW480 exosomes and SW620 exosomes
Table C.11	Cer sum compositions, their positive ionization mode m/z for MS analysis and molecular lipids identified for SW480 cells, SW620 cells, SW480 exosomes and SW620 exosomes
Table C.12	Hex-Cer sum compositions, their positive ionization mode m/z for MS analysis and molecular lipids identified for SW480 cells, SW620 cells, SW480 exosomes and SW620 exosomes
Table C.13	TG sum compositions, their positive ionization mode m/z for MS analysis and molecular lipids identified for SW480 cells, SW620 cells, SW480 exosomes and SW620 exosomes
Table C.14	DG sum compositions and their positive ionization mode m/z for MS analysis for SW480 cells, SW620 cells, SW480 exosomes and SW620 exosomes

Table C.15	MG sum compositions, their positive ionization mode m/z for MS analysis and molecular lipid identities for SW480 cells, SW620 cells, SW480 exosomes and SW620 exosomes	.264
Table C.16	Chol Ester sum compositions, their positive ionization mode m/z for MS analysis and molecular lipid identities for SW480 cells, SW620 cells, SW480 exosomes and SW620 exosomes	.265

LIST OF FIGURES

Figure 1.1	Example of fatty acyl structure, FA _(18:1, n-9)	2
Figure 1.2	General glycerophospholipid structure and headgroup variations	5
Figure 1.3	Example of the structure of the sphingolipids and their notation including the sphingoid backbone (sphingosine), Ceramide and Sphingomyelin	6
Figure 1.4	Structure of cholesterol (Chol) and cholesterol esters (Chol Ester)	7
Figure 1.5	The four types of MS/MS scans utilized by a triple quadrupole mass spectrometer: product ion scan, precursor ion scan, neutral loss scan and SRM Scan.	33
Figure 2.1	Positive ion mode ESI high-resolution mass spectrometric analysis of a crude lipid extract from the SW480 human adenocarcinoma cell line. Expanded regions (m/z 744-751) of the ESI-mass spectrum obtained from the (A) underivatized crude lipid extract and (B) reaction with the amine-specific derivatization reagent, d ₆ -DMBNHS. The insets to each panel show an expanded region of the spectrum from m/z 748.4-748.8	69
Figure 2.2	Positive ion mode ESI high-resolution mass spectrometric analysis of a crude lipid extract from the SW480 human adenocarcinoma cell line. Expanded regions (m/z 800-887) of the ESI-mass spectrum obtained from the (A) underivatized crude lipid extract and (B) reaction with the amine-specific derivatization reagent, d ₆ -DMBNHS	71
Figure 2.3	Positive ion mode ESI high-resolution mass spectrometric analysis of a crude lipid extract from the SW480 human adenocarcinoma cell line following mild formic acid hydrolysis. (A) Expanded region (m/z 744-751) of the ESI-mass spectrum and (B) expanded region (m/z 880-887) of the ESI-mass spectrum	75
Figure 2.4	Positive ionization mode ESI high-resolution mass spectrometric analysis of a mixture of PC, PE and TG synthetic lipid standards, including two plasmenyl ether containing PC and PE lipids (A) without derivatization and (B) after reaction with iodine and methanol. The insets to each panel show an expanded region (<i>m/z</i>	

	760-825) of the mass spectra containing the underivatized plasmenyl PC and PE lipids	77
Figure 2.5	Positive ionization mode ESI high-resolution HCD-MS/MS analysis of the synthetic lipid standard PC _(P-18:0/22:6) (A) without derivatization and (B) after reaction with iodine and methanol. The horizontal arrows in panel B indicate the fragmentation pathways that were observed upon performing ion trap multistage CID-MS ⁿ of the derivatized PC precursor ion	81
Figure 2.6	Positive ionization mode ESI high-resolution HCD-MS/MS analysis of the synthetic lipid standard PE _(P-18:0/22:6) (A) without derivatization and (B) after reaction with iodine and methanol. The horizontal arrows in panel B indicates the fragmentation pathways that were observed upon performing ion trap multistage CID-MS ⁿ of the derivatized PE precursor ions	83
Figure 2.7	Positive ion mode ESI high-resolution mass spectrometric analysis of a crude lipid extract from the SW480 human adenocarcinoma cell line following d ₆ -DMBNHS derivatization followed by mild formic acid hydrolysis. (A) Expanded region (m/z 744-751) of the ESI-mass spectrum and (B) expanded region (m/z 880-887) of the ESI-mass spectrum.	87
Figure 2.8	Positive ionization mode ESI high-resolution mass spectrometric analysis of a crude lipid extract from the SW480 human adenocarcinoma cell line (A) after reaction with the amine-specific derivatization reagent, ¹³ C-DMBNHS and (B) after reaction with ¹³ C-DMBNHS and iodine and methanol	88
Figure 2.9	Positive ionization mode ESI high-resolution HCD-MS/MS analysis of the synthetic lipid standard $PE_{(P-18:0/22:6)}$ (A) after derivatization with $^{13}C_1$ -DMBNHS, and (B) after derivatization with $^{13}C_1$ -DMBNHS followed by reaction with iodine and methanol. The horizontal arrows in panels A and B indicate the fragmentation pathways that were observed upon performing ion trap multistage CID-MS n of the derivatized PE precursor ions	91
Figure 3.1	Positive ion mode ESI high-resolution mass spectrometric analysis (m/z 600-1000) of crude lipid extract from the human adenocarcinoma cell line (A) SW480 and (B) its metastatic counterpart SW620	90

Figure 3.2	Positive ion mode ESI high-resolution mass spectrometric analysis of a crude lipid extract from the SW620 human adenocarcinoma cell line. (A) Expanded region (m/z 744-751) and (B) expanded region (m/z 880-887) of the ESI-mass spectrum obtained after reaction with the amine-specific derivatization reagent, d ₆ -DMBNHS
Figure 3.3	Expanded regions of the positive ion mode ESI high-resolution mass spectrometric analysis of a crude lipid extract after reaction with d ₆ -DMBNHS and formic acid from the SW620 human adenocarcinoma cell lines for (A) m/z 744-751 and (B) m/z 880-887103
Figure 3.4	Quantitation of PC lipids from the d_6 -DMBNHS derivatized SW480 and SW620 cell crude lipid extracts. (A) Percent individual PC ion abundances compared to the total ion abundance for all PC lipids. (B) Percent total ether-linked PC ion abundance compared to the total PC lipid ion abundance. (C) Percent total PC ion abundance compared to the total ion abundance for all identified lipids. $n = 5$, * = $p < 0.01$
Figure 3.5	Quantitation of LPC lipids from the d_6 -DMBNHS derivatized SW480 and SW620 cell crude lipid extracts. (A) Percent individual LPC ion abundances compared to the total ion abundance for all LPC lipids. (B) Percent total ether-linked LPC ion abundance compared to the total LPC lipid ion abundance. $n = 5$, * = $p < 0.01$
Figure 3.6	Quantitation of PE lipids from the d_6 -DMBNHS derivatized SW480 and SW620 cell crude lipid extracts. (A) Percent individual PE ion abundances compared to the total ion abundance for all PE lipids. (B) Percent total ether-linked PE ion abundance compared to the total PE lipid ion abundance. (C) Percent total PE ion abundance compared to the total ion abundance for all identified lipids. $n = 5$, * = $p < 0.01$
Figure 3.7	Quantitation of LPE lipids from the d_6 -DMBNHS derivatized SW480 and SW620 cell crude lipid extracts. (A) Percent individual LPE ion abundances compared to the total ion abundance for all LPE lipids. (B) Percent total ether-linked LPE ion abundance compared to the total LPE lipid ion abundance. $n = 5$, * = $p < 0.01$
Figure 3.8	Quantitation of TG lipids from the d ₆ -DMBNHS derivatized SW480 and SW620 cell crude lipid extracts. (A) Percent individual TG ion abundances compared to the total ion abundance for all PE lipids.

	(B) Percent total ether-linked TG ion abundance compared to the total TG lipid ion abundance. (C) Percent total TG ion abundance compared to the total ion abundance for all identified lipids. n = 5, * = p < 0.01
Figure 4.1	Positive ion mode ESI high-resolution mass spectrometric analysis (m/z 600-1100) of crude lipid extracts derivatized with 13 C ₁ -DMBNHS followed by Iodine and Methanol from the human adenocarcinoma cell lines, (A) SW480 and (B) SW620, and their secreted exosomes, (C) SW480 Exosomes and (D) SW620 Exosomes. The internal standard lipid PC _(28:0) was included to enable relative quantification of the observed lipid species
Figure 4.2	Distribution of normalized lipid ion abundance/ μ g protein for each lipid sub-class from the $^{13}C_1$ -DMBNHS and iodine/methanol derivatized SW480 and SW620 cell and exosome crude lipid extracts. * = p < 0.01
Figure 4.3	Diacyl, alkyl (O-) and alkenyl (P-) distribution of each lipid sub-class from the 13 C ₁ -DMBNHS and iodine/methanol derivatized SW480 and SW620 cell and exosome crude lipid extracts: (A) PE, (B) PC, and (C) PS lipids. * = p < 0.01
Figure 4.4	Quantification of PE lipids from the 13 C ₁ -DMBNHS and iodine/methanol derivatized SW480 and SW620 cell and exosome crude lipid extracts for individual lipid sum composition normalized abundances/µg protein above 10. * = p < 0.01132
Figure 4.5	Quantification of PC lipids from the 13 C ₁ -DMBNHS and iodine/methanol derivatized SW480 and SW620 cell and exosome crude lipid extracts for individual lipid sum composition normalized abundances/µg protein above 5. * = p < 0.01134
Figure 4.6	Quantification of PS lipids from the 13 C ₁ -DMBNHS and iodine/methanol derivatized SW480 and SW620 cell and exosome crude lipid extracts of individual normalized lipid sum composition abundances/µg protein. * = p < 0.01137
Figure 4.7	Quantification of SM from the ¹³ C ₁ -DMBNHS and iodine/methanol derivatized SW480 and SW620 cell and exosome crude lipid extracts. Individual normalized lipid sum composition abundances/ug protein. * = p < 0.01

Figure 4.8	Quantification of Cer from the $^{13}C_1$ -DMBNHS derivatized SW480 and SW620 cell and exosome crude lipid extracts. Individual normalized lipid sum composition abundances/µg protein. * = p < 0.01
Figure 4.9	Quantification of TG lipids from the 13 C ₁ -DMBNHS derivatized SW480 and SW620 cell and exosome crude lipid extracts. (A) Individual normalized lipid sum composition abundances/µg protein and (B) tiacyl, alkyl (O-) and alkenyl (P-) distribution. * = p < 0.01142
Figure 4.10	Distribution of fatty acids for the sum composition species from Figure 4.4 shown in order: SW480 cells, SW620 cells, SW480 exosomes and SW620 exosomes. (A) Percentages of the longest, most unsaturated fatty acids of the two fatty acyl chains for diacyl PE species. (B) Percentages of the O- chain for each plasmanyl PE species. (C) Percentages of the P- chain for each plasmenyl PE species.
Figure 4.11	Distribution of fatty acids for the sum composition species from Figure 4.5 shown in order: SW480 cells, SW620 cells, SW480 exosomes and SW620 exosomes. (A) Percentages of the longest, most unsaturated fatty acids for diacyl PC species. (B) Percentages of the O- chain for each plasmanyl PC species
Figure 4.12	Distribution of fatty acids for the sum composition species from Figure 4.6 shown in order: SW480 cells, SW620 cells, SW480 exosomes and SW620 exosomes. (A) Percentages of the longest, most unsaturated fatty acids for diacyl PS species. (B) Percentages of the O- chain for each plasmanyl PS species
Figure 4.13	Distribution in percentage of fatty acyls for the sum composition species of the triacyl TG from Figure 4.9 shown in order: SW480 cells, SW620 cells, SW480 exosomes and SW620 exosomes
Figure A.1	Quantitation of PA lipids from the d_6 -DMBNHS derivatized SW480 and SW620 cell crude lipid extracts. (A) Percent individual PA ion abundances compared to the total ion abundance for all PA lipids. (B) Percent total ether-linked PA ion abundance compared to the total PA lipid ion abundance. (C) Percent total PA ion abundance compared to the total ion abundance for all identified lipids. $n = 5$, $* = p < 0.01$
Figure A.2	Quantitation of PS lipids from the d ₆ -DMBNHS derivatized SW480 and SW620 cell crude lipid extracts. (A) Percent individual PS ion abundances compared to the total ion abundance for all PS lipids.

	(B) Percent total ether-linked PS ion abundance compared to the total PS lipid ion abundance. (C) Percent total PS ion abundance compared to the total ion abundance for all identified lipids. n = 5, * = p < 0.01	174
Figure A.3	Quantitation of LPS lipids from the d_6 -DMBNHS derivatized SW480 and SW620 cell crude lipid extracts. (A) Percent individual LPS ion abundances compared to the total ion abundance for all LPS lipids. (B) Percent total LPS ion abundance compared to the total ion abundance for all identified lipids. $n = 5$, $* = p < 0.01$	175
Figure A.4	Quantitation of PG lipids from the d_6 -DMBNHS derivatized SW480 and SW620 cell crude lipid extracts. (A) Percent individual PG ion abundances compared to the total ion abundance for all PG lipids. (B) Percent total PG ion abundance compared to the total ion abundance for all identified lipids. $n = 5$, $* = p < 0.01$	176
Figure A.5	Quantitation of PI phospholipids from the d_6 -DMBNHS derivatized SW480 and SW620 cell crude lipid extracts. (A) Percent individual PI ion abundances compared to the total ion abundance for all PI lipids. (B) Percent total ether-linked PI ion abundance compared to the total PI lipid ion abundance. (C) Percent total PI ion abundance compared to the total ion abundance for all identified lipids. $n = 5$, * = $p < 0.01$.	177
Figure A.6	Quantitation of DG phospholipids from the d_6 -DMBNHS derivatized SW480 and SW620 cell crude lipid extracts. (A) Percent individual DG ion abundances compared to the total ion abundance for all DG lipids. (B) Percent total ether-linked DG ion abundance compared to the total DG lipid ion abundance. (C) Percent total DG ion abundance compared to the total ion abundance for all identified lipids. $n = 5$, $* = p < 0.01$	178
Figure A.7	Quantitation of MG phospholipids from the d $_6$ -DMBNHS derivatized SW480 and SW620 cell crude lipid extracts. (A) Percent individual MG ion abundances compared to the total ion abundance for all MG lipids. (B) Percent total ether-linked MG ion abundance compared to the total MG lipid ion abundance. (C) Percent total MG ion abundance compared to the total ion abundance for all identified lipids. $n = 5$, $* = p < 0.01$	179
Figure A.8	Quantitation of SM from the d ₆ -DMBNHS derivatized SW480 and SW620 cell crude lipid extracts. (A) Percent individual SM ion abundances compared to the total ion abundance for all SM lipids.	

	(B) Percent total SM ion abundance compared to the total ion abundance for all identified lipids. $n = 5$, $* = p < 0.01$
Figure A.9	Quantitation of Cer from the d_6 -DMBNHS derivatized SW480 and SW620 cell crude lipid extracts. (A) Percent individual Cer ion abundances compared to the total ion abundance for all Cer lipids. (B) Percent total Cer ion abundance compared to the total ion abundance for all identified lipids. $n = 5$, $* = p < 0.01$
Figure A.10	Quantitation of cholesterol (Chol) and cholesterol esters (Chol ester) from the d_6 -DMBNHS derivatized SW480 and SW620 cell crude lipid extracts. (A) Percent of total Chol ion abundance compared to the total ion abundance for all lipid peaks identified. (B) Percent individual Chol ester ion abundances compared to the total ion abundance for all Chol ester lipids. (C) Percent total Chol ester ion abundance compared to the total ion abundance for all identified lipids. $n = 5$, $n = 0$ 0.01
Figure C.1	Quantification of Lyso PE (LPE) lipids from the 13 C ₁ -DMBNHS derivatized SW480 and SW620 cell and exosome crude lipid extracts. (A) Individual normalized lipid sum composition abundances/µg protein and (B) acyl, O- and P- distribution of LPE species. * = p < 0.01
Figure C.2	Quantification of LPC lipids from the 13 C ₁ -DMBNHS derivatized SW480 and SW620 cell and exosome crude lipid extracts. (A) Individual normalized lipid sum composition abundances/µg protein and (B) acyl, O- and P- distribution of LPC species. * = p < 0.01203
Figure C.3	Quantification of Lyso PS (LPS) lipids from the 13 C ₁ -DMBNHS derivatized SW480 and SW620 cell and exosome crude lipid extracts. (A) Individual normalized lipid sum composition abundances/µg protein and (B) acyl, O- and P- distribution of LPS species. * = p < 0.01
Figure C.4	Quantification of PG lipids from the $^{13}C_1$ -DMBNHS derivatized SW480 and SW620 cell and exosome crude lipid extracts. (A) Individual normalized lipid sum composition abundances/µg protein and (B) acyl, O- and P- distribution. * = p < 0.01204
Figure C.5	Quantification of LPG lipids from the $^{13}C_1$ -DMBNHS derivatized SW480 and SW620 cell and exosome crude lipid extracts. (A) Individual normalized lipid sum composition abundances/µg protein and (B) acvl. O- and P- distribution. * = p < 0.01204

Figure C.6	Quantification of PI lipids from the $^{13}C_1$ -DMBNHS derivatized SW480 and SW620 cell and exosome crude lipid extracts. (A) Individual normalized lipid sum composition abundances/µg protein and (B) acyl, O- and P- distribution of PI species. * = p < 0.01	.205
Figure C.7	Quantification of Hex-Cer from the $^{13}C_1$ -DMBNHS derivatized SW480 and SW620 cell and exosome crude lipid extracts. Individual normalized lipid sum composition abundances/µg protein. * = p < 0.01.	.205
Figure C.8	Quantification of DG lipids from the $^{13}C_1$ -DMBNHS derivatized SW480 and SW620 cell and exosome crude lipid extracts. (A) Individual normalized lipid sum composition abundances/µg protein and (B) diacyl, O- and P- distribution. * = p < 0.01	.206
Figure C.9	Quantification of MG lipids from the 13 C ₁ -DMBNHS derivatized SW480 and SW620 cell and exosome crude lipid extracts. (A) Individual normalized lipid sum composition abundances/µg protein and (B) acyl, O- and P- distribution. * = p < 0.01	.206
Figure C.10	Quantification of individual Chol Ester lipids from the $^{13}C_1$ -DMBNHS derivatized SW480 and SW620 cell and exosome crude lipid extracts as normalized lipid sum composition abundances/µg protein. * = p < 0.01.	.207

LIST OF SCHEMES

Scheme 1.1	Adapted fragmentation mechanism for MS ³ analysis of [PC _(O-16:1/18:1) - CH ₃ - H] ⁻ [208]
Scheme 1.2	Adapted fragmentation mechanism for MS^3 analysis of $[PC_{(P-16:0/18:1)} - CH_3 - H]^{-}[208]$
Scheme 2.1	Reaction of plasmenyl phospholipids with iodine and methanol76
Scheme 2.2	Proposed CID-MS/MS fragmentation mechanisms for the plasmenyl ether containing $PC_{(P-18:0/22:6)}$ lipid, prior to and following reaction with iodine and methanol. The m/z values shown correspond to the calculated masses of the various product ions80
Scheme 2.3	Proposed CID-MS/MS fragmentation mechanisms for the plasmenyl ether containing $PE_{(P-18:0/22:6)}$ lipid, prior to and following reaction with iodine and methanol. The m/z values shown correspond to the calculated masses of the various product ions84
Scheme 2.4	Proposed CID-MS/MS fragmentation mechanisms for the 13 C ₁ -DMBNHS derivatized plasmenyl ether containing PE _(P-18:0/22:6) lipid, prior to and following reaction with iodine and methanol. The m/z values shown correspond to the calculated masses of the various product ions
Scheme 4.1	Workflow for exosome isolation, lipid extraction, derivatization and data analysis using $^{13}\text{C}_1\text{-DMBNHS}$ followed by iodine and methanol derivatization method for lipid analysis
Scheme 4.2	Acyl and alkenyl chain identification and headgroup confirmation for the derivatized plasmenyl PE lipid, PE _(P-16:0/18:1) , by MS/MS in positive ionization mode
Scheme 4.3	Acyl chain identification and headgroup confirmation for the PC lipid, PC _(16:0/18:1) , by MS/MS in negative ionization mode148

Chapter 1

An Overview of Analytical Strategies for Lipidome Analysis

1.1 Introduction to Lipid Structure and Function

Lipids are a diverse class of biomolecules that consist of fats, waxes, sterols, etc. and can be defined as, "hydrophobic or amphipathic small molecules that originate entirely or in part by carbanion-based condensations of thioesters and/or by carbocation-based condensations of isoprene units" according to the Lipid Maps Consortium [1]. Lipids function in three main areas: structure, signaling and energy storage. A single, all encompassing definition of lipid structure does not exist; however, lipids are generally divided into eight classes divided by their distinct individual base structures: fatty acyls, glycerolipids, glycerophospholipids, sphingolipids, sterols, prenols, saccharolipids and polyketides [1,2].

1.1.1 Structure and Nomenclature of Lipid Classes

As mentioned above, lipids can be divided into eight classes.; however, there are several possibilities for lipid classification depending on the degree to which a lipid has been or can be identified. Lipids can be defined by the following: lipid class or sub-class, sum composition, molecular lipid identity or

structurally defined molecular lipid [3]. Sum composition is defined as the lipid class/sub-class as well as the total number of carbons and double bonds in the fatty acyl chains [3]. Molecular lipid identity is defined as the lipid class/sub-class with the total number of carbons and double bonds identified in each individual fatty acyl chain [3]. Structurally defined molecular lipids are defined as the molecular lipid identity with the position of the double bond positions defined [3].

Fatty acyls (FA) have several sub-classes including fatty acids, fatty alcohols, cyclic fatty acids, hydrocarbons and more [1,2]. As a class, they consist of chains of methylene groups with or without branching with zero to several degrees of unsaturation in varying positions along the aliphatic chain. In several cases, fatty acids are labeled by different names based on their structure and/or function. Oleic acid, for example, is a fatty acid consisting of 18 carbons and 1 double bond starting at the ninth carbon from the end (Figure 1.1). It can also be notated as FA_(18:1,n-9), where 'n' denotes the position of the double bond from the terminal carbon. Many complex lipids in the other classes have FA constituents and are also notated by their composition.

Figure 1.1 Example of fatty acyl structure, FA_(18:1, n-9).

Glycerolipids are a class of lipids that contain a glycerol backbone [1,2]. The most commonly known glycerolipids are either mono- di- or tri-substituted with fatty acids or fatty alcohols: monoglycerol (MG), diglycerol (DG) and

triglycerols (TG) (Table 1.1), respectively. The fatty acyl constituents attached to the glycerol backbone may be either fatty acids or fatty alcohols with or without a vinyl double bond. Sn position may or may not be known for specific fatty acyl constituents. Therefore, a naming convention has been proposed by Liebisch et al indicating either a positive sn position identification (fatty acyls separated by a "/" in order from sn-1 to sn-3) or limited to identification of the fatty acyl substituent identities without knowledge of sn position (fatty acyls separated by a " " in order of shortest to longest chain and degree of unsaturation) glycerolipids with a fatty alcohol (also called alkyl or plasmanyl) substituent are notated with an "O-" (ex. TG_(O-16:0/18:1/16:0) or TG_(O-50:1)) and a fatty alcohol with a vinyl ether bond (also called alkenyl or plasmenyl) with a "P-" (ex. TG_(P-16:0/18:1/16:0) or TG_(P-50:1)) [4] (Table 1.1). Glycerolipids can also have one or more sugar residues attached by glycosidic linkages to the glycerol backbone which are called glyceroglycolipids [1,2,5].

Table 1.1 Examples of level of identification, symbol and structures of the glycerolipids, $TG_{(16:0/18:1, n-9/16:0)}$, $TG_{(O-16:0/18:1, n-9/16:0)}$ and $TG_{(P-16:0/18:1, n-9/16:0)}$.

Level of Identification	Symbol	Structure
Sum Composition	TG _(50:1)	
Molecular Lipid	TG _(16:0/18:1/16:0)	0 sn-1 0-sn-2
Structurally Defined Molecular Lipid	TG _(16:0/18:1, n-9/16:0)	sn-3
Sum Composition	TG _(O-50:1)	
Molecular Lipid	TG _(O-16:0/18:1/16:0)	
Structurally Defined Molecular Lipid	TG _(O-16:0/18:1, n-9/16:0)	
Sum Composition	TG _(P-50:1)	
Molecular Lipid	TG _(P-16:0/18:1/16:0)	
Structurally Defined Molecular Lipid	TG _(P-16:0/18:1, n-9/16:0)	

Glycerophospholipids are a class of lipids defined by a glycerol backbone with a phosphate at the *sn*-3 position and one (lyso) or two fatty acyl groups at the *sn*-1 and/or *sn*-2 position [1,2]. There are several sub-classes of glycerophospholipids differentiated by the headgroup attached to the phosphate group including choline (PC), ethanolamine (PE), Serine (PS), Inositol (PI), glycerol (PG), no group at all as phosphatidic acid (PA) (Figure 1.3) or another PG as with cardiolipin (CL). As with glycerolipids, the position of the individual fatty acyl substituent(s) may not be known; therefore, the "/" or "_" convention described above is also followed for glycerophospholipids [4]. Furthermore, the

presence of an alkyl ether or vinyl ether bond rather than an ester bond for the fatty acyls is signified by an "O-" or "P-", respectively (Figure 1.3). The alkyl or alkenyl chain is typically on the *sn*-1 position but may also be present on the *sn*-2 position, or both [1,2].

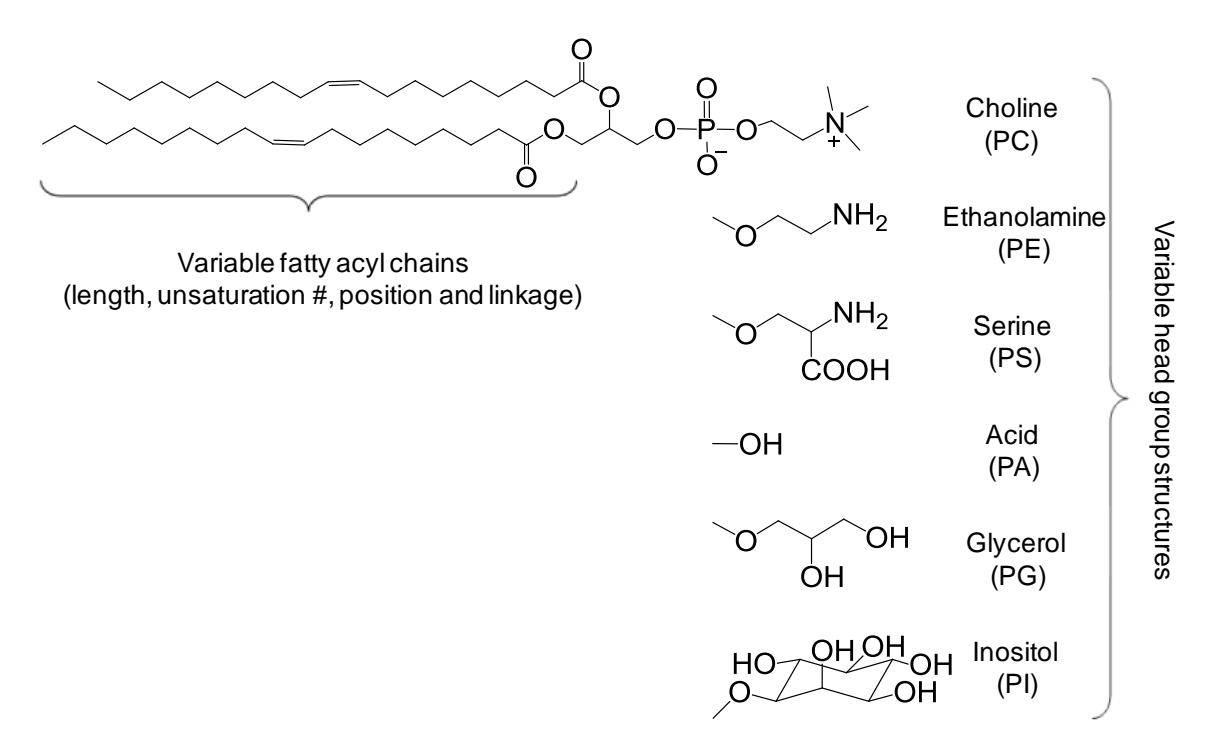


Figure 1.2 General glycerophospholipid structure and headgroup variations.

Sphingolipids are a class of lipids that contain a sphingoid base [1,2]. Sphingosine is a common sphingoid base which has a trans double bond on the fourth carbon from the terminal hydroxyl group (area shaded green in Figure 1.3) while sphinganine is a sphingoid base that lacks the double bond. The sphingoid base is designated with a "d" for 1,3-dihydroxy chain base (as shown in Figure 1.3) or a "t" for 1,3,4-trihydroxy variations [1,2]. There are many potential additions to the sphingoid bases which include a phosphate (Sphingosine-1-phosphate), an amide-linked fatty acid (Ceramide) (area shaded red in Figure

1.3), an amide-linked fatty acid and phosphate (Ceramide-1-phosphate), an amide-linked fatty acid and a phosphocholine group (Sphingomyelin) (area shaded blue in Figure 1.3) and more complex variations such as Gangliosides [1,2]. There could also be branching and hydroxyl groups included on the sphingoid base in various positions [1,2].

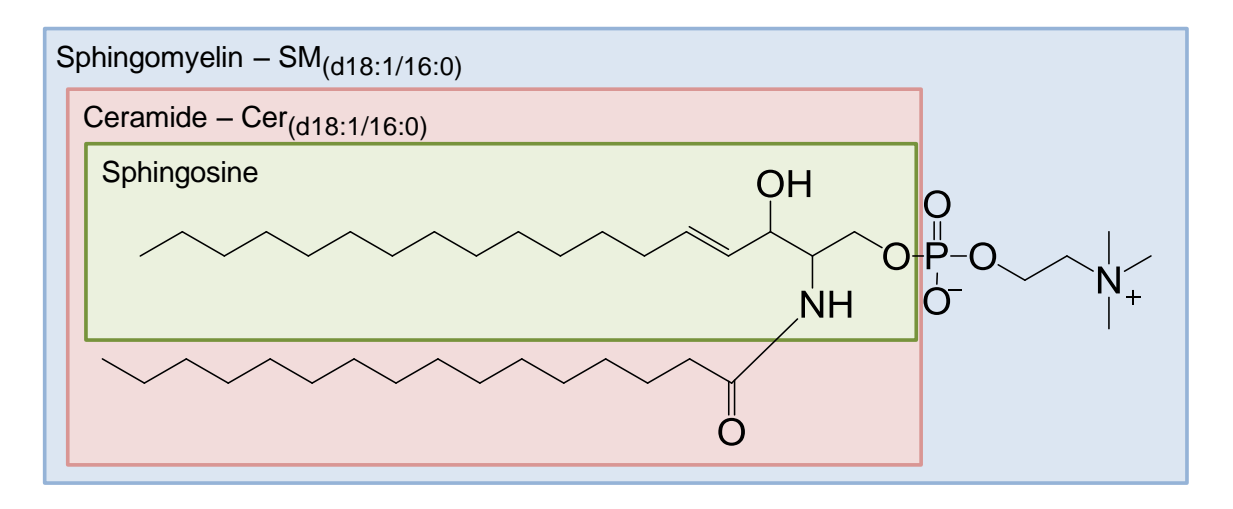


Figure 1.3 Example of the structure of the sphingolipids and their notation including the sphingoid backbone (sphingosine), Ceramide and Sphingomyelin.

Sterol lipids include cholesterol and its derivatives that contain a fused 4 ring structure (Figure 1.4) [1,2]. Cholesterol esters are a type of sterol lipid with a cholesterol core and an ester-bonded fatty acid substituted for the carbon-3 hydroxyl group (for example, Chol_(18:1)). Other derivatives of sterol lipids include C18 steroids (estrogens), C19 steroids (androgens), C21 steroids (progestogens, glucocorticoids and mineralocorticoids), those with B ring cleavage of the core structure (Vitamin D variants) and oxidized derivatives (bile acids).

$$R = H = Chol$$

$$R = H = Chol$$

$$C_XH_Y$$

Figure 1.4 Structure of cholesterol (Chol) and cholesterol esters (Chol Ester).

Prenol lipids, saccharolipids and polyketides are the final three classes of lipids, according to the Lipid Maps Consortium [1,2]. Prenol lipids are made from the isopentenyl diphosphate and dimethylallyl diphosphate precursors. Saccharolipids are similar to glycerolipids and glycerophospholipids, but have sugar residues in place of the glycerol backbone. The fatty acids can attach via an ester linkage or amide linkage and often have branched hydroxyl groups in which another ester linked fatty acid may reside. Many secondary metabolites of most living organisms are polyketides. Polyketides have great structural diversity and often have many modifications and are synthesized from acetyl and propionyl subunit polymerization.

The focus of this work is on the analysis of complex lipids in mammalian cells. For this reason, glycerophospholipids, glycerolipids, sphingolipids and sterol lipids will be discussed further.

1.1.2 Lipid Function in Mammalian Cells

1.1.2.1 Lipids as Structural Components

Lipids, especially phospholipids, compose the majority of the matrix of cellular membranes [6]. Specifically, PC accounts for over 50% of the phospholipids in membranes of eukaryotic cells [6]. The plasma membrane has an asymmetrical lipid bilayer with the non-polar acyl chains as the core. The outer layer of the bilayer consists of mostly PC while PE and PS are located primarily on the cytosol side [6]. This is due to the cylindrical shape of PC lipids and an overall conical shape to PE [6]. PE, when moved to the outer layer of the plasma membrane, puts curvature stress on the membrane which aids in fission, fusion and budding [7]. Several other organelles in the eukaryotic cell are either monolayers or bilayers composed mostly of phospholipids. Sphingolipids, such as sphingomyelin, and cholesterol are also major components of the cellular membrane and are enriched in lipid rafts [8,9] in a liquid ordered phase [9,10]. The sphingolipids are orientated similarly to the phospholipids (fatty acid chains toward the center of the bilayer) and cholesterol situated with the hydroxyl group interacting with the phosphate headgroups of sphingomyelin and phospholipids [11].

1.1.2.2 Cellular Signaling Roles of Lipids

Fatty acids are essential in not only in the structures of complex lipids, but also in their ability to regulate signaling of cellular functions [12]. Free fatty acids

(FFAs) and fatty acid metabolism are also involved in insulin secretion of pancreatic β-cells [13]. For example, arachidonic acid (AA) metabolizes to form prostaglandins which sensitize nerves in areas of inflammation [14,15]. Dietary polyunsaturated fatty acids (PUFAs) inhibit n-9 fatty acid biosynthesis which reduces n-9 incorporation in the plasma membrane and the activity of Δ^9 desaturase from the lack of substrate [12]. Saturated fatty acids can also engorge white adipose tissue leading to apoptosis which can cause low-grade inflammation by recruiting macrophages and neutrophils [16,17]. This chronic inflammation can further lead to insulin resistance in muscle tissues [17].

Complex lipids, such as sphingolipids and glycerophospholipids, act as second messengers for cellular signaling [6,11]. One of the largest groups of second messengers are those present in the sphingolipid pathway, especially Cer which is an intermediate for the biosynthesis/metabolism of many other molecules in the sphingolipid pathway including Ceramide-1-Phosphate (Cer-1-P) and Sphingosine-1-Phosphate (S-1-P). Cer mediates cellular responses to stress which may include signaling for cellular growth, differentiation [18] and apoptosis [19,20]. Cer is also involved in many immune responses such as Tumor Necrosis Factor- α (TNF- α) [18,21], Interleukin-1 (IL-1) [21], and interferon γ [18]. Cer-1-P has also been shown to be involved in apoptosis, some immune responses, and proliferation and cell survival [22-24]. S-1-P, when present on the outer leaflet of membranes, can activate G protein-coupled receptor pathways [25,26].

Similar to the role that Cer plays in the sphingolipid pathway, DG formed from glycerophospholipids through the enzyme phospholipase C [27] serves as the second messenger for phosphatidylinositol phosphate (PI-P) signaling [28]. After enzymatic degradation of phosphatidylinositol biphosphate (PI-P₂), DG can help activate protein kinase C by phosphorylation [27]. PI-P2s contribute to calcium homeostasis and membrane trafficking [29]. Phosphatidylinositol triphosphate (PI-P₃) can also contribute to the activation of protein kinase C [27] as well as protein kinase B, which affects cell survival and increases extracellular protein binding [30]. Lysophospholipids, although low in concentration compared to many diacyl species in cells and tissues, are also involved in many cellular signaling cascades [31]. Lysophosphatidic acids (LPA) effect blood pressure, contraction of smooth muscle and even platelet activation [31] whereas lysophosphatidylcholine (LPC) is involved with inflammatory diseases [31] and couples with the G-protein coupled receptor, G2A, to promote apoptosis [32].

1.1.2.3 Lipids as Fuel and Energy Storage Molecules

Lipids are also important energy storage molecules. TG are the main lipids used for energy storage in lipid droplets of adipocytes [6]. Intracellular TG lipids are metabolized by skeletal muscle for ATP production via β -oxidation [33]. Production of energy through β -oxidation of TG lipids provides over twice the energy of carbohydrates or proteins per mass [34].

1.1.3. The Role of Lipids in Disease

1.1.3.1 Lipid Alterations in Various Disease States

Alterations in lipid species have been reported for several diseases and disorders including diabetes [35-40], Alzheimer's disease [41-45], peroxisomal disorders [46,47] and many more [39,46,47]. Busik et al. have reported significant differences in the abundance and fatty acyl constituents of some glycerophospholipids [38] and a decrease in n-3 polyunsaturated fatty acids [40] in diabetic rat retina compared to their non-diabetic control littermates. Others have reported remodeling of cardiolipin fatty acyl constituents in diabetic rats which may lead to diabetic cardiomyopathy [35,37].

Plasmalogen lipids have been observed to be altered in Alzheimer's disease [41-45,48] and the Peroxisomal disorder, Zellweger's syndrome [49]. Overall glycerophospholipid content was originally determined to be decreased in Alzheimer's disease patients when compared to age-matched control brains [41] which was caused by a loss of plasmenyl PE species [48]. This was thought to be a result of the elevation of enzymatic activity of plasmalogen-specific phospholipase-A₂ (PLA₂) [43]. Han et al. also observed a decrease in plasmenyl PE content in the cerebellar white matter in the brains of transgenic mice and humans with Alzheimer's disease [44]. The reduction of plasmenyl PE content was not, however, reflected in the cerebellar grey matter, regardless of their clinical dementia ratings [44]. Infants with Zellweger syndrome, a lethal disease,

were observed to not only lack peroxisomes in their livers and kidneys and have mitochondrial defects, but also have only 10% of the plasmenyl PE expected of normal infants and a marked decrease in the amount of plasmenyl PC in their heart and muscle tissues [49].

1.1.3.2 Lipid Alterations in Cancer

Several lipid classes have also been demonstrated to have altered content in malignant tumors [50]. For example, increases in 16:0 and 18:1 fatty acyl containing PC lipids were observed in liver tumors of transgenic mice [51]. N-3 and especially n-6 polyunsaturated fatty acids (PUFAs) were increased in breast cancer tissue compared to normal breast tissue whereas several other fatty acids such as 14:0, 18:1, 18:2, 18:3 were decreased [52]. However, n-3 fatty acids were suggested to have a protective effect in normal breast tissue against cancer [53] and in mice against hepatocellular cancer [54]. Many of these alterations in lipid content of tumor cells are suspected to be linked to increased activity of fatty acid synthase (FASN) [55,56].

Total ether lipid content in glycerophospholipids has been associated with invasiveness of cancer, demonstrating a positive correlation with ether lipid abundance and proliferation [57-61]. Plasmenyl (vinyl ether) and plasmanyl (alkyl ether) PE and PC content increased in human breast [61-63], lung [63] and prostate cancer [63] tissues compared to normal and benign tumor tissues [63]. Plasmenyl PC and plasmenyl PE in colon cancer tumors were observed to

increase by 45% and 58%, respectively compared to control human mucosa [64]. These alterations were suggested to be caused by a decrease in Phospholipase C and Phospholipase D activity, while Phospholipase A₁ and A₂ activity were observed to remain unchanged [64].

Lyso lipids have been suggested to play a role in the activation of ovarian [65-67], breast [65,68] and colorectal cancer [69]. Specifically, LPA, lysophosphatidylserine (LPS) and sphingosinephosphocholine (SPC) induced increases in calcium ion concentration and threonine phosphorylation in ovarian and breast cancer cells with LPA positively affected proliferation [65]. Lysophosphatidylinositol (LPI) as well as LPA concentrations were elevated in the serum of patients with ovarian cancer [70]. LPC concentration was detected to increase in a study of human malignant colon tissues [71].

Other glycerophospholipid species have been demonstrated to have altered lipid profiles in cancer tissues including diacyl glycerophospholipid species within the PC, PE, PS and PI sub-classes that were altered in the urine of human subjects with prostate cancer compared to samples from controls [72]. Further studies have shown alterations in the concentrations of ether lipids (plasmanyl and/or plasmenyl) in malignant tumor cells and tissues [59,71,73,74]. Although plasmenyl PC, like LPC, was observed to increase in human malignant colon tissues, plasmenyl PE was determined to decrease [71]. Alkyl lipid content in the membranes of transplantable rat mammary tumors was positively correlated with the metastatic potential of each cell type whereas there was no detectable correlation with plasmenyl lipid content [73]. Furthermore, knockout of

the key enzyme for ether lipid biosynthesis lead to the reduction of ether lipids levels in melanoma, breast and prostate cancer cells which lowered cell survival, cell migration and invasion of the cells in culture [75].

The correlation of ether linkage (plasmanyl or plasmenyl) to tumorigenicity is not limited to glycerophospholipids only, but also occurs in glycerolipids [57,59]. Plasmanyl TG and Plasmenyl TG content was elevated in breast, lung and prostate cancer tissues compared to control human tissue and benign tumors [63]. Both plasmanyl TG and plasmenyl TG were increased in transplantable mouse and rat liver tumors with varying invasiveness [59,74,76]. Plasmanyl TG content was also increased in human liver tumors compared to normal tissue [77,78]. Overall neutral lipid content, including glycerolipids and cholesterol esters, were positively correlated with human brain tumor grade [79].

Sphingolipids are signaling molecules, therefore it is not surprising that several sphingolipids are associated with tumor suppression, promotion [80,81] and chemotherapeutic resistance [81]. Ceramide, a pro-apoptotic molecule, was decreased in ovarian tumors when compared to normal tissue and was inversely correlated to the malignancy of brain tumors [80]. Sphingosine-1-phosphate (S-1-P), an anti-apoptotic molecule, was shown to be important in proliferation and survival of breast cancer tumors [82,83]. Total SM content was observed to increase in breast cancer cell lines with low and high degrees of aggression when compared to non-malignant breast cancer epithelial cells including an enrichment of SM(34:1) [68].

1.1.3.3 Lipids in Secreted Cancer Exosomes

Exosomes are 40-100nm vesicles formed within multivesicular bodies and secreted upon fusion of the late endosome with the cellular membrane [84]. They contain a variety of molecules including proteins, RNAs and lipids [85] and have been implicated to play roles in several disorders [86] and diseases [87,88]. They are able to transfer mRNAs, microRNAs and proteins intercellularly which facilitates local and system wide cellular communication [89-91] and can affect cells in the immune system [92]. An increasing amount of research in cancer suggest that exosomes are involved in the promotion of angiogenesis, migration and cancer metastasis [88,89,93] by converting potential locations of metastasis into "pre-metastatic niches" [93]. Latent TGF- β is present in some exosomes [94,95] which can trigger SMAD-3 and α -SMA expression and can change the morphology of fibroblasts [95]. This is especially important since there is a higher amount of secretion of exosomes in cancer as opposed to non-malignant cells [96,97].

Although there is an increasing amount of research being performed on exosomes, there is still limited information on the lipid compositions with most lipid information limited to the lipid class level of identification (i.e. PC, PE, SM, etc.) [98-100]. A more in depth exosomal lipidomic study was performed by Llorente, et al. which was able to identify and quantify 280 lipid species at the molecular lipid level of identification from PC-3 prostate cancer cell secreted exsomes [101]. More research on the lipidomes of exosomes would be beneficial

since exosomal membrane lipids may impact exosome secretion, fusion, uptake and target cell functional response [98,102,103].

1.2 Lipid Extraction

Several methods have been developed for the extraction of lipids, with variable goals depending on the lipid class of interest or type of tissue/cell being extracted [104]. No matter which extraction method is used, there are precautions that need to be made to ensure the samples are not degraded or contaminated. Storage of samples and extracts is highly important since lipids can readily degrade [105] and/or oxidize [104]. For example, double bonds of unsaturated and plasmenyl lipids are readily oxidized by exposure to ambient air [106]. Due to the non-polar properties of lipids, all methods utilize organic solvents which can degrade plastics used for storing and performing analyses, thus contaminating the extracts. For this reason, glass containers with Teflon lined caps should be used whenever possible. It may also be necessary to homogenize tissues if looking for total lipid content since tissues may have different lipid content depending on the area from which it is taken [107].

One of the most common extraction techniques for extraction of total lipids is the Folch extraction [108]. The original method involves homogenization of tissue in a 20-fold excess of 2:1 CHCl₃/MeOH, assuming 1g of tissue is approximately 1mL. The homogenate is then filtered through fat-free paper into a glass stoppered container and 20% of the volume of extract quantity of water is

added to the container, mixed thoroughly and allowed to separate completely by either letting the vessel stand or by centrifugation. The top layer is carefully siphoned off then the remaining interface is washed 3 times with water and aspirated without disrupting the lower phase. Methanol is added until one continuous phase is achieved and the extract is diluted with 2:1 CHCl₃/MeOH until the desired volume is achieved. This procedure has been the basis of several modified extraction procedures for mammalian tissues which simplified the process [109-111]. Although the aim of this method is the extraction of total lipid content, very polar lipids such as gangliosides are partitioned into the aqueous layer and mostly lost unless separate extraction of the aqueous layer is performed [112].

Another common extraction technique is the Bligh and Dyer method [113]. This method, which was originally performed on frozen fish tissue, is meant for total lipid extraction on large amounts of tissue with very high water content [104]. Briefly, the tissue is homogenized with 1:2 CHCl₃/MeOH which is miscible with the water in the tissue. After homogenization, enough CHCl₃ and water are added until two distinct phases are formed with the lipids extracted into the organic (lower) layer. After centrifugation, the organic layer is removed and more CHCl₃ is added to the aqueous phase for re-extraction. The organic phase is removed, added to previous organic portion and dried with anhydrous sodium sulfate. Like the Folch method, extraction of total lipid content is the aim and

several methods have been adapted for different tissues [114,115]; however it is a much faster method which lends itself well to large sample sets.

A more recently developed method is the use of methyl-tert-butyl ether (MTBE) for total lipid extraction [116]. In short, MeOH is added to the sample to be extracted then vortexed. MTBE is added and shaken at room temperature for 1 hour followed by the addition of water for phase separation. Samples are set at room temperature for 10 minutes, centrifuged and the upper phase (MTBE) is removed prior to re-extraction with the solvent mixture (10:3:2.5 MTBE/MeOH/H₂O by volume). The organic phases are combined and dried completely. This method is comparable to the Folch as well as Bligh and Dyer methods, but has the potential to obtain cleaner extraction(less water and cellular debris in the organic phase) since the lipid extract is in the upper phase.

There are numerous other extractions methods that are tailored for specific lipid types. For example, sphingolipids can be extracted using the Folch or Bligh and Dyer methods, but loss of the already low abundant polar sphingolipids is a concern. Therefore, the sphingolipids are extracted with 2:1 MeOH/CHCl₃, heated and exposed to KOH to degrade interfering lipids such as glycerophospholipids to allow concentration of sphingolipids in the samples [117]. Svennerholm and Fredman developed an extraction method that is specific for extraction gangliosides involved of which also the removal of alycerophospholipids [118]. Extraction of total lipids can also be achieved by two separate extraction steps [119], which will be discussed in section 1.2.6.3.2.

1.3 Strategies for Lipidome Analysis

1.3.1 Thin Layer Chromatography (TLC)

TLC is an analytical method in which extracted lipids are adsorbed on a solid phase and separated using an organic solvent mixture which migrates lipids based on their polarity/affinity for the solvent used. Typically the solid phase is silica gel, but alumina and kieselguhr are also utilized [120]. Although TLC was previously the gold standard for lipid quantification by densiometry or in conjunction with other separation methods such as GC, the development of high performance liquid chromatography (HPLC) has largely taken the place of TLC separation.

1.3.1.1 Methodologies for TLC Analysis

The ability of TLC to separate a complex lipid mixture depends highly on the stationary phase and solvent mixture employed. Normal phase TLC uses a silica gel stationary phase with a non-polar mobile phase which has a high concentration of either chloroform or hexane. This is useful for the separation of phospholipid classes based on the polarities of their headgroups. Modifications to the stationary phase will alter the separation performed. For example, silver nitrate impregnated in the stationary phase allows for separation of non-polar lipids such as triglycerols, fatty acids, and phospholipids based on their degree of

unsaturation [121]. Solvent systems for normal phase TLC include 25:15:4:2 chloroform/methanol/acetic acid/water or 65:25:4 chloroform/methanol/water for the separation of phospholipids [122,123] and 70:30:1 hexane/diethylether/acetic acid for separation of neutral lipids [79,124,125], and many others [120].

Reverse phase TLC uses a non-polar stationary phase such as silicone or a hydrocarbon and a polar mobile phase [126]. It is used to separate lipids based on their degrees of unsaturation. For example, siliconized chromaplates have been used to separate saturated and unsaturated methyl esters in menhaden oil using acetonitrile/acetic acid/ water or acetic acid/water solutions [127]. Reverse phase TLC was also used with hydrocarbon, undecyl and octadecyl bonded stationary phases, to separate sterols, which only differ in some cases by a single double bond [128,129].

Two-dimensional TLC uses different mobile phases in order to separate those lipid classes that wouldn't ordinarily separate in a traditional normal or reverse phase TLC experiment, such as highly acidic lipids, PS and PE [120]. The first dimension of TLC separation is typically by a less polar mobile phase and the second is more polar to separate the phospholipid which co-elute in the first separation [130-132].

1.3.1.2 Benefits and Drawbacks of TLC

TLC, whether normal phase, reverse phase or two dimensional, has several benefits for lipid analysis. It is a simple method of placing the lipid extract

on a substrate and allowing the mobile phase to migrate the lipids along the substrate. It is inexpensive, as it doesn't require any expensive equipment or equipment maintenance which also makes it a convenient method that can be used in any lab. The amount of solvent required for TLC is very small which adds to the inexpensive and convenient aspect along with the added benefit of less waste. For one dimensional TLC, several extracts can be analyzed on a single plate which saves time, materials and enables easy comparison of samples.

However, despite its many benefits, TLC has several drawbacks for lipid analysis. First, since TLC separations are performed in ambient conditions, the lipids are exposed to the atmosphere which can lead to oxidation of the double bonds. The extent of oxidation depends on the duration of exposure before analysis and can lead to errors in the measurements. Although there are several substrates and solvent systems available for separation of complex lipid extracts, finding a system that works best for an unknown mixture may be difficult and time consuming. Once the optimum system is found, there's still the drawback of low resolution as certain classes of lipids may not fully separate from each other. Finally, TLC cannot separate individual molecular species of complex lipid mixtures and is limited to either separation by lipid sub-class or degree of unsaturation of a more purified extract.

1.3.2 Gas Chromatography (GC)

GC is a chromatographic technique to separate gas phase analytes and can be divided into two types: Gas-Liquid Chromatography (GLC) and Gas-Solid Chromatography (GSC). Both techniques use inert gas such as He as the mobile phase, but GLC separates analytes by partitioning between a liquid stationary phase column and the mobile phase whereas GSC uses adsorption to a solid stationary phase within the column. Analysis of lipids is more commonly performed with GLC than GSC. There are several detectors used by GC including thermo conductivity (TCD), flame ionization (FID) and mass spectrometry (MS). Analysis by GC-MS will be discussed in 1.2.6.1.

1.3.2.1 Methodologies, Including Derivatization, for GC Analysis

Analysis of lipids using GC requires either transesterification of complex lipids, derivatization and/or conversion of free FA into fatty acid methyl esters (FAMES) [133]. This is accomplished by base catalyzed reagents, acid catalyzed reagents, diazomethane and many others [133]. For example, FAMES and dimethylacetals (DMA) were formed by a boron fluoride-methanol reagent and extracted with pentane and sodium hydroxide at 0°C [134-136]. O-alkyl TGs have also been saponified, extracted with CHCl₃ and derivatized to trimethylsilyl ethers[137] and diacetyl [138] derivatives [77,78]. Each method is specific to the lipid content of the samples of interest since many of the methods are not universal and can have undesired effects such as forming contaminants which can be incorrectly identified as lipids, incomplete conversion/derivatization, and

changing the original FA composition by oxidation, degradation, or forming geometric isomers [133].

1.3.2.2 Drawbacks and Benefits of GC

GC in an efficient analysis tool and is also very sensitive with as low as sub-picogram detection limits depending on the detector used, which is beneficial for small amount of samples [139]. Quantitation by GC is possible and analysis can be achieved quickly. Analysis by GC is easily automated, relatively inexpensive and is well-established for fatty acid composition. Unfortunately, analysis of intact complex lipids is not feasible using GC as most intact lipids are not volatile and would need to be derivatized. Complex lipids are also susceptible to thermal degradation. Although quantitation is possible, many internal standards would be needed which may not be readily available and can make analysis expensive.

1.3.3 Liquid Chromatography (LC)

LC is another chromatographic technique which separates analytes based on their interactions with both the stationary phase and the mobile phase. There are several types of LC techniques with varying columns to be used depending on the properties of the analytes desired to be separated. These techniques include Ion Exchange (IEC), Affinity (AC) and Size Exclusion chromatography

(SEC) [140] but further focus will be on two types of partition chromatography: normal phase and reversed phase. Like GC, there are several detectors available including absorbance (UV or diode array), fluorescence, refractive index, evaporative light-scattering and MS [141]. LC techniques may also include derivatization to improve the sensitivity of detection [142]. LC-MS will be discussed in section 1.2.6.1.

1.3.3.1 Normal Phase and Reverse Phase LC

Normal phase liquid chromatography (NP-LC) is characterized by the use of a polar stationary phase such as unmodified silica or silica modified with either amine or diol functional groups with a non-polar mobile phase. NP-LC separates phospholipids based on their polar headgroups leading to several methods with varying columns and solvent systems being established [143-145]. Reversed phase liquid chromatography (RP-LC) uses a non-polar stationary phase and a polar mobile phase such as a mixture of acetonitrile, methanol and water. Analytes are eluted depending on lengths and degrees of unsaturation of the fatty acyls as well as headgroup polarity of lipids. Derivatization of some lipid classes is required for UV detectors [142,146,147] (see section 1.2.6.3.4), but the light-scattering mass detector can be used universally, albeit with a higher detection limit. NP-LC and RP-LC are also easily linked to mass spectrometric detectors which will be discussed in 1.2.6.1.

1.3.3.2 Drawbacks and Benefits of LC

LC is a powerful tool for lipid analysis since it is suitable for non-volatile samples and can separate lipids by headgroup or acyl chain composition. It also allows for quantitation if all standards are available. LC is easily automated with most current instrumentation. However, separation of lipids via LC can be very time consuming and due to their complex structures, lipid species may co-elute and/or tail leading to incorrect quantitation and mis-identification. Quantification requires many internal standards which may not be available and can be very expensive. Detection of underivatized lipids can be difficult as many underivatized lipids do not absorb visible and UV light effectively.

1.3.4 Nuclear Magnetic Resonance (NMR)

NMR is a spectroscopic technique which uses static and oscillating magnetic fields to identify the resonance of nuclei in molecules. It can be used to gain structural information of simple molecules by one-dimensional NMR and larger, more complex molecules such as proteins using two-dimensional NMR. Information gained by one dimensional NMR includes the chemical shift in ppm which gives information on the local environment of the nuclei, fine structure such as doublet or singlet indicating the number of close similar nuclei and the intensity that establishes how many nuclei are giving rise to that peak. The latter

can be used for structural identification in pure samples or for quantitation of a number of a specific species in a mixture [148].

1.2.4.1 Methodologies for NMR

¹H and ¹³C NMR can be used for structural characterization of all lipids whereas ³¹P is useful for phospholipids including glycerophospholipids and phosphorylated sphingolipids such as SM. ¹H NMR was used following a perchloric acid extraction to determine the effects of indomethacin on phosphatidylcholine metabolism of breast cancer cell lines; quantifying the amplitudes of the shifts belonging to glycerophosphocholine, phosphocholine and choline [149]. ¹H and ¹³C NMR were used to identify, characterize and quantify lipids of normal kidney, malignant renal tumors and benign oncocytomas [150] and characterize colorectal cancer tumors [151]. Phosphorus containing metabolites of rabbit lens [152] and phospholipid profiles of colorectal cancer tumors [71] were identified and quantified utilizing ³¹P NMR. Since very complex mixtures can have thousands of peaks, two dimensional or three dimensional NMR is used for many lipidomic analyses. Standard methods for structural determination of PI, Chol and SM using ¹H NMR, Chol using ¹³C NMR and a mixture of phospholipids for profiling in solution using two dimensional ³¹P-¹H NMR have been described [148].

1.3.4.2 Drawbacks and Benefits of NMR

NMR is a non-destructive technique, unlike many other analysis methods which allows for further analysis by another technique [153]. It can be quantitative and ¹H NMR is beneficial for structural analysis of purified molecules [153]. NMR also has a large dynamic range of over 4 orders of magnitude on modern instruments [154]. There are several drawbacks to NMR including low sensitivity leading to the inability to analyze very small amount of samples. In complex mixtures, spectra are mostly dominated by PC and Chol, making identification of other lipids difficult. Peak broadening, which also occurs in aqueous solutions for ³¹P NMR, is an additional concern with NMR.

1.3.5 Mass Spectrometry (MS) Based Lipid Analysis

Mass spectrometry is an analysis technique in which spectra are acquired from ionized analytes that have been separated based on their mass to charge ratios and may provide the mass of an analyte of interest and/or structural information by characteristic fragment formation upon performance of tandem mass spectrometry (MS/MS) [155]. The use of mass spectrometry for lipid analysis ranges from use as a detector for fatty acids after separation to direct analysis without previous separation [156]. Various ionization methods can be used for many of these techniques including electron ionization (EI), matrix-assisted laser desorption/ionization (MALDI) and electrospray ionization (ESI)

[156]. EI is used to form radical ions from gas phase analytes and is typically coupled with GC. EI forms reproducible fragments which enable structural characterization, but may not include a molecular ion [M⁺] which may lead to difficulty in lipid identification. The development of soft ionization techniques such as MALDI and ESI has enabled the ionization of analytes that are not easily volatile in the gas phase, such as intact complex lipids. MALDI-MS is used for lipid detection after TLC separation as well as lipid mapping of tissues [155]. ESI-MS combines well with LC separation or can be used for direct injection of lipid extracts in the case of 'shotgun' analysis [155], which is the main focus of this dissertation.

1.3.5.1 Sample Introduction Methods for MS

MS has been used as a detector with many separation techniques such as TLC and capillary electrophoresis (CE), but most commonly with GC and LC. GC-MS has traditionally been used to investigate free fatty acids, sterols and fatty acid methyl esters (FAMES) [156] due to their abilities to readily go into the gas phase. GC-MS of other lipids, such as intact lipids, requires separation and additional sampling steps involving saponification or enzymatic digestion with Phospholipase C, and derivatization prior to GC separation [146]. Curstedt described a method for analysis of ether linked PC lipids which involved several separation steps by LC, enzymatic digestion, derivatization and hydrolysis in order to form the trimethylsilylethers suitable for GC-MS analysis [157]. Although

direct analysis of intact lipids is not feasible, analysis of FAMES and FAME derivatives using GC-MS gives important structural information. For example, double bond position of FAMES has been achieved by derivatization with pyrrolididine [158], 4,4-dimethyloxazoline [159] or dimethyl disulfide [160-165] prior to traditional higher energy EI (70eV) GC-MS or by use of lower energy EI (30eV) GC-MS [166].

LC-MS has proven to be a powerful tool for the analysis of highly complex lipid samples without the need for derivatization for detection. Several methods have been developed for use of MS as a detector for either RP-LC [114,142,167,168] or NP-LC [115,117,169], depending on the type of lipids of interest or the information desired. LC-MS/MS has been utilized for determining the structures of unknown lipids and the fatty acid compositions of the *sn*-1 and *sn*-2 positions of intact lipids [114]. Specific information for identification of lipids by characteristic headgroups or fatty acid fragments is found in sections 1.2.6.2.2 and 1.2.6.2.3. Although LC-MS is a more universal technique for lipidomic analysis, there are drawbacks including unresolved chromatographic peaks, lengthy analysis time and the need for many internal standards for quantitation and method development.

Direct infusion or "shotgun" lipidomics involves sample introduction to the mass spectrometer without prior separation by chromatography [170]. Current lipidomic analysis techniques by direct infusion MS or MS/MS rely on differential extraction/class specific extraction or, more commonly, characteristic fragmentation scans performed by the mass spectrometer using tandem mass

spectrometry (MS/MS) to separate isobaric lipid ions that may be present within the crude unresolved lipid mixture [171,172]. Analysis of lipids by characteristic fragmentation can be performed by inherent fragments, such as the phosphocholine headgroup of PC and SM ions, or by specific fragmentation due to lipid class specific derivatization [173,174]. These fragmentation techniques with and without derivatization will be discussed in future sections.

Regardless of the sample infusion method, the ability to differentiate individual ions in a mass spectrum depends heavily on the resolving power and mass accuracy (i.e. the difference between the observed m/z in the spectrum and the calculated theoretical mass, in Da or ppm) of the mass spectrometer utilized. Resolving power is defined as the m/z of a specific ion (M) divided by the resolution (Δm), where resolution (according to the % valley definition) is the m/z difference between ions that can be separated [175]. Ions are considered resolved according to the % valley method by having a 10-20% overlap in the valley between the two peaks. Many mass spectrometers, such as the quadrupole ion trap or triple quadrupole, have nominal mass resolution meaning that $\Delta m = 1$. If at m/z 400 $\Delta m = 1$, then the resolving power of the instrument at m/z 400 = 400. Resolution may also be defined using full width at half maximum (FWHM) of a peak, which may also be termed as ∆m, which will result in a resolution value that is double the value of that obtained by the % valley definition. For this reason, a qualifier stating the method by which resolution is defined must be used when reporting the resolving power of an instrument. Instruments with an Orbitrap, Ion Cyclotron Resonance (ICR) and some time-offlight (TOF) mass analyzers can have mass resolving power (FWHM) of over 100,000 at m/z 400 [176,177].

1.3.5.2 Tandem Mass Spectrometry (MS/MS)

1.3.5.2.1 Traditional Instrumentation and Methods of CID-MS/MS

Two types of collision induced dissociation (CID) MS/MS, tandem in time and tandem in space [178], are utilized in lipidomics for different purposes. Tandem in time MS/MS is performed in an ion trap, such as a linear ion trap. In this case, lipid ions are trapped by an applied RF potential in the presence of a bath gas such as Helium (He). Once trapped, a specific m/z is isolated and a supplemental RF potential is applied at the same frequency as the ion of interest. The ion collides with the He in the trap, the kinetic energy is converted to internal energy and the ion fragments. Since He is very small, many collisions must take place which results in fragmentation at the most labile position. Ion traps also have MSⁿ capabilities since fragments from MS/MS can also be trapped and subsequent fragmentation is possible [178]. This phenomenon is beneficial for identifying fragmentation mechanisms of lipids and is also very fast which is beneficial for use with LC [140].

Tandem in space MS/MS occurs when isolation and fragmentation are performed in different chambers of the mass spectrometer [178]. A common instrument used in lipidomics is the triple quadrupole as the RF and DC

potentials applied to the quadrupoles can be set to control ion transmission and monitor characteristic fragmentation patterns (see Figure 1.5) [178]. Triple quadrupoles can identify lipids by MS, but provide only nominal mass resolution performance; thus, every peak in the mass spectrum can consist of several lipid ions. For this reason, several types of CID-MS/MS are utilized for lipid analysis: product ion scans, precursor ion scans (PIS), neutral loss scans (NLS) and selected reaction monitoring (SRM) [156]. This enables lipids to be identified and/or categorized by headgroup, fatty acyl of interest, or other characteristic fragments, thereby separating complex mixtures and simplifying spectra for analysis of only the lipids intended. Unlike the ion trap, ions are not trapped and isolated prior to fragmentation. For this reason, the triple quadrupole utilizes a larger collision gas, Argon (Ar), which enables fragmentation to be achieved in the short amount of time that is required in order to travel through the second quadrupole [179].

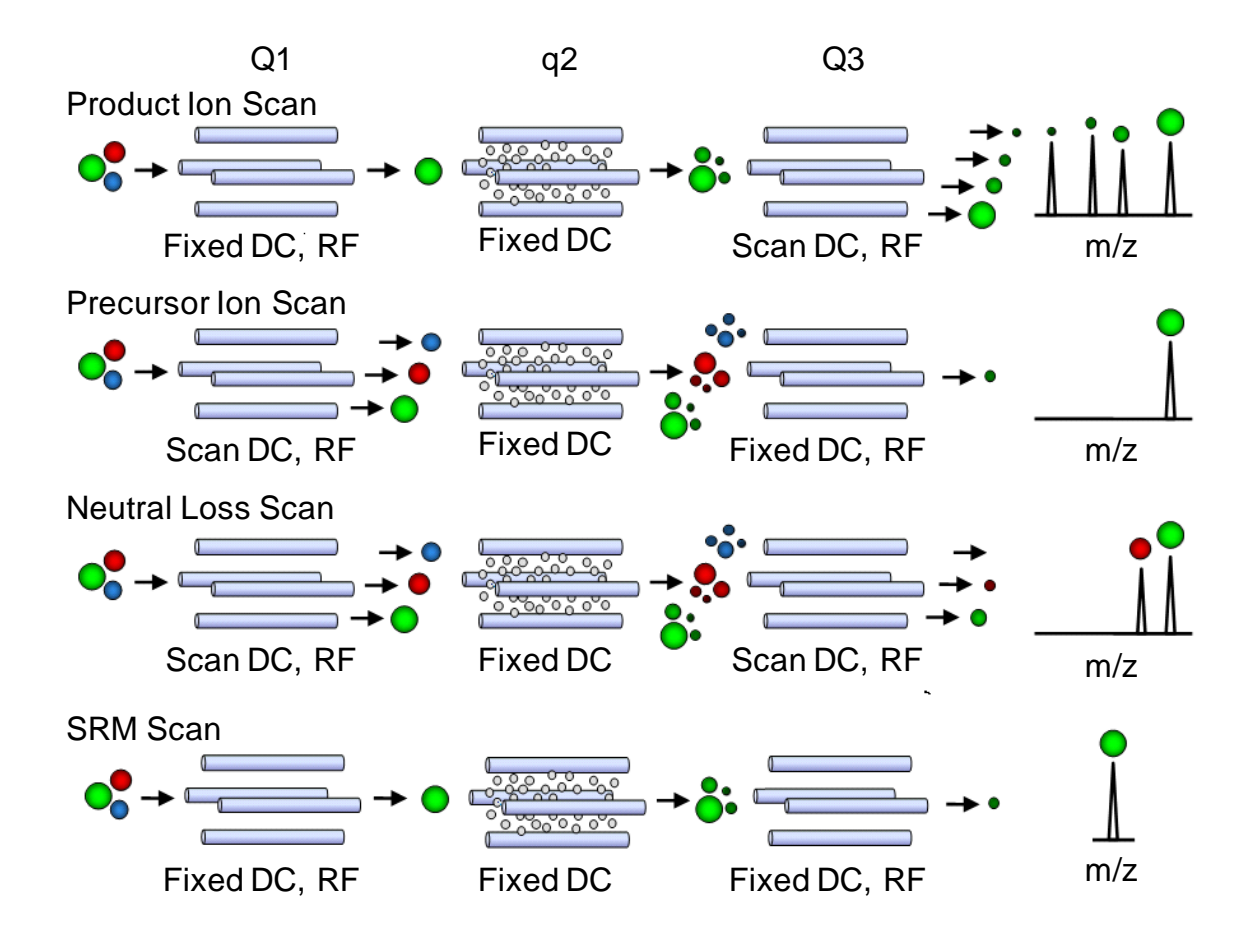


Figure 1.5 The four types of MS/MS scans utilized by a triple quadrupole mass spectrometer: product ion scan, precursor ion scan, neutral loss scan and SRM Scan.

Several methods have been developed for both types of MS/MS analysis using both HPLC and direct infusion, as well as other MS systems such as a quadrupole-time-of-flight (Q-TOF) [156]. The specific fragmentation patterns for each type of lipid are described in 1.2.6.2.2 and 1.2.6.2.3. Lipidomic analysis via characteristic MS/MS fragmentation has several benefits such as simplification of spectra (only lipid sub-classes with specific characteristics are shown) and ease of analysis. However, ion traps and triple quadrupole instruments have only

nominal mass resolution and cannot differentiate between ether-linked and odd numbered carbon chain lipids which may be present in complex mixtures.

1.3.5.2.2 Lipid Class Identification by Characteristic Head Group Fragmentation Behaviors upon CID-MS/MS

A common approach for using mass spectrometry to identify lipids is by taking advantage of characteristic fragmentation behavior [171]. The fragments formed depend not only on the polarity of the lipid ions but also the ionizing adduct (i.e. H⁺, Na⁺, HCO₂⁻, etc.) [173]. Characteristic fragmentation behavior enables lipid identification on instruments with nominal mass resolution, such as the triple quadrupole, without prior chromatographic separation [180].

PC can be readily protonated through electrospray ionization (ESI) due to the quaternary nitrogen atom of the choline headgroup. Protonated PC yields the characteristic fragment of phosphocholine (m/z 184.0739) upon performing CID-MS/MS [173,181-183]. Other common adducts for positive mode ionization of PC include Na⁺ and Li⁺. Sodiated PC yields a product ion at m/z 146.9823 [184] as well as an ion formed from the neutral loss of 205.0480 Da [184,185]. CID-MS/MS of lithiated PC ions give rise to the neutral losses of 183.0660 Da., 59.0735 Da. and 189.0812 Da., albeit at different efficiencies depending on whether they are diacyl, plasmenyl, plasmanyl or lyso species [174] (Table 1.2). lonization of PC in negative ion mode, however, must use negatively charged adducts, due to the quaternary nitrogen fixed positive charge which needs to be

neutralized. Several adducts for deprotonating PC have been investigated including chloride (Cl $^-$), iodide (l $^-$), fluoride (F $^-$), bromide (Br $^-$), acetate (CH₃CO₂ $^-$), formate (HCO₂ $^-$), methyl carbonate (CH₃OCO₂ $^-$) and several more [183,186].

Table 1.2 Summary of the characteristic fragments for PC lipid ions in positive and negative ionization mode with various common adducts.

Lipid Type	Precursor Ion	m/z or	Ion Formed
Lipid Type	FIECUISOI IOII	Neutral Loss	ion i onned
		(NL)	
	ΓN Λ . LJ1 ⁺	` '	
PC, O-PC,	[M+H] ⁺	m/z 184.0739	
P-PC, LPC			HO-P-O
			ÓН
PC, O-PC,	[M+Na] ⁺	m/z 146.9823	O Na ⁺
P-PC, LPC			ll l
			HO-P-O
			Ó
PC, O-PC,	[M+Na] ⁺	NL 205.0480	R_{1}
P-PC			R_1 O R_2
			~Õ+
PC, O-PC,	[M+Na] ⁺	NL 59.0735	0 + +
P-PC, LPC	[M+Li] ⁺		R ₁ O Na/Li
	[IVI+LI]		$R_{2} \downarrow O-P-O$
			0
			0
PC, O-PC,	[M+Na] ⁺	NL 183.0660	_ O√Na/Li ⁺
P-PC, LPC	[M+Li] ⁺		R ₁ ONa/Li
	[IVI+LI]		
			R_2
PC, O-PC,	[M+Li] ⁺	NL 189.0812	R_1 $O \longrightarrow R_2$
P-PC, LPC	[141.1 -1]		
			\ \ \ \ \ \ \ \ \ \ \ \ \ \ \ \ \ \ \
			Ú—′ 11

Table 1.2 (cont'd)

PC, O-PC,	[M+CI]	NL 49.9923	R_1 0
P-PC, LPC	[M+Br]	NL 93.9418	R_2 O-P-O N
	[M+I] ⁻	NL 141.9279	0
	[M+F] ⁻	NL 34.0219	
	[M+CH ₃ CO ₂]	NL 74.0368	
	[M+HCO ₂]	NL 60.0211	
PC, O-PC, P-PC, LPC	[M+CH ₃ OCO ₂]	NL 135.0895	R_1
			0-P-0
PC, O-PC, P-PC, LPC	[M+CH ₃ OCO ₂]	NL 161.1052	R ₁ O O
			R ₂ O-P-OH O-

PE can also be analyzed in both positive and negative ionization mode. In positive mode, the most common fragment for PE is the neutral loss of 141.0191 Da which is formed from either the protonated PE or sodiated PE precursor ions [173,181] (Table 1.3). This loss is observed as an efficient fragmentation pathway for diacyl and lyso PE lipids, but is not as efficient for plasmanyl or plasmenyl lipids [110,187]. Sodiated diacyl, lyso, plasmenyl and plasmanyl PE lipids also give rise to a neutral loss of 43.0422 Da and a product ion at m/z 164.0089 [110,184]. The neutral loss of 43 Da also results from the lithium adduct of PE [188]. In negative ionization mode, CID-MS/MS of deprotonated PE gives rise to a product ion at m/z 196.0375, albeit not at high abundance for the detection of low abundant species [110,185]. A neutral loss of 35.9767 Da is observed from the chloride adduct of PE in negative ionization mode CID-MS/MS which is much more efficient and therefore a better choice of analysis method if

one is choosing to use negative ionization mode to detect and quantitate PE lipids [182].

Table 1.3 Summary of the characteristic fragments for PE lipid ions in positive and negative ionization mode with various common adducts.

Lipid Type	Precursor Ion	m/z or Neutral Loss (NL)	Ion Formed
PE, O-PE, P-PE, LPE	[M+H] ⁺	NL 141.0191	R_1 R_2 R_1 R_2 R_2 R_2 R_2 R_2 R_2 R_2
PE, O-PE, P-PE, LPE	[M+Na] ⁺	m/z 164.0089	HO P O NH ₂
PE, O-PE, P-PE, LPE	[M+Na] ⁺ [M+Li] ⁺	NL 43.0422	R ₁ O Na/Li [†] R ₂ O-P-OH OH
PE, O-PE, P-PE, LPE	[M-H] ⁻	m/z 196.0375	O O O O O O O O O O
PE, O-PE, P-PE, LPE	[M+CI]¯	NL 35.9767	R ₁ O O O O NH

PS lipids, like PE and PC lipids, are characterized in both positive and negative ionization mode CID-MS/MS. In positive mode, a fragment formed from the neutral loss of 185.0089 Da can arise from either the [M+H]⁺ [189,190] or [M+Na]⁺ [180,182,190] (Table 1.4). The neutral loss of 190.0162 Da and product ion at m/z 191.0240 form from the lithiated precursor ion, [M+Li]⁺ [189]. In negative ion mode, the characteristic fragment formed from the deprotonated PS ion is the neutral loss of 87.0320 Da [180,189].

Table 1.4 Summary of the characteristic fragments for PS lipid ions in positive and negative ionization mode with various common adducts.

Lipid Type	Precursor Ion	m/z or Neutral Loss (NL)	Ion Formed
PS, O-PS, P-PS, LPS	[M+H] ⁺ [M+Na] ⁺	NL 185.0089 NL 185.0089	H [†] /Na [†] O
	[M+Li] ⁺	NL 190.0162	R_1 R_2
			R ₁ H ⁺ O R ₂ '
			R_2 O R_1
PS, O-PS, P-PS, LPS	[M+Li] ⁺	m/z 191.0241	O Li [†] HO-P-O NH ₂
			OH HOOO

Table 1.4 (Cont'd)

PS, O-PS, P-PS, LPS	[M-H] ⁻	NL 87.0320	R_1 O
,			R_2 O-P-OH

PI lipids can be identified in positive ionization mode by the neutral loss of 277.0563 Da from the [M+NH₄]⁺ ion and 282.0117 Da from the [M+Na]⁺ [190] and in negative ionization mode, the product ion at m/z 241.0113 from the [M-H] [185,191,192] (Table 1.5). A product ion at m/z 152.9953 also forms from the fragmentation of deprotonated PI in negative ionization mode CID-MS/MS [191]. Ammoniated PG ([M+NH4]⁺) forms an ion with a neutral loss of 189.0402 Da from positive ion mode CID-MS/MS [192] and a product ion at m/z 152.9953 in negative ionization mode from its [M-H] precursor [185,192,193] (Table 1.6). PA is identified in positive ionization mode from its [M+NH₄]⁺ ion via a neutral loss of 115.0034 Da [182] (Table 1.7). Like PG, PA forms a product ion from [M-H] at m/z 152.9953 in negative ionization mode [185,192,194]. Since ion at m/z 152.9953 is formed from PI, PG and PA, it is not an ideal choice for a characteristic ion for absolute identification of these lipids.

Table 1.5 Summary of the characteristic fragments for PI lipid ions in positive and negative ionization mode with various common adducts.

Lipid Type	Precursor Ion	m/z or	Ion Formed
Lipid Type	1 10001301 1011	Neutral Loss	ion i onned
		(NL)	
PI, O-PI,	[M+NH ₄] ⁺	NL 277.0563	⊔ ⁺
P-PI, LPI	[M+Na] ⁺	NL 282.0117	D 0
	[IVI+IVa]	112 202.0117	R_1
			R ₂
			$R_1 H^+$
			0,0
			O R ₂ '
			R_2 O
			$O R_1'$
PI, O-PI,	[M-H] ⁻	m/z 241.0113	O _I
P-PI, LPI			O P
			/ 6 \
			1.0
			HOOH
			HÓ ÒH
PI, O-PI,	[M-H] ⁻	m/z 152.9953	HO
P-PI, LPI			
			0 0

Table 1.6 Summary of the characteristic fragments for PG lipid ions in positive and negative ionization mode with various common adducts.

Lipid Type	Precursor Ion	m/z or Neutral Loss (NL)	Ion Formed
PG, O-PG, P-PG, LPG	[M+NH ₄] ⁺	NL 189.0402	R_1 R_2 R_1 R_2 R_1 R_2
			$ \begin{array}{c c} & O \\ & O \\ & R_2' \end{array} $ $ \begin{array}{c c} & R_2' \\ & R_2 \end{array} $
PG, O-PG, P-PG, LPG	[M-H]	m/z 152.9953	HO O O

Table 1.7 Summary of the characteristic fragments for PA lipid ions in positive and negative ionization mode with various common adducts.

Lipid Type	Precursor Ion	m/z or Neutral Loss (NL)	Ion Formed
PA, O-PA, P-PA, LPA	[M+NH ₄] ⁺	NL 115.0034	R ₁ R ₂
PA, O-PA, P-PA, LPA	[M-H] ⁻	m/z 152.9953	HO O O O

SM can be identified by some of the same fragments as PC including all PIS and NLS above for PC except NLS 205 and NLS 189 [182,184,195] (Table 1.8). SM and Cer can also be identified by the characteristic fragment of the sphingo-backbone which will be discussed in the next section.

Table 1.8 Summary of the characteristic fragments for SM lipid ions in positive and negative ionization mode with various common adducts.

Linid Type	Precursor Ion	m/z or	Ion Formad
Lipid Type	Precursor ion	Neutral Loss	Ion Formed
		(NL)	
SM	[M+H] ⁺	m/z 184.0739	0 /
	[IVI+FI]	, =	
			HO-P-O
014	+	/ 440,000	OH +
SM	[M+Na] ⁺	m/z 146.9823	Q Na [†]
			HO-P-Q
			o
SM	[M+Na] ⁺	NL 59.0735	OH Na/Li
	[M+Li] ⁺		I Na/Li
	[1411 = 1]		R ₁ ' O-P-O
			$\mid NH \rightarrow \mid$
			R_2
SM	[M+Na] ⁺	NL 183.0660	Na/Li
	[M+Li] ⁺		Han El OH
			R ₁ '
			N1
			R_2 NH
SM	[M+CI]	NL 49.9923	ОН О
	[M+Br]	NL 93.9418	
	[M+I]	NL 141.9279	R ₁ '
	[M+F]	NL 34.0219	R_2 NH O
	[M+CH ₃ CO ₂]	NL 74.0368	_
	[M+HCO ₂]	NL 60.0211	

Table 1.8 (Cont'd)

SM	[M+CH ₃ OCO ₂]	NL 135.0895	OH O-P-O NH O
SM	[M+CH ₃ OCO ₂]	NL 161.1052	OH OH O-P-OH R ₂ NH O

The ammonium adduct of cholesterol can be identified in MS mode, but upon fragmentation, has only a characteristic loss of water and ammonia [196] (Table 1.9). Cholesterol esters are identified by a common cholestane fragment at m/z 369.3521 [196,197] which, along with the m/z of the [M+NH₄]⁺ ion, enables full structural identification. All fatty acyl specific fragments will be discussed in the fatty acyl substituent identification section (1.2.6.2.3).

Table 1.9 Characteristic fragment for ammoniated Chol Ester in positive ionization mode.

Lipid Type	Precursor Ion	m/z or Neutral Loss (NL)	Ion Formed
Chol Ester	[M+NH ₄] ⁺	m/z 369.3521	+

1.3.5.2.3 Fatty Acyl Substituent Identification by CID-MS/MS

Many phospholipids are identified through neutral loss or precursor ion scans in positive ionization mode, but structural identification is much more difficult using positive ionization mode CID-MS/MS since the characteristic headgroup loss is highly abundant. For this reason, MS³ of the neutral loss fragment would be required for identification of the fatty acid substituents. PS in positive ionization mode has a neutral loss of 185 Da corresponding to the loss of phosphoserine (see 1.2.6.2.2). For example, CID-MS³ of the neutral loss fragment of PS lipids (NL 185.0089 Da) will generate fragments corresponding to the neutral loss of each fatty acid moiety as ketenes, thereby giving the information pertaining to each individual fatty acyl chain. This is also the case for diacyl PE, PA and PG [173]. However, these fragments are typically of low abundance and therefore of limited value for the characterization of these species in complex mixtures where the original [M + H]⁺, [M + Na]⁺ or [M + NH₄]⁺ ions are observed at low abundance compared to several other lipid classes. Conversely, the ion formed from protonated PC lipids is not abundant and therefore MS³ is not typically possible.

Plasmenyl PE lipids fragment efficiently in positive ionization mode giving fragments that correspond to the losses of both the acyl and the plasmenyl groups as ketenes with sufficient abundance for identification of even low abundant species [187]. For example, upon CID-MS/MS fragmentation, [PE_{(P-}

18:0/18:1) + H]⁺ (m/z 730.5745) yields three dominant peaks: m/z 589.5554, m/z 392.2929 and m/z 339.2899. These peaks correspond to the neutral loss of the phosphoethanolamine headgroup only, the neutral loss of the phosphoethanolamine headgroup and the plasmenyl group as a fatty alcohol, and a rearrangement product ion consisting of the plasmenyl group directly attached to the phosphoethanolamine headgroup, respectively [187]. The mechanism for dissociation of protonated plasmenyl PE will be discussed in chapter 2.

Ammoniated TG and DG lipids are identified through a neutral loss scan of their characteristic neutral loss of ammonia and a fatty acyl group [198-201]. This fragmentation yields an oxonium ion [202] in which the information on one of the fatty acyl moieties can be elucidated. Structural characterization can be achieved using a product ion scan and by identifying the neutral losses of individual fatty acyls from the $[M + NH_4]^+$ peaks. These scans will, in most circumstances, yield several peaks corresponding to oxonium ions of the neutral losses of all fatty acyls present in a mixture. For simple TG mixtures, the fatty acyls of the TG species in question is as simple as adding up the fatty acyls identified by neutral loss and ensuring they add up to the m/z in question. For example, a $[TG_{(52:1)} + NH_4]^+$ (m/z 878.8171) which yields ions at m/z 605.5510 (neutral loss of 273.2661 = 16:0 + NH₃), m/z 579.5354 (neutral loss of 299.2817 = 18:1 + NH₃) and m/z 577.5198 (neutral loss of 301.2973 = 18:0 + NH₃), would be identified as

TG(16:0_18:0_18:1) without specificity to *sn* position. In complex TG mixtures, several more possibilities of peaks may arise including those corresponding to 14:0, 14:1, 16:1, 20:0, 20:1, 22:0, 22:1, 24:0 and 24:1. Using only this information, 12 different TG identities may be found [199] if the assumption is made that all possible species will be present in any given mixture. However, if more certainty is needed, MS³ must be performed on these neutral loss peaks to reveal acylium ions of the other fatty acyl moieties to match up [200]. DG lipids, however, only require MS/MS for complete identification since there are only 2 fatty acids and therefore identification of one fatty acid provides the information of the second fatty acid [203].

For the analysis of Cer in positive ionization mode, Cer ions exist as either a protonated or lithiated adduct [204]. Protonated Cer first loses water by loss of the terminal hydroxyl group followed by formation of ions pertaining to the remaining sphingoid backbone prior to and after subsequent loss of an additional water molecule [205]. A d18:1 backbone forms ions at m/z 282.2797 and m/z 264.2691, respectively. Lithiated Cer will form the same doubly dehydrated backbone ion that protonated ceramide forms, but more readily forms a fragment consisting of the lithiated amide chain [206]. For Cer(d18:1/24:1), m/z 264.2691 for the sphingoid backbone and m/z 372.3887 for the lithiated fatty amide will form. Other than the major phosphocholine fragment, protonated SM forms a minor dehydrated sphingoid fragment following the neutral loss of the phosphocholine headgroup [207]. As with ceramide, a d18:1 sphingoid backbone forms the ion at m/z 264.2691. Lithiated SM(d18:1/16:0) forms the ion at m/z 264.2691 but also an

ion at m/z 280.2640 corresponding to the protonated fatty amide with a three positioned ring on the terminal nitrogen [195]. This fragmentation pattern holds true for sodiated and potassiated SM, forming the same fragment ions [195].

Fatty acid substituent identification of most glycerophospholipids is also achievable through fragmentation in negative ionization mode, in which all glycerophospholipids lose fatty acyls that form deprotonated carboxylate ions. This simplifies identification of the fatty acyl substituents as the individual fatty acyls will add up to equal the sum composition. For example, a [PE(34:1) - H] will have a total of 34 carbons and one double bond in the fatty acyl chains. If fragment ions at m/z 253.2167 ([FA(16:1) - H]), m/z 255.2324 ([FA(16:0) - H]), m/z 281.2180 ([FA(18:1) - H]) and m/z 283.2637 ([FA(18:0) - H]) are in the spectrum, the parent ion can be identified as a mixture of [PE(16:0 18:1)-H] and [PE(16:1 18:0)-H]. This method of identification does not give information about sn position of the fatty acids and is ambiguous in complex mixtures where many different lipids may be present at the same nominal m/z and will yield the same product ions. Moreover, fatty alcohols (alkyl and alkenyl linkages) do not form deprotonated fragments. In these cases, it is necessary to identify characteristic ions formed after the neutral loss of a sn-2 fatty acyl as the ketene or neutral acid. Negatively charged glycerophospholipids form ions from the neutral losses of fatty acyls as R'CH=C=O and R'COOH more readily at the sn-2 position aiding in molecular ion identification [173].

Acetate and formate adducts of PC more readily form ions from the loss of R2'CH=C=O ketene after the initial loss of methyl acetate or methyl formate. For example, for $[PC_{(16;1/18;1)} + B]$, a major product ion at m/z 478.2933, a smaller product ion at m/z 460.2828 corresponding to the neutral loss of the ketene and neutral fatty acid, respectively, and the deprotonated fatty acid ions at m/z 253.2167 and m/z 281.2180 are all observed [173,184]. [PC(O-16:1/18:1) + B] will form only ions at m/z 464.3141 (neutral loss of R2'CHCO), m/z 446.3035 (neutral loss of R2'COOH) and m/z 281.2180 ([FA(18:1) - H]) [208] (Scheme 1.1). However, $[PC_{(P-16:0/18:1)} + B]^{-}$, which has the same precursor ion mass as $[PC_{(O-16;1/18;1)} + B]$, will also form ions at m/z 464.3141 (neutral loss of R2'CHCO), m/z 446.3035 (neutral loss of R2'COOH) and m/z 281.2180 $([FA_{(18;1)}-H]^{T}[208]$ (Scheme 1.2). Differentiation of $[PC_{(O-16;1/18;1)} + B]^{T}$ and $[PC_{(P-16:0/18:1)} + B]^{-}$ requires MS³ on the ion at m/z 464.3141 which will form fragment ions at m/z 224.0688, m/z 168.0426 and lose neutral 135.9925 to form m/z 251.2739 if $[PC_{(P-16:0/18:1)} + B]$. If $[PC_{(Q-16:1/18:1)} + B]$ is present, ions at m/z 152.9953, 134.9847 and loss of neutral 138.0082 to form m/z 249.2582 will result.

Scheme 1.1 Adapted fragmentation mechanism for MS^3 analysis of $[PC_{(O-16:1/18:1)} - CH_3 - H]^{-}$ [208].

Scheme 1.2 Adapted fragmentation mechanism for MS³ analysis of [PC_(P-16:0/18:1) - CH₃ - H]⁻ [208].

Deprotonated diacyl PE also forms the neutral loss of R₂'CH=C=O more readily than R₂'COOH [184]. Plasmanyl PE and plasmenyl PE have similar fragmentation patterns as those seen in Scheme 1.1 [208]. Unfortunately, after the initial loss of methyl acetate or methyl formate of the PC ions, PC and PE fragments differ by 2 carbons. Therefore, there is some ambiguity in identifying the lipids solely by the neutral loss of the *sn-2* acyl chain and it is important to ensure the complimentary fatty acyl carboxylate is also present in the spectrum. For example, a negative ionization mode fragmentation of m/z 776.6 may include

 $[PC_{(32:1)} - HCO_2]^{-}$ and $[PE_{(39:6)} - H]^{-}$. A fragment at m/z 478.2933 would represent $[PC_{(16:1)} - CH_3 - H]^{-}$ and/or $[PE_{(18:1)} - H]^{-}$. The PC fatty acyl composition is identified as $PC_{(16:1/16:0)}$ if m/z 255.2324 for $[FA_{(16:0)} - H]^{-}$ is present and the PE fatty acyl composition is $PE_{(18:1/21:5)}$ if m/z 315.2324 for $[FA_{(21:5)} - H]^{-}$ is in the spectrum.

Deprotonated diacyl PS, PI, PG and PA also form ions corresponding to the neutral loss of R2'CH=C=O and R2'COOH, but unlike PE and PC, the neutral loss of R2'-COOH is the dominant fragment. PI, PG and PA form these ions directly whereas PS forms them after an initial loss of neutral serine, leaving a fragment identical to a deprotonated PA ion. This can cause some ambiguity with fatty acyl/alkyl/alkenyl identification similar to the PC and PE issue described above, but can be resolved by the presence of the complimentary fatty acyl. All neutral loss fragments formed by PS, PI, PG and PA are of odd nominal mass due to the lack of nitrogen, but, other than PS and PA described above, form unique neutral loss exact masses.

Sphingolipids, Cer and SM, may be structurally characterized in both positive and negative ionization modes [204]. Cer lipids are analyzed from either their deprotonated [209-211] acetate adducts [212] in negative ion mode. Deprotonated Cer first loses HCHO from the terminal hydroxyl end with a subsequent loss of the fatty acid group as a ketene [211]. For example, a d18:1 sphingosine base ceramide yields an ion at m/z 268.2640. In negative ionization

mode, the formate adduct of SM is characterized by the neutral loss methyl formate followed by the fatty chain [183]. For example, $[SM_{(d18:1/16:0)} + HCO_2]^T$ (parent mass at m/z 747.5652) yields an ion at m/z 449.3144 as the neutral loss methyl formate and the 16:0 fatty chain from which the rest of the structure can be deduced [183]. The same ions are formed from the acetate adduct following the neutral loss of methyl acetate and the fatty chain [212].

1.3.5.2.4 Derivatization Techniques for MS Based Lipid Identification

FAMES have been derivatized for analysis by GC-MS to improve their gas chromatographic properties and sensitivity, but derivatization has also been a powerful tool for individual lipid identification using ESI-MS. Derivatization of free fatty acids to form 3-acyl-oxymethyl-1-methylpyridinium iodide (AMMP) enhanced their sensitivity by 2500-fold in positive ionization mode over the deprotonated fatty acids in negative ionization mode [213]. Tris(2,4,6,trimethoxyphenyl)phosphonium acetic acid (TMPP-AA) was used to derivatize cholesterol to improve the ionization sensitivity as well as help identify other endogenous lipids in serum [214]. A quaternary ammonium ion of DG was formed using N-chlorobetainyl chloride by Li, et al. improving their intensities by over two-fold compared to their underivatized sodiated adducts [215]. PE and LPE have been derivatized using fluorenylmethoxylcarbonyl (Fmoc) chloride by Han, et al. to improve the ionization efficiency in negative ionization mode [216]. Cholesterol-3-sulfate was created from free cholesterol by Sandhoff, et. al. to improve the sensitivity of detection by MS/MS [217]. The use of derivatization reagents for quantitation will be discussed in section 1.2.6.4.

1.3.5.3 High Resolution MS (HRMS)

Until recently, the gold standard for lipidomic analysis was by either using LC-MS/MS or "shotgun" CID-MS/MS on triple quadrupole mass spectrometer platforms to monitor for the characteristic product ions or neutral losses for each lipid class. However, quantification is difficult and in complex lipid extracts, the possibilities of having nominal mass overlaps and the same characteristic fragmentation exists. For example, $[PC_{(33:1)} + H]^+$ and $[PC_{(O-34:1)} + H]^+$ both have a m/z of 746 and both yield a characteristic fragment for the phosphocholine headgroup at m/z 184. Differentiation of these two ions may be accomplished by fragmentation in negative ionization mode, but the two species can give some of the same nominal fragments if both are present. Ether lipids do not yield deprotonated fatty alcohol ions so require the presence of ions which have lost the fatty acyl as a neutral carboxylic acid. However, a diacyl lipid ion which has lost the even carbon chain may yield the same ion as the ether lipid which has lost the acyl chain (i.e. $[PE_{(33;1)} - FA_{(16;0)} - H]^{-} = m/z$ 464.2777, $[PE_{(O-34:1)} - FA_{(16:0)} - H]^{-} = m/z$ 464.3141). For mammalian systems, the assumption made by many researchers is that the peak would be the ether lipid since mammals do not synthesize odd chain fatty acids [218]. However, odd chain fatty acids may be present [219]. The presence of numerous relatively abundant odd carbon fatty acid-containing phospholipids have recently been reported using lipidomic analysis of macrophages and other human tissue and cell extracts [115]. High resolution mass spectrometers (mass resolving power of 100,000) have the ability to differentiate between these lipid ions and therefore can alleviate this issue.

1.3.5.3.1 Instrumentation for HRMS

High resolution/high mass accuracy mass spectrometers enable lipid analysis based on exact m/z value and not necessarily through MS/MS fragmentation. Quadrupole-Time of Flight (Q-TOF) instruments are useful for lipidomic analysis as they are capable of > 10,000 mass resolving power (Full Width at Half Max (FWHM)), <2 ppm mass accuracy and can perform rapid CID-MS/MS product ion scans [111,220]. Fourier Transform Ion Cyclotron Resonance (FT-ICR) and Orbitrap mass spectrometers are capable of over 100,000 mass resolving power (at FWHM) and high mass accuracy (< 2ppm) [101,143,176,221]. These instruments, whether used as mass analyzers following LC separation or direct infusion, can differentiate ether-linked lipids from odd numbered carbon chain lipids by their exact mass measurements for assignment at the sum composition level.

1.3.5.3.2 Differential Extraction for HRMS

No matter how high the mass resolving power of an instrument is, there are multiple exact mass overlaps of lipid ions that are possible for complex mixtures. One method that has been used to overcome this problem is using differential extraction to separate the apolar lipids from the polar lipids for analysis of a yeast lipidome [119]. First, apolar lipids are extracted with 17:1 CHCl3/MeOH which includes ergosterol, DG, TG, PC, LPC, PE, LPE, PG, and Cer. Then, polar lipids (PA, LPA, PS, LPS, PI, LPI, CL, long-chain base (IPC), phosphate (LCBP), inositolphosphoceramide mannosylinositolphosphoceramide (MIPC), and mannosyl-diinositolphosphoceramide (M(IP)₂C)) are extracted with 2:1 CHCl₃/MeOH. These fractions are run separately by direct infusion assuming all lipids contain only even chain species. The drawbacks are that this technique requires additional sample handling (additional extraction) and does not allow for odd chain lipid species to be differentiated from even chain species (i.e. $[PC_{(31:0)} + H]^{\dagger} = [PE_{(34:0)} + H]^{\dagger}$).

1.3.5.3.3 High Resolution MS/MS

High resolution mass spectrometers with CID-MS/MS capabilities enhance the unambiguous identification of lipids by having the ability to differentiate between species which produce fragments with the same nominal mass, but different exact masses. Even with high resolution, MS identification of sum composition identity, only nominal mass isolation for CID-MS/MS can be achieved. Thus, high resolution detection MS/MS is needed. This ability for identification of lipid fatty acid moieties has been demonstrated by Schuhmann, et al. using an Orbitrap mass analyzer to identify 221 molecular lipids in rat retina [222] as well as 331 and 222 molecular lipid species in bovine heart extract and human blood plasma, respectively, using polarity switching [223].

1.3.5.4 Lipid Quantification and Data Analysis

1.2.6.4.1 Internal Standard Methods

MS or MS/MS based quantitation of lipids can be achieved by the use of several exogenous internal standards which can be added before [185] or after [224] lipid extraction. Lipid ionization efficiency, ion transmission through the mass spectrometer and fragmentation efficiency for PIS and NLS can be affected by lipid type (i.e. phospholipid headgroup) which can limit the utility of internal standards for quantitative analysis. Typically, all lipids of a lipid sub-class are quantified by comparison of a single internal standard (e.g. all PE lipids are compared to PE_(28:0) internal standard). Unfortunately, ion transmission can also be affected by carbon length and degree of unsaturation. For these reasons, the use of several internal standards for each sub-class of interest would be needed for absolute lipid ion quantitation [225]. This may not be feasible with complex

lipid extracts as hundreds of exogenous lipid standards may not be commercially available.

1.3.5.4.2 Derivatization Strategies

Isotope encoded derivatization reagents have also been employed to enable the quantitation of lipids. These multiplexing techniques have been focused on identifying alterations in relative abundance among lipids in samples. Yang, et al. performed quantitative analysis of fatty acids by using 3-acyloxymethyl-1-methyl-d₃-pyrididinium iodide derivatized standard fatty acid solutions compared to serum fatty acids derivatized with 3-acyl-oxymethyl-1methyl-pyrididinium iodide [213]. Han et al previously described a method involving 9-fluorenylmethoxylcarbonyl chloride (Fmoc-Cl) derivatization of phosphoethanolamine-containing lipids (PE and lysoPE) in extracts from mouse retinas, to provide enhanced sensitivity for their identification and quantification in negative ion mode using MS and MS/MS [216]. Zemski Berry et al. reported a similar strategy, involving the use of isotopically labeled N-methylpiperazine acetic acid NHS ester [226,227] or 4-(dimethylamino)benzoic acid NHS ester [228,229] reagents for the comparative quantitative analysis of diacyl, ether, and plasmalogen PE lipids in a RAW 264.7 macrophage cell line. Sandhoff, et al. used sulfated ¹³C isotope encoded cholesterol standards to quantify free cholesterol from serum derivatized to cholesterol-sulfate [217]. Importantly, Han et al. also noted an additional significant benefit of derivatization, i.e., that PE species are shifted in mass from the region of the mass spectrum where they could potentially overlap in nominal mass with other lipid classes (e.g., phosphatidylinositol) [216], thereby facilitating quantification of both the derivatized and non-derivatized lipids.

1.3.5.4.3 Software for MS Lipid Data Analysis

With the extensive amount of data that can be acquired through MS and MS/MS lipidomic methods, it is necessary to have software that can process the data by peak identification and isotope correction. There are two different types of software with these functions: software utilizing either a predefined or in-silico generated library database. Fatty Acid Analysis Tool (FAAT) [230], LipID [231], LipidProfiler [224], LipidSearch [232], Lipid Mass Spectrum Analysis (LIMSA) [233] are examples of software that are based on predefined lipid library databases. However, lipid library databases are time consuming to set up as each lipid ion along with its various adducts/fragments must be added individually. However, once the databases are complete, these software tools can be beneficial to many different analysis strategies. In contrast, LipidXplorer [234,235] and Lipid Qualitative/Quantitative Analysis (LipidQA) [236] generate the lipid structures in-silico prior to data analysis. LipidXplorer identifies peaks based on a query language which is set up by the user and selected by lipid class for each analysis; queries are created with molecular ion and/or fragment information for identification. With even 100,000 resolution, "shoulders" of peaks

still exist which can be seen and corrected for in profile mode, but may be combined in centroid mode. LipidQA requires MS/MS spectra to be collected as it uses an in-silico generated library of MS/MS spectra and established fragmentation behaviors (as described in section 1.2.6.2) to identify lipids from the MS spectra. Many of these software analysis tools were established with a specific workflow/instrument in mind and therefore require some modification to language or code for utilization with other lipidome profiling methods.

Chapter 2

Development of a Sequential Derivatization Strategy for High Resolution MS

Based Comprehensive Lipidome Analysis

2.1 Introduction

Mass spectrometry is an excellent choice for comprehensive lipidome analysis because of its capabilities for rapid and sensitive monitoring of the molecular compositions and abundances of individual lipid species in complex lipid extracts obtained from limited quantities of sample tissue, with only minimal need for sample preparation, as well as the potential for structural characterization of individual lipid species using tandem mass spectrometry (MS/MS) methods [155,171,172]. However, there are several caveats associated with the use of MS methods for lipidome analysis. First and foremost is the structural diversity and complexity of the lipid mixtures that can result from extraction of a given cell or tissue. Adding to the diversity of the lipid classes and sub-classes discussed in Chapter 1, fatty acyl chains typically linked to the *sn*-1 position may alternatively be substituted with an ether linkage; a plasmenyl vinyl-

Part of the results described in Chapter Two were published in:

Fhaner, C. J., Liu, S., Ji, H., Simpson, R. J., Reid, G.E., Comprehensive lipidome profiling of isogenic primary and metastatic colon adenocarcinoma cell lines. *Anal. Chem.* **2012**, *84*, 8917-8926.

Fhaner, C. J., Liu, S., Zhou, X., Reid, G. E., Functional group selective derivatization and gas-phase fragmentation reactions of plasmalogen glycerophospholipids. *Mass Spectrom.* **2013**, *2*, S0015.

ether (i.e., -O-alk-1'-enyl or plasmalogen) bond, or a plasmanyl alkyl-ether (i.e., 1-O-alkyl) bond. Also, hydrolysis of the acyl chain from the sn-2 position results in the formation of a lysophospholipid species. Individual lipid ions containing different head group and acyl chain compositions, but with the same nominal mass values (e.g., phosphatidylserine (PS) [PS_(16:1/22:6) + H]⁺ and [PC_(16:0/22:6) + H]⁺, Δm = 0.0727), can typically not be identified on the basis of their m/z values alone when using mass analyzers with only unit mass resolving power (e.g., ion traps or triple quadrupoles). Furthermore, other lipids belonging to different subclasses, but with isomeric molecular structures, can yield ions with the same exact m/z, and therefore cannot be distinguished from one other even when using high resolution/accurate mass instrumentation. For example, plasmanyl-ether lipids containing one additional site of unsaturation compared to plasmenyl-ether containing lipids, with the same head group (e.g., [PC(P-36:0) + $H_{1}^{+} = [PC_{(O-36:1)} + H_{1}^{+})$, are observed at the same exact m/z in positive ionization mode. Additionally, isomeric lipid species with the same head group, but differing in their individual sn-1 and sn-2 acyl chain compositions (e.g., $PC_{(16:0/22:5)}$ and $PC_{(18:1/20:4)}$), will all be present at the same exact m/z value. Also, certain lipids that have different *molecular* elemental compositions may actually yield ions with the same ionic elemental compositions (i.e., the same exact m/z), depending on the ionic adduct that is formed upon electrospray ionization (ESI) MS. For example, during positive ion mode ESI-MS in the presence of ammonium salts, phosphatidic acid (PA), phosphatidylglycerol (PG)

and phosphatidylinositol (PI) lipid ions are observed as ammonium adducts whereas PC, PE and PS lipids are observed as protonated ions. Under these conditions, PA lipids containing 2 additional carbons and 1 double bond in their acyl chains can yield ions with the same exact m/z as a protonated PE lipid. Similarly, PG lipids containing the same number of carbons and 2 additional double bonds will have the same m/z as a protonated PS lipid (e.g., [PA(36:2) + $NH_4]^+ = PE_{(34:1)} + H]^+$ and $[PG_{(34:3)} + NH_4]^+ = PS_{(34:1)} + H]^+$). The protonated ions of certain lipid species containing an even number of carbons in their acyl chains can overlap at the same exact m/z with lipids containing an odd number of carbons in their acyl chains but with different head groups (e.g., $[PC_{(33:2)}+H]^+$ = $[PE_{(36:2)}+H]^{+} = [PA_{(38:3)}+NH_{4}]^{+}$). Finally, low abundance lipid species that are present at or below the level of chemical noise present within a mass spectrum are typically not identified by MS measurements alone, particularly when using low resolution instruments.

Traditionally, to overcome these issues when using direct infusion 'shotgun' MS approaches [155], identification, structural characterization and quantitative analysis of the individual members of a given lipid class that may be present within a complex unfractionated lipid mixture has been accomplished by using a series of neutral loss and precursor ion MS/MS scans in triple quadrupole mass spectrometers [182,237], or by using product ion MS/MS scans in an 'ion mapping' mode in high resolution quadrupole time-of-flight mass spectrometers [111,220], based on the characteristic fragmentation behavior of their individual

headgroup or acyl chain substituents. Although such methods are well established and widely used, the throughput of these approaches can be limited, as individual scans are required for the analysis of each different lipid class (for the triple quad approach) or precursor ion m/z value (for the quadrupole time-of-flight approach). For example, for the glycerophospholipids, each of the 7 different head groups have their own characteristic fragmentation patterns and require separate neutral loss and precursor ion MS/MS scans for their identification and quantification [182,237]. Also, for other lipid classes or subclasses, such as glycerolipids and some sphingolipids, additional sample preparation steps are commonly required to remove other potentially interfering lipids prior to MS/MS analysis [117,182].

Liquid chromatography (LC) [167,169] may be employed for the separation of lipids prior to MS and/or MS/MS [114] analysis, resulting in less complex spectra and potentially enabling the separation of individual lipids with the same nominal or exact m/z values. However, the analysis times associated with these approaches can be relatively slow, and the quantitation of individual lipids can be compromised in complex mixtures due to excessive tailing [238] or overlap of peaks in the chromatogram [185].

The recent development of ultra-high resolution/accurate mass analyzers based on FT-ICR or Orbitrap platforms has opened the door to the possibility of employing high-throughput direct infusion 'shotgun' mass spectrometry for the simultaneous analysis of multiple lipid classes without prior separation, and with a reduced need for extensive MS/MS analysis [119,208,222,223,239]. Ultra-high

resolution (≥100,000) readily provides the ability to separate lipid ions with the same nominal m/z values, with substantially improved signal-to-noise and dynamic range compared to lower resolution instruments for the detection of low abundance lipid species that may be present within a complex crude lipid extract. Unfortunately, the differentiation of isobaric mass lipid ions remains an issue. One approach that has been employed to overcome the exact mass overlap problem has been to perform multistep lipid extractions to separate apolar lipids (including PE and PG) from polar lipids (including PA and PS) [119]. However, these methods require additional extraction steps which could result in increased experimental error for subsequent quantitative analysis. Performing MS analysis in negative ion mode can be used to eliminate the possibility of m/z overlap for certain lipids; however, the ionization efficiency of many lipid classes in negative ionization mode can be much lower than in positive ionization mode, unless different solvent systems are used for positive and negative ion modes [119], thereby limiting the ability to identify lipids present at trace abundances using this method alone. Furthermore, similar to that described above for positive ionization mode MS analysis, some lipids that have different molecular elemental compositions can also yield ions with the same m/z in negative ionization mode, depending on the ionic adduct that is formed. For example, the acetate adducts of PC lipid ions can overlap in exact m/z with deprotonated PS lipids containing four additional acyl chain carbons and one less double bond (e.g., PC(32:2) + $C_2H_3O_2$ = [PS_(36:1) - H], while formate adducts of PC lipids can overlap with deprotonated PS lipids containing 3 additional acyl chain carbons and one less

double bond (e.g., $[PC_{(32:2)} + CHO_2]^- = [PS_{(35:1)} - H]^-)$. Finally, while differentiation of isobaric mass plasmenyl- and plasmanyl-ether containing glycerophospholipid species can be achieved by the use of CID-MS³ methods [208], the practical application of this approach is limited for the analysis of very low abundant species that may be present in complex extracts. Thus, further development is required in order for ultra-high resolution/accurate mass spectrometry methods to become more generally applicable for use in quantitative lipidome profiling.

In this chapter, a 'shotgun' lipidomics strategy consisting of sequential functional group selective chemical modification reactions coupled with high-resolution / accurate mass spectrometry and 'targeted' tandem mass spectrometry (MS/MS) analysis is developed and applied to the complex, crude lipid extract of the primary colorectal cancer cell line, SW480. Selective chemical derivatization of glycerophosphoethanolamine and glycerophosphoserine lipids using a 'fixed charge' sulfonium ion containing and isotopically labeled (either d₆-or ¹³C₁-), S,S'-dimethylthiobutanoylhydroxysuccinimide ester (DMBNHS) reagent was used to eliminate the possibility of isobaric mass overlap of these species with the precursor ions of all other lipids in the crude extract thereby enabling their unambiguous assignment. Further subsequent selective mild acid hydrolysis using formic acid, or derivatization with iodine and methanol, of plasmenyl containing lipids enabled these species to be readily differentiated from isobaric mass plasmanyl containing lipids. Additionally, the positive

ionization mode tandem mass spectrometry fragmentation behavior of the iodine/methanol derivatized plasmenyl ether containing glycerophosphocholine and glycerophosphoethanolamine lipids are shown yield abundant characteristic product ions that directly enable the assignment of their molecular lipid identities.

2.2 Selective Derivatization of Aminophospholipids with d $_6$ -S,S'-Dimethylthiobutanoylhydroxysuccinimide Ester (d $_6$ -DMBNHS) and $^{13}\mathrm{C}_1$ -DMBNHS

Derivatization of aminophospholipids was achieved by use of d₆ and ¹³C₁ isotopically labeled and N-hydroxysuccinimide containing ester, S,S'-dimethylthiobutanoylhydroxysuccinimide ester (DMBNHS) [240]. Although this reagent was originally synthesized for use in analysis of peptides, it is useful in the derivatization of aminophospholipids as well since both aminophospholipid sub-classes (PE and PS) have isobaric overlaps with other sub-classes (PC/PA and PG, respectively).

2.2.1 Characterization of the Reactivity and Specificity of Aminophospholipids with DMBNHS

An SW480 cell extract was used to monitor the reactivity and specificity of the derivatization of primary amine functional group containing

lipids, PE and PS. The cells were extracted using a modified Folch [108,110] method (See Chapter 5) and spiked with $PC_{(14:0/14:0)}$, $PE_{(14:0/14:0)}$ and $PS_{(14:0/14:0)}$ internal standards. Samples were derivatized using concentrations of d₆-DMBNHS of 0M, 0.5M, 0.25M, 0.125M, 0.0625M, 0.05M and 0.025M in CHCl₃ with 1.1x TEA and reaction times of 5, 10, 20, 30 and 60 minutes (data not shown). A concentration of 0.125M for 30 min. was chosen as the best reaction conditions for derivatization.

Figures 2.1A and 2.1B show the high resolution mass spectra acquired from the crude SW480 lipid extracts prior to and following derivatization with d₆-DMBNHS, respectively, in m/z ranges 744-751. It can be seen that several ions have either disappeared or are reduced in abundance in figure 2.1B compared to the underivatized spectrum (Figure 2.1A), indicative of the presence of PE and PS lipids. For example, m/z 744.5545 in Figure 2.1A, that could potentially contain both $[PE_{(36:2)}+H]^+$ and $[PA_{(38:3)}+NH_4]^+$ lipids, is not present in Figure 2.1C, and therefore can be assigned exclusively as containing [PE(36:2)+H]+. Similarly, m/z 748.5279, m/z 748.5487 and m/z 750.5433 can assigned as exclusively containing $[PE_{(P-38:6)}]$ and/or $PE_{(O-38:7)}+H]^+$, $[PS_{(P-34:0)}]$ and/or $PS_{(O-34:1)}+H]^+$ and $[PE_{(P-38:5)}$ and/or $PE_{(O-38:6)}+H]^+$ lipids, respectively. In contrast, the ion at m/z 746.5707 in Figure 2.1A was observed to decrease in relative abundance but not disappear upon derivatization of the crude lipid extract, indicating the presence of both $[PE_{(36:1)}+H]^+$ and $[PA_{(38:2)}+NH_4]^+$ lipid

species at this m/z. The ratio of the ion abundances observed before and after derivatization can be used to obtain some qualitative measure of the relative abundance of the two species at this m/z (i.e., approx. 30% [PE(36:1)+H]+ and 70% [PA_(38:2)+NH₄]⁺, assuming similar ionization efficiencies). Other ions in the spectrum, corresponding to non-derivatized lipids, were observed to undergo a uniform decrease in absolute abundance after the d₆-DMNBHS derivatization reaction, presumably due to the presence of the excess derivatization reagent causing some ionization suppression in the sample. However, the relative abundance of these lipids compared to the internal standard PC(14:0/14:0) lipid were not altered between the derivatized and non-derivatized samples, indicating that the ability to perform relative quantitative analysis based on the observed % total ion abundances would not be impaired. Using this reagent, the ability to separate PE lipid ions from PC and PA lipid ions and the ability to separate PS lipid ions from PG lipid ions is successfully achieved.

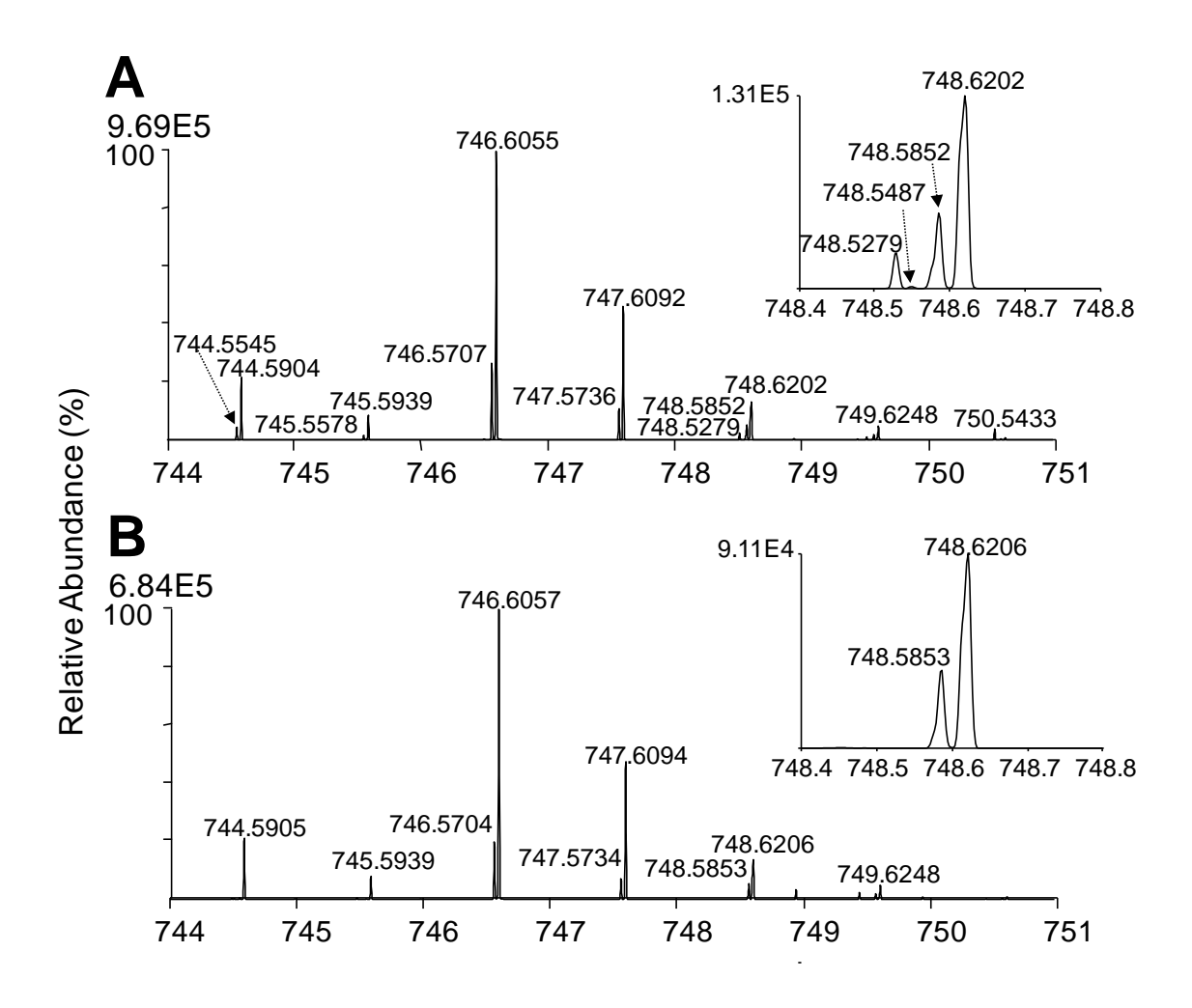


Figure 2.1 Positive ion mode ESI high-resolution mass spectrometric analysis of a crude lipid extract from the SW480 human adenocarcinoma cell line. Expanded regions (m/z 744-751) of the ESI-mass spectrum obtained from the (A) underivatized crude lipid extract and (B) reaction with the amine-specific derivatization reagent, d_6 -DMBNHS. The insets to each panel show an expanded region of the spectrum from m/z 748.4-748.8.

To account for the individual contributions of the potentially overlapping even chain length $[PA + NH_4]^+$ ions and odd chain length $[PC + H]^+$ ions at a given m/z value in the positive ion mode MS spectra, the lipid extracts were also analyzed in negative ionization mode (data not shown). No overlap of PA lipids with other lipid species occurs in negative ion mode, and similar sensitivity was

obtained for the deprotonated PA lipids compared to the positive ion mode ammoniated PA adducts (determined here by comparing the ion abundances of a series of PA lipid standards analyzed in both negative and positive ion modes: data not shown). Thus, assignment of the PA lipids in this study was performed using the negative ion mode data. Importantly, using the experimental conditions described in Chapter 5, the precursor ion abundances for all the other lipid classes and subclasses reported in this study were determined to be greater in positive ion mode, so assignment of these species was performed using the positive ion mode data. The contribution of the PA lipids to the positive ion mode odd chain PC lipid ion abundances were then subtracted after applying a correction factor determined by measuring the ratio of ion abundances for the series of PA lipid standards measured in both positive and negative ion modes. After performing this correction, with the exception of four cases in which both even-numbered chain length PA and odd-numbered chain length PC ions were found to be present (and when overlap was possible), only the odd-numbered chain length PC lipids were observed. For example, m/z 748.5853 in Figure 2.1B, could be exclusively assigned as containing $[PC_{(33:0)}+H]^+$ rather than [PA_(38:1)+NH₄]⁺.

Figures 2.2A and 2.2B show expanded regions from m/z 880-887 which correspond to the m/z regions in which the PE and PS lipids from Figure 2.1A and 2.1B are relocated, respectively, after the d_6 -DMBNHS derivatization reaction. This region of the mass spectrum is also occupied by ions corresponding to the ammonium ion adducts of PI and TG containing lipids (e.g.,

 $[PI_{(36:2)}+NH_4]^+$ and $[PI_{(36:1)}+NH_4]^+$ at m/z 880.5909 and 882.6065, respectively, and $[TG_{(52:0)}+NH_4]^+$ at m/z 880.8326), but there is no mass overlap with the PE and PS species that appear upon derivatization (e.g., $PE_{(36:2)}$ at m/z 880.6366, $PE_{(36:1)}$ at m/z 882.6520, $PE_{(P-38:6)}$ and/or $PE_{(O-38:7)}$ at m/z 884.6104, $PE_{(P-38:5)}$ and/or $PE_{(O-38:6)}$ at m/z 886.6257, and $PS_{(P-34:0)}$ and/or $PS_{(O-34:1)}$ at m/z 884.6316).

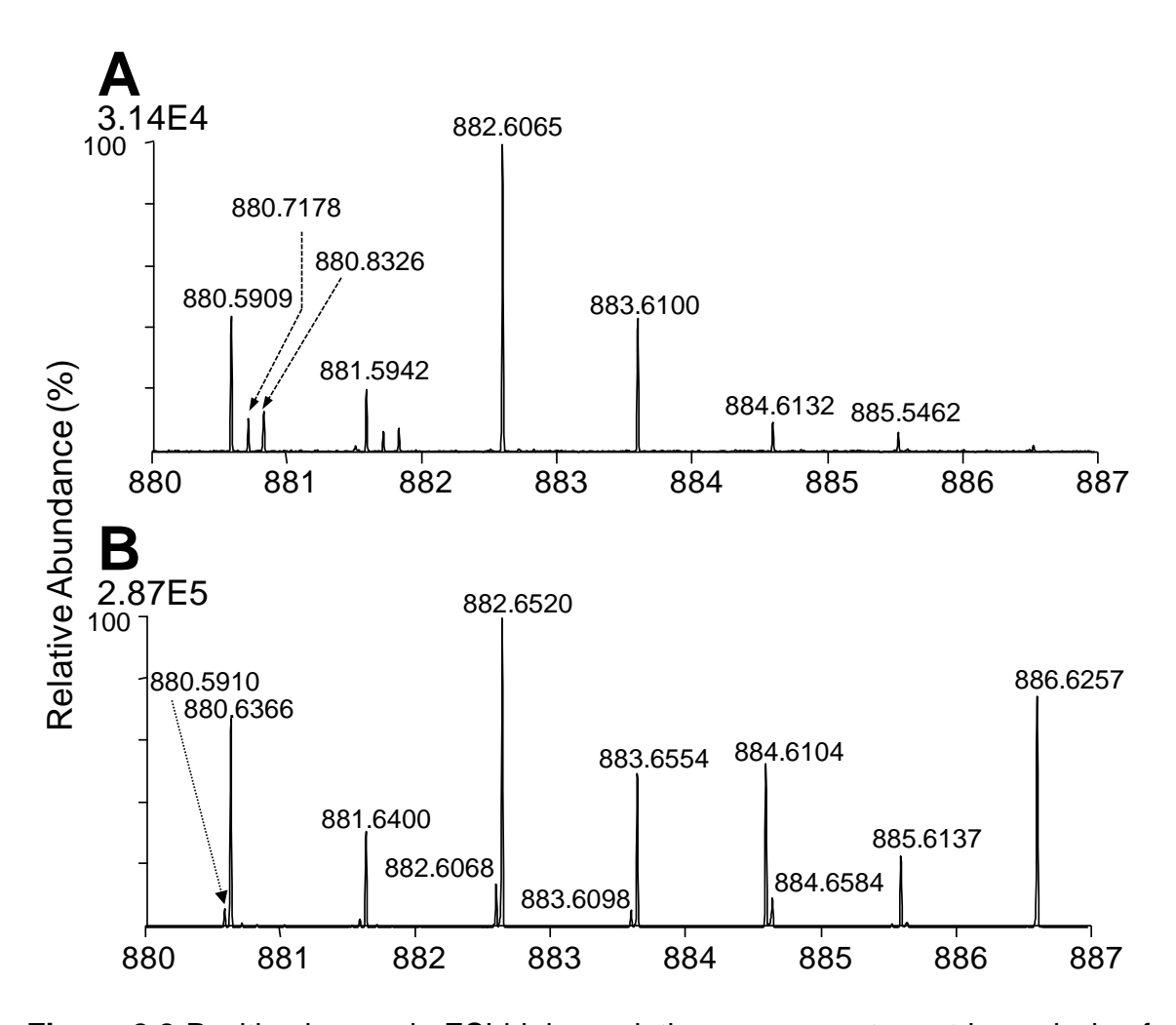


Figure 2.2 Positive ion mode ESI high-resolution mass spectrometric analysis of a crude lipid extract from the SW480 human adenocarcinoma cell line. Expanded regions (m/z 800-887) of the ESI-mass spectrum obtained from the (A)

Figure 2.2 (Cont'd) underivatized crude lipid extract and (B) reaction with the amine-specific derivatization reagent, d₆-DMBNHS.

2.2.2 Sensitivity Enhancement of DMBNHS Derivatized Aminophospholipids

Along with the ability to resolve the PE lipids from PC and PA, and PS lipids from PG, derivatization with the d₆-DMBNHS reagent also provides an additional benefit of significantly increasing the PE and PS lipid ionization efficiencies, thereby enhancing the dynamic range for their detection and quantification. For example, the PE lipid ion at m/z 750.5433 in Figure 2.1A, which contains either $[PE_{(P-38:5)} + H]^{+}$ or $[PE_{(O-38:6)} + H]^{+}$, had an intensity of 3.48E4, whereas its d₆-DMBNHS derivatized ion at m/z 886.6257 in Figure 2-1B was observed with an intensity of 2.13E5. Similarly, the PS lipid at m/z 748.5487, either $[PS_{(P-34:0)} + H]^+$ or $[PS_{(O-34:1)} + H]^+$, had an intensity of 1.26E3 in the underivatized spectrum in Figure 2.1A, (note that this ion is present at a relative abundance of only 0.05% compared to the most abundant ion in Figure 2.1A), but yielded a derivatized ion at m/z 884.6316 in Figure 2.2B with an intensity of 2.99E3. Overall, the average fold change increase in intensity after derivatization was found to be 6.08 ± 0.39 for the PE lipids and 3.31 ± 0.37 for the PS lipids. These results are similar to those previously reported using other methods for aminophospholipid derivatization [216,226-229], as well as to those recently reported from the use of the DMBNHS reagent to enhance the ionization sensitivity of derivatized phosphopeptides subjected to RP-HPLC-ESI-MS [241]. Notably, the increase in ion intensity observed here allows numerous PE and PS lipids to be identified from the d_6 -DMBNHS derivatized spectrum, that otherwise would be too low in abundance to assign from the underivatized spectrum.

2.3 Derivatization and Selective Differentiation of Ether Lipids

The most common types of phospholipids and glycerolipids have fatty acids linked by an ester bond to the glycerol moiety. Ether bonds are also observed and can either be in the form of an alkyl ether (plasmanyl or O-) or a vinyl ether (plasmenyl or P-) (see Figure 1.1). In this case, unsaturation sites further down the chain make isobaric overlaps between plasmanyl and plasmenyl lipids possible (i.e. PE(P-34:0) = PE(O-34:1)).

2.3.1 Identification of Plasmalogen Lipids by Acid Hydrolysis

The d₆-DMNBHS derivatization reaction allowed the PE and PS ions to be effectively resolved from PC and/or PA and PG lipids at the same m/z, respectively, thereby allowing their separate identification and quantification. However, the differentiation of isobaric mass unsaturated plasmanly-ether lipids from plasmenyl-ether containing lipids could not be achieved using this strategy alone. Murphy *et al.* previously demonstrated that plasmenyl lipids can be selectively acid hydrolyzed by performing lipid extraction in a 0.2N HCl solution [187,242]. However, this technique requires an additional liquid-liquid extraction

step prior to analysis, which may result in increased sample loss or increased variance for subsequent quantitative analysis.

In contrast, it was determined here that 80% formic acid can also be used to selectively and completely hydrolyze plasmenyl-ether containing lipids, without degradation of diacyl or plasmanyl-ether lipid containing species, and without a requirement for an additional extraction step prior to analysis. For example, expanded regions of the mass spectrum obtained following mild formic acid hydrolysis of crude lipid extract from the SW480 cell line are shown in Figures 2.3A and 2.3B. The ion at m/z 746.6055 in Figure 2.1A, potentially containing $[PC_{(O-34:1)}+H]^{+}$ and/or $[PC_{(P-34:0)}+H]^{+}$ lipids, underwent essentially no change in abundance after formic acid treatment in Figure 2.3A, and therefore can be assigned as exclusively containing the $[PC_{(O-34:1)}+H]^+$ plasmanyl-ether lipid species. In contrast, m/z 744.5904, whose accurate mass indicated the presence of $[PC_{(O-34:2)}+H]^{+}$ and/or $[PC_{(P-34:1)}+H]^{+}$ lipids, decreased in abundance by approximately 50%, indicating that this ion contains both plasmanyl- and plasmenyl-ether PC lipid species. In figure 2.3B, ions containing the diacyl PI and triacyl TG lipids remain at roughly the same abundances present in Figure 2.2A, as expected.

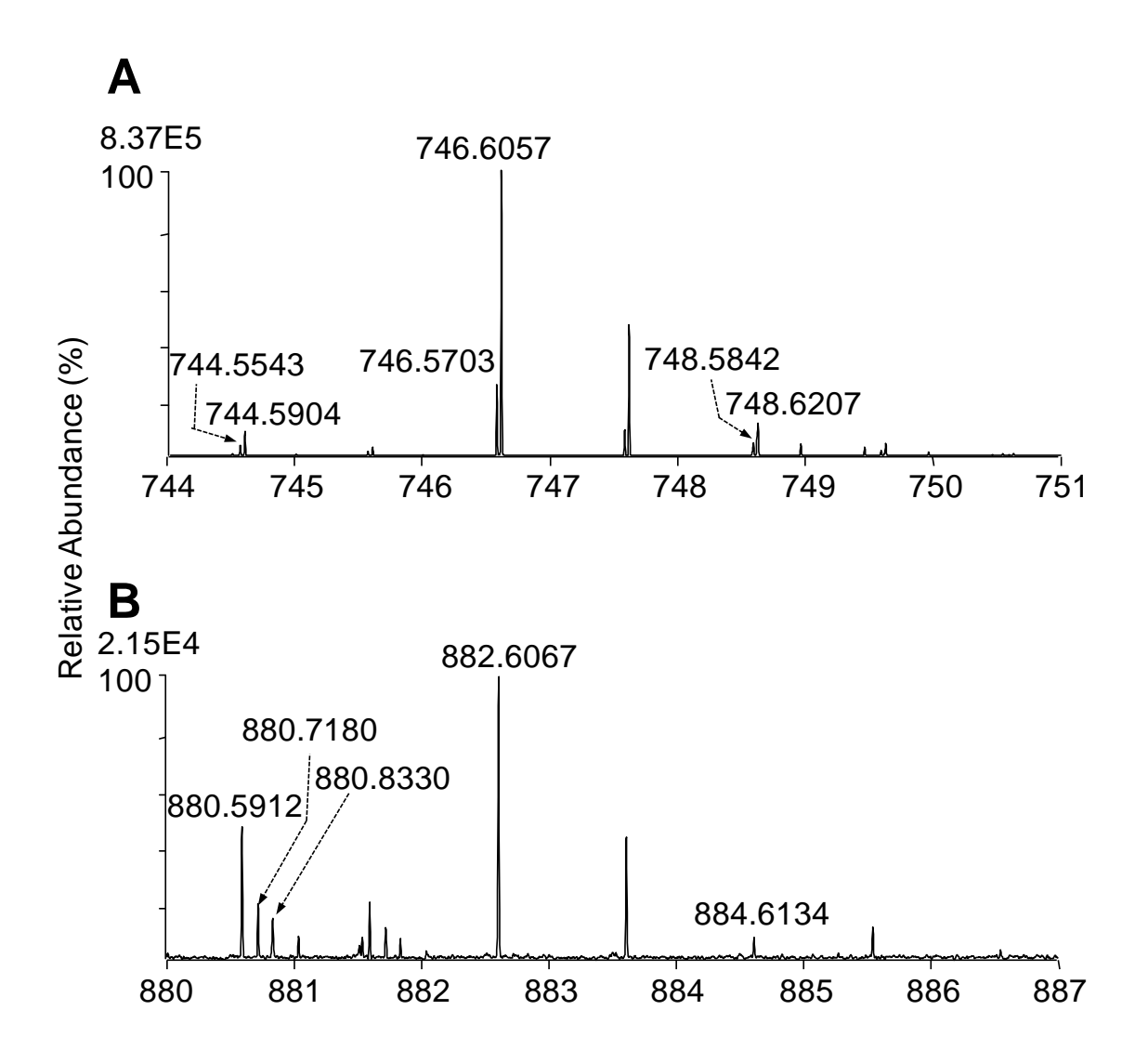


Figure 2.3 Positive ion mode ESI high-resolution mass spectrometric analysis of a crude lipid extract from the SW480 human adenocarcinoma cell line following mild formic acid hydrolysis. (A) Expanded region (m/z 744-751) of the ESI-mass spectrum and (B) expanded region (m/z 880-887) of the ESI-mass spectrum.

2.3.2 Identification of Plasmalogen Lipids via Derivatization with Iodine and Methanol

Although it is possible to differentiate between plasmanyl and plasmenyl lipids by comparing the acid hydrolyzed samples to the non-hydrolyzed samples,

this requires the collection of separate spectra and more time for data analysis. Also, quantitation is difficult. In 1946, Siggia and Edsberg described a simple method for labeling vinyl alkyl ether bonds with iodine and methanol, with quantification by titration [243]. The method was later adapted for the quantification of plasmenyl ether lipids by back titration [244] and, later, potentiometry [245]. This method, as described in Chapter 5, was adapted here for the analysis of plasmenyl lipid by MS and MS/MS by buffering the reaction with ammonium bicarbonate (NH₄HCO₃). Adjusting the solvent and iodine concentration and performing the reaction at 0°C prevents acid hydrolysis by the formation of HI during the reaction and ensures the reaction is specific to the vinyl ether bond of the plasmenyl lipids. An overall scheme for this reaction is shown in Scheme 2.1.

Scheme 2.1 Reaction of plasmenyl phospholipids with iodine and methanol.

To demonstrate the selectivity and completeness of the iodine and methanol reaction conditions described above for the derivatization of plasmenyl ether lipids, the positive ion mode high-resolution mass spectra acquired from a mixture of synthetic lipid standards ($PE_{(18:0/22:6)}$, m/z 792.5494, $PC_{(18:1/18:1)}$, m/z 786.5963, $PC_{(18:2/18:2)}$, m/z 782.5652, $TG_{(14:0/16:1/14:0)}$, m/z 766.6880,

TG_(16:0/16:0/18:1), m/z 850.7812, TG_(18:1/16:0/18:1), m/z 876.7966 and TG_(18:0/18:0/18:1), m/z 906.8432), including two plasmenyl ether glycerophospholipids (PE_(P-18:0/22:6), m/z 776.5551 and PC_(P-18:0/22:6), m/z 818.6014), before and after reaction with iodine/CH₃OH, are shown in Figures 2.4A and 2.4B, respectively.

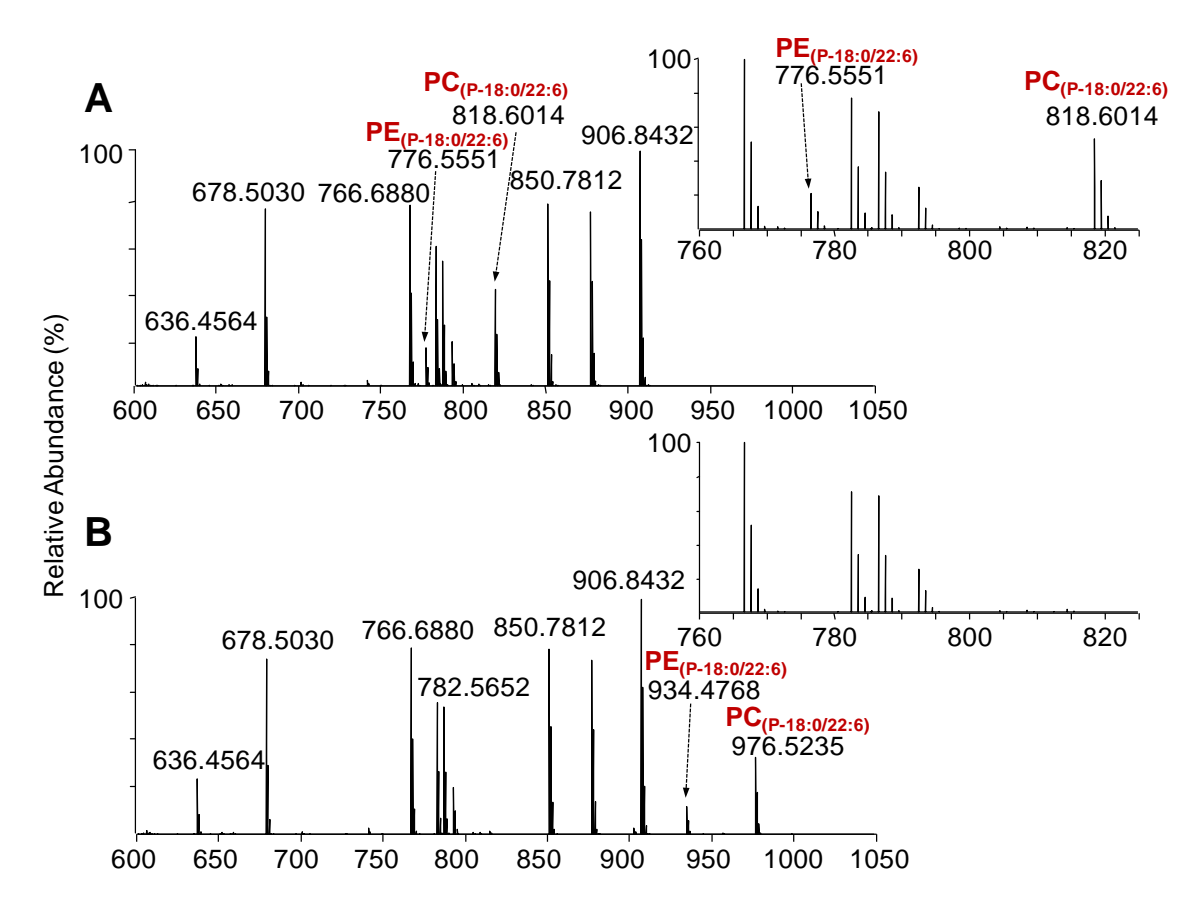


Figure 2.4 Positive ionization mode ESI high-resolution mass spectrometric analysis of a mixture of PC, PE and TG synthetic lipid standards, including two plasmenyl ether containing PC and PE lipids (A) without derivatization and (B) after reaction with iodine and methanol. The insets to each panel show an expanded region (m/z 760-825) of the mass spectra containing the underivatized plasmenyl PC and PE lipids.

From these spectra, it can be seen that complete and selective reaction of the plasmenyl ether lipids within the mixture had occurred, with new ions corresponding to the derivatized plasmenyl PE and PC lipids appearing at *m/z* 934.4768 (i.e., the addition of 157.9217 Da) and *m/z* 976.5235 (i.e., the addition of 157.92221 Da), respectively, consistent with the addition of I+OCH₃ (calculated mass 157.9229 Da). A low abundance ion at *m/z* 902.4502 corresponding to the in-source loss of methanol from the [PE(P-18:0/22:6) + H + I + OCH₃]⁺ ion was also observed. Importantly, despite the presence of numerous mono- and poly-unsaturated fatty acids within the other lipids in the standard mixture, no reaction of these lipids was observed. Furthermore, no change in the relative sensitivity was observed for any of the underivatized or derivatized lipids following the reaction.

2.3.3 Characterization of the Fragmentation Behavior of DMBNHS Derivatized Lipids

Derivatization of PE and PS lipids with DMBNHS not only removes isobaric overlaps with other species and increases the ionization sensitivity in positive ionization mode, it also changes the fragmentation behavior of both types of lipids. The DMBNHS derivatized diacyl PE and PS fragmentation behavior was investigated by a former member of the group and discussed in her thesis [246]. Note that plasmanyl and plasmenyl species, which lack the carbonyl

oxygen on the *sn*-1 position undergo different fragmentation pathways. Plasmanyl PE and PS fragmentation is similar to that of diacyl PE and PS without the loss of the *sn*-1 fatty alcohol chain. MS/MS spectra and proposed fragmentation mechanisms for the plasmenyl species will be discussed in the next few sections.

2.3.3.1 Characterization of the Fragmentation Behavior of Iodine/Methanol Derivatized Plasmalogen PC Lipids

CID-MS/MS of protonated plasmenyl ether PC lipids in positive ionization mode results in the formation of a dominant product ion fragment at *m/z* 184.0739, corresponding to the phosphocholine headgroup (Scheme 2.2, pathway *a*), while the product ion corresponding to characteristic loss of the plasmenyl chain as a neutral alkenyl alcohol (note that an analogous loss is not observed for plasmanyl ether containing PC lipids) (Scheme 2.2, pathway *b*) [247], is observed only at very low abundance. An example is shown in Figure 2.5A for HCD-MS/MS of the PC(P-18:0/22:6) lipid from Figure 2.4A. In negative ionization mode, CID-MS/MS of the acetate or formate adducts of plasmenyl PC lipids results in initial loss of methyl acetate or methyl formate, followed by the formation of a low abundance product ion corresponding to neutral loss of the *sn*-2 fatty acid. However, as this dissociation behavior does not allow the differentiation of plasmenyl or plasmanyl ether chains, further dissociation by MS³ is typically required [208]. Thus, the low abundance of the characteristic

product ion in positive ion mode MS/MS, and the necessity for MS³ in negative ion mode, can severely limit the applicability of these methods for the analysis of very low abundant plasmalogen PC lipids that may be present within a complex crude lipid extract.

Scheme 2.2 Proposed CID-MS/MS fragmentation mechanisms for the plasmenyl ether containing $PC_{(P-18:0/22:6)}$ lipid, prior to and following reaction with iodine and methanol. The m/z values shown correspond to the calculated masses of the various product ions.

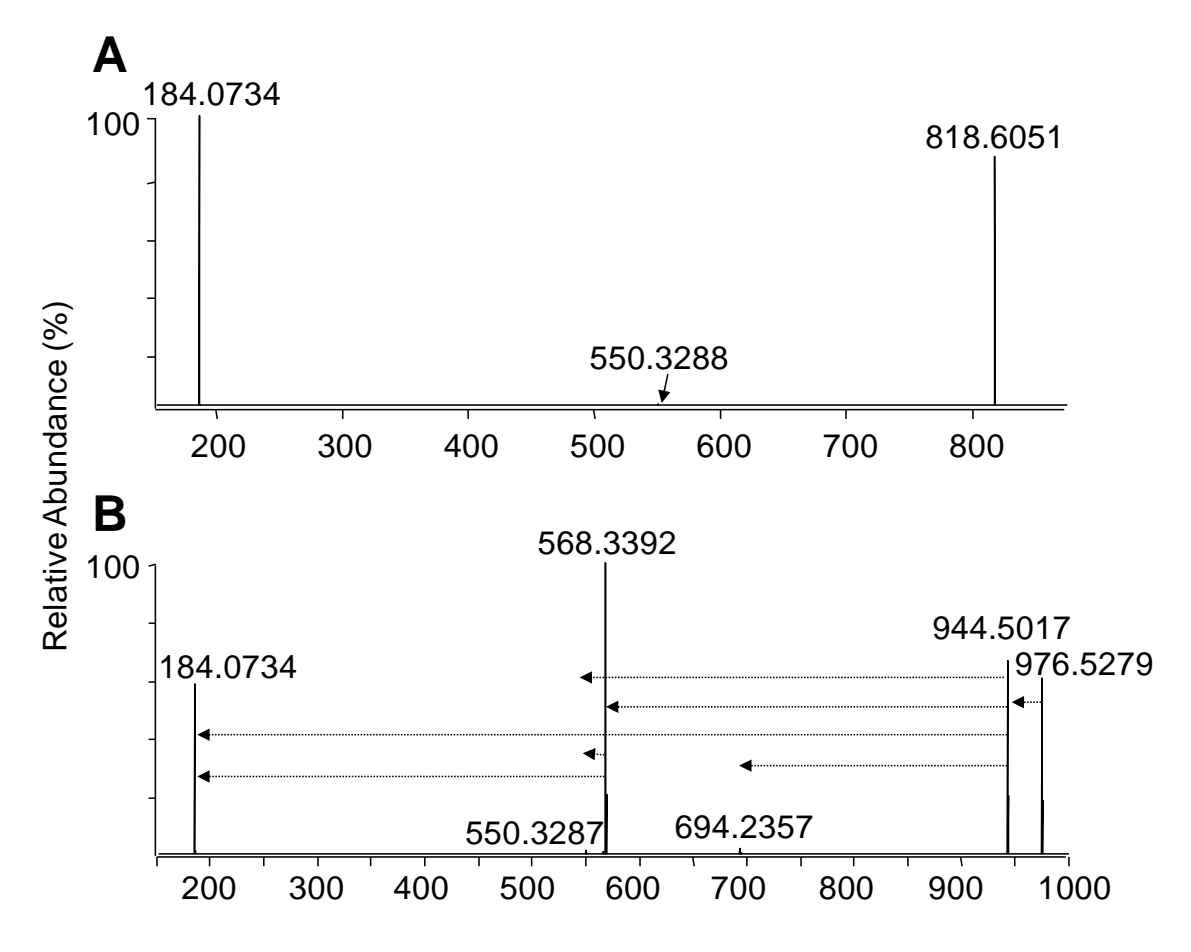


Figure 2.5 Positive ionization mode ESI high-resolution HCD-MS/MS analysis of the synthetic lipid standard $PC_{(P-18:0/22:6)}$ (A) without derivatization and (B) after reaction with iodine and methanol. The horizontal arrows in panel B indicate the fragmentation pathways that were observed upon performing ion trap multistage CID-MSⁿ of the derivatized PC precursor ion.

In contrast, positive ion mode HCD-MS/MS of the iodine/CH₃OH derivatized plasmenyl PC lipid (i.e., $[PC_{(P-18:0/22:6)} + I + OCH_3 + H]^+$ (m/z 976.5279) from Figure 2.4B) (Figure 2.5B), resulted in the formation of a dominant product ion corresponding to characteristic cleavage of the derivatized plasmenyl ether chain with neutral loss of a characteristic R₁'CICHOCH₃ alkene (m/z 568.3392), that directly enabled assignment of the molecular lipid identity

(i.e., $PC_{(P-18:0/22:6)}$ rather than $PC_{(O-18:1/22:6)}$), as well as an abundant product ion at m/z 944.5017 corresponding to the loss of methanol, both of which also underwent further dissociation to yield the abundant PC headgroup specific ion at m/z 184.0734. Mechanistic proposals for formation of each of these product ions, supported by the high resolution/accurate mass performance of the Orbitrap mass spectrometer, and data acquired via ion trap multistage CID-MSⁿ experiments (the sequential fragmentation pathways observed from these experiments are shown as dotted lines in the Figures), are shown in Scheme 2.2, pathways c and d, respectively. Note that the low abundance ion at m/z 694.2357 in Figure 2.5B, corresponding to loss of the sn1 alkenyl chain as a neutral R'CHCHOCH₃ alkene via the pathway proposed in Scheme 2.2, pathway e, is likely to be observed only for C22:6 fatty acyl chain containing plasmenyl lipids, due to the specific sites of unsaturation located within this particular acyl chain.

2.3.3.2 Characterization of the Fragmentation Behavior of Iodine/Methanol Derivatized Plasmalogen PE Lipids

A comparison of the HCD-MS/MS spectra acquired from the protonated and iodine/CH₃OH derivatized plasmenyl ether $PE_{(P-18:0/22:6)}$ lipid precursor ions, are shown in Figure 2.6A and B, respectively. The abundant product ions at m/z 385.2738 and m/z 392.2924 observed upon dissociation of the underivatized

protonated plasmenyl PE lipid from Figure 2.4A (Figure 2.6A), corresponding to loss of the *sn*-2 acyl and *sn*-1 alkenyl chains, respectively, directly enable assignment of the molecular lipid identity. These products are consistent with those previously reported by Zemski Berry and Murphy, who also provided a sound mechanistic rationale for their formation (Scheme 2.3, pathways *a* and *b*) [187].

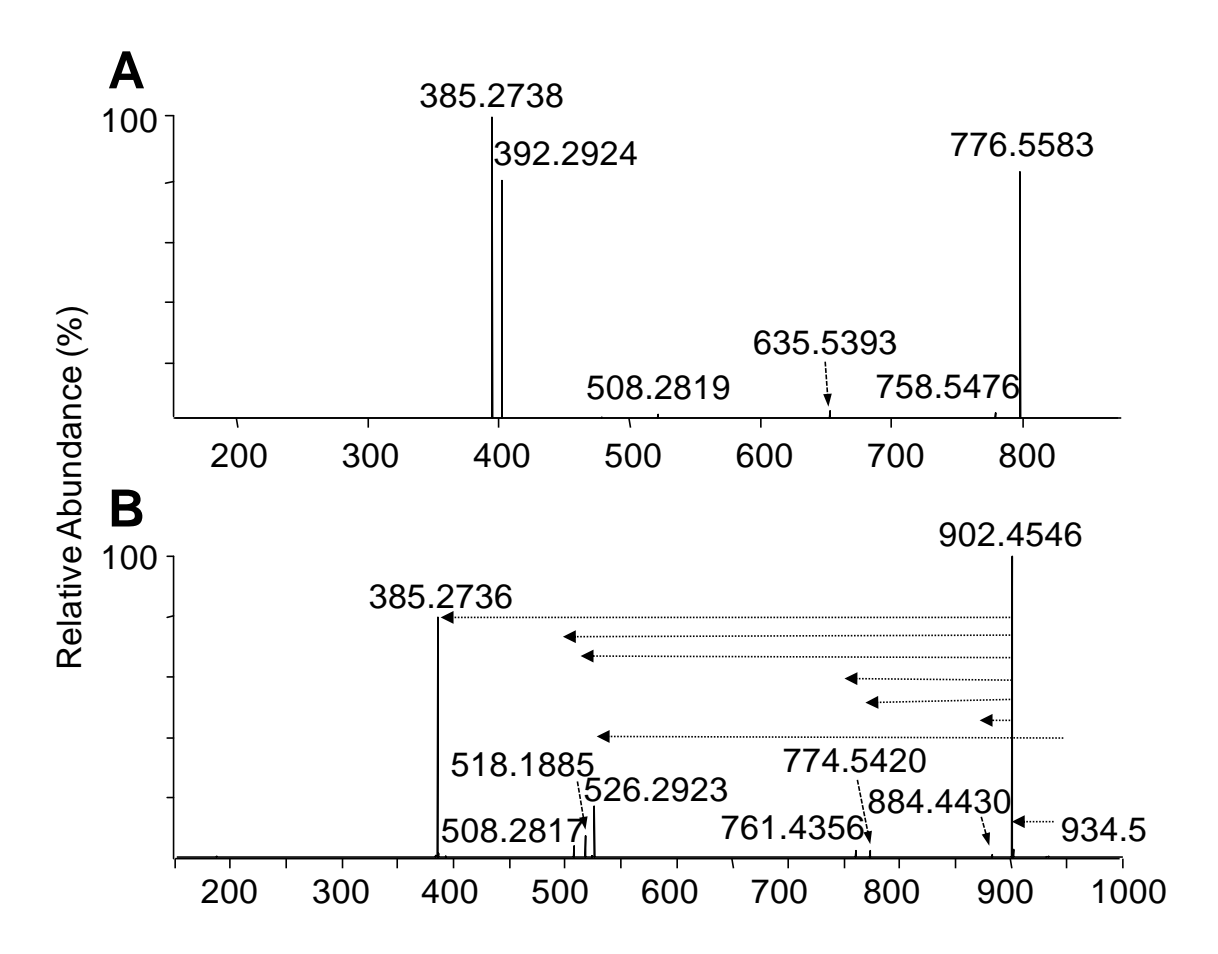


Figure 2.6 Positive ionization mode ESI high-resolution HCD-MS/MS analysis of the synthetic lipid standard $PE_{(P-18:0/22:6)}$ (A) without derivatization and (B) after reaction with iodine and methanol. The horizontal arrows in panel B indicates the fragmentation pathways that were observed upon performing ion trap multistage CID-MSⁿ of the derivatized PE precursor ions.

Scheme 2.3 Proposed CID-MS/MS fragmentation mechanisms for the plasmenyl ether containing $PE_{(P-18:0/22:6)}$ lipid, prior to and following reaction with iodine and methanol. The m/z values shown correspond to the calculated masses of the various product ions.

In contrast, the primary fragmentation pathway for the iodine/CH₃OH derivatized plasmenyl ether $PE_{(P-18:0/22:6)}$ lipid from Figure 2.4B (Figure 2.6B) corresponded to the loss of methanol (m/z 902.4546) (Scheme 2.3, pathway c). A lower abundance product ion formed via the neutral loss of the characteristic

 R_1 'CICHOCH₃ alkene (m/z 526.2923) (Scheme 2.3, pathway d) was also observed, analogous to that proposed in Scheme 2.2, pathway c for the iodine/CH₃OH derivatized plasmenyl PC lipid, from which the molecular lipid identity could be directly assigned (i.e., PE(P-18:0/22:6)) rather than PE(O-18:1/22:6)). Further dissociation of the m/z 902.4546 product ion during HCD-MS/MS (or by CID-MS³) resulted in the formation of product ions similar to those observed for the underivatized PE lipid (e.g., compare Scheme 2.3, pathways e and e for the formation of e 385.2736 and e 518.1885, with Scheme 2.3, pathways e and e and e respectively). Several other minor products were also observed, including e 508.2817, formed via the pathway proposed in Scheme 2-5 pathway e as well as e 884.4430, e 774.5420 and e 761.4356 formed via the losses of e H₂O, HI and the phosphoethanolamine head group, respectively.

2.4 Seguential Modification of Aminophospholipid and Plasmalogen Lipids

Derivatization of the aminophospholipids enables the differentiation of protonated PE lipids from protonated PC and ammoniated PA lipids as well as protonated PS lipids from ammoniated PG lipids, but cannot differentiate between plasmanyl and plasmenyl lipids. Furthermore, acid hydrolysis and derivatization with iodine and methanol allow differentiation between plasmanyl and plasmenyl lipids, but do not determine the headgroup of the phospholipids.

Sequential reaction, first with DMBNHS followed by either acid hydrolysis of a portion of the sample or followed by derivatization with iodine and methanol enables both lipid sub-class identification but also the nature of the ether bond of the plasmanyl or plasmenyl lipids.

2.4.1 d₆-DMBNHS and Acid Hydrolysis

Figures 2.7A and B show expanded regions, 744-751 and 880-887, respectively, of the mass spectra from the SW480 cellular extract derivatized with d₆-DMBNHS followed by acid hydrolysis. Figure 2.7A is very similar to Figure 2.3A as many of the PE species present in this region of the mass spectrum correspond to plasmenyl species which were hydrolyzed in Figure 2.3. Upon formic acid hydrolysis, ions in Figure 2.7B containing the diacyl PI and PE lipids and triacyl TG lipids remained at essentially the same abundances as those in Figure 2.2B, as expected. The ion at m/z 884.6316 also remained at the same abundance, and therefore could be assigned as exclusively containing PS_{(O-} 34:1). In contrast, the ion at m/z 884.6104 had completely disappeared, and therefore was assigned as exclusively containing PE(P-38:6). Finally, the ion at m/z 886.6257 had decreased in abundance by approximately 80%, indicating that while this ion primarily contains the plasmenyl-PE(P-38:5) lipid species, a low abundance plasmanyl-PE(O-38:6) lipid was also present.

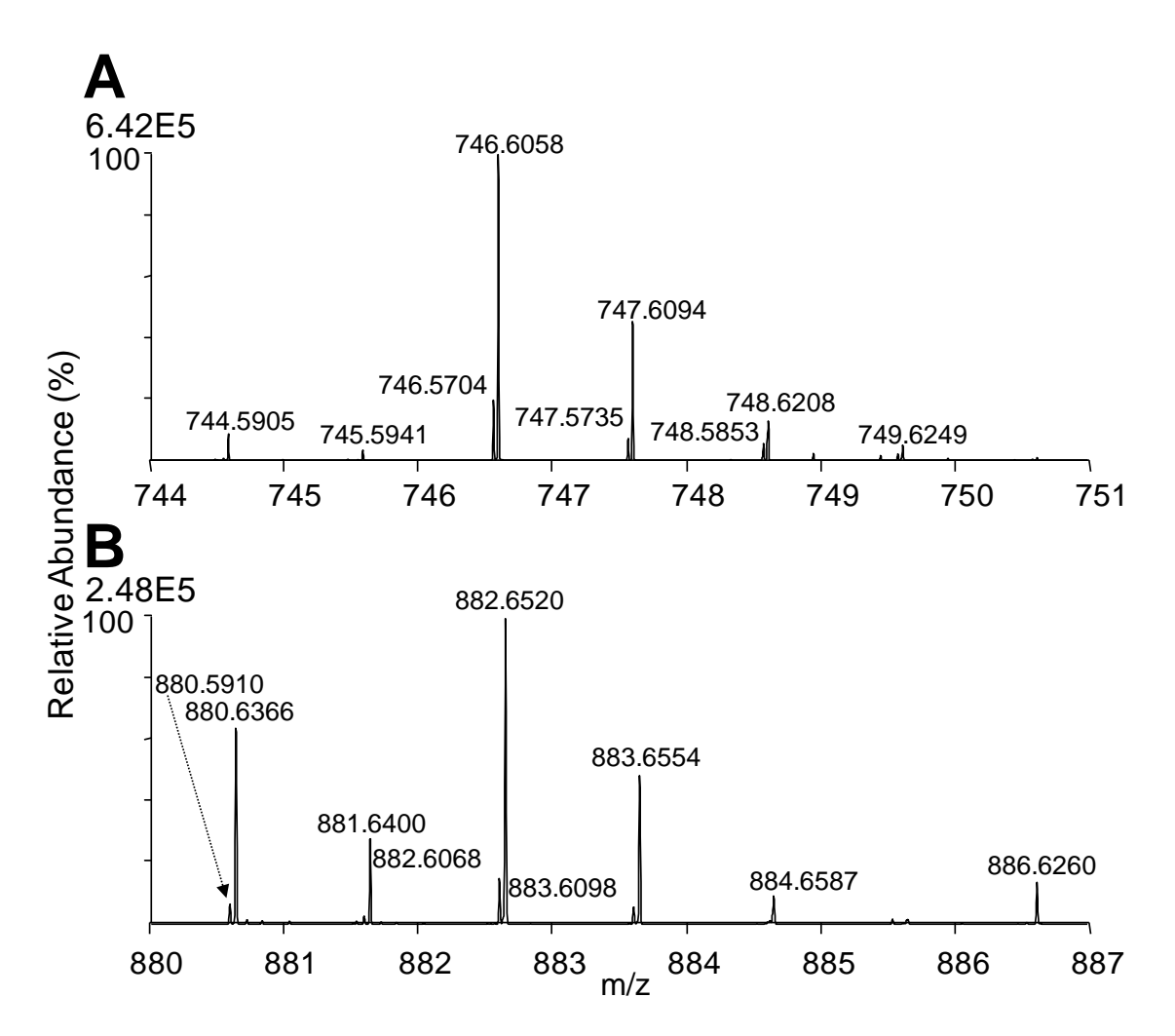


Figure 2.7 Positive ion mode ESI high-resolution mass spectrometric analysis of a crude lipid extract from the SW480 human adenocarcinoma cell line following d₆-DMBNHS derivatization followed by mild formic acid hydrolysis. (A) Expanded region (m/z 744-751) of the ESI-mass spectrum and (B) expanded region (m/z 880-887) of the ESI-mass spectrum.

2.4.2 ¹³C₁-DMBNHS and Iodine/Methanol

The selective iodine/CH₃OH plasmalogen derivatization method was applied to the SW480 cell line crude lipid extract that had first been subjected to

functional group selective derivatization of the PE and PS aminophospholipids within the mixture using $^{13}C_1$ -DMBNHS, as described in Chapter 5. The positive ion mode high-resolution mass spectrum obtained following the reaction with the $^{13}C_1$ -DMBNHS reagent is shown in Figure 2.8A.

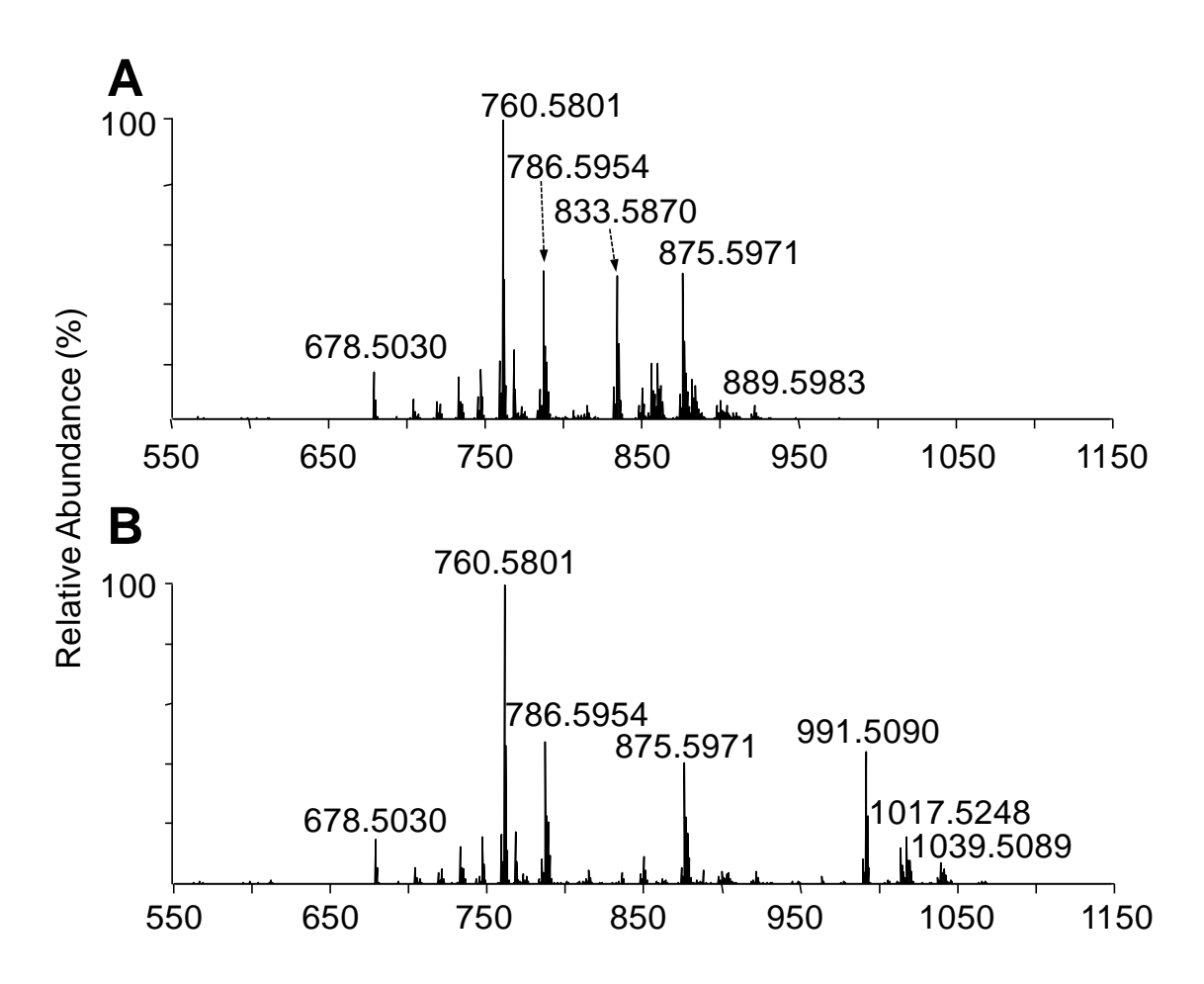


Figure 2.8 Positive ionization mode ESI high-resolution mass spectrometric analysis of a crude lipid extract from the SW480 human adenocarcinoma cell line (A) after reaction with the amine-specific derivatization reagent, ¹³C-DMBNHS and (B) after reaction with ¹³C-DMBNHS and iodine and methanol.

Upon further treatment of the 13 C₁-DMBNHS labeled lipid extract with methanol and iodine (Figure 2.8B), numerous lipids appeared at m/z values

shifted by 157.9229 Da, indicating the presence of plasmenyl lipids via the addition of I + OCH₃. For example, m/z 833.5870 in Figure 2.8A had largely shifted to m/z 991.5090 (Figure 2.8B) indicating the presence of PE_(P-34:1), while the residual ion abundance at m/z 833.5870 indicated the presence of PE_(O-34:2). Consistent with the results from the standard lipid mixture, no change in abundances were observed for any of the other diacyl or alkyl ether containing ions in the crude lipid extract (e.g., m/z 875.5971 corresponding to the 13 C₁-DMBNHS derivatized diacyl PE_(36:2), and m/z 746.6017 corresponding to the protonated plasmanyl PC_(O-34:1)). Interestingly, no in-source fragmentation corresponding to the loss of methanol from the 13 C₁-DMBNHS derivatized PE plasmenyl lipids derivatized with iodine and methanol were observed, suggestive of an improved stability of the DMBNHS derivatized lipid ions.

2.4.2.1 Characteristic Fragmentation of Sequentially ¹³C₁-DMBNHS and Iodine/Methanol Derivatized Plasmalogen PE

Derivatization of the plasmenyl PE lipid with the 13 C₁-DMBNHS reagent, resulting in the introduction of a 'fixed charge' sulfonium ion, significantly altered the gas-phase fragmentation behavior (Figure 2.9A). Here, the dominant initial product ion at m/z 844.5860 was formed via the neutral loss of 63.0024 Da (i.e., 13 C₁-dimethylsulfide), resulting in a 5 membered protonated iminohydrofuran

ring on the headgroup (Scheme 2.4, pathway a). This was followed by further dissociation similar to that seen for the plasmenyl PC lipid in Figure 2.5A, yielding a dominant product ion corresponding to the derivatized phosphoethanolamine headgroup at m/z 210.0532, its complementary 209 Da neutral loss product at m/z 635.5407 formed via intra-complex proton transfer (Scheme 2.4, pathway b), as well as a low abundance product ion at m/z 576.3090 formed via characteristic loss of the plasmenyl chain as a neutral alkenyl alcohol (Scheme 2.4, pathway c) from which direct assignment of the molecular lipid identity (i.e., PE(P-18:0/22:6)) rather than PE(O-18:1/22:6)) could be achieved, albeit with poor detection sensitivity.

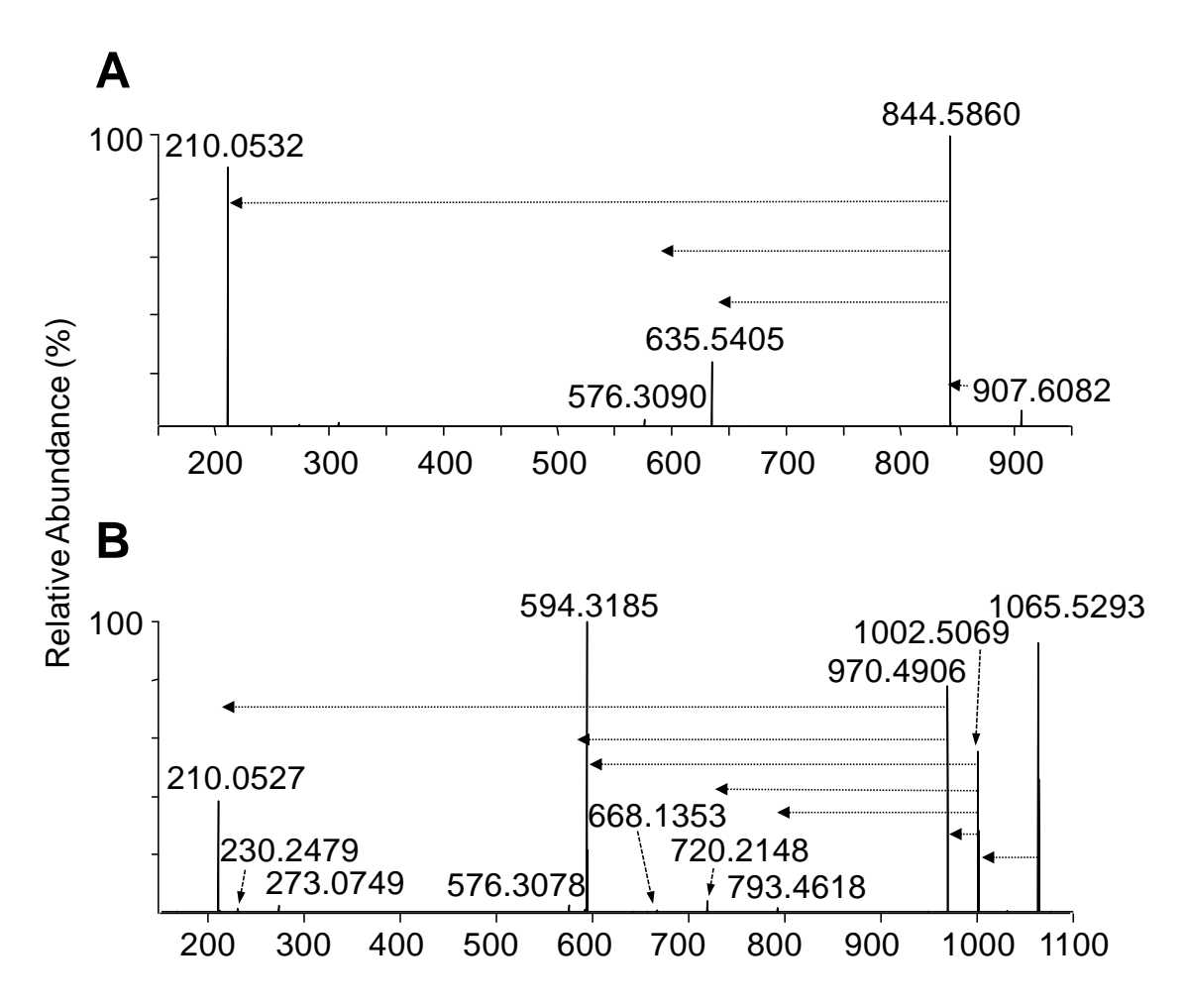


Figure 2.9 Positive ionization mode ESI high-resolution HCD-MS/MS analysis of the synthetic lipid standard $PE_{(P-18:0/22:6)}$ (A) after derivatization with $^{13}C_1$ -DMBNHS, and (B) after derivatization with $^{13}C_1$ -DMBNHS followed by reaction with iodine and methanol. The horizontal arrows in panels A and B indicate the fragmentation pathways that were observed upon performing ion trap multistage CID-MS n of the derivatized PE precursor ions.

Scheme 2.4 Proposed CID-MS/MS fragmentation mechanisms for the 13 C₁-DMBNHS derivatized plasmenyl ether containing PE_(P-18:0/22:6) lipid, prior to and following reaction with iodine and methanol. The m/z values shown correspond to the calculated masses of the various product ions.

Finally, the spectrum acquired upon HCD-MS/MS of the sequentially 13 C₁-DMBNHS and iodine/CH₃OH derivatized plasmenyl ether PE_(P-18:0/22:6) lipid is shown in Figure 2.9B. Similar to the plasmenyl PE lipid derivatized only with 13 C₁-DBMNHS, the dominant neutral loss of 13 C₁-dimethylsulfide (m/z

1002.5069) was observed as the primary fragmentation pathway (Scheme 2.4. pathway d). Then, further dissociation of this initial product ion was found to be essentially identical to that observed from the iodine/CH3OH derivatized plasmenvl PC lipid in Figure 2.5B, with the major product ion formed via neutral loss of the characteristic R₁'CICHOCH₃ alkene (m/z 594.3185), that directly enabled assignment of the molecular lipid identity (i.e., PC_(P-18:0/22:6) rather than PC_(O-18:1/22:6)) (Scheme 2.4, pathway e), as well as an abundant product ion corresponding to the loss of methanol (m/z 970.4906) that also underwent further dissociation to yield the abundant derivatized PE headgroup specific ion at m/z 210.0527 (Scheme 2.4, pathway f) and its low abundance complementary 209 Da neutral loss product at m/z 793.4618. Interestingly, the minor product ion at m/z 720.2148, corresponding to loss of the sn-1 alkenyl chain as a neutral R'CHCHOCH₃ alkene via a pathway the same as that proposed in Scheme 2.3, pathway e for the iodine/CH₃OH derivatized plasmenyl PC lipid, was not observed for the plasmenyl PE lipid that had only been derivatized with iodine/CH₃OH (i.e., no ¹³C₁-DMBNHS), suggesting that this reaction pathway is only energetically competitive under 'non-mobile' protonation conditions.

2.5 Conclusions

The results shown herein indicate that sequential functional group specific lipid derivatization reactions can be successfully developed and applied to fully resolve, identify the presence of, and characterize the molecular lipid compositions of plasmenyl ether containing lipid species from within crude complex lipid extracts based on the characteristic mass shifts observed upon 'shotgun' high resolution/accurate mass spectrometry, and/or the characteristic product ions formed upon tandem mass spectrometry analysis of their mass selected precursor ions. The reactions are simple, fast, and proceed to completion without non-specific modification of other lipids that may be present within a given mixture. Coupled with its ability to significantly reduce or eliminate the need for chromatographic fractionation or additional lipid extraction steps prior to analysis, this approach represents an attractive strategy for use in future studies aimed at developing an improved understanding of the structures and functions of plasmenyl and plasmanyl ether lipids in health and disease.

Chapter 3

Comprehensive Lipidome Profiling of Isogenic Primary and Metastatic Colon Adenocarcinoma Cell Lines

3.1 Introduction

Lipids comprise the majority of cellular membranes and are necessary for several cellular functions including structure and signaling [6,248,249]. A large number of studies have demonstrated that disruption of lipid metabolism and/or signaling are associated with the onset and progression of numerous conditions including obesity [39], diabetes [36-38,40,250,251], coronary heart disease [39,252], Alzheimer's disease [44], as well as several human cancers including lung [63], prostate [63,72], breast [63,68], brain [253], liver [51,54] and colorectal [64,71,136,254-256]. Notably, changes in the abundances of ether-linked PC and PE lipids have been correlated with malignancy and metastatic potential in various cancers [63]. For example, in colorectal cancer, the third leading cause of cancer deaths in the United States [256], increased levels of alkyl ether linked plasmanyl-PC lipids have previously been reported between normal and malignant tissue [64,71], while significantly decreased vinyl ether linked plasmenyl-PE lipid levels observed malignant have been in

Part of the results described in Chapter Three were published in:

Fhaner, C. J., Liu, S., Ji, H., Simpson, R. J., Reid, G.E., Comprehensive lipidome profiling of isogenic primary and metastatic colon adenocarcinoma cell lines. *Anal. Chem.* **2012**, *84*, 8917-8926.

compared to non-malignant colon cancer tissue samples [71]. At present, however, little information is available regarding the changes in 'global' lipid profiles that occur between normal and diseased cells, tissues or readily accessible bodily fluids (e.g., tumor interstitial fluid, blood plasma or serum) as a function of the onset and progression of colon cancer. Such information could provide further insights into the biological mechanisms by which lipids are associated with cancer development, or lead to the identification of effective biomarker signatures of the disease, e.g., to differentiate between benign, primary versus metastatic cancers, or as targets for therapeutic intervention.

3.2 High Resolution MS Based Lipidomic Analysis of SW480 and SW620 Cellular Extracts

The recent development of ultra-high resolution/accurate mass analyzers based on FT-ICR or Orbitrap platforms has opened the door to the possibility of employing high-throughput direct infusion 'shotgun' mass spectrometry for the simultaneous analysis of multiple lipid classes without prior separation, and with a reduced need for extensive MS/MS analysis [119,208,223,239]. High resolution (≥100,000) readily provides the ability to separate lipid ions with the same nominal m/z values, with substantially improved signal-to-noise and dynamic range compared to lower resolution instruments for the detection of low abundance lipid species that may be present within a complex crude lipid extract. However, the differentiation of isobaric mass lipid ions remains an issue. In this

chapter, the 'shotgun' lipidomics strategy consisting of sequential functional group selective chemical modification reactions coupled with high-resolution/accurate mass spectrometry described in Chapter 2 was applied toward the comprehensive identification, characterization and quantitative analysis of changes in relative abundances of individual glycerophospholipid, glycerolipid, sphingolipid and sterol lipids between the primary colorectal cancer cell line, SW480, and its isogenic lymph node metastasized derivative, SW620.

3.2.1 Sample Preparation for MS Analysis

Cells from each of the SW480 and SW620 adenocarcinoma cell lines were routinely cultured as described in Chapter 5. Once confluent, cells were washed, trypsinized, resuspended in PBS, snap frozen and lyophilized. Lyophilized cells were extracted by a modified Folch method [108,110]. Stock solutions were prepared by dissolving the crude lipid extracts in 4:2:1 IPA/MeOH/CHCl₃. Three aliquots of each crude lipid extract were placed into separate vials with internal lipid standards (PC_(14:0/14:0), PE_(14:0/14:0) and PS_(14:0/14:0)) and were dried under a stream of nitrogen. One aliquot was derivatized with d₆-DMBNHS, a separate aliquot was derivatized with d₆-DMBNHS followed by mild formic acid hydrolysis as described in Chapters 2 and 5, and one was left underivatized. Immediately prior to ESI-MS analysis, each

re-dissolved in 200 μ L of 4:2:1 IPA/MeOH/CHCl $_3$ containing 20mM ammonium formate (NH $_4$ HCO $_2$).

3.2.2 High Resolution MS Analysis of SW480 and SW620 Cellular Extracts

Samples were loaded into a Whatman multichem 96-well plate (Sigma Aldrich, St. Louis, MO) and sealed with Teflon Ultra Thin Sealing Tape (Analytical Sales and Services, Prompton Plains, NJ). Samples were introduced to the mass spectrometer via nanoESI using an Advion Triversa Nanomate (Advion, Ithaca, NY). High resolution mass spectra were acquired across the range of m/z from 200-2000 using the FT analyzed (100,000 resolving power) and were signal averaged for 3 minutes.

3.2.2.1 High Resolution MS of Underivatized Cellular Extracts

The mass spectra (m/z 600-1000) obtained following positive ionization mode ESI-MS analysis of the crude lipid extracts from the primary colorectal cancer cell line, SW480, and its isogenic metastatic derivative, SW620, are shown in Figures 3.1A and 3.1B, respectively. The addition of 20 mM ammonium formate to the spray solution was found to provide an approximately two-fold increase in ion abundance in positive ion mode compared to the use of 20 mM ammonium acetate (data not shown); therefore, ammonium formate was employed for all the results shown herein. A number of qualitative differences in

the presence and/or abundance of several ions between the SW480 and SW620 cell lipid extracts are immediately apparent. For example, the ion at m/z 746.6055 and numerous ions within the m/z range of 800-920 have all increased in abundance between the SW480 and SW620 extracts, relative to that of the internal standard $PC_{(14:0/14:0)}$ lipid, while the ion at m/z 760.5861 has decreased in abundance.

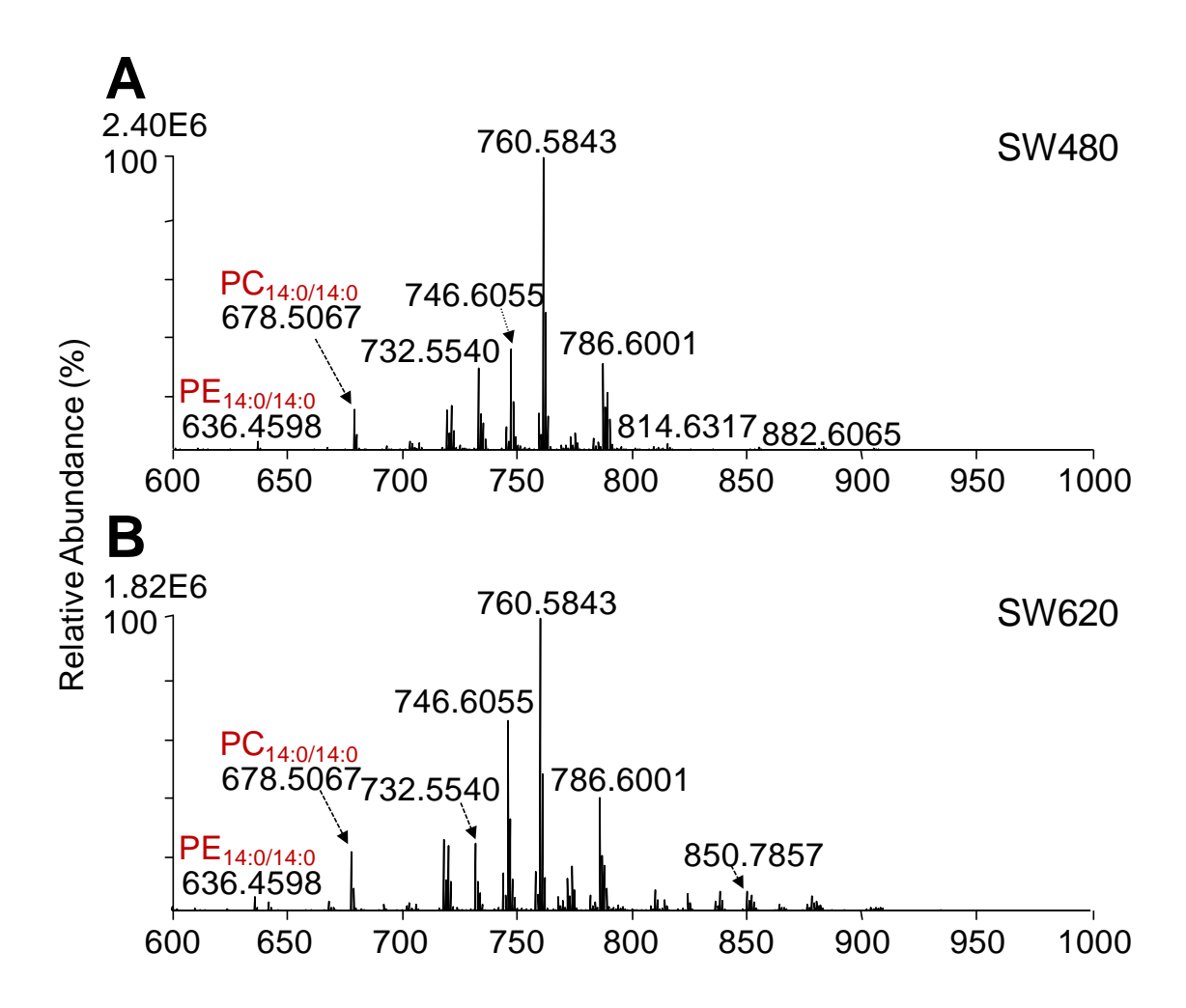


Figure 3.1 Positive ion mode ESI high-resolution mass spectrometric analysis (m/z 600-1000) of crude lipid extract from the human adenocarcinoma cell line (A) SW480 and (B) its metastatic counterpart, SW620.

Based on the high resolution performance and accurate mass values obtained using the Orbitrap, the sum compositions [3] of the glycerolipid, sphingolipid, cholesterol, cholesterol ester and PI lipid ions, including (i) assignment of the head group identities, (ii) the nature of their hydrophobic chain linkages (i.e., diacyl versus plasmanyl- or plasmenyl-ether) and (iii) the total number of carbons and double bonds that were present within their hydrophobic chains, could be automatically assigned by in silico comparison with the calculated masses of a database of hypothetical lipid compounds, using the LIMSA software [233]. For example, m/z 850.7857 in Figure 3.1A was assigned as the ammonium ion adduct of a TG_(50:1) lipid (calculated m/z 850.7858), with the experimental and calculated m/z values differing by only 0.0001 Da (0.08 ppm). For saturated plasmanyl-ether containing lipids, assignment of the lipid identity was also straightforward, while for ether linked lipids containing at least one site of unsaturation, assignment of lipid identity was more complicated as these could overlap in exact mass with plasmenyl-ether containing lipid ions with the same total number of carbons but one less site of unsaturation.

3.2.2.2 High Resolution MS of Cellular Extracts Derivatized with d₆-DMBNHS

As discussed in chapter 2, PC, PE, PA, lipid species may not be assigned directly from their accurate mass values alone, due to the possibility of exact mass overlap between protonated PE lipid ions with the ammonium ion adducts of PA lipids containing 2 additional carbons and 1 additional double bond, as well

as with odd chain length protonated PC ions containing 3 additional carbons. Protonated PS lipids can also overlap in exact mass with the ammonium ion adducts of PG lipids containing 2 additional double bonds. Figure 3.2 shows the expanded regions (m/z 744-751 and m/z 880-887) of the SW620 cell crude lipid extracts derivatized with d_6 -DMBNHS.

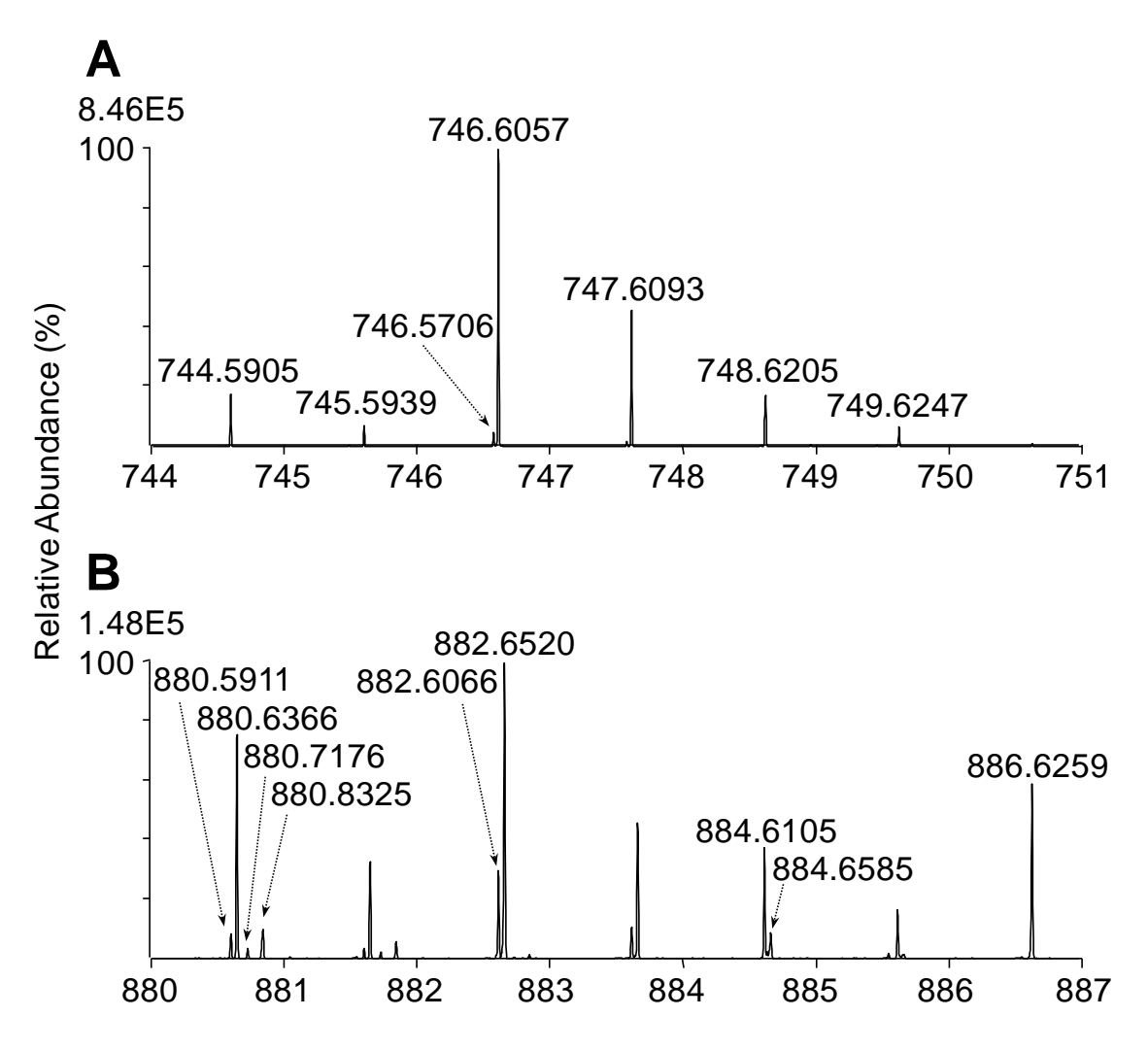


Figure 3.2 Positive ion mode ESI high-resolution mass spectrometric analysis of a crude lipid extract from the SW620 human adenocarcinoma cell line. (A) Expanded region (m/z 744-751) and (B) expanded region (m/z 880-887) of the ESI-mass spectrum obtained after reaction with the amine-specific derivatization reagent, d_6 -DMBNHS.

The higher m/z region of the mass spectra is occupied by the derivatized PE and PS ions as well as those ions corresponding to the ammonium ion adducts of PI and TG containing lipids (e.g., $[PI_{(36:2)}+NH_4]^+$ and $[PI_{(36:1)}+NH_4]^+$ at m/z 880.5909 and 882.6065, respectively, and $[TG_{(52:0)}+NH_4]^+$ at m/z 880.8326. There is no mass overlap with the PE and PS species that appear upon derivatization (e.g., $PE_{(36:2)}$ at m/z 880.6366, $PE_{(36:1)}$ at m/z 882.6520, $PE_{(P-38:6)}$ and/or $PE_{(O-38:7)}$ at m/z 884.6104, $PE_{(P-38:5)}$ and/or $PE_{(O-38:6)}$ at m/z 886.6257, and $PS_{(P-34:0)}$ and/or $PS_{(O-34:1)}$ at m/z 884.6316.

3.2.2.3 High Resolution MS of Cellular Extracts Derivatized with d₆-DMBNHS and Acid Hydrolyzed

The expanded regions (m/z 744-751 and m/z 880-887) of the mass spectra obtained following mild formic acid hydrolysis of the d₆-DMNBHS derivatized crude lipid extracts from the SW620 cell lines are shown in Figure 3.3 A and B, respectively. The same expanded regions of the SW480 d₆-DMBNHS derivatized and d₆-DMBNHS derivatized with formic acid hydrolysis are shown in Figures 2.7 A and B, respectively. Upon formic acid hydrolysis, ions containing the diacyl PI, TG and PE lipids remain at essentially the same abundances when comparing Figure 3.2 to Figure 3.3, as expected, whereas the ion at m/z

884.6104 had completely disappeared, and therefore was assigned as exclusively containing PE_(P-38:6).

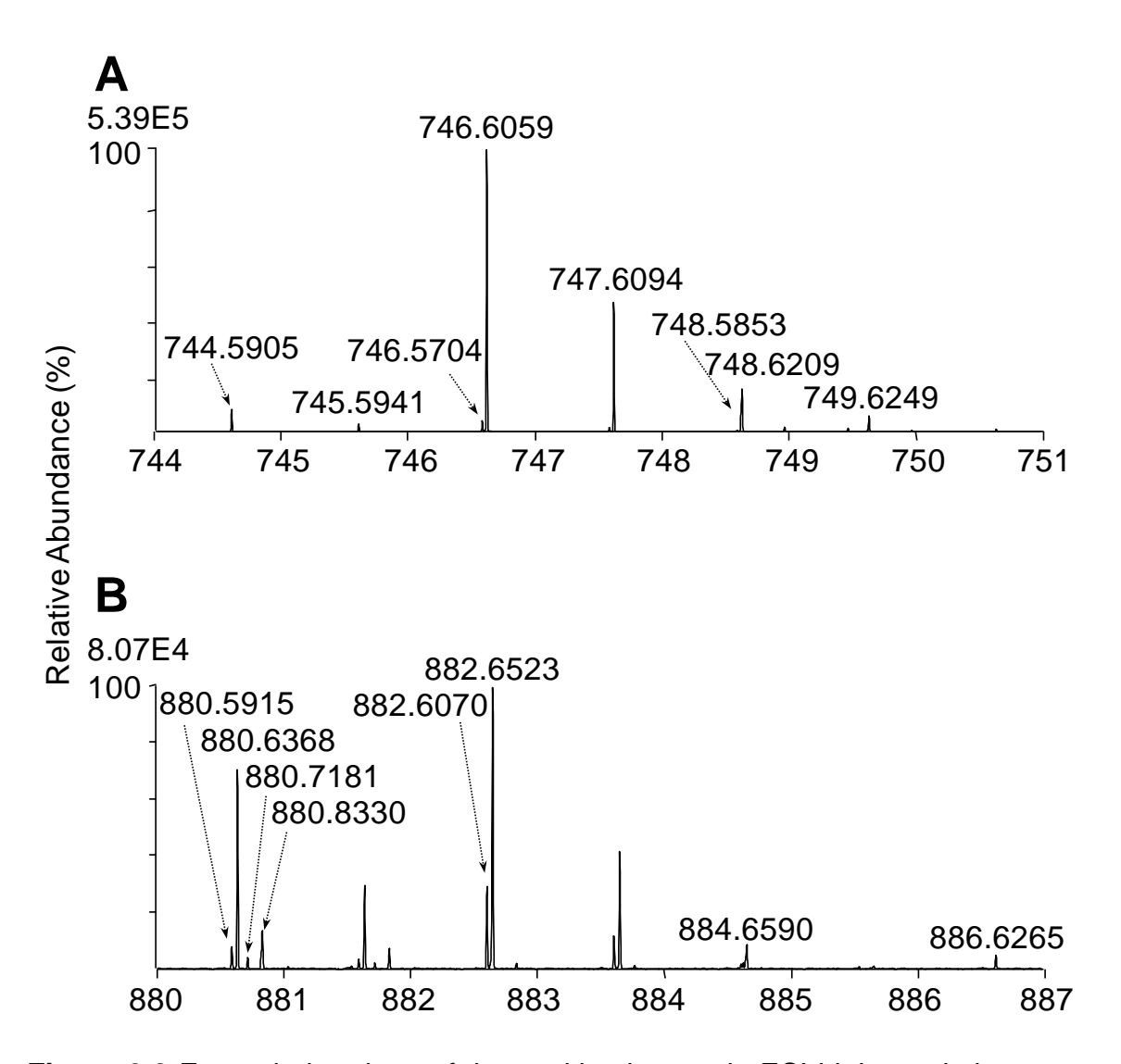


Figure 3.3 Expanded regions of the positive ion mode ESI high-resolution mass spectrometric analysis of a crude lipid extract after reaction with d_6 -DMBNHS and formic acid from the SW620 human adenocarcinoma cell lines for (A) m/z 744-751 and (B) m/z 880-887.

3.2.2.4 MS Data Analysis for Relative Quantification

Relative quantification of lipid ion abundances was performed by comparison of each lipid ion abundance compared to the ion abundance of the PC_(14·0/14·0) internal standard. Sum composition assignment of all lipid ion peaks in the mass spectra obtained following d₆-DMBNHS derivatization was performed using LIMSA and determination of the nature of the ether bond (plasmanyl vs. plasmenyl) was performed by comparison of the individual peaks in the derivatized and acid hydrolyzed spectra. No attempts were made to quantitatively correct for different ESI responses of individual lipids due to concentration, acyl chain length or degree of unsaturation. Thus, the abundance of the ions corresponding to individual molecular species within each lipid class, normalized to the abundance of the PC_(14:0/14:0) internal standard, are reported here as the percentage of the total lipid ion abundance for each class, and do not represent the absolute concentrations of each lipid or lipid class. The internal standards $PE_{(14:0/14:0)}$ and $PS_{(14:0/14:0)}$ were included to monitor the completeness of the d₆-DMBNHS reaction. All lipid classes (PC, PE, PS, PG, PI, LPC, LPE, LPS, TG, DG, MG, SM, Cer, Chol and Chol esters) except for PA were identified and quantified from the d₆-DMBNHS derivatized spectra. Determination of the abundance of PA lipids was performed in negative ionization mode, then a correction was applied to the positive ion mode spectra to remove the contribution of these lipids to the PC lipid ion abundances, as described in Chapter 2. In the results described below, lipids whose identities of their headgroup and fatty acyl, alkyl and/or alkenyl chains could be unambiguously assigned by manual analysis of their individual MS/MS spectra are classified as Molecular Lipids (Mol Lipids) [3], while 'Total' includes the combined number of Molecular Lipids as well as those lipids where only the Sum Compositions could be assigned from the high resolution d₆-DMBNHS derivatized and mild formic acid hydrolyzed ESI-MS data.

3.3 Implications in Colon Cancer Metastasis from Lipidomic Changes Identified

The abundances of the ions corresponding to each assigned lipid were then expressed as a percentage of the total lipid ion abundance for a given lipid class, to allow quantitative comparison between the SW480 and SW620 cell lines. It has been well established that alterations in lipid content have several implications in the progression of diseases [60,63,136,257]. These quantitative comparisons may suggest the progression of colorectal cancer from the primary cells to metastatic cells.

3.3.1 Glycerophospholipid Alterations

Figure 3.4 shows the changes observed in individual PC lipid % ion abundances between the d₆-DMBNHS derivatized SW620 and SW480 cell crude lipid extracts, for all ions whose abundances were found to correspond to greater than 0.1% of the total ion abundance in each lipid class. Pair-wise comparisons

between individual lipids between the two cell lines resulted in numerous statistically significant changes (p<0.01) to be observed. Most notably are the alterations with respect to increases in the abundances of plasmanyl-ether containing PC lipids between the SW620 and SW480 cell crude lipid extracts, and a corresponding decrease in the abundance of their diacyl counterparts (e.g., the PC_(O-34:1) ion at m/z 746.6058 versus the PC_(34:1) ion at m/z 760.5850) (Figure 3.4A). Overall, the % total ether-linked PC ion abundance (corresponding to approximately 30% of the total PC lipid ion abundance) increased by approximately 50% percent (Figure 3.4B), whereas the % total PC ion abundance compared to the total ion abundance for all identified lipids increased by only a small amount (Figure 3.4C). A similar significant increase was observed in the abundance of the major plasmanyl-LPC lipid present in the lipid extracts i.e., LPC_(O-16:0)), along with an overall increase in the % total LPC ion abundance between the SW620 and SW480 cells (Figure 3.5).

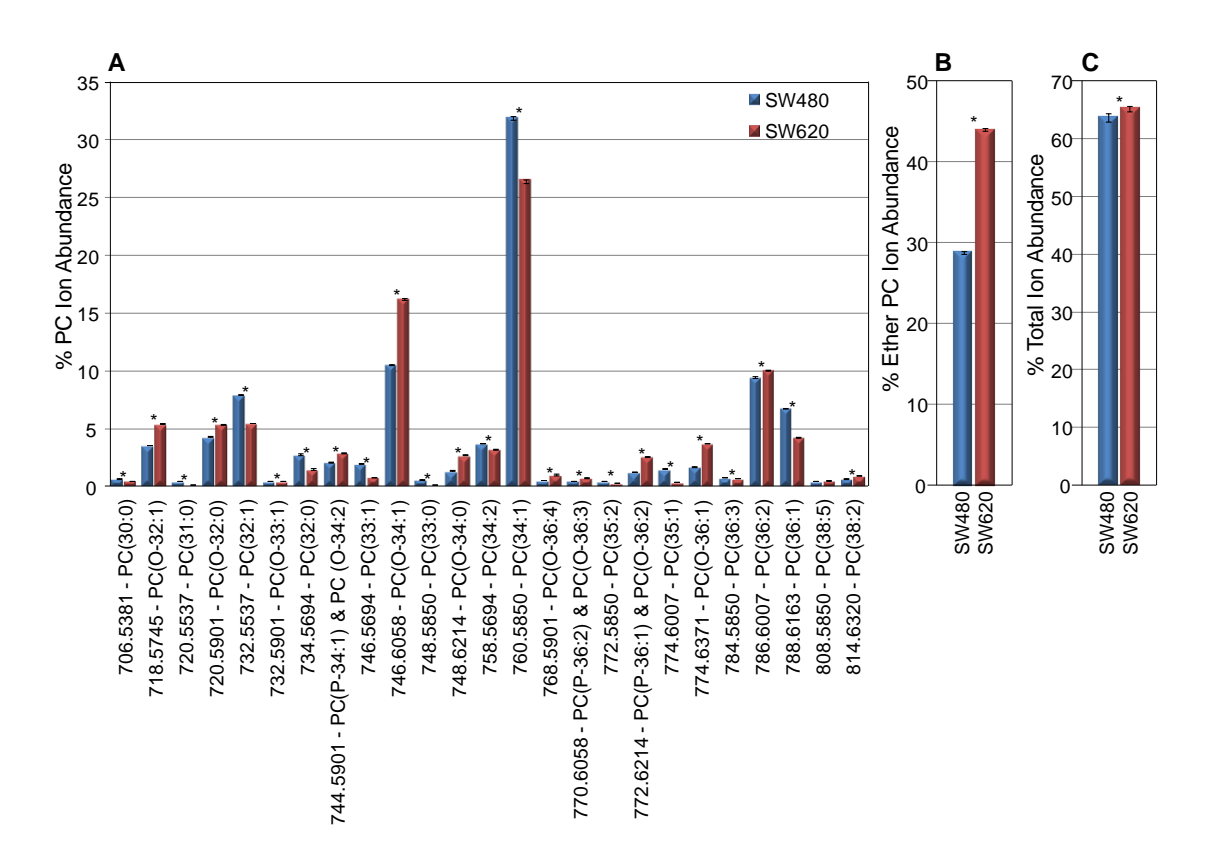


Figure 3.4 Quantitation of PC lipids from the d₆-DMBNHS derivatized SW480 and SW620 cell crude lipid extracts. (A) Percent individual PC ion abundances compared to the total ion abundance for all PC lipids. (B) Percent total etherlinked PC ion abundance compared to the total PC lipid ion abundance. (C) Percent total PC ion abundance compared to the total ion abundance for all identified lipids. n = 5, m = 5, m = 6, m = 6.

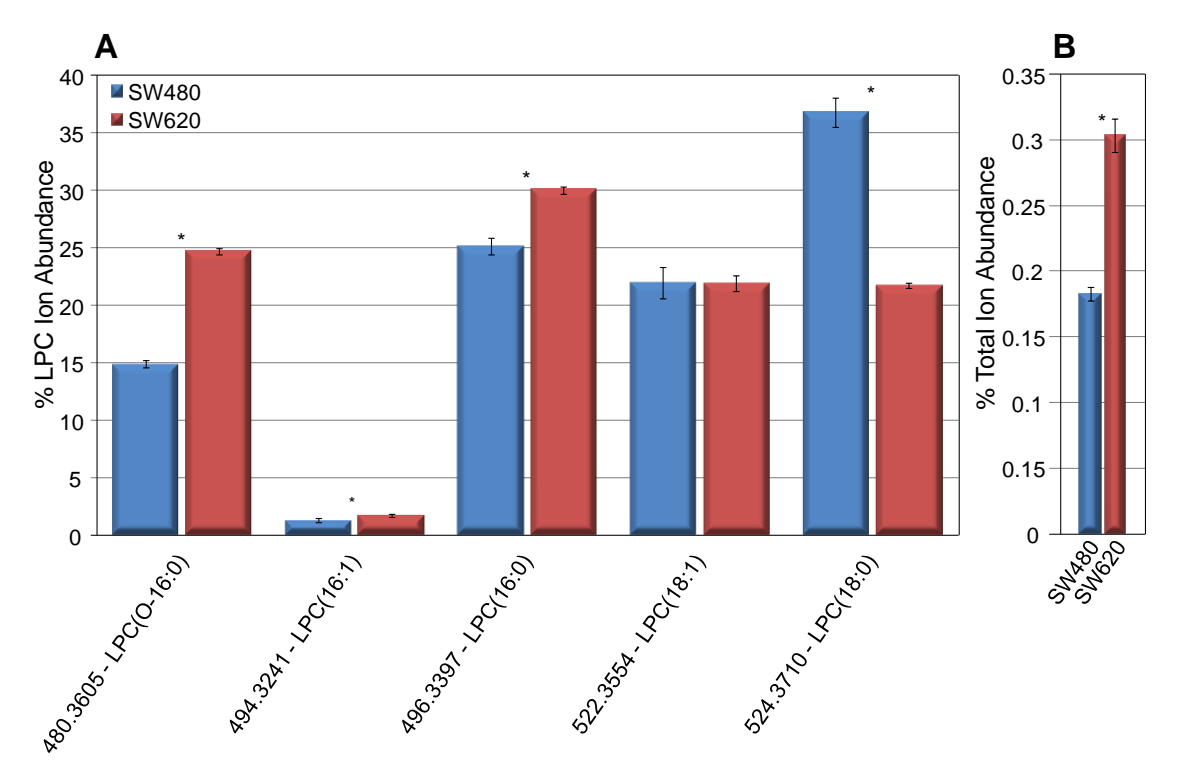


Figure 3.5 Quantitation of LPC lipids from the d₆-DMBNHS derivatized SW480 and SW620 cell crude lipid extracts. (A) Percent individual LPC ion abundances compared to the total ion abundance for all LPC lipids. (B) Percent total etherlinked LPC ion abundance compared to the total LPC lipid ion abundance. n = 5, * = p < 0.01.

Numerous statistically significant changes in PE lipid ion abundances were also observed between the d₆-DMBNHS derivatized SW620 and SW480 cells (Figure 3.6A). In contrast to the PC lipids, an increase in the % abundance of diacyl-PE lipid containing ions was generally observed, with a corresponding decrease in the % ion abundance of plasmenyl- and plasmanyl-ether containing PE lipids, particularly for shorter chain length species, e.g., the abundant d₆-DMBNHS derivatized PE_(P-34:1) and PE_(O-34:2) lipids at m/z 838.6261, as well as PE_(P-32:1) at m/z 810.5948 and PE_(O-34:1) at m/z 840.6417. Similar changes

were also observed for the LPE lipids (Figure 3.7). Overall decreases in both the % total ether-linked PE ion abundance compared to the total PE lipid ion abundance (Figure 3.6B), as well as the % total PE ion abundance compared to the total ion abundance for all identified lipids (Figure 3.6C), were also observed. Finally, the abundance of odd chain PC and PE lipid species (diacyl, plasmanyl and plasmenyl), as well as odd chain length LPE lipid species, were all observed to significantly decrease in abundance between the SW620 and SW480 cells.

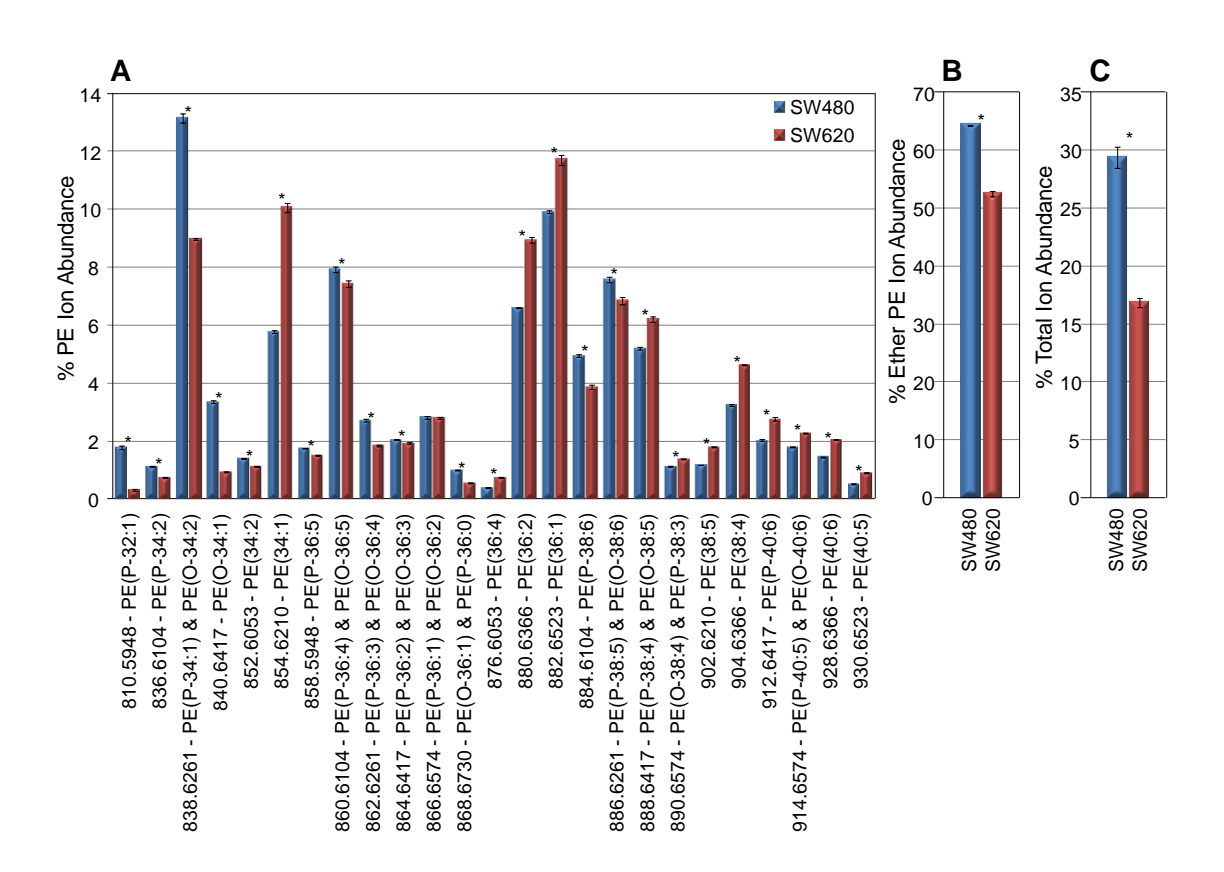


Figure 3.6 Quantitation of PE lipids from the d₆-DMBNHS derivatized SW480 and SW620 cell crude lipid extracts. (A) Percent individual PE ion abundances compared to the total ion abundance for all PE lipids. (B) Percent total etherlinked PE ion abundance compared to the total PE lipid ion abundance. (C) Percent total PE ion abundance compared to the total ion abundance for all identified lipids. n = 5, m =

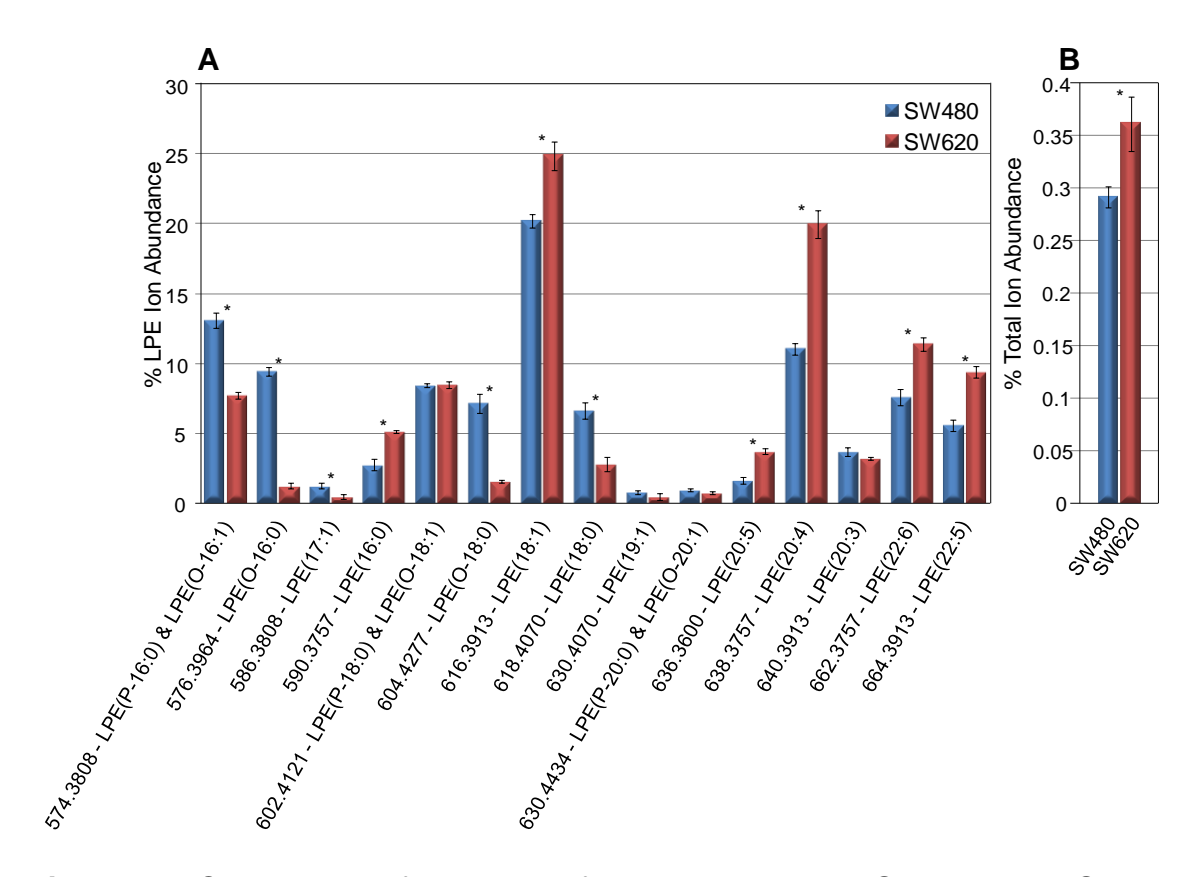


Figure 3.7 Quantitation of LPE lipids from the d₆-DMBNHS derivatized SW480 and SW620 cell crude lipid extracts. (A) Percent individual LPE ion abundances compared to the total ion abundance for all LPE lipids. (B) Percent total etherlinked LPE ion abundance compared to the total LPE lipid ion abundance. n = 5, * = p < 0.01.

It has been known for some time that elevated levels of alkyl ethers of glycerol (and to a somewhat lesser extent, alkyl-phosphogylcerides) are present between normal and neoplastic human tissues [74]. Howard *et al.* have suggested that a correlation exists between the rate of tumor growth and the glyceryl-ether content in phospholipids, and ether-lipid levels have been shown to be at higher concentrations in cells that are more rapidly growing than other cells observed [58]. Notably, a recent study involving the overexpression and knockout of the rate limiting enzyme for ether lipid synthesis enzyme, alkylglycerone

phosphate synthase (AGPS), revealed that cells with increased ether lipids had higher cell survival, motility and growth whereas cells that had AGPS knocked out, exhibited decreased survival, proliferation, migration and invasion [75]. Furthermore, increased plasmanyl-PC levels have previously been reported between normal and malignant tissue [64,71] in patients with colon cancer, and have been correlated with malignancy and metastatic potential in various other cancers [63,68]. In contrast, significantly decreased plasmenyl-PE lipid levels have been reported in malignant colon cancer tissue samples compared to non-malignant tissue [71], and between MCF7 human breast cancer cells and primary cultures of normal human mammary epithelial cells [62]. These results are consistent with those determined here, given that the SW620 cells originated from a metastatic tumor, which is more proliferative than the primary adenocarcinoma SW480 cell line.

Although the functional role of changes in ether-lipid metabolism, and particularly plasmanyl-lipids, to malignancy and metastasis are still poorly understood, it is well established that changes in the physical properties of the cellular membrane (e.g., structure, fluidity, dynamics and fusion) as a function of its plasmalogen lipid composition [258] may play an important role in regulating cell growth, fusion, intracellular transport and signal transduction [46,259-261]. Benjamin, et al. found that arachidonic acid (AA) was preferentially incorporated into diacyl glycerophospholipids, thereby lowering the availability of AA for eicosanoid synthesis, upon knockdown of the rate limiting enzyme for ether lipid synthesis, alkylglycerone phosphate synthase (AGPS) [75]. Alterations in

membrane properties may also influence the sensitivity of cells to certain forms of therapy [61,262].

The results obtained for the PA, PS, LPS, PG and PI lipids are shown in Appendix A: Figures A.1-A.5, respectively. An overall significant increase in the % total ether-linked (primarily plasmanyl) PA ion abundance compared to the total PA lipid ion abundance was observed between the SW620 and SW480 cells, whereas the % total PA ion abundance underwent a significant decrease. There was an increase in the % total ion abundance of both PS and PG lipids in the SW620 compared to the SW480 cells, as well as an increase in the % total ether-linked PS [115,263,264] ion abundance. No ether-linked or odd chain species were observed for the PG lipids. The most abundant LPS lipid in the SW480 cells (LPS_(19:0) at m/z 676.4125 in the d₆-DMBNHS derivatized spectrum) underwent a significant decrease in abundance, thereby following the trend observed for the other phospholipids. Notably however, significant increases in the % ion abundance of multiple odd chain length PS species were observed in the SW620 cells compared to the SW480 cell extract, in direct contrast to the other phospholipid and glycerolipids examined here. Interestingly, ether-linked PI lipids were only observed in the SW480 cells.

3.3.2 Glycerolipid Alterations

Quantitative analysis of the TG lipids (Figure 3.8) revealed a dramatic increase in the total % TG ion abundance in the SW620 cells, along with similar

trends in the changes in the % ion abundances of individual monoether-linked (primarily plasmanyl) and triacyl-TG lipids as those observed for the PC lipids e.g., increased TG_(O-48:0), TG_(O-50:1) and TG_(O-50:0) and correspondingly decreased TG_(48:0), TG_(50:1) and TG_(50:0). Notably, numerous long chain length TG lipids (>56 total carbons) were observed exclusively in the SW620 cell lipid extract. Consistent with the other lipid classes (except PS, see below), the abundances of odd chain length TG lipids were decreased in the SW620 cells. The increase in overall TG species (including the ether-linked TG lipids that are the likely source of the increase in ether-linked phospholipids observed here) is likely due to increased de novo fatty acid synthesis in malignant cells which is used to supply the membrane with fatty acids for increased proliferation [55,56,265]. Also, increases in ether-linked TG content has been shown to be correlated with malignancy and metastasis in mouse and rat liver [59,76] and mammary tissue [73]. This finding is also consistent with an increase in alkylglycerol lipid abundances previously reported for malignant human hepatocellular carcinoma tissues compared to normal liver tissue [77].

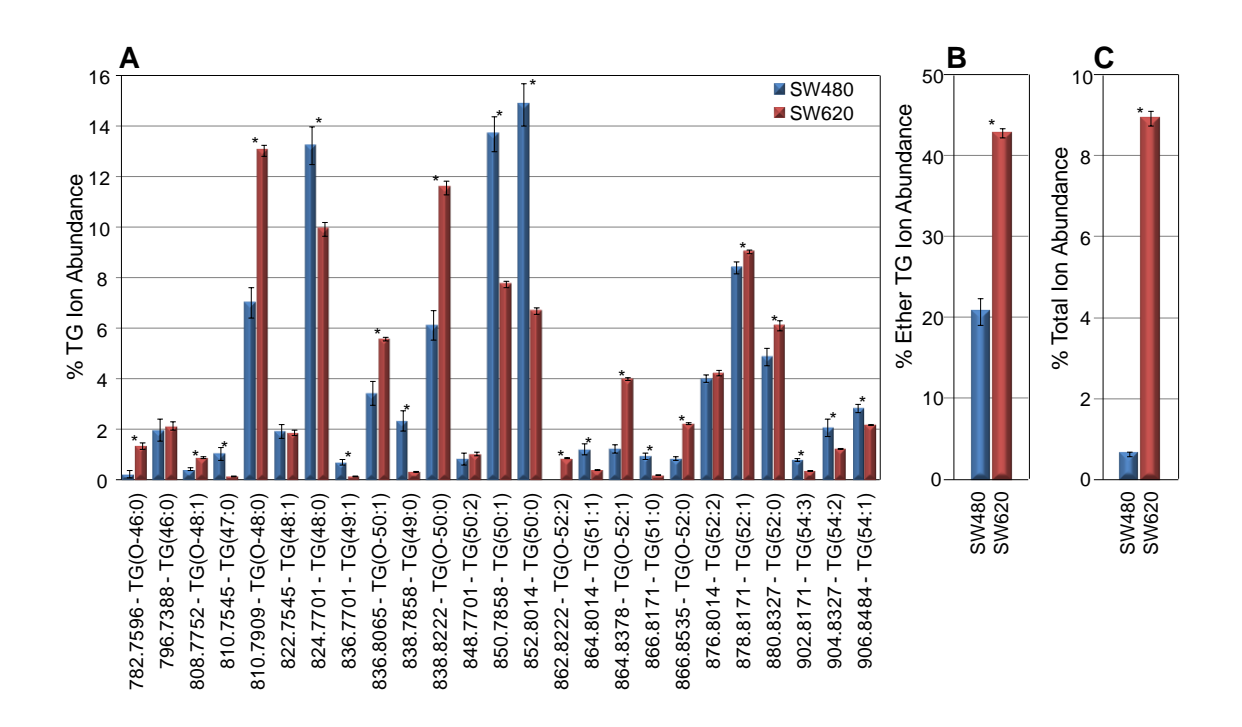


Figure 3.8 Quantitation of TG lipids from the d₆-DMBNHS derivatized SW480 and SW620 cell crude lipid extracts. (A) Percent individual TG ion abundances compared to the total ion abundance for all PE lipids. (B) Percent total etherlinked TG ion abundance compared to the total TG lipid ion abundance. (C) Percent total TG ion abundance compared to the total ion abundance for all identified lipids. n = 5, * = p < 0.01.

The results obtained from quantitative analysis of the DG and MG lipids are shown in Appendix A: Figures A.6 and A.7. Small increases in total DG and MG lipid ion abundances were observed between the SW620 and SW480 cells. For the individual DG lipids, the most obvious difference arose from a decrease in $DG_{(32:0)}$ and an increase in $DG_{(34:0)}$ lipids.

3.3.3 Sphingolipid Alterations

Significantly decreased $SM_{(42:1)}$ and $Cer_{(42:1)}$ lipid abundances (i.e., $SM_{(d18:1/16:0)}$ and $Cer_{(d18:1/16:0)}$) were observed in the SW620 cells, despite an overall increase in SM and Cer % total ion abundances (Appendix A: Figures A.8 and A.9, respectively). Importantly, numerous reports in the literature have previously associated decreased C_{16} -ceramide levels with the resistance of cells toward the activation of apoptotic signaling [254,266,267].

3.3.4 Sterol Lipid Alterations

No overall change was found in the level of Chol (Appendix A: Figure A.10). However, a dramatic approximately 80 fold increase was observed in the % lipid abundance of Chol esters. Large increases in sterol esters have previously been reported in human glioblastomas [253]. Furthermore, Chol ester abundances have also been positively correlated to increases in plasmalogen content [268].

3.2.4.2 High Resolution MS/MS Data Analysis for Molecular Lipid Characterization

For the phospholipids, HCD-MS/MS was performed in negative ionization mode on the deprotonated precursor ions, with the exception of PC lipids, which were analyzed as their formate adducts. Similarly, the sphingolipids were also

analyzed as their formate adducts in negative ionization mode [212]. It is important to note that formate adducts were employed here as opposed to the common acetate adduct, in order to eliminate the possibility of nominal mass overlap between the acetate adducts of ether-linked PC lipids with deprotonated ether-linked PE lipids. This is especially significant because the structural identification of ether-linked phospholipids relies heavily on observation of the acyl chain neutral loss product ions, and the fragments of ether PC and ether PE lipids containing 2 more carbons would have identical exact masses. example, $[PC_{(O-16;1/16:0)} + Ac]$ and $[PE_{(O-18;0/22:6)} - H]$ both have a nominal m/z of 776. During negative ion fragmentation, the PC lipid initially loses methyl acetate, forming [dimethyl PE(O-16:1/16:0) - H], that subsequently dissociates via the loss of 16:0 R'CHCO and RCOOH fatty acyl chains to give rise to product ions at m/z 464.3141 and 446.3035, respectively, which would have the same exact m/z values as a PE ion that had lost 22:6 R'CHCO and RCOOH fatty acyl chains. However, as the m/z of the formate adduct is 14 Da less than the acetate adduct, this overlap is not problematic and MS/MS and MS³ can be performed without ambiguity.

For the characterization of TG lipid ions, positive ion mode HCD-MS/MS (or CID-MS/MS followed by HCD-MS³) spectra were acquired to observe the neutral loss of characteristic fatty acids from the ammonium ion adducts at each of the identified precursor ion m/z values for these lipids, as previously described. The assignment of the fatty acyl chains for these lipids (Supplemental Tables,

Fhaner, et al. [269]) are listed in order from the shortest to the longest acyl chain, and not in terms of their *sn* position. Unfortunately, the ammonium adducts for the ether TG lipids and DG lipids were not sufficiently stable to allow their isolation for MS/MS or MS³ analysis. Therefore, these species are expressed simply in terms of their sum compositions.

From the information provided from the high-resolution/accurate mass, d₆-DMBNHS derivatization and formic acid treated MS spectra described above, a total of 354 and 368 lipid containing ions from the SW480 and SW620 cell lipid extracts, respectively, could initially be unambiguously assigned in terms of their molecular lipid identities (Table 3.1). Following isolation and fragmentation of the identified ions, 490 and 573 lipids could be characterized in the SW480 and SW620 derivatized lipid extracts at the molecular lipid level. Altogether, 600 and 694 individual lipid species in the SW480 and SW620 crude lipid extracts, respectively, were identified by either their sum composition or molecular lipid identity.

Table 3.1 Summary of the number of assigned lipid ions, identified lipids, and total lipid species from crude lipid extracts derived from the SW480 and SW620 cell lines.

	SW480			SW620		
Sub- Class	Sum Comp	Mol Lipids	Total	Sum Comp	Mol Lipids	Total
PC	85	93	130	80	125	154
PE	77	154	164	60	149	158
PA	15	30	30	12	26	26
PS	25	62	62	27	74	74
PI	24	33	39	19	32	36
PG	7	9	9	7	9	9
LPC	4	4	4	5	5	5
LPE	15	18	18	15	19	19
LPS	5	5	5	5	5	5
SM	17	1	17	17	1	17
Cer	6	0	6	6	0	6
TG	30	60	68	59	96	133
DG	24	0	27	26	0	30
MG	14	15	15	14	16	16
Chol	1	1	1	1	1	1
Chol Ester	5	5	5	15	15	15
Total	354	490	600	368	573	694

3.4 Conclusions

In the results described herein, we have demonstrated that selective functional group derivatization reactions combined with high resolution/accurate mass spectrometry can serve as an effective 'chemical' strategy to resolve isobaric mass lipids from within complex mixtures, as well as to enhance the ionization sensitivity and detection of low abundance lipid species, without requirement for chromatographic fractionation or differential extraction steps prior to analysis. The application of this novel 'shotgun' lipidomics approach to identify

and quantify differences in the abundances of >600 individual lipids in 4 major lipid classes and 36 lipid subclasses from the SW480 and SW620 cell lines, represents the most comprehensive study to date to analyze differences in 'global' lipid profiles between primary and metastatic colon cancer cells. The results obtained therefore may provide important new insights into the role of aberrant lipid metabolism in the onset and progression of colon cancer.

Chapter 4

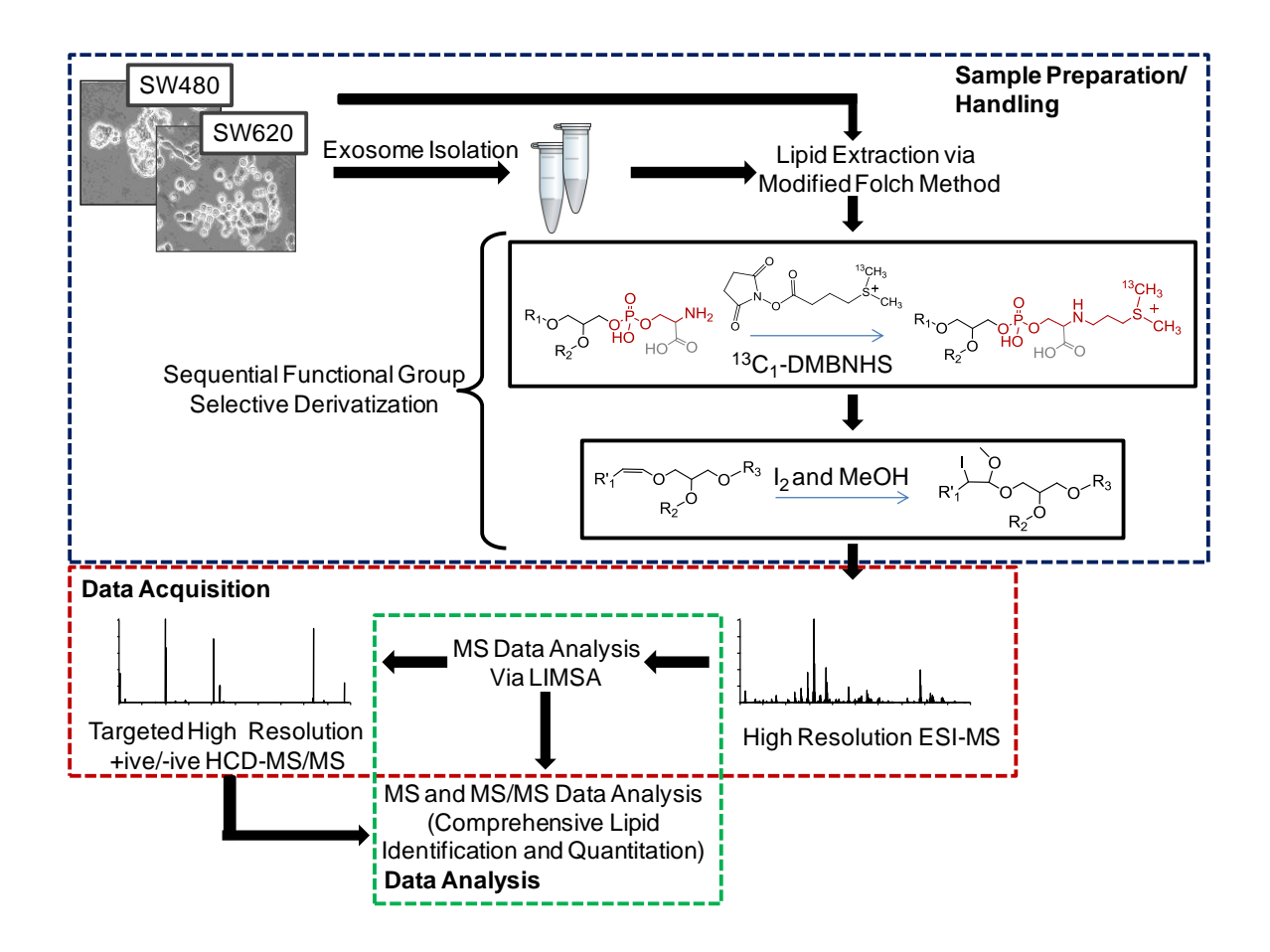
Lipidome Analysis of Colorectal Cancer Cells and their Secreted Exosomes

4.1 Introduction

As discussed in Chapter 1, exosomes have been implicated in the promotion and progression of cancer metastasis. However, the specific exosomal molecules responsible for these functional responses, and exploration of the potential of exosome derived lipid profiles as biomarkers of colorectal cancer malignancy and metastatic capacity, not been explored. It has been demonstrated previously that lipids are highly involved with the process by which exosomes interact with cells [270] and may act as lipid mediators [271]. The make-up of their lipid membrane has an affect how the exosomes interact with cells whether by fusion, staying on cell surfaces or taken up by endocytosis [272]. Engulfed exosomes enable target cells to concentrate bioactive lipids and exosomal contents in their endosomes [273]. Development of the 'shotgun' mass spectrometric lipidome analysis methods described in chapter 2 that allows complete lipidomic profiling from small amounts of starting material and with limited sample handling provides the ability to analyze these small vesicles to identify possible biomarkers. Furthermore, differentiation of exosome lipidomes from parent cell lipidomes may identify novel roles for lipid species in cancer exosome function and promotion of metastasis.

4.2 HRMS Lipidomic Analysis of SW480 and SW620 Cells and Exosomes

The previous chapters have outlined methods for high resolution mass spectrometry (HRMS) based lipidome analysis. For this experiment, lipid identification and analysis by HRMS involves initial isolation of cells and exosomes followed by crude lipid extraction of non-polar lipids, sequential functional group derivatization using ¹³C₁-DMBNHS plus iodine/methanol, and high-resolution direct infusion MS and CID-MS/MS analysis (Scheme 4.1).



Scheme 4.1 Workflow for exosome isolation, lipid extraction, derivatization and data analysis using $^{13}C_1$ -DMBNHS followed by iodine and methanol derivatization method for lipid analysis.

4.2.1 Isolation, Extraction and Derivatization of Cells and Crude Exosomes

Exosomes were isolated every 3-4 days by differential centrifugation from the spent medium of routinely cultured SW480 and SW620 cells [274]. Cells were also collected. Protein concentration of cells and exosomes was determined by 1D-sodium dodecyl sulfate-polyacrylamide gel electrophoresis (SDS-PAGE)/SYPRO® Ruby protein staining/densitometry [275]. Protein

concentration was determined to be 352 μ g/10⁶ SW480 cells and 249 μ g/10⁶ SW620 cells. Total exosome protein amount for the exosomes was determined to be 110 μ g and 72 μ g for the SW480 and SW620 crude exosomes, respectively. Cell and exosome lipids were extracted using a modified Folch method [108,110] then subjected to amine specific derivatization with 13 C₁-DMBNHS followed by reaction with iodine and methanol as outlined in Chapter 2. All materials and methods are described in Chapter 5.

4.2.2 HRMS of Cell and Exosome Lipid Extracts Derivatized with ¹³C₁-DMBNHS and Iodine/Methanol

Full derivatization of the lipid extracts with ¹³C₁-DMBNHS and lodine/Methanol (as explained in Chapters 2 and 5) enabled the collection of data with the high-resolution instrument, LTQ Orbitrap Velos, from a single spectrum without the need for comparison to underivatized spectra, as is the case with d₆-DMBNHS derivatization and mild acid hydrolysis. All samples were analyzed via 'shotgun' nano ESI-MS. High resolution mass spectra were acquired across the range of m/z from 200-2000 using the FT analyzer (100,000 resolving power) and were signal averaged for 2 minutes. Data analysis was performed using LIMSA [233] as described in chapters 1 and 3. The data from the LIMSA output was then normalized to the protein content of each sample, to give a normalized ion abundance/μg of protein. One-way ANOVA (Microsoft Excel Software) was

used to evaluate differences (p<0.01) among SW480 and SW620 cells and exosomes. Student's t-test with 2 tailed distribution, two sample unequal variance was used to evaluate differences in the individual ion abundances between the SW480 and SW620 cell extracts, SW480 cell and exosome extracts, SW620 cell and exosome extracts, and SW480 and SW620 exosome extracts, with p < 0.01 considered statistically significant.

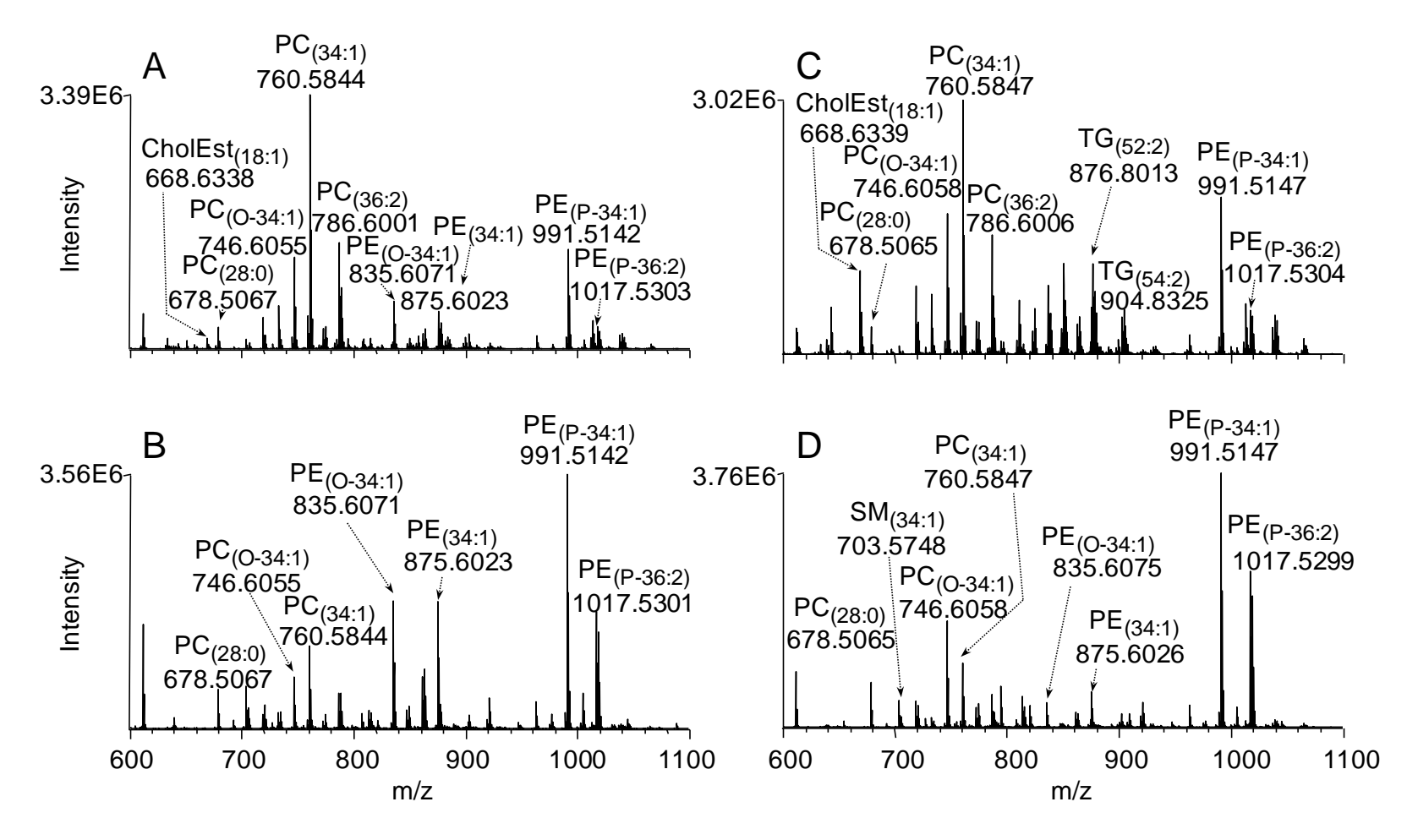


Figure 4.1 Positive ion mode ESI high-resolution mass spectrometric analysis (m/z 600-1100) of crude lipid extracts derivatized with 13 C₁-DMBNHS followed by Iodine and Methanol from the human adenocarcinoma cell lines, (A) SW480 and (B) SW620, and their secreted exosomes, (C) SW480 Exosomes and (D) SW620 Exosomes. The internal standard lipid PC_(28:0) was included to enable relative quantification of the observed lipid species.

The high resolution/accurate mass spectra of the ${}^{13}\mathrm{C}_1\text{-DMBNHS}$ and iodine/methanol derivatized SW480 and SW620 cell and exosome lipid extracts are shown in Figures 4.1A - 4.1D. Comparison of the SW480 and SW620 cellular lipid extracts were discussed in Chapter 3. From the spectra shown in this figure, several qualitative changes are observed between the exosomes and their respective cells. Figures 4.1A and 4.1B show the SW480 cell and exosome extracts, respectively. Relative to the internal standard, PC_(14:0/14:0), the ions at m/z 760.5844 representing $PC_{(34:1)}$ and m/z 786.6001 ($PC_{(36:1)}$) (i.e., the two most abundant diacyl PC lipids) decreased in the exosomes by approximately 60%. Although the ion at m/z 746.6058 ($PC_{(O-34:1)}$) (i.e., the most abundant plasmanyl PC lipid) has also decreased, the ratio of that ion compared to m/z 760.5844 has increased. Conversely, the PE lipid ions at m/z 835.6071, m/z 875.6023, m/z 991.5142 and m/z 1017.5303 assigned as PE(34:1), PE(36:2), PE_(P-34:1), and PE_(P-36:2), respectively, increased significantly indicating an overall enrichment of PE lipids in the exosome population and an increase in the ratio of plasmalogen PE to diacyl PE species. Similarly in the SW620 cells and exosomes (Figures 4.1C and 4.1D, respectively), the diacyl and plasmanyl PC lipid ions at m/z 760.5847 and m/z 786.6006 decreased, while the plasmenyl PE lipid ions at m/z 991.5147 (PE(P-34:1)) and m/z 1017.5303 (PE(P-36:2)) increased significantly. However, the plasmanyl PC ion at m/z 746.6058 (PC_(O-34·1)) only decreased slightly in relation to the internal standard, m/z 678.5065, in the SW620 exosomes and there was a slight decrease in the diacyl PE lipids at m/z 835.6075 and m/z 875.6026. As was discussed in Chapter 3, the TG and Chol Ester concentrations were significantly higher in the SW620 cells compared to the SW480 cells. The Chol Ester (m/z 668.6338, Chol Ester_(18:1)) and TG (m/z 850.7858, TG_(50:1) and m/z 876.8013, TG_(52:2)) species observed in the SW620 cells were of much lower abundance the SW620 exosomes.

Comparison of the SW480 and SW620 exosome lipid extracts also revealed alterations in their lipid content. For example, a decrease in the abundant diacyl $PC_{(34:1)}$ and $PE_{(34:1)}$ species was observed from the SW480 to SW620 exosomes compared to the internal standard. $PC_{(O-34:1)}$ increased by nearly 2-fold compared to the internal standard whereas $PE_{(O-34:1)}$ (m/z 835.6071) and $PE_{(34:1)}$ (m/z 875.6023) decreased by almost 4- and 3-fold, respectively, in the SW620 exosome lipid extracts.

4.3 Comparison of Total Lipids from SW480 and SW620 Cell and Exosome Lipid Extracts

Peak lists including intensities were extracted from re-calibrated high-resolution MS spectra of the derivatized lipid extracts and placed into a Microsoft Excel workbook. Data analysis utilizing LIMSA and an in-house database of over 21,000 lipid identities gave identification and relative quantitation of lipid peaks in the MS spectra. Tables containing lipid sub-structures and chemical formulas as

well as formulas for building the lipid ions with the adducts utilized in this method are located in Appendix B. The output of relative concentration for each lipid identified was then divided by the total amount of protein (in µg) for each sample. Figure 4.2 exhibits the relationships of lipid ion abundances normalized to the internal standard (PC_(28:0) at 500nM) of each individual lipid sub-class expressed as normalized abundance per µg of total protein. As expected from the spectra in Figure 4.1, the normalized PE lipid ion abundance increased significantly in the exosomes compared to their respective cells. The observed alterations in total PE was mirrored for total LPE, albeit at a lower abundance. Although the spectra in Figure 4.1 appear to indicate that PC abundance decreased in the exosomes, when normalized to the total protein concentration, the total PC abundance was determined to slightly increase in the exosomes compared to the cells. Large increases in PS, PG (SW620 exosomes only) and SM species were also found in the exosomes compared to their respective cells, while decreases in total TG and Chol Est were observed.

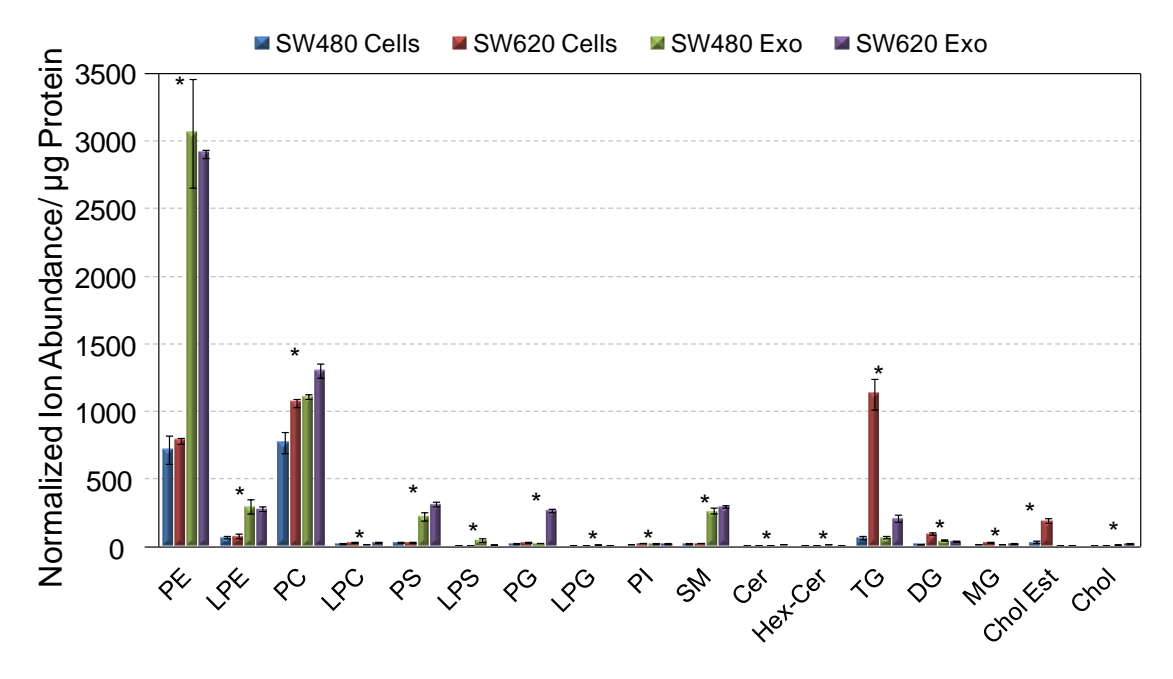


Figure 4.2 Distribution of normalized lipid ion abundance/ μ g protein for each lipid sub-class from the $^{13}C_1$ -DMBNHS and iodine/methanol derivatized SW480 and SW620 cell and exosome crude lipid extracts. * = p < 0.01.

The acyl, plasmanyl (O-) and plasmenyl (P-) distributions for PE, PC and PS in the cell and exosome lipid extracts are shown in Figure 4.3A-C. Statistically significant (p < 0.01) increases in plasmanyl and plasmenyl containing phospholipids among the cells and exosomes were observed with the largest increases in plasmenyl PE and plasmanyl PC and PS, especially in the SW620 exosomes. Increases in the normalized diacyl abundances were also detected in the PS population.

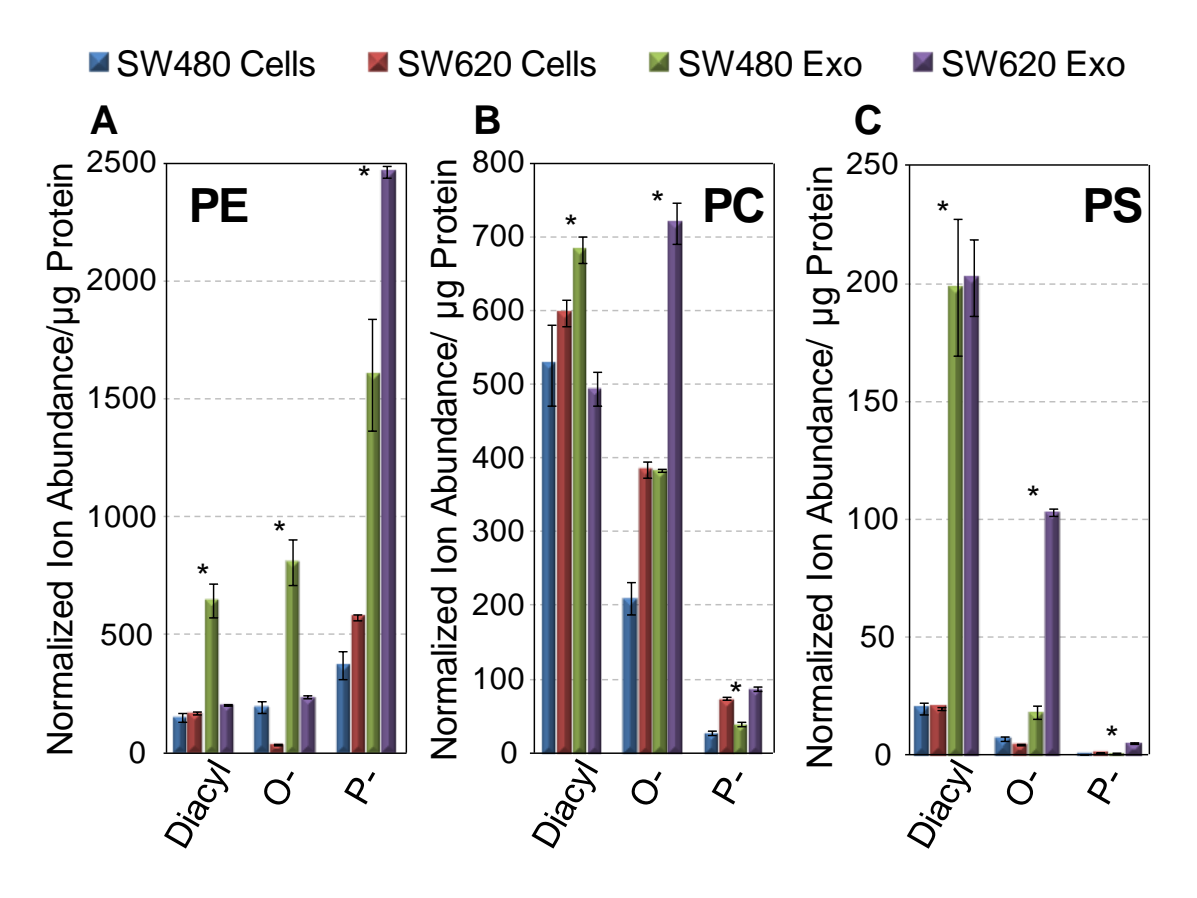


Figure 4.3 Diacyl, alkyl (O-) and alkenyl (P-) distribution of each lipid sub-class from the $^{13}\text{C}_1$ -DMBNHS and iodine/methanol derivatized SW480 and SW620 cell and exosome crude lipid extracts: (A) PE, (B) PC, and (C) PS lipids. * = p < 0.01.

The alterations observed in lipid sub-classes are similar to those reported previously [98,101] with the exosomes being enriched in the phospholipid and sphingolipid sub-class compared to their parent cells.

4.4 Comparison of Lipid Sum Composition Alterations Among SW480 and SW620 Cells and Exosomes

4.4.1 Glycerophospholipids of SW480 and SW620 Cell and Exosome Extracts

The PE lipids represent a lipid sub-class that underwent the largest alterations in abundance in Figures 4.1 and 4.2. Figure 4.4 illustrates the changes in individual PE lipid sum composition normalized abundances (only species above normalized ion abundances of 10/µg protein are shown) among the cell and exosome extracts. The majority of the total PE lipid ion abundance corresponded to species containing between 32 and 36 carbons, with one or two carbon-carbon double bonds. Notably, nearly 70% of the PE lipid ion abundance in the SW620 exosomes arises from three plasmenyl species: PE(P-34:1), PE(P-36:1) and PE(P-36:2). Plasmanyl PE species, on the other hand, albeit lower in the SW620 samples, are also most abundant in the same region for the exosomes with PE(O-34:1), PE(O-36:1) and PE(O-36:2) increasing in the exosomes compared to the cells.

The increase in both types of ether PE in the exosomes could affect how exosomes to interact with surrounding cells and/or target cells for metastasis, whether by fusion or endocytosis, thereby aiding the transfer exosomal materials [93,100,272,273,276]. The antioxidative properties of the plasmenyl lipids [277] may protect exosomes from degradation as they travel through the bloodstream to the target site.

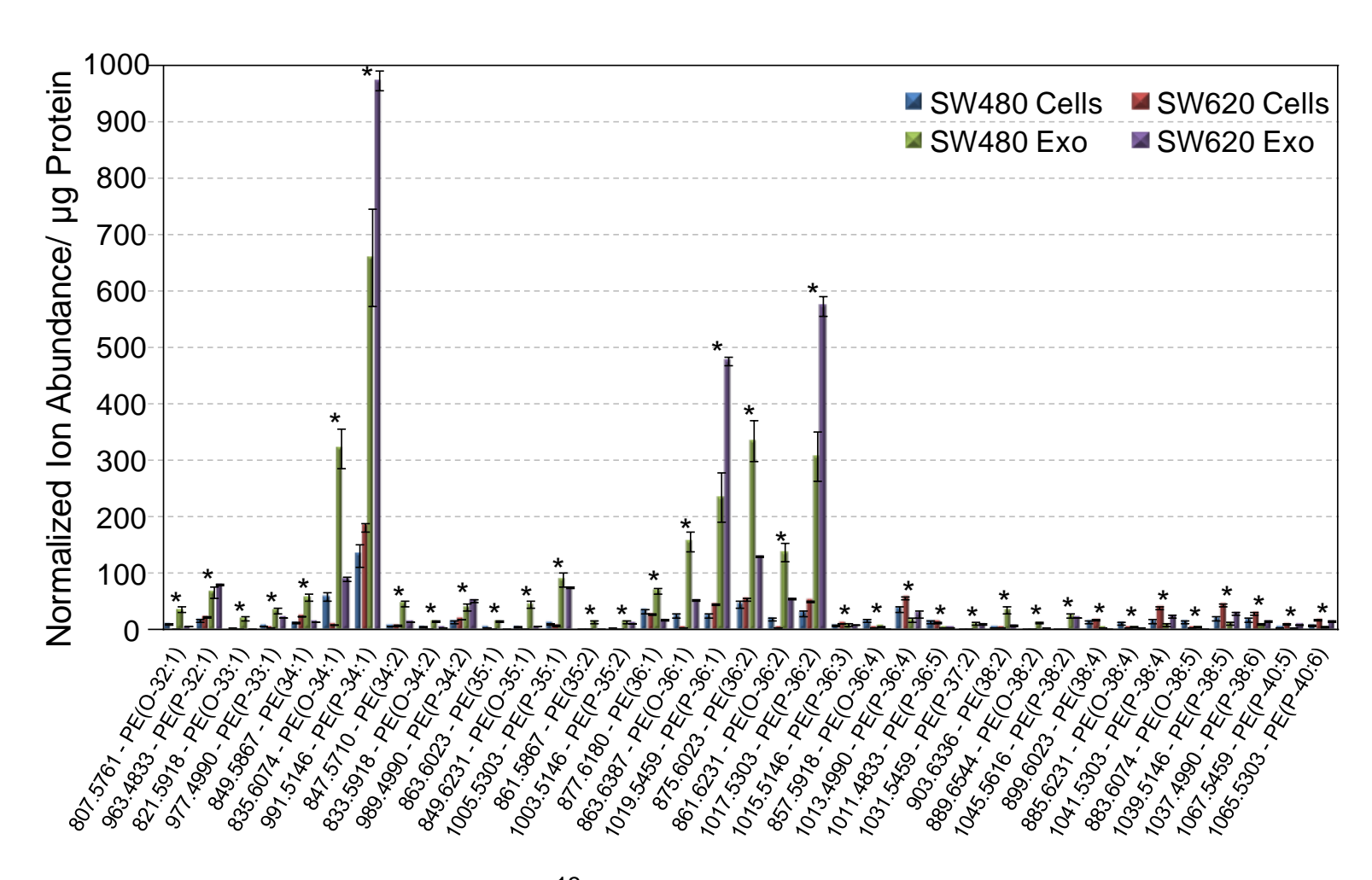


Figure 4.4 Quantification of PE lipids from the 13 C₁-DMBNHS and iodine/methanol derivatized SW480 and SW620 cell and exosome crude lipid extracts for individual lipid sum composition normalized abundances/µg protein above 10. * = p < 0.01.

Figure 4.5 demonstrates the alteration in the lipid sum compositions of the PC lipids present in the SW480 and SW620 cells and exosomes. The largest alteration is in the amount of PC_(O-34:1) in the exosomes compared to the cells and each other; the amount in the SW620 exosomes is over 2x the amount in the SW620 cells and the SW480 exosomes. This is also the case with other plasmanyl PC lipids such as PC_(O-36:1) and PC_(O-36:2). Plasmenyl PC species, PC_(P-34:1), PC_(P-36:1) and PC_(P-36:2), are also higher in concentration in the SW620 cells and exosomes than the SW480 cells and exosomes. A higher abundance of plasmanyl and plasmenyl PC lipids was also found previously in lung, breast and prostate cancer cells when compared to benign tumors and normal similar tissue [63], and were also reported to be higher in prostate cancer exosomes compared to their parent cells [101].

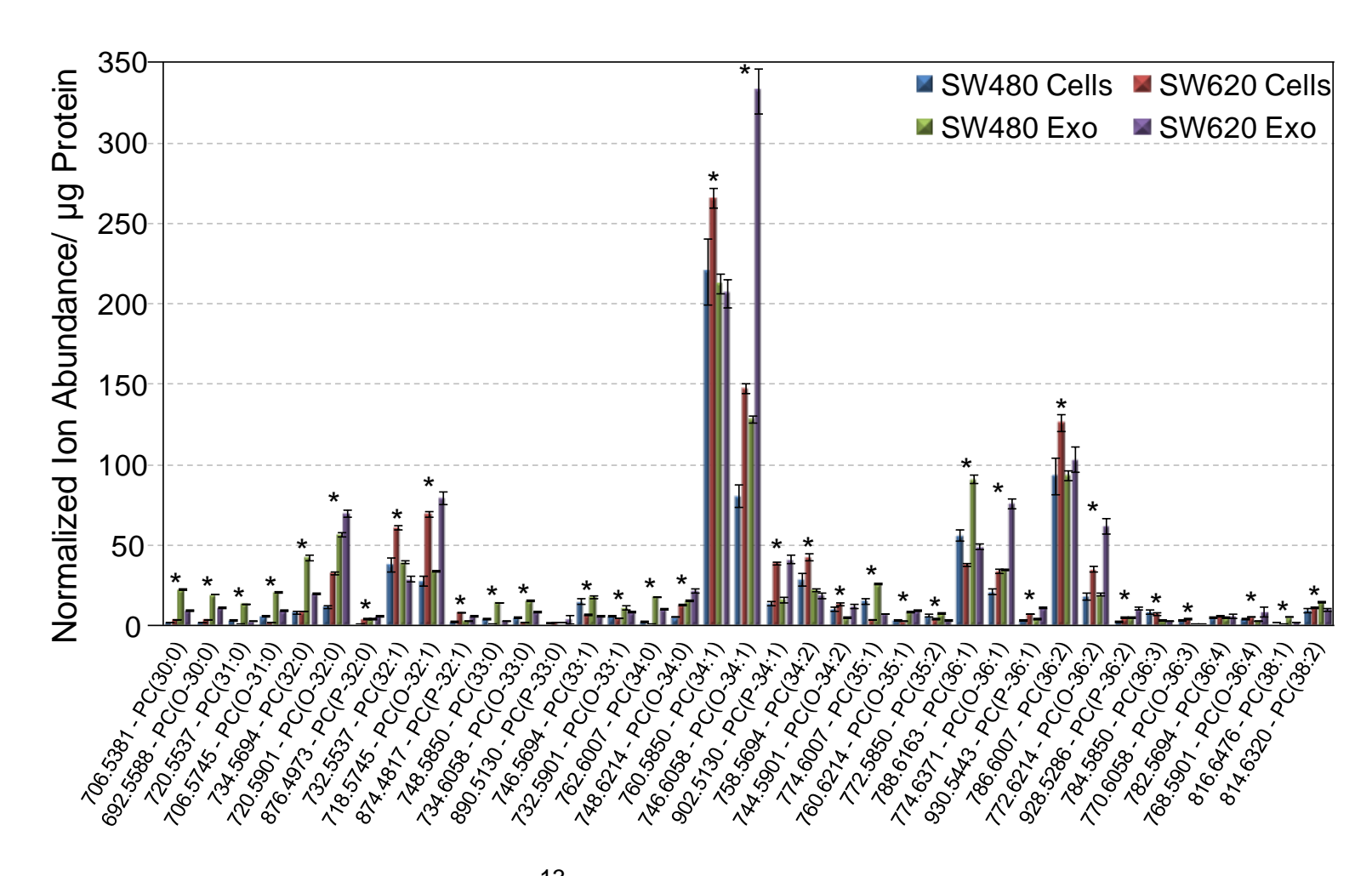


Figure 4.5 Quantification of PC lipids from the 13 C₁-DMBNHS and iodine/methanol derivatized SW480 and SW620 cell and exosome crude lipid extracts for individual lipid sum composition normalized abundances/µg protein above 5. * = p < 0.01.

PS lipids are highly enriched in the exosomes, as shown in Figure 4.2. Similar to PC, the plasmanyl PS lipid sub-class increased in the exosomes when compared to their parent cells, especially in the SW620 exosomes. Individual PS sum compositions are compared in Figure 4.6. Although the distribution of plasmanyl PS species is similar to PC lipids in Figure 4.2, the sum compositions contributing to those alterations differ. For PS, the largest enrichment in plasmanyl species is in PS(O-36:0) and PS(O-36:1) as opposed to PC(O-34:1). Also, the exosomes are enriched in diacyl PS with vast contributions from PS(36:1), PS(36:2), PS(38:2) and PS(40:2).

The enrichment of PS in exosomes compared to their parent cells was also observed in the PC-3 prostate cancer cells by Llorente, et al [101] including the increase in PS_(36:1). Interestingly, vesicles made for drug delivery to cancer cells were more successful when there was a higher ratio of PS in the membrane and were unsuccessful without PS [278]. Two reasons are possible: the conical shape of PS enables vesicles' small size which allows more contact points with cells and/or the PS enhances signaling to the cells via receptor binding which releases the drug [278]. Since smaller vesicles with lower PS amount did not have the same enhanced drug affect, it is more likely that PS signaling is the contributing factor. This may also be the case for cell lines with higher metastatic potential. Since exosomes have been implicated in 'educating' cells for metastasis, PS may be a key component needed for the delivery of exosomal materials.

One of the most remarkable alterations between the cells and exosomes is the enrichment in plasmanyl and plasmenyl glycerophospholipids. This is especially important to note with respect to the role that these species play in the physical properties of membranes, such as structure, fluidity and dynamics [258] and their subsequent effect may play an important role in regulating fusion or endocytosis, intracellular transport and signal transduction [259-261,272]. These properties may positively affect the exosomes' ability to interact with cells to pass on their biological information. This data is consistent with the recent implication of exosomes 'educating' cells at potential sites of metastasis [93] as the more metastatic exosomes (i.e., SW620) have the largest amount of ether lipids present per µg of protein. Furthermore, as mentioned in Chapter 3, Benjamin, et al. revealed that cells with increased AGPS expression and ether lipid content displayed higher cell survival and tumor growth [75]. Notably, exosomes display remarkably higher ether lipid content than their parent cells, and the more metastatic exosomes (SW620) contain a higher ether lipid content than the SW480 exosomes. Therefore, it is possible that the lipid composition of the exosomal membranes may be directly associated with the development of the "pre-metastatic niche" and promotion of tumor metastasis.

All other glycerophospholipid sub-class sum composition comparisons, including LPE, LPC, LPS, PG, LPG and PI are present in Appendix C.

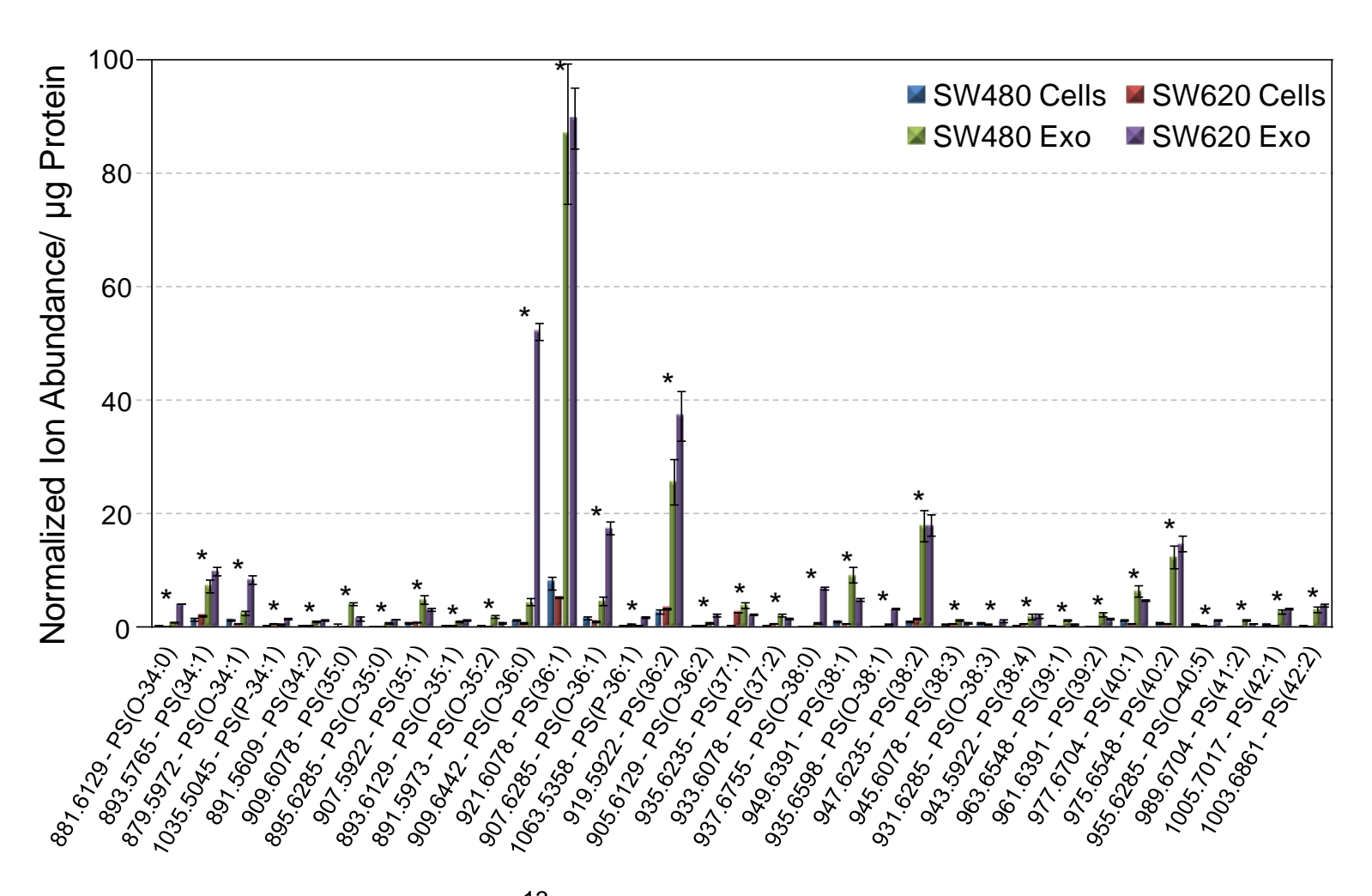


Figure 4.6 Quantification of PS lipids from the 13 C₁-DMBNHS and iodine/methanol derivatized SW480 and SW620 cell and exosome crude lipid extracts of individual normalized lipid sum composition abundances/µg protein. * = p < 0.01.

4.4.2 Sphingolipids of SW480 and SW620 Cell and Exosome Extracts

A large contribution to the enrichment of SM in the exosomes compared to the cells shown in Figure 4.2, is due to SM(34:1) and the long chain SM species, $SM_{(42:1)}$ and $SM_{(42:2)}$ (Figure 4.7). Increases in total SM in exosomes were also observed from mast cells and dendritic cells [279]. The same acyl chains are largely responsible for the enrichment in Cer in the exosomes, along with Cer_(34:0) (Figure 4.8). Ceramides have been implicated in promoting exosome budding from the endosomes; thus not only are they enriched, but also are important in the formation of exosomes [98]. Interestingly, C16:0, C24:0 and C24:1 containing Cer species were reported to be enriched in tumors compared to normal tissues in patients with head and neck squamous cell carcinoma [280] which are also more abundant in the SW620 exosomes than the SW480 exosomes. The increased abundances of sphingolipids (including Hex-Cer found in Appendix C, Figure C.7), were also observed by Llorente, et al. in the prostate cancer exosomes [101]. The presence of gangliosides were also observed in the prostate cancer exosome samples [98,101]. Unfortunately however, these more polar lipids are most likely lost in the aqueous partition of the modified Folch extraction employed here and therefore not observed in the spectra obtained from the SW480 and SW620 cells or exosomes.

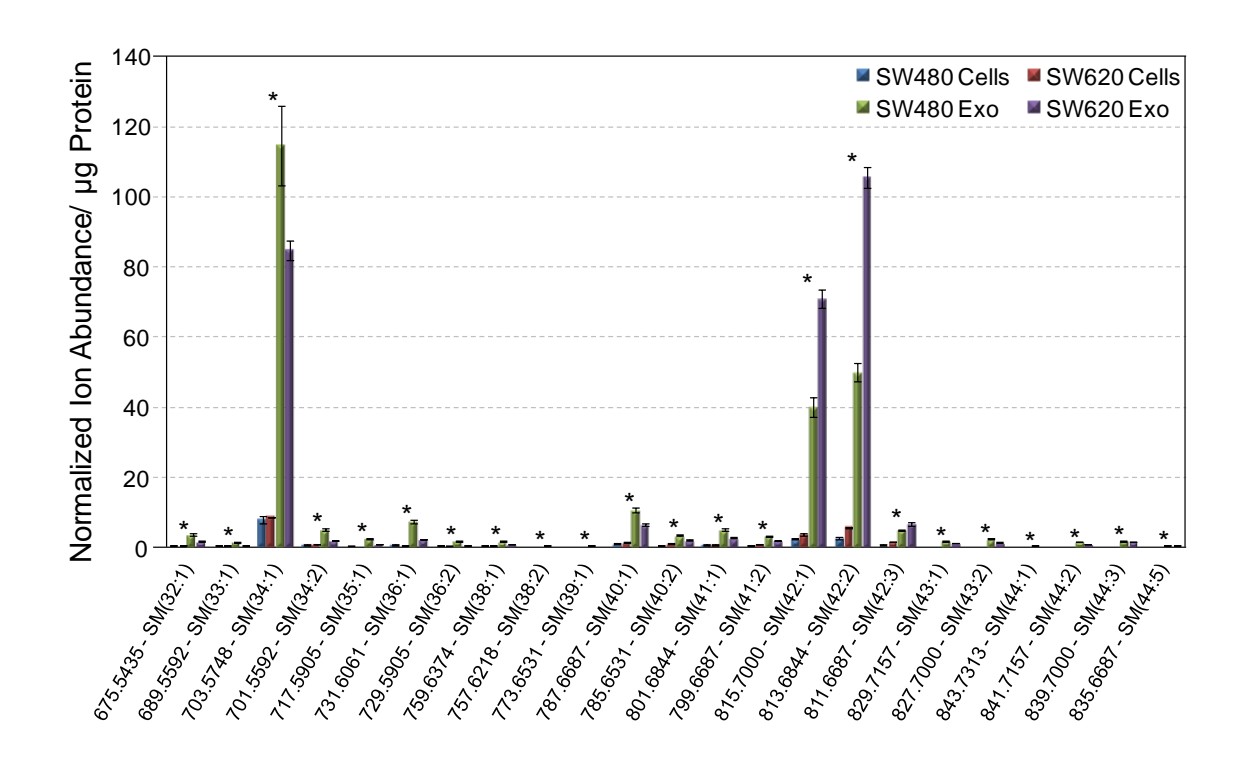


Figure 4.7 Quantification of SM from the $^{13}C_1$ -DMBNHS and iodine/methanol derivatized SW480 and SW620 cell and exosome crude lipid extracts. Individual normalized lipid sum composition abundances/µg protein. * = p < 0.01.

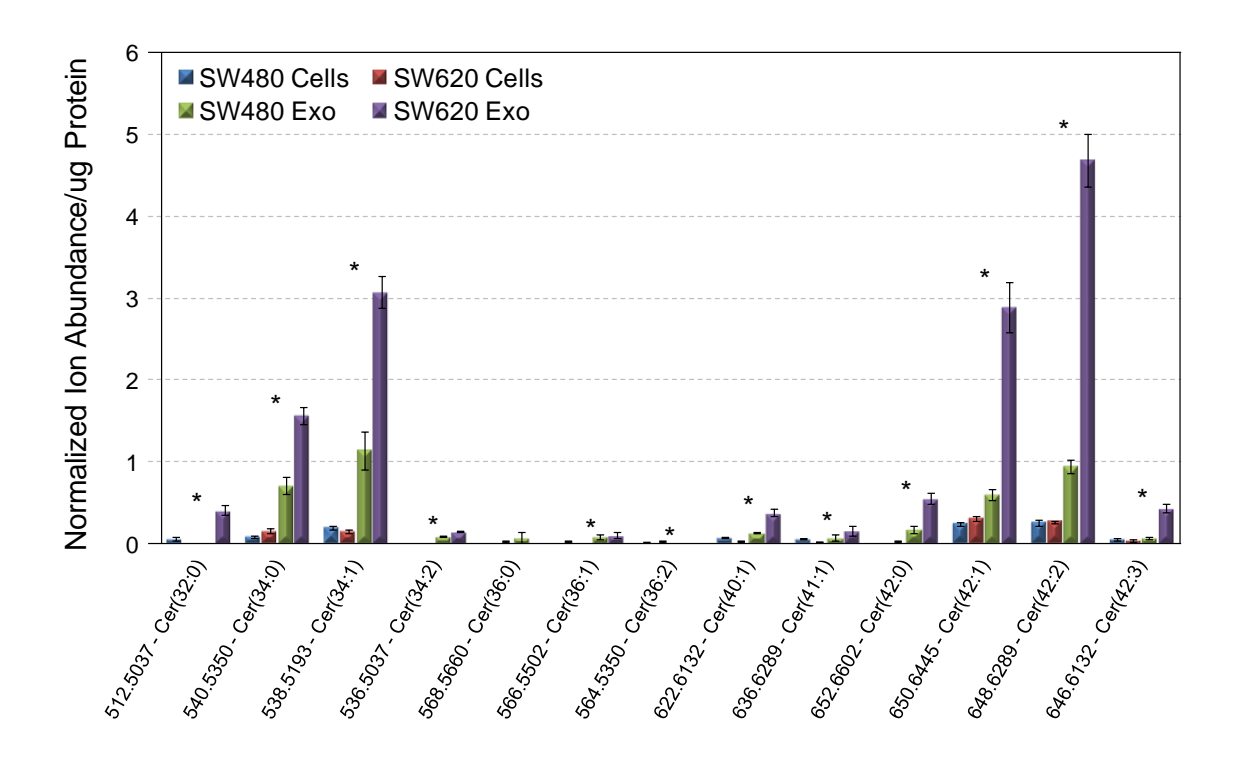


Figure 4.8 Quantification of Cer from the 13 C₁-DMBNHS derivatized SW480 and SW620 cell and exosome crude lipid extracts. Individual normalized lipid sum composition abundances/µg protein. * = p < 0.01.

4.4.3 Glycerolipids of SW480 and SW620 Cell and Exosome Extracts

In contrast to the enrichment of glycerophospholipids seen in Figure 4.2, the glycerolipids in the exosomes were decreased compared to their cells. Figure 4.9 illustrates the normalized lipid abundances/ μ g of protein of the sum compositions of the most abundant TG species found in the cells and exosomes. The plot is mostly dominated by the presence of TG lipids in the SW620 cells, albeit with a few species (TG(52:3), TG(54:4) and TG(54:5)) being more abundant in the SW620 exosomes. The increase in TG species in the SW620 cells compared to the SW480 cells is likely due to increased *de novo* fatty acid

synthesis used to supply the membrane with fatty acids for increased proliferation [55,56,265]. Ether-linked TG lipids are also increased in the SW620 cells in comparison to the SW480 cells which are the likely source of the increase in ether-linked glycerophospholipids in the cells, such as PC. However, since exosomes are formed inside the cells, there is no need for a *de novo* synthesis of structural lipids within the exosomes, which is consistent with the lack of alkyl or alkenyl linked TG lipids in the exosomes. The large increase in plasmanyl PC, which is not formed by *de novo* synthesis in the exosomes, suggests a change in the makeup of the endosomes or organelles from which the exosomes are formed within the SW480 and SW620 cells [281].

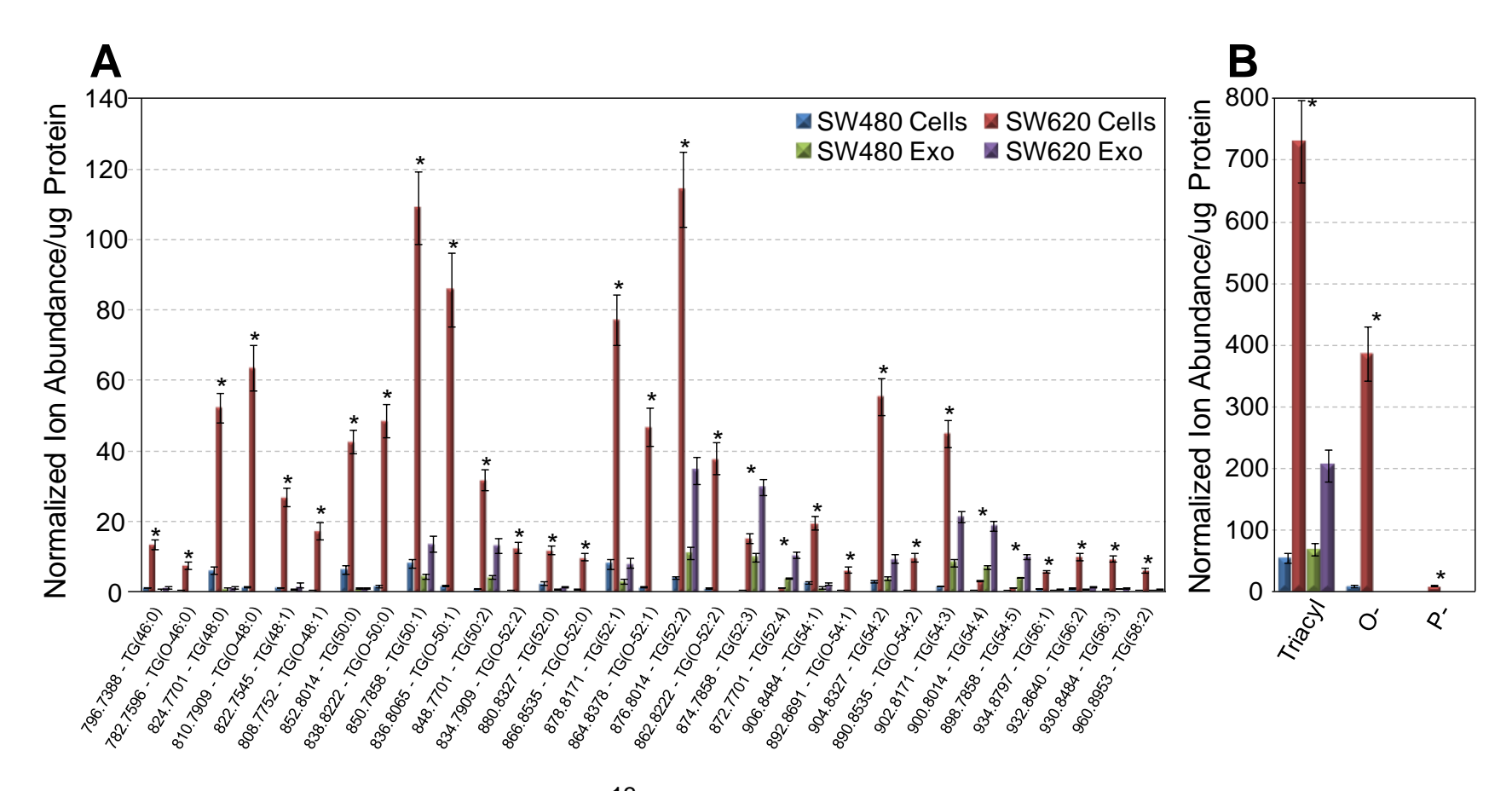


Figure 4.9 Quantification of TG lipids from the 13 C₁-DMBNHS derivatized SW480 and SW620 cell and exosome crude lipid extracts. (A) Individual normalized lipid sum composition abundances/µg protein and (B) tiacyl, alkyl (O-) and alkenyl (P-) distribution. * = p < 0.01.

DG and MG sum composition comparisons are found in Appendix C, Figure B.6. The abundances of DG and MG in the cells and exosomes were much lower than that of the TG lipids. However, the abundances of each sum composition among the cells and exosomes were much more similar for DG and MG lipids than they were for the TG species.

4.4.4 Sterol Lipids of SW480 and SW620 Cell and Exosome Extracts

The trend of enriched lipid content in the exosomes continues with free cholesterol (Chol), which is up in both exosome samples compared to their parent cells. However, Chol Esters (Appendix C, Figure C.8) are virtually not detected in the exosomes, with only one Chol Ester species being present in the SW620 exosomes and none in the SW480 exosomes. Like TG, this is to be expected since the function of Chol Esters is in fatty acid trafficking and metabolism within cells and not as part of the lipid membrane.

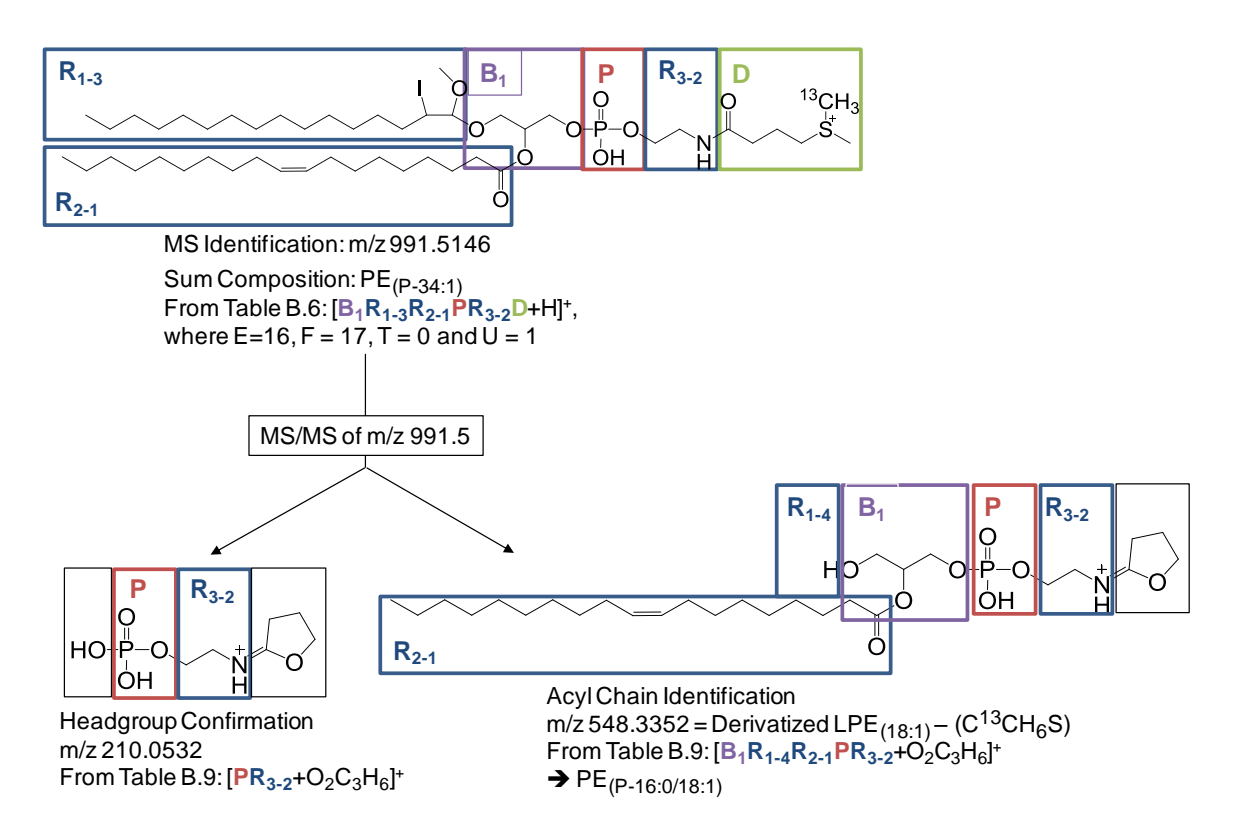
4.5 HCD-MS/MS Analysis for Molecular Lipid Characterization of HRMS Identified Lipids

As discussed in Chapters 1 and 3, MS identification of lipid ions provides sum composition information only. In order to confirm the lipid headgroup and identify the individual fatty acyl/alkyl/alkenyl substituents, MS/MS must be performed. For complete lipid structural identification, both positive and negative

ionization mode HCD-MS/MS is utilized. Tables containing the methods and specific fragments used for lipid sub-class verification and fatty acyl/alkyl/alkenyl substituent identification in both positive and negative ionization mode are located in Appendix B.

4.5.1 Positive Ionization Mode HCD-MS/MS

Fragmentation of the lipid ions identified from the lipid extracts derivatized with ¹³C₁-DMBNHS and iodine/methanol was performed in positive ionization mode for fatty acyl/alkenyl substituent identification and headgroup verification for plasmenyl phospholipids, TG, Cer and SM. Plasmenyl PC lipids were verified by the presence of an ion at m/z 184.0739. Plasmenyl PS and PE lipids were verified by the presence of ions at m/z 254.0430 and m/z 210.0532, respectively, as described in Chapter 2. Plasmenyl PC, PE and PS fatty acyl/alkenyl substituents were identified by the loss of the iodine/methanol derivatized *sn*-1 chain. An example of how the characterization of a species of plasmenyl PE lipid, PE(P-34:1), was achieved is shown in Scheme 4.2.



Scheme 4.2 Acyl and alkenyl chain identification and headgroup confirmation for the derivatized plasmenyl PE lipid, PE_(P-16:0/18:1), by MS/MS in positive ionization mode.

The presence of SM lipids was verified by the presence of the phosphocholine headgroup at m/z 184.0739. The identity of the sphingoid backbone, and indirectly the fatty amide, was found by the presence of an ion corresponding to the loss of water from the protonated sphingoid backbone. The sphingoid backbone of ceramide species were found by isolating and fragmenting the $\left[\operatorname{Cer} + \operatorname{H} - \operatorname{H}_2\operatorname{O}\right]^+$ precursor ion, which is readily formed in the ion source. Similar to SM, the protonated sphingosine/sphinganine fragment ion indirectly provides information on the identity of the fatty amide [195].

The fatty acyls that make up TG lipids were identified by the neutral loss of ammonia and the fatty acids from the ammoniated adducts. Masses pertaining to

the neutral losses of odd and even chain fatty acids were identified and grouped together to make the number of carbons and double bonds in three fatty acids equal the sum composition of the TG lipid that was isolated, without duplication for *sn* position [199]. For example, a TG_(52:1) precursor ion that yielded fatty acid neutral losses corresponding to ammonia and FA_(14:0), FA_(16:0), FA_(16:1), FA_(17:0), FA_(18:0), FA_(18:1), FA_(19:1), FA_(20:0) and FA_(20:1) was assigned as TG_(14:0_18:0_20:1), TG_(14:0_18:1_20:0), TG_(16:0_16:0_20:1), TG_(16:0_16:1_20:0), TG_(16:0_16:0_10:1) and TG_(17:0_16:0_19:1). Unfortunately, O-TG and P-TG lipid fatty acyl/alkyl/alkenyl substituents were unable to be identified by this method due to a lack of ion isolation efficiency in the ion trap associated with low ammonium ion adduct stability.

4.2.3.2 Negative Ionization Mode HCD-MS/MS

All phospholipids, other than the plasmalogens, were characterized using negative ionization mode HCD-MS/MS. Prior to introduction to the mass spectrometer, samples were derivatized with iodine and methanol (i.e. not additionally with DMBNHS) simply to separate plasmenyl species from plasmanyl species. Diacyl and plasmanyl PC were fragmented from their formate adducts in negative ionization mode. Upon isolation and fragmentation, a loss of methyl formate verified the choline headgroup (NL 60.0221) and two other fragments identified the fatty acyl/alkyl chains. Lipid identification including classification of

the *sn* position, required the fragments associated with the neutral loss of the fatty acyl as a ketene [173] as well as the presence of the deprotonated fatty acid associated with the *sn*-2. If the parent ion was too low in abundance to form the deprotonated lysodimethylethanolamine fragment, the acyl chains could still be identified by the presence of the two deprotonated fatty acids which, when combined, total the number of carbons and double bonds of the sum composition. However, *sn* position cannot be assigned in these cases and the lipid was then notated with a "_" in place of the "/" [4]I, as described in Chapter 1. An example of how characterization of diacyl PC lipids is performed is shown in Scheme 4.3.

Scheme 4.3 Acyl chain identification and headgroup confirmation for the PC lipid, PC_(16:0/18:1), by MS/MS in negative ionization mode.

Verification of the headgroup of diacyl PE and plasmanyl PE in negative ionization mode was achieved by the presence of an ion at m/z 196.0375; however, this ion is not typically highly abundant and was not present in many cases due to other, more favorable fragmentation pathways. Similar to PC, fatty acyl/alkyl identification including classification of the *sn* position, required the fragments associated with the neutral loss of the *sn*-2 fatty acyl as a ketene [173] as well as the presence of the deprotonated fatty acid associated with the *sn*-2 position. Both fragments are required if the nominal m/z isolated includes both

the formate adduct of a PC and deprotonated PE because the Iyso PE fragment formed is the same exact m/z as the Iysodimethylethanolamine formed from PC with 2 less carbons on the *sn*-1 chain. For example, if [PE(18:1/22:0) - H] and [PC(16:1/18:2) + Form] are both present, the ion at m/z 478.2933 could be assigned as [PE(18:1) - R2'CH=C=O - H] or [PC(16:1) -R2'CH=C=O - CH3 - Form - H] or both. Verification of the presence of both would be made by the presence of the corresponding deprotonated fatty acyl: [FA(22:0) - H] for PE and [FA(18:2) - H] for PC. Like PC, if the parent ion is too low in abundance to obtain the deprotonated Iysoethanolamine fragment, acyl chains may still be identified albeit without *sn* chain assignment and the "" is used.

Diacyl PS and plasmanyl PS were verified by the presence of a fragment with a neutral loss of m/z 87.0320 from the deprotonated precursor. Acyl and/or alkyl chain identification was determined by further fragmentation leading the [PS - C₃H₅O₂N - R₂'-COOH - H]. An ion with the same exact m/z is formed by the fragmentation of [PA-H] ions. Therefore, just like PC and PE, it is important for the corresponding deprotonated fatty acid to also be present for both PS and PA if there is a possibility for both ions to be present.

PI ions were verified by the presence of a fragment at m/z 241.0113 from the isolated deprotonated precursor. PA, PI and PG ions form an ion at m/z 152.9953; therefore, there is not one specific ion for the verification of PA or PG ions. These classes, as well as PI ions, could be considered verified by the

presence of their $[M - R_2'COOH]^{-1}$ ions with the presence of the corresponding deprotonated fatty acid.

4.5.3 Comparison of Fatty Acyl Distributions Among SW480 and SW620 Cells and Exosomes

Fatty acyl, alkyl and alkenyl distribution for the diacyl, plasmanyl and plasmenyl PE lipids described in Figure 4.4 are shown in Figure 4.10A-4.10C. Figure 4.10A shows the longer of the two acyl chains (higher number of carbons and most double bonds) of the diacyl PE species. Figure 4.10B represents the alkyl chain of the plasmanyl PE species and figure 4.10C shows the alkenyl chain of the plasmenyl PE species. Although the distributions in the cells and exosomes were not exact, many of the sum compositions contained the same fatty acyls at similar ratios. The most substantial differences appeared to be present in the longer carbon chain species and more unsaturated lipids such as PE(38:4) where the exosomes had a preference toward the less unsaturated acyl chain FA_(20:3) over FA_(20:4) incorporation. Another notable difference was the presence of a FA_(P-20:5) in the PE_(P-40:6) lipid in the exosomes, which was not present in the cells and was contradictory to the fatty acyl preference in the diacyl PE species.

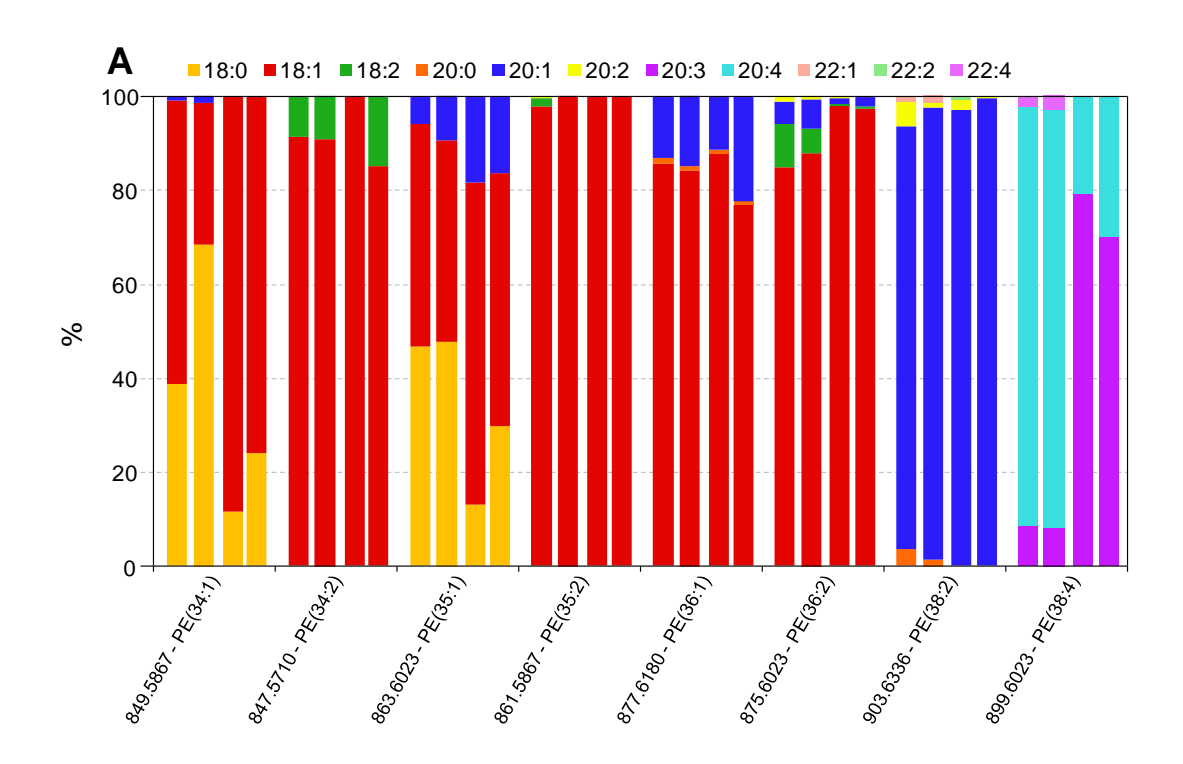
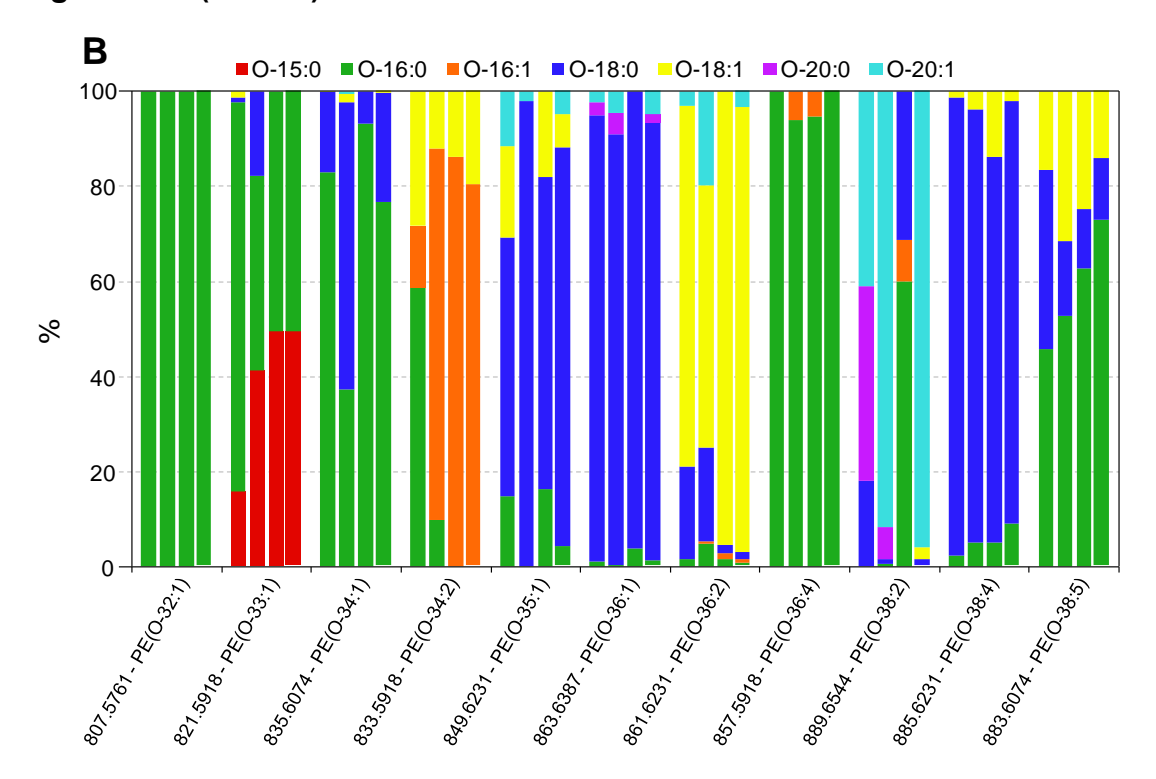
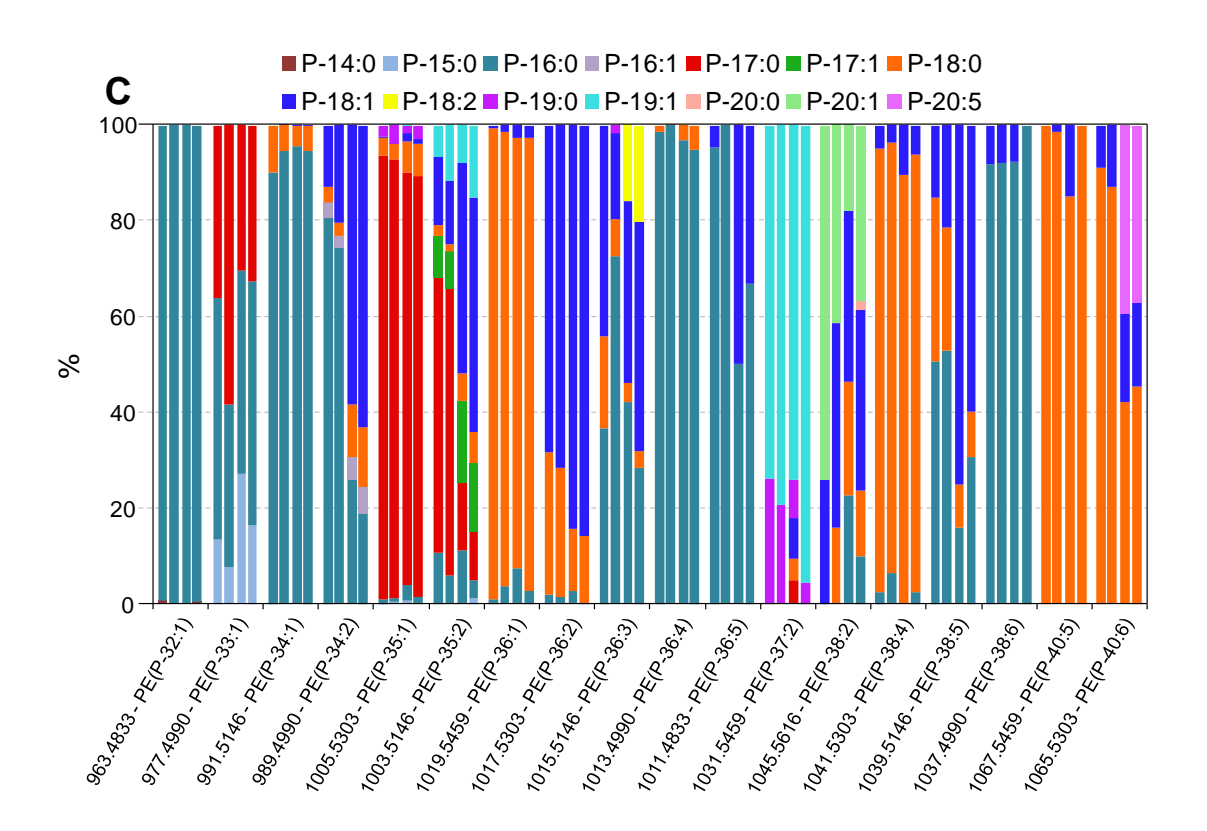


Figure 4.10 Distribution of fatty acids for the sum composition species from Figure 4.4 shown in order: SW480 cells, SW620 cells, SW480 exosomes and SW620 exosomes. (A) Percentages of the longest, most unsaturated fatty acids of the two fatty acyl chains for diacyl PE species. (B) Percentages of the O- chain for each plasmanyl PE species. (C) Percentages of the P- chain for each plasmenyl PE species.

Figure 4.10 (Cont'd)





The fatty acyl and alkyl distributions among the PC lipid sum compositions present in Figure 4.5 are found in Figure 4.11A and 4.11B, respectively. The fatty acyl/alkenyl distributions were similar in the cells to each other and the distributions were similar in the exosomes to each other, but the cells were different than the exosomes (for example, $PC_{(32:1)}$, $PC_{(33:1)}$ and $PC_{(36:4)}$. The plasmenyl PC graph was not shown as not all molecular lipids could be identified for the few species included in Figure 4.5. This may be due PC functioning as a main structural lipid [6,11]. The sheer size difference in the exosomes compared to the cells may be a large contributing factor. Interestingly for $PC_{(O-34:0)}$, the cells are nearly identical to their exosomes, but not to each other.

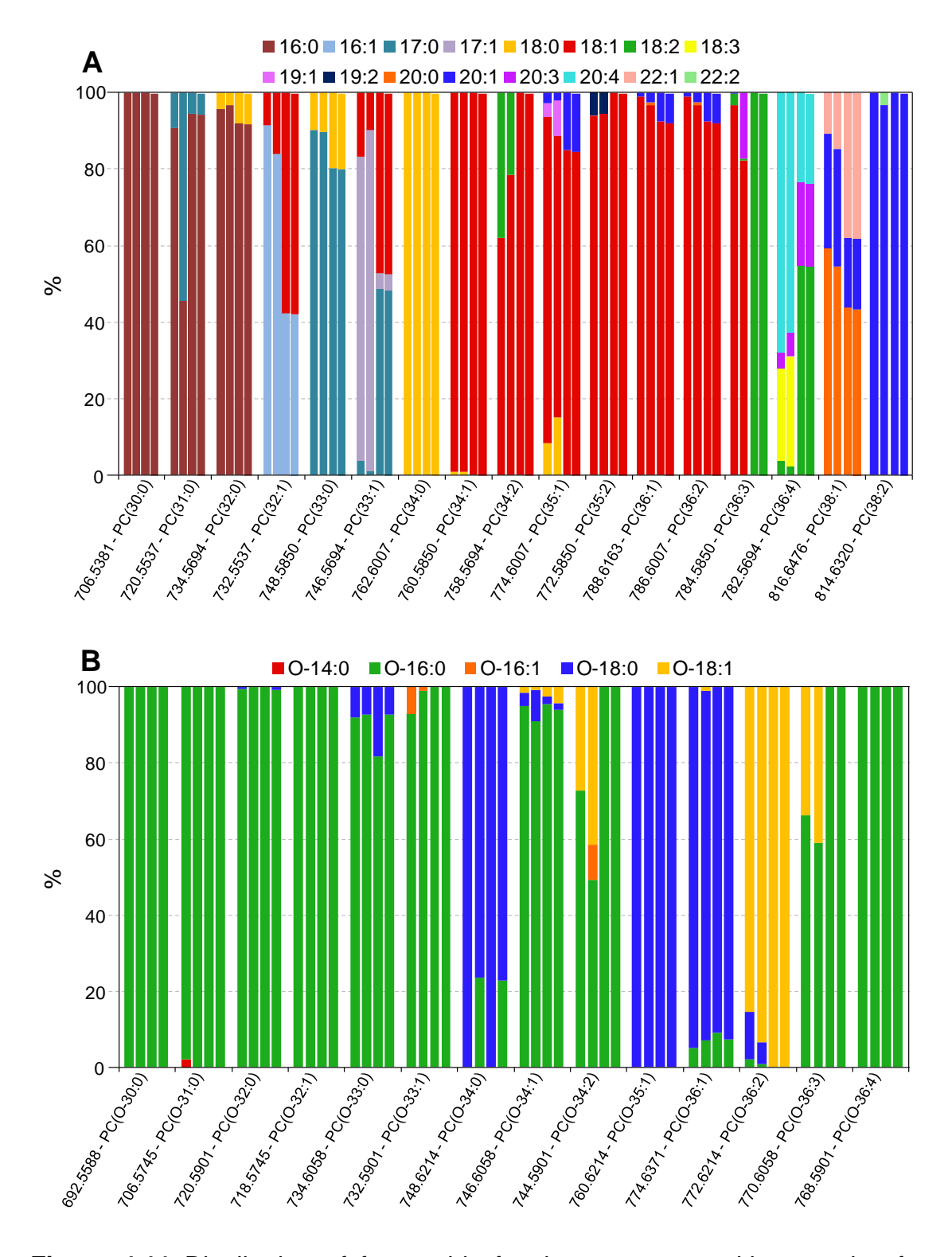


Figure 4.11 Distribution of fatty acids for the sum composition species from Figure 4.5 shown in order: SW480 cells, SW620 cells, SW480 exosomes and SW620 exosomes. (A) Percentages of the longest, most unsaturated fatty acids for diacyl PC species. (B) Percentages of the O- chain for each plasmanyl PC species.

Distribution of the fatty acyl and alkyl species of PS lipids are shown in Figures 4.12A and 4.12B. Like PC, most sum compositions have very little alteration in fatty acyl/alkyl components within the cells and exosomes. However, the alkyl chain of the PS species for the SW620 lipid extracts included in Figure 4.12B are altered in some cases from both the SW480 cells and the SW620 exosomes. For example, $PS_{(O-35:1)}$ contains mostly $PS_{(O-16:0/17:1)}$ with a minor amount of $PS_{(O-17:0/16:1)}$ in the SW620 cells. The SW480 cells and both exosome samples consist of mostly $PS_{(O-17:0/16:1)}$.

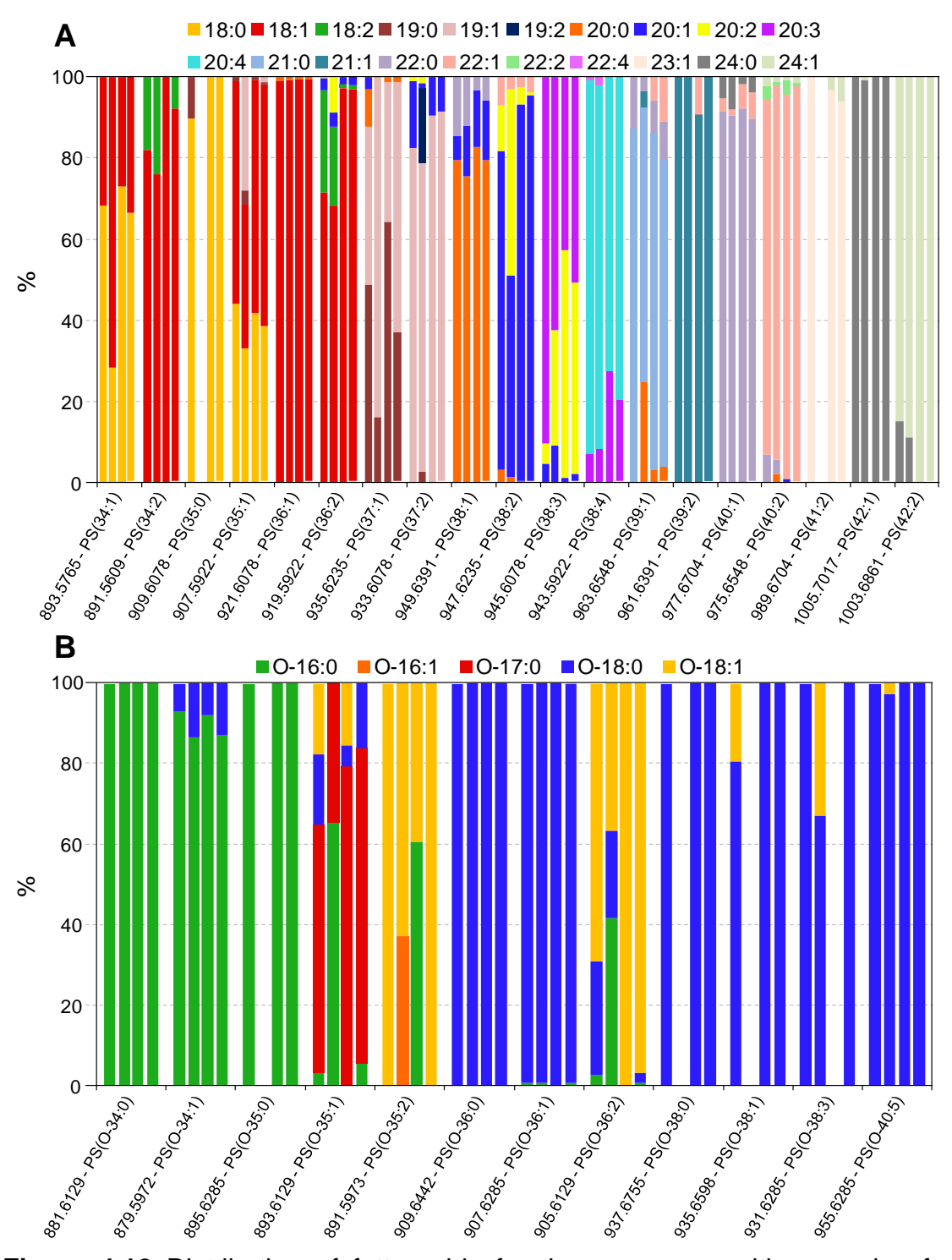


Figure 4.12 Distribution of fatty acids for the sum composition species from Figure 4.6 shown in order: SW480 cells, SW620 cells, SW480 exosomes and SW620 exosomes. (A) Percentages of the longest, most unsaturated fatty acids for diacyl PS species. (B) Percentages of the O- chain for each plasmanyl PS species.

The overall distribution of fatty acyls present in the TG species of the cells and exosomes are shown in Figure 4.13. Although not identical, the distributions of fatty acyls in the exosomes are similar to those in the cells.

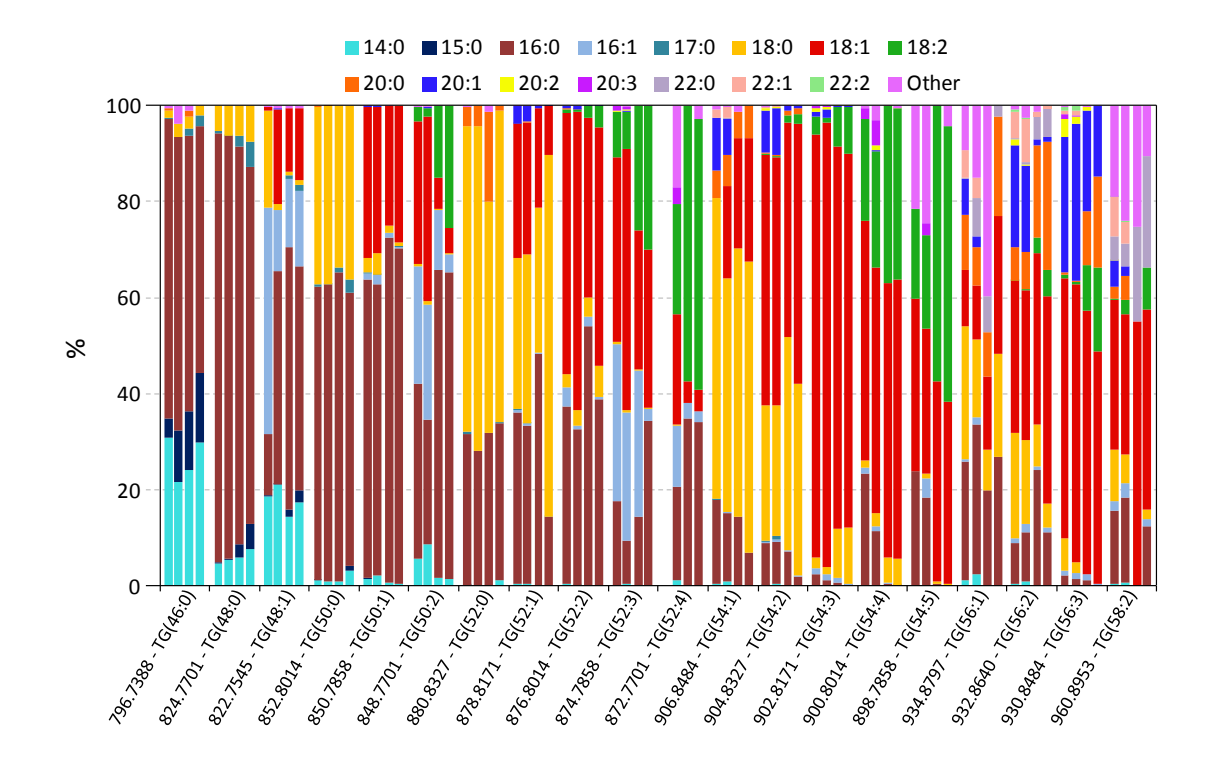


Figure 4.13 Distribution in percentage of fatty acyls for the sum composition species of the triacyl TG from Figure 4.9 shown in order: SW480 cells, SW620 cells, SW480 exosomes and SW620 exosomes.

Table 4.1 shows the number of lipids identified by sum composition and molecular lipid composition using the HRMS and HRMS/MS method described here. Sum composition consists of those lipids identified by HRMS. The number of molecular lipids pertains to the number of lipid species with identified fatty acyl/alkyl/alkenyl chains by MS/MS. Total lipids consists of those species identified at the molecular lipid level as well as those that were only identified by sum composition. A total of 1338 and 1626 lipid species were identified in the

SW480 and SW620 cells, respectively. Also, 828 and 829 lipid species were found to be contained in the SW480 and SW620 exosomes, respectively. The number of identified sum compositions and molecular lipid species is remarkably higher than the previous method using d₆-DMBNHS and acid hydrolysis for the cells (Chapter 3) and the 277 molecular lipid species identified in PC-3 exosomes [101]. The identities of the individual lipid in each of the lipid classes and subclasses are listed in Appendix C, Tables C.1-C.16.

Table 4.1 Summary of the number of assigned sum compositions (Sum Comp), identified lipids (ID Lipids), and total lipid species (Total) from crude lipid extracts from SW480 and SW620 colorectal cancer cell lines and secreted exosomes.

	SW	/480 Cel	ls	SW	/620 Ce	lls	SW48	0 Exoso	omes	SW62	0 Exoso	omes
Sub- Class	Sum Comp	Mol Lipids	Total									
PE	51	130	132	46	124	124	48	71	81	32	70	70
O-PE	39	96	97	27	76	78	43	77	84	33	78	79
P-PE	44	73	83	42	85	91	48	96	107	43	79	89
LPE	15	15	15	13	13	13	18	18	18	16	16	16
O-LPE	5	5	5	4	4	4	4	4	4	4	4	4
P-LPE	4	4	4	4	4	4	4	4	4	4	4	4
PC	47	82	95	42	78	80	47	54	69	38	48	51
O-PC	42	40	58	39	41	55	34	22	39	32	26	39
P-PC	31	31	44	30	24	38	15	8	17	17	9	17
LPC	9	9	9	8	8	8	6	6	6	3	3	3
O-LPC	3	3	3	3	3	3	3	3	3	3	3	3
P-LPC	1	1	1	1	1	1	0	0	0	1	1	1
PS	29	78	79	26	83	85	30	71	72	30	75	77
O-PS	18	26	28	17	28	29	15	15	20	21	24	29
P-PS	3	2	3	4	4	5	3	2	3	6	3	6
LPS	0	0	0	1	1	1	2	2	2	2	2	2
O-LPS	4	4	4	4	4	4	6	6	6	4	4	4
P-LPS	2	2	2	2	2	2	2	2	2	2	2	2
PI	16	28	31	16	33	35	12	23	24	9	15	16
O-PI	6	7	9	2	2	3	4	3	4	2	2	2
P-PI	0	0	0	1	0	1	2	0	2	1	0	1
PG	9	12	13	12	17	20	5	4	6	13	6	15
O-PG	15	0	15	14	0	14	12	0	12	14	0	14
P-PG	1	0	1	0	0	0	1	0	1	1	0	1
O-LPG	4	4	4	3	3	3	2	2	2	2	2	2
SM	17	6	18	14	6	15	24	7	24	21	9	22
Cer	10	18	18	10	15	16	11	18	19	11	18	19
Hex- Cer	4	0	4	3	0	3	4	0	4	4	0	4
TG	56	454	463	97	719	735	44	152	154	48	194	195
O-TG	20	0	20	52	0	52	0	0	0	0	0	0
P-TG	0	0	0	10	0	10	0	0	0	0	0	0
DG	23	0	23	28	0	28	19	0	19	13	0	13
O-DG	13	0	13	16	0	16	7	0	7	8	0	8
P-DG	1	0	1	5	0	5	1	0	1	2	0	2
MG	18	18	18	16	16	16	9	9	9	11	11	11
O-MG	8	8	8	7	7	7	2	2	2	6	6	6
P-MG	0	0	0	1	1	1	0	0	0	0	0	0
Chol	1	1	1	1	1	1	1	1	1	1	1	1
Chol Ester	16	16	16	20	20	20	0	0	0	1	1	1
Total	585	1173	1338	641	1423	1626	488	682	828	459	716	829

4.6 Conclusions and Future Directions

The derivatization method described in Chapter 2 involving the use of \$^{13}\$C_1-DMBNHS and iodine/methanol derivatization has been used for the comprehensive lipidome analysis of the adenocarcinoma cell lines SW480 and SW620 and their secreted exosomes. The method developed is especially beneficial where sample is limited as only a small amount of material is required for analysis and there is minimal sample handling. Although there is currently little focus on the individual lipid species (i.e. PC(34:1) or PC(16:0/18:1)) or fatty acid distributions within each lipid class in disease progression or biomarker discovery, the ability to profile tissues, cells and exosomes to this extent may lead to information about individual fatty acid substrate preference and/or lipid metabolism. This information may also lead to more specific biomarker discovery, such as at the molecular lipid level, as opposed to the lipid class or sub-class level.

Profiling lipids and tissues of disease states leads to many questions about lipid metabolism and why the alterations are happening. Exploring the functional aspects of why several of these lipid sub-classes are enriched, such as the plasmalogens, PS, SM and Cer, etc., could lead to a larger understanding of how and why these alterations occur. For example, Benjamin, et. al. reported lower proliferation, migration and invasion as well as fatty acid remodeling in cell lines with AGPS knocked down [75]. A continuation of a similar experiment with the SW480 and SW620 cells with expansion to include the exosomes also could be beneficial to understanding how plasmanyl and plasmenyl lipids affect exosome secretion, uptake/fusion, or lipid remodeling in exosome formation. This

information could be beneficial for understanding the mechanisms by which cells and exosomes communicate with each other. Furthermore, many more models for cancer progression and metastasis could also be explored, including some model organisms and clinical samples. Lipids are only one part of cellular functionality. Other biomolecules such as proteins, RNAs and metabolites would be beneficial to analyze in conjunction with the lipids for a higher understanding of the metabolic pathways of cancer metastasis. These large amounts of data need to be correlated to one another to make sense of what is happening in the cells/tissues as a whole.

CHAPTER 5

Experimental Methods

5.1 Materials

SW480 cells were purchased from American Type Culture Collection (ATCC) (Manassas, VA). RPMI 1640 medium, penicillin and streptomycin antibiotic mix and 0.25% Trypsin-EDTA, were obtained from Invitrogen (Carlsbad, CA). LC grade water, methanol (MeOH), chloroform (CHCl₃) and ACS grade isopropanol (IPA) were purchased from Macron Chemicals (Center Valley, PA). Iodine, N,N-dimethylformamide (DMF) and triethylamine (TEA) were from Jade Scientific (Westland, MI). Dichloromethane (DCM) was from Mallinckrodt Chemicals (Phillipsburg, NJ, USA). 99% formic acid was purchased from Spectrum Scientific (Irvine, CA). Acetonitrile (CH₃CN) was purchased from EMD Chemicals (San Diego, CA, USA). Ammonium formate was obtained from Alfa Aesar (Ward Hill, MA). Ammonium bicarbonate was from J.T. Baker (Phillipsburg, NJ), USA). Synthetic lipid standards were from Avanti Polar Lipids, Inc. (Alabaster, AL). ¹³C-iodomethane (99% ¹³C) was obtained from Sigma Aldrich (St. Louis, MO, USA).

5.2 Cell Culture Conditions and Protocols

SW480 and SW620 cells were routinely cultured in RPMI1640 medium supplemented with 10% FBS, 100 unit/mL penicillin and 100 µg/mL streptomycin (complete culture medium) at 37°C and 5% CO₂ atmosphere. Approximately 2 x 10⁶ cells were seeded into 75 cm² culture flask containing 10mL of the complete culture medium and cultured until cell density reached 80% confluence.

5.2.1 Cell Counting

The cells were washed three times with PBS and lifted off the culture plates with 0.25% Trypsin-EDTA. Cell suspensions were centrifuged at 1000 rpm at 20°C for 5 minutes. The medium was then carefully aspirated and the cells were resuspended in clean medium. Cells were then counted using a hemocytometer or by a cell counter.

5.2.2 Exosome Isolation

In order to generate conditioned medium for crude exosome isolation, approximate 2×10^6 cells were plated into 150 mm diameter cell culture dishes (30 dishes per cell line) in 25 mL of medium and cultured until the cell density reached 70-80% confluence. The cells were washed four times with RPMI1640 medium and then cultured in 15 mL of serum-free culture medium (RPMI1640

medium supplemented with 0.8% insulin, selenium and transferrin (ITS), 60 μ g/mL benzylpenicillin and 100 μ g/mL streptomycin) for 24 h before the collection of conditioned medium.

Conditioned media were collected after SW480 or SW620 cells were cultured under the serum free condition for 24 h (RPMI1640 medium supplemented with 0.8% ITS). The conditioned media were centrifuged at 400g for 5 min to remove floating cells then 2,000g for 10 min to remove cell debris. The resultant supernatant was centrifuged at 10,000g for 30 min at 4°C to pellet and remove shed micro-vesicles. The supernatant was further centrifuged at 100,000g for 1 h at 4°C to pellet crude exosomes. The isolated crude exosomes were resuspended in PBS and lyophilized for further lipid extraction.

5.3 Modified Folch Lipid Extraction

Extraction of lipids from SW480 and SW620 cells and exosomes was performed using a modified Folch method, as previously described [108,110]. Briefly, $10^6 - 2x10^7$ lyophilized or freshly trypsinized cells, or lyophilized isolated exosomes were suspended in 2mL 40% MeOH in 15mL test tubes with PTFE lines screw caps. 4mL 2:1 CHCl₃/MeOH was added to the cell suspensions and vortexed on high for 1 minute. Cell suspensions were centrifuged for 10 minutes at 3000g at 20° C. The organic phase (bottom) was transferred to a separate test tube. 4mL CHCl₃ was added to the aqueous phase, vortexed on high for 1

minute and centrifuged for 10 minutes at 3000g at 20° C. The organic phase was removed and added to the previous organic phase. Organic solvent was dried completely under a stream of N₂(g). Dried lipid extracts were either redissolved in CHCl₃, transferred to a separate test tube and re-dried with N₂(g) or placed under reduced pressure overnight to ensure complete drying occurred. Stock solutions were prepared by dissolving the dried crude cell lipid extracts in 600 µL of 4:2:1 IPA/MeOH/CHCl₃. Crude exosome extracts were suspended in 200 µL of 4:2:1 IPA/MeOH/CHCl₃. Lipid extracts were stored in 2 mL glass vials with PTFE lined caps (Fisher Scientific, Fairlawn, NJ) at -80° C prior to further analysis.

5.4 High Resolution MS (HRMS) Analysis

Samples (n=3-5 replicates) were loaded into a Whatman multichem 96-well plate (Sigma Aldrich, St. Louis, MO) and sealed with Teflon Ultra Thin Sealing Tape (Analytical Sales and Services, Prompton Plains, NJ). The samples were then introduced into a high resolution/accurate mass Thermo Scientific model LTQ Orbitrap Velos mass spectrometer equipped with a dual pressure ion trap and an HCD multipole collision cell (San Jose, CA) using an Advion Triversa Nanomate nano-electrospray ionization (nESI) source (Advion Ithaca, NY) with a spray voltage of 1.4 kV and a gas pressure of 0.3 psi. The ion source interface

settings (inlet temperature of 100°C and S-Lens value of 50%) were optimized to maximize the sensitivity of the precursor ions while minimizing 'in-source' fragmentation. High resolution mass spectra were acquired in positive and negative ionization mode using the FT analyzer operating at 100,000 resolving power, across the range of m/z from 200-2000, and were signal averaged for 2-3 minutes. Mass spectra were initially acquired at a range of different dilutions of the lipid extracts to determine the range at which linearity in the response of specific lipids was observed, and to ensure that the ratio of specific lipid ion abundances compared to other lipids within the mixture, or compared to the internal standards, remained constant. External calibration of the instrument was initially performed using the standard Thermo LTQ calibration mixture. Automated Gain Control (AGC) target numbers were maintained at the default settings for all MS experiments.

5.4.1 Aminophospholipid Derivatization with DMBNHS

d₆-DMBNHS was synthesized as previously reported [240]. 13 C₁-DMBNHS was also synthesized as previously reported [282]. 5 μL of the stock lipid extract, 10 μL each of 10 μM PC_(14:0/14:0) and PE_(14:0/14:0) and 3.25 μL PS_(14:0/14:0) were dried under a stream of nitrogen, then redissolved in 40 μL of 39:1.1 CHCl₃ containing 0.0125 M TEA and vortexed for 30 seconds. 1 μL of 0.0125 M d₆-DMBNHS or 13 C₁-DMBNHS in DMF was then added to the lipid

mixture and vortexed for 30 min. The reaction was quenched by drying under a stream of nitrogen then re-dissolved in 200 µL 4:2:1 IPA/MeOH/CHCl₃ containing 20 mM ammonium formate for immediate analysis by ESI-MS.

5.4.2 Acid Hydrolysis of Plasmalogen Lipids

Following derivatization with d₆-DMBNHS, then drying under N₂ as described above, 40 μ L of 80% formic acid in 4:2:1 IPA/MeOH/CHCl₃ was added to the sample and allowed to react for 1 min. The solvent was then immediately evaporated under reduced pressure and samples were re-dissolved in 200 μ L 4:2:1 IPA/MeOH/CHCl₃ containing 20 mM ammonium formate for immediate analysis by ESI-MS.

5.4.3 Iodine and Methanol Derivatization of Plasmalogen Lipids

For lipid standard reactions, 10µL each of 100µM lipid standards ($PE_{(P-18:0/22:6)}$, $PC_{(P-18:0/22:6)}$, $PE_{(14:0/14:0)}$, $PE_{(18:0/22:6)}$, $PC_{(14:0/14:0)}$, $PC_{(18:1/18:1)}$, $PC_{(18:2/18:2)}$, $PC_{(14:0/16:1/14:0)}$, $PC_{(16:0/16:0/18:1)}$, $PC_{(18:1/16:0/18:1)}$ and $PC_{(18:0/18:0/18:1)}$) were dried under a stream of nitrogen then redissolved in 60µL ice cold 2:1 CHCl₃/CH₃OH with 2 mM ammonium bicarbonate and 0.167 mM

iodine (i.e., a 5 fold molar excess with respect to the total plasmenyl lipid concentration). For cell extract reactions, 5 μ L of the stock SW480 lipid extract and 10 μ L each of 10 μ M PC_(14:0/14:0) and PE_(14:0/14:0) were combined then dried under a stream of nitrogen, then redissolved in 60 μ L ice cold 2:1 CHCl₃/CH₃OH with 2mM ammonium bicarbonate and 1.33 mM iodine (estimated to be a 10 fold molar excess with respect to the total plasmenyl lipid concentration). The solutions were reacted in an ice bath for 5 minutes and dried under a stream of nitrogen. The resulting products were then re-dissolved in 200 μ L 4:2:1 IPA/CH₃OH/CHCl₃ containing 20 mM ammonium formate for immediate analysis by MS.

5.5 HRMS and MS/MS Data Analysis Strategies

5.5.1 HRMS Data Analysis Using LIMSA

Post acquisition internal mass calibration was performed using the recalibration software in Xcalibur (Thermo Scientific, San Jose, CA), using a peak list consisting of the calculated m/z values of the protonated $PE_{(14:0/14:0)}$, $PC_{(14:0/14:0)}$ and $PS_{(14:0/14:0)}$ internal standards, and an abundant $PC_{(36:2)}$ lipid present in the extract in positive ionization mode, and the calculated m/z values of the formate adducts of the internal standard $PC_{(28:0)}$ lipid, and the formate

adduct of the PC(34:2) and deprotonated PA(34:0) and PI(36:1) lipids present in the extract in negative ionization mode (the identities of these lipids were all first confirmed using MS/MS). Peak lists containing the recalibrated masses and intensities were then transferred to Microsoft Excel, then lipid identification (i.e., assignment of the lipid headgroup, the nature of the linkage of the hydrophobic tails (i.e., diacyl versus alkyl or alkenyl) and the total number of carbons and degree of unsaturation) and quantitation was performed using the Lipid Mass Spectrum Analysis (LIMSA) v.1.0 software linear fit isotope correction algorithm [233], in conjunction with an 'in-house' developed database of hypothetical lipid compounds (Appendix B), for automated peak finding (using a peak width tolerance of 0.003 and a sensitivity of 0.1%) and for the correction of ¹³C isotope effects. Peaks originally picked by LIMSA that were outside the 95% confidence level of the experimental mass accuracy (determined to be 2.57ppm) were removed. No attempts were made to quantitatively correct for different ESI responses of individual lipids due to concentration, acyl chain length or degree of unsaturation. Thus, the abundance of the ions corresponding to individual molecular species within each lipid class, normalized to the abundance of the PC_(14:0/14:0) internal standard, are reported here as the percentage of the total lipid ion abundance for each class, and not the absolute concentrations. All lipid classes (PC, PE, PS, PG, PI, LPC, LPE, LPS, TG, DG, MG, SM, Cer, Hex-Cer, Chol and Chol esters) except for PA were identified and quantified from the d₆or ¹³C₁-DMBNHS and lodine/Methanol derivatized spectra. **DMBNHS**

Determination of the abundance of PA lipids was performed in negative ion mode, then a correction was applied to the positive ion mode spectra to remove the contribution of these lipids to the PC lipid ion abundances. An appropriate correction factor was determined using the negative and positive ion abundances measured using a series of PA lipid standards analyzed under the same conditions as the lipid extracts. For data described in Chapter 3, bar graphs represent the percent of each lipid sum composition as a function of the total abundance of each lipid sub-class. For data described in Chapter 4, sum composition bar graphs represent the lipid abundance normalized to the internal standard, PC_(14:0/14:0), per µg of total protein. For chapter 3, student's t-test with 2 tailed distribution, two sample unequal variance was used to evaluate differences in the individual ion abundances between the SW480 and SW620 cell line crude lipid extracts, with p < 0.01 considered statistically significant. For chapter 4, one-way ANOVA (Microsoft Excel Software) was used to evaluate differences (p<0.01) among SW480 and SW620 cells and exosomes. Student's ttest with 2 tailed distribution, two sample unequal variance was used to evaluate differences in the individual ion abundances between the SW480 and SW620 cell extracts, SW480 cell and exosome extracts, SW620 cell and exosome extracts, and SW480 and SW620 exosome extracts, with p < 0.01 considered statistically significant. Data were presented as mean ± standard deviation.

5.5.2 MS/MS Molecular Lipid Identification and Relative Quantification

Lipids were derivatized with both 13 C₁-DMBNHS and iodine and methanol for analysis in positive ionization mode, but only derivatized with iodine and methanol for negative ionization mode experiments to resolve vinyl ether lipids from the alkyl ether lipids. For the phospholipids, HCD-MS/MS was performed in negative ionization mode on the deprotonated precursor ions, with the exception of PC lipids, which were analyzed as their formate adducts. For TG lipid ions, positive ion mode HCD-MS/MS spectra were acquired to observe the neutral loss of characteristic fatty acids from the ammonium ion adducts at each of the identified precursor ion m/z values for these lipids, as previously described [199]. SM characterization was performed on the protonated ions in positive ionization mode [195] whereas Cer was characterized by fragmentation of the [Cer – H_2O + H_1^+ peaks. All lipid characterization for 'shotgun' experiments is explained in the specifications spelled out in Appendix B.

APPENDICES

APPENDIX A

This appendix contains supplemental figures for chapter 3.

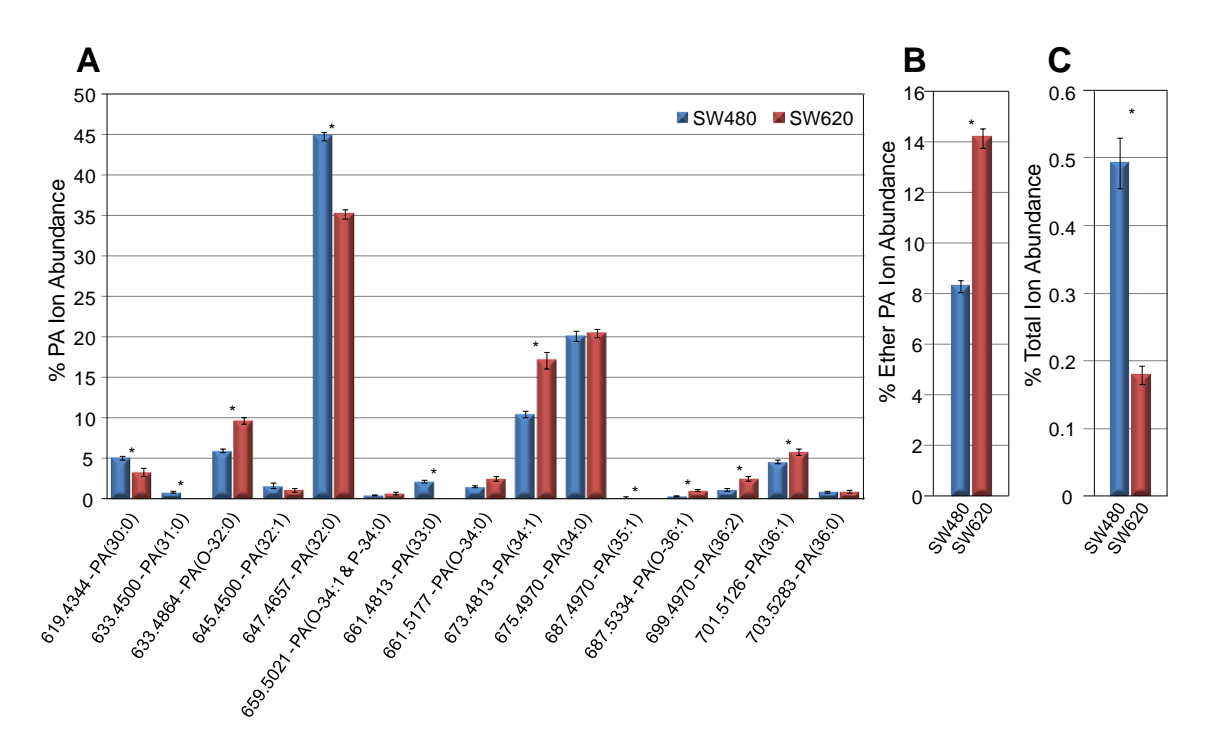


Figure A.1 Quantitation of PA lipids from the d₆-DMBNHS derivatized SW480 and SW620 cell crude lipid extracts. (A) Percent individual PA ion abundances compared to the total ion abundance for all PA lipids. (B) Percent total etherlinked PA ion abundance compared to the total PA lipid ion abundance. (C) Percent total PA ion abundance compared to the total ion abundance for all identified lipids. n = 5, * = p < 0.01.

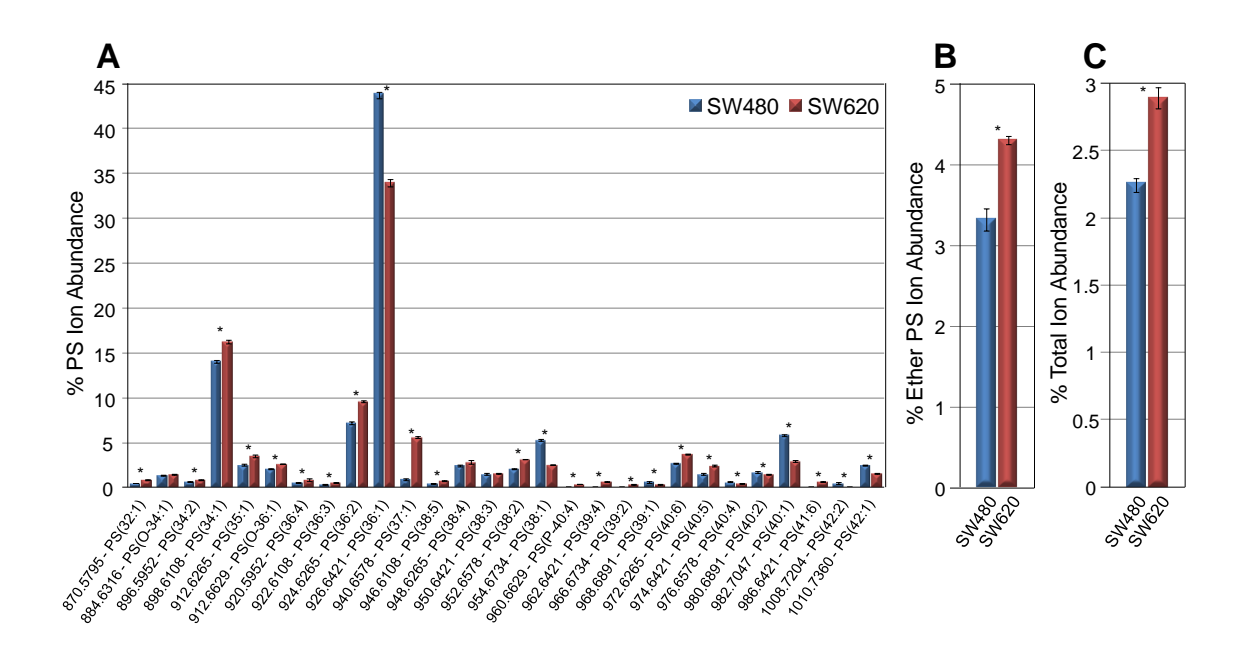


Figure A.2 Quantitation of PS lipids from the d₆-DMBNHS derivatized SW480 and SW620 cell crude lipid extracts. (A) Percent individual PS ion abundances compared to the total ion abundance for all PS lipids. (B) Percent total etherlinked PS ion abundance compared to the total PS lipid ion abundance. (C) Percent total PS ion abundance compared to the total ion abundance for all identified lipids. n = 5, * = p < 0.01.

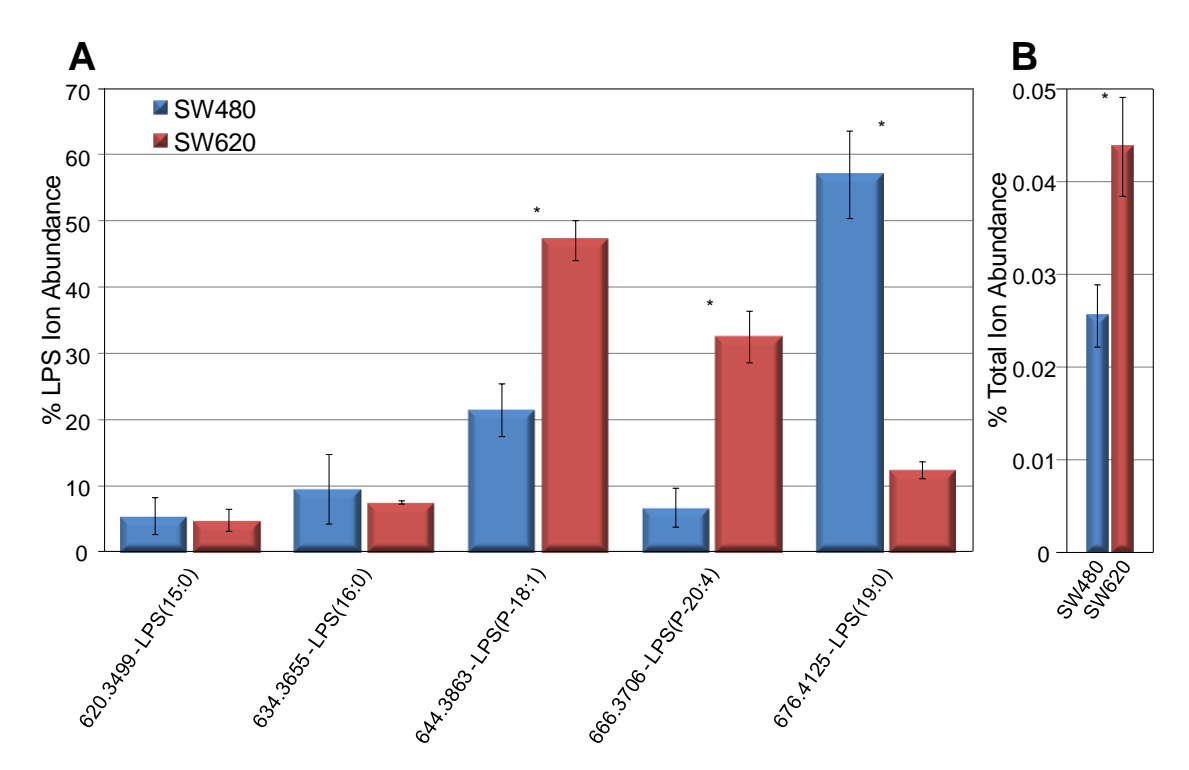


Figure A.3 Quantitation of LPS lipids from the d₆-DMBNHS derivatized SW480 and SW620 cell crude lipid extracts. (A) Percent individual LPS ion abundances compared to the total ion abundance for all LPS lipids. (B) Percent total LPS ion abundance compared to the total ion abundance for all identified lipids. n = 5, * = p < 0.01.

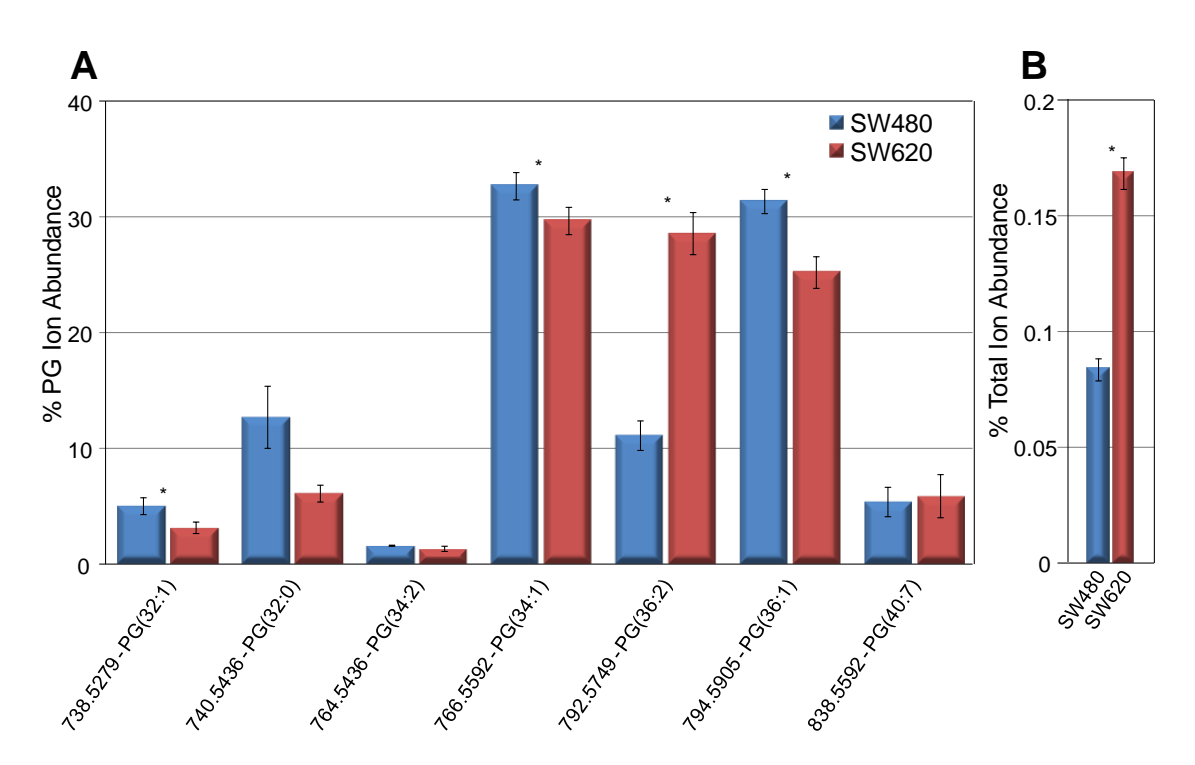


Figure A.4 Quantitation of PG lipids from the d₆-DMBNHS derivatized SW480 and SW620 cell crude lipid extracts. (A) Percent individual PG ion abundances compared to the total ion abundance for all PG lipids. (B) Percent total PG ion abundance compared to the total ion abundance for all identified lipids. n = 5, * = p < 0.01.

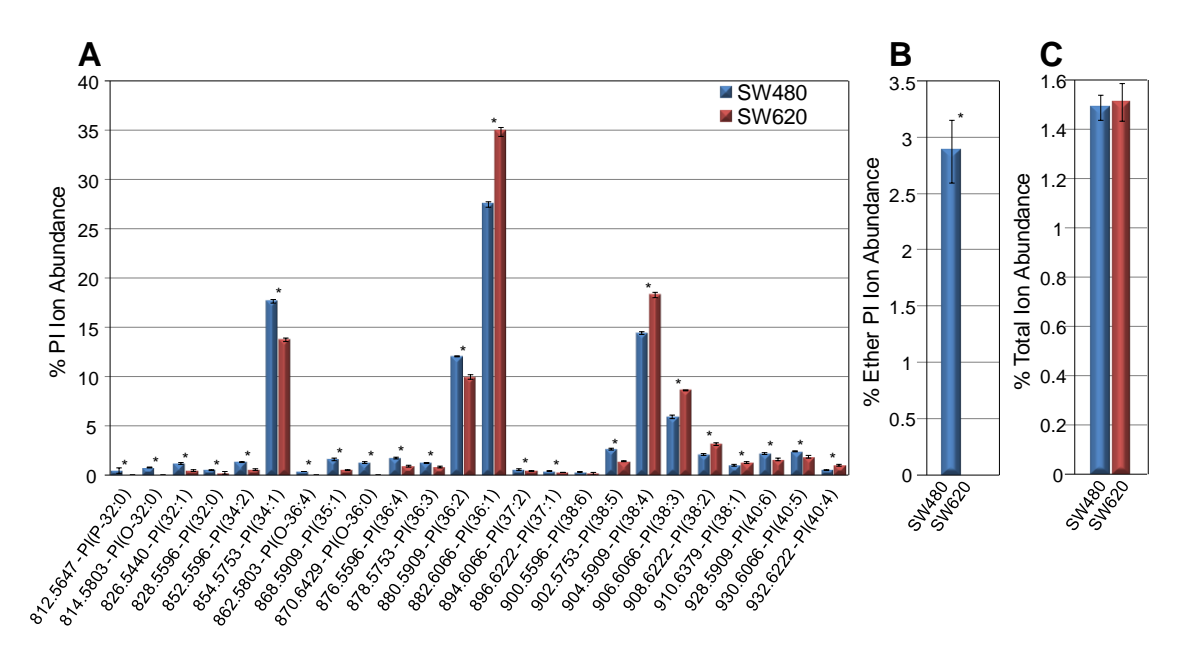


Figure A.5 Quantitation of PI phospholipids from the d_6 -DMBNHS derivatized SW480 and SW620 cell crude lipid extracts. (A) Percent individual PI ion abundances compared to the total ion abundance for all PI lipids. (B) Percent total ether-linked PI ion abundance compared to the total PI lipid ion abundance. (C) Percent total PI ion abundance compared to the total ion abundance for all identified lipids. n = 5, * = p < 0.01.

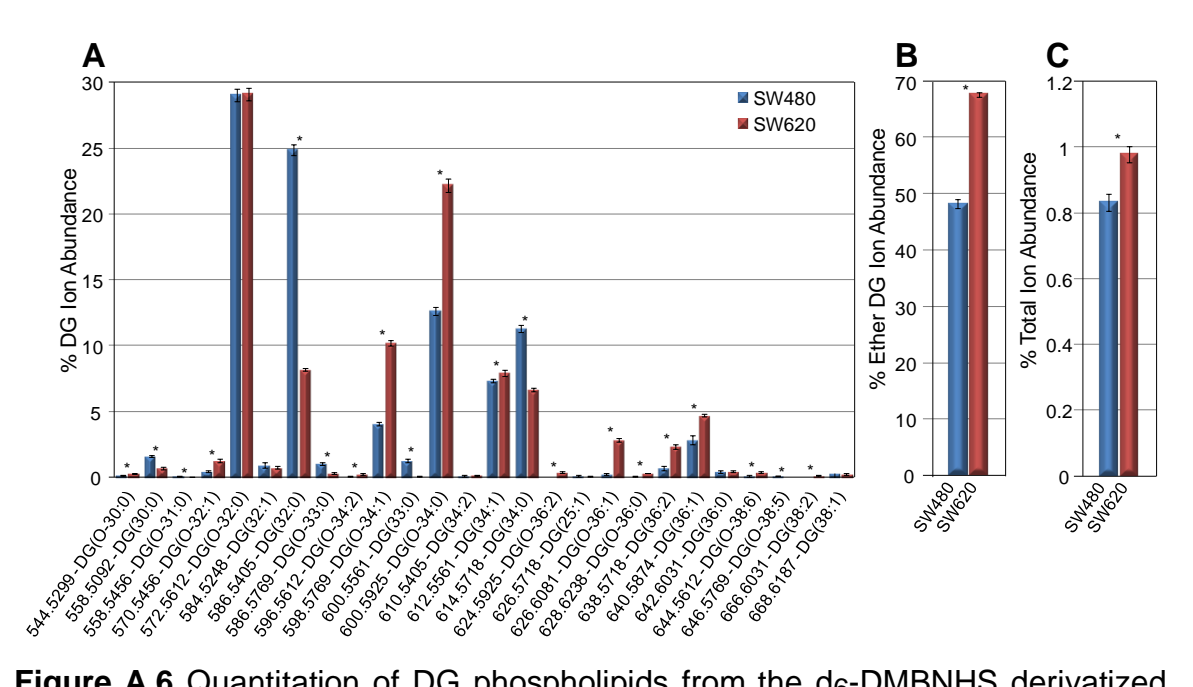


Figure A.6 Quantitation of DG phospholipids from the d_6 -DMBNHS derivatized SW480 and SW620 cell crude lipid extracts. (A) Percent individual DG ion abundances compared to the total ion abundance for all DG lipids. (B) Percent total ether-linked DG ion abundance compared to the total DG lipid ion abundance. (C) Percent total DG ion abundance compared to the total ion abundance for all identified lipids. n = 5, * = p < 0.01.

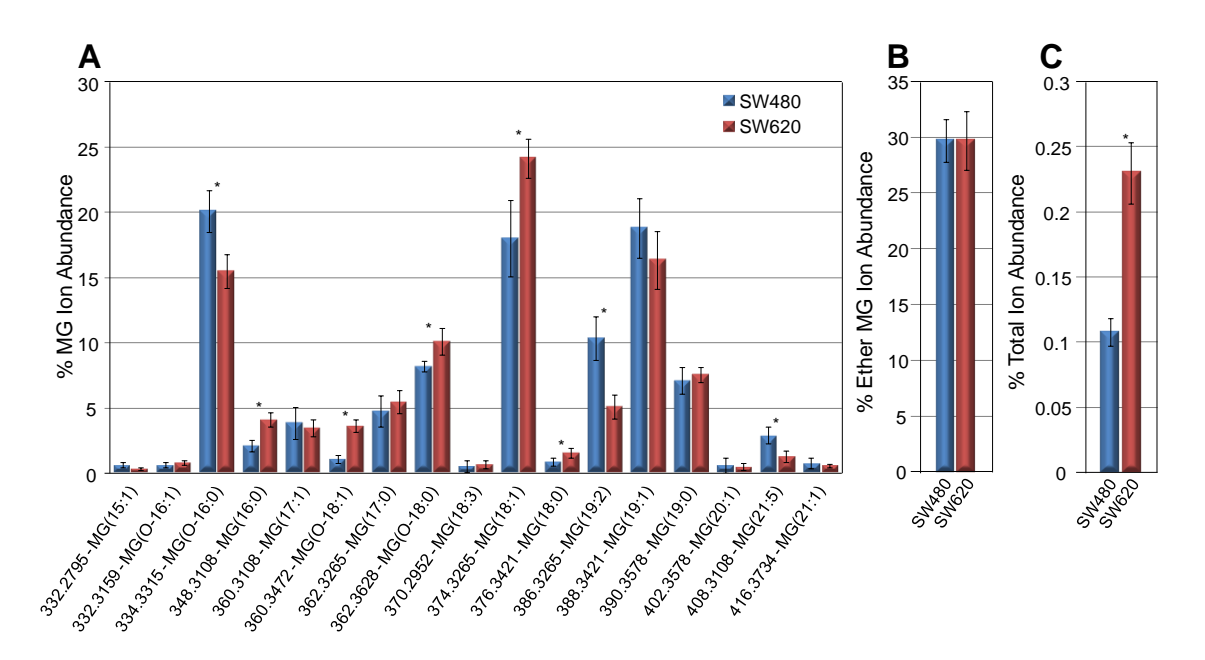


Figure A.7 Quantitation of MG phospholipids from the d_6 -DMBNHS derivatized SW480 and SW620 cell crude lipid extracts. (A) Percent individual MG ion abundances compared to the total ion abundance for all MG lipids. (B) Percent total ether-linked MG ion abundance compared to the total MG lipid ion abundance. (C) Percent total MG ion abundance compared to the total ion abundance for all identified lipids. n = 5, * = p < 0.01.

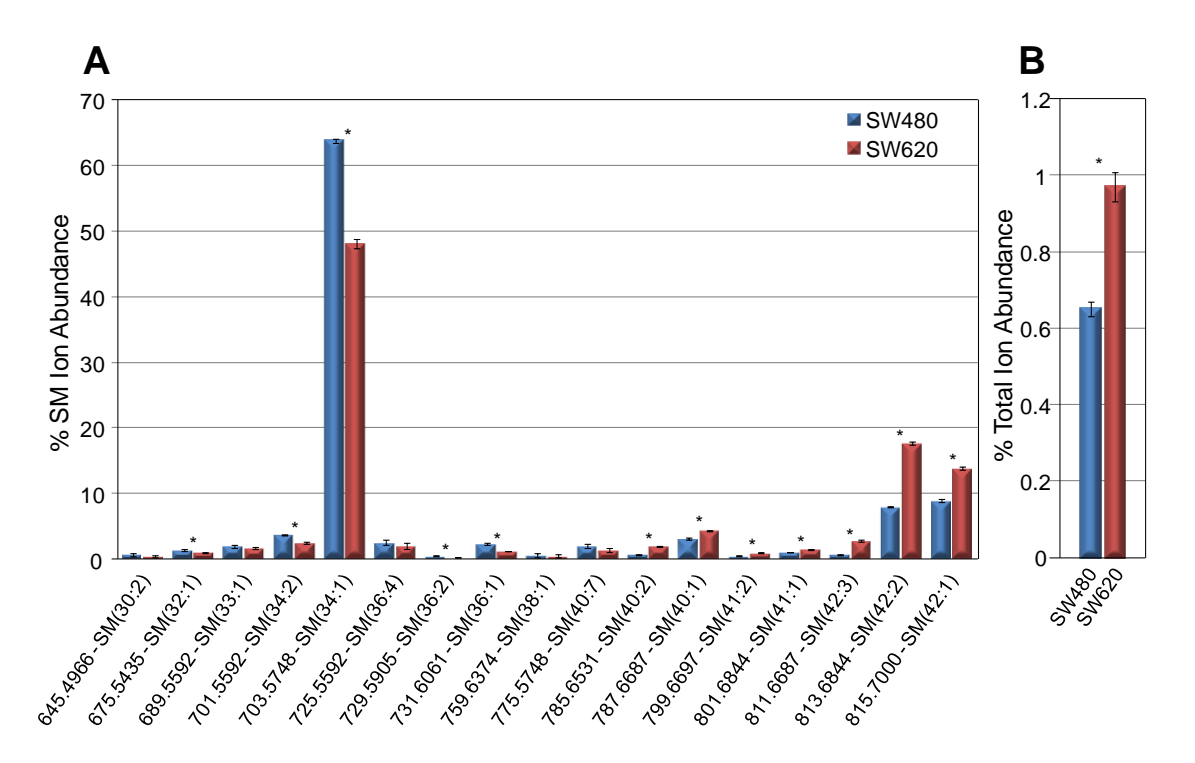


Figure A.8 Quantitation of SM from the d_6 -DMBNHS derivatized SW480 and SW620 cell crude lipid extracts. (A) Percent individual SM ion abundances compared to the total ion abundance for all SM lipids. (B) Percent total SM ion abundance compared to the total ion abundance for all identified lipids. n = 5, * = p < 0.01.

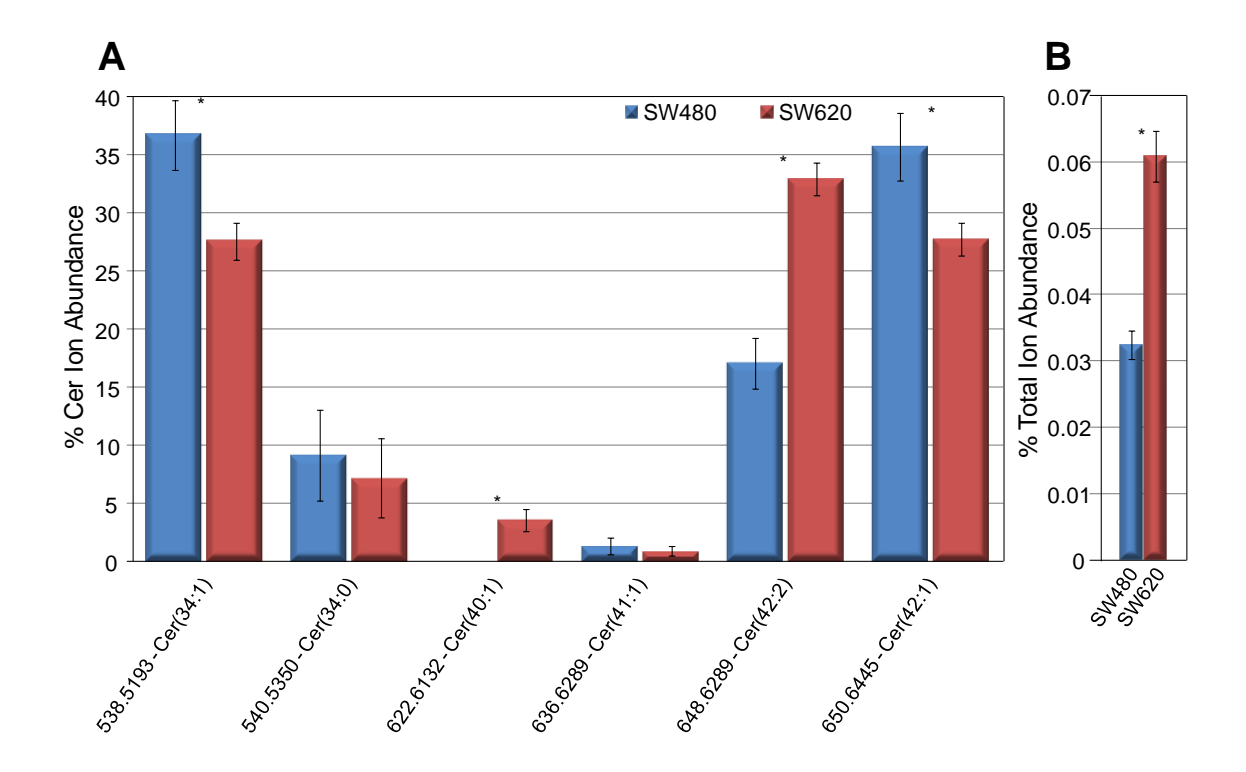
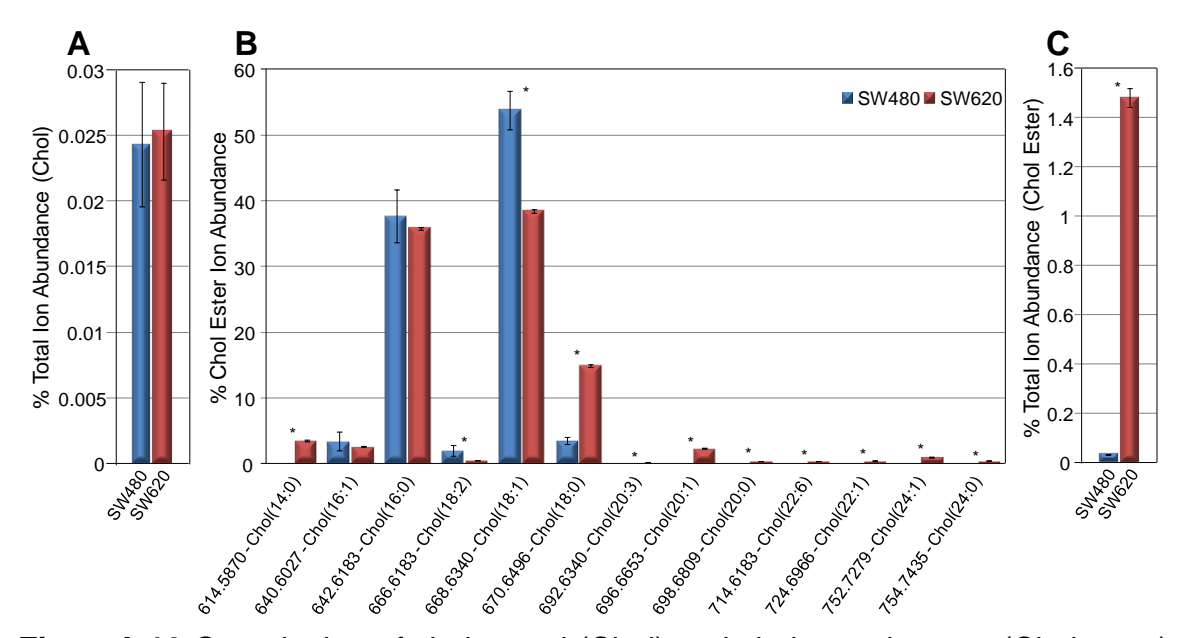


Figure A.9 Quantitation of Cer from the d₆-DMBNHS derivatized SW480 and SW620 cell crude lipid extracts. (A) Percent individual Cer ion abundances compared to the total ion abundance for all Cer lipids. (B) Percent total Cer ion abundance compared to the total ion abundance for all identified lipids. n = 5, * = p < 0.01.



FigureA.10 Quantitation of cholesterol (Chol) and cholesterol esters (Chol ester) from the d_6 -DMBNHS derivatized SW480 and SW620 cell crude lipid extracts. (A) Percent of total Chol ion abundance compared to the total ion abundance for all lipid peaks identified. (B) Percent individual Chol ester ion abundances compared to the total ion abundance for all Chol ester lipids. (C) Percent total Chol ester ion abundance compared to the total ion abundance for all identified lipids. n = 5, * = p < 0.01.

APPENDIX B

This appendix contains information on identification and characterization of lipids based on sub-structures including base structures, R-groups and possible alterations. The "Formula to be Used" column contains the molecular formula to be used when determining the m/z of whole lipids and fragments. They are altered from the formula of the structure in order to maintain neutrality.

Table B.1 Base structures for lipid building blocks: Symbol used in the "code" tables, Molecular structure of the base and formula of the base to be used when summing the parts of each lipid of the code.

Symbol	Structure	Formula to be Used
B ₁	R ₁ , O, C, R ₃	C ₃ H ₅ O ₃
B ₂	R_1 O_{∞} R_3 HN_{∞} R_2	C ₂ H ₄ O ₂ N
В3	R ₁ v ₀	C ₂₇ H ₄₅ O

Table B.2 R-group structures for lipid building blocks labeled with R_1 : Symbol used in the "code" tables, Molecular structure of the R-group and formula of the R-group to be used when summing the parts of each lipid of the code. (Note: F = number of Carbons and T = number of double bonds).

Symbol	Structure	Formula
R ₁₋₁	O C(E-1)H(2E-1-2T)	C _E H _(2E-1-2T) O
R ₁₋₂	C(E-1)H(2E-1-2T)	C _E H _(2E+1-2T)
R ₁₋₃	O I C(E-2)H(2E-3-2T)	C _E H _(2E+2-2T) OI
R ₁₋₄	H	Н

Table B.3 R-group structures for lipid building blocks labeled with R_2 : Symbol used in the "code" tables, Molecular structure of the R-group and formula of the R-group to be used when summing the parts of each lipid of the code. (Note: F =number of Carbons and U =number of double bonds).

Symbol	Structure	Formula
R ₂₋₁	O C _(F-1) H _(2F-1-2U)	C _F H _(2F-1-2U) O
R ₂₋₂	C(F-1)H(2F-1-2U)	C _F H _(2F+1-2U)
R ₂₋₃	O I C _(F-2) H _(2F-3-2U)	C _F H _(2F+2-2U) OI
R ₂₋₄	H	Н

Table B.4 R-group structures for lipid building blocks labeled with R_3 : Symbol used in the "code" tables, Molecular structure of the R-group and formula of the R-group to be used when summing the parts of each lipid of the code. (Note: G = number of Carbons and V = number of double bonds).

Symbol	Structure	Formula
R ₃₋₁	N+ vvv	C ₅ H ₁₂ N
R ₃₋₂	NH ₂	C ₂ H ₆ N
R ₃₋₃	NH ₂	C ₃ H ₆ O ₂ N
R ₃₋₄	OH OH OH	C ₆ H ₁₁ O ₅
R ₃₋₅	OH OH	C ₃ H ₇ O ₂
R ₃₋₆	H	Н
R ₃₋₇	C _(G-1) H _(2G-1-2V)	C _G H _(2G-1-2V)

Table B.5 Additional alteration structures for lipid building blocks: Symbol used in the "code" tables, Molecular structure of the alteration and formula of the additional block to be used when summing the parts of each lipid of the code.

Symbol	Structure	Formula
P	0	HO₃P
D	O 13CH ₃ + S	C ₅ ¹³ CH ₁₀ OS

Table B.6 Codes and Lipid Sum Composition readout for positive ionization mode MS analysis. (Note: E, F, G and X = number of C where E + F + G = X. T, U, V and Y = number of double bonds where T + U + V = Y).

lon Observed ([M + adduct] ⁺)	Lipid Sum Composition
[B ₁ R ₁₋₁ R ₂₋₁ PR ₃₋₁ + H] [†]	PC _(X:Y)
$[B_1R_{1-2}R_{2-1}PR_{3-1} + H]^{+}$	PC _(O-X:Y)
[B ₁ R ₁₋₃ R ₂₋₁ PR ₃₋₁ + H] ⁺	PC _(P-X:Y)
[B ₁ R ₁₋₁ R ₂₋₄ PR ₃₋₁ + H] ⁺	LPC(X:Y)
[B ₁ R ₁₋₂ R ₂₋₄ PR ₃₋₁ + H] ⁺	LPC _(O-X:Y)
[B ₁ R ₁₋₃ R ₂₋₄ PR ₃₋₁ + H] ⁺	LPC(P-X:Y)
$[B_1R_{1-1}R_{2-1}PR_{3-2}D + H]^{+}$	PE(X:Y)
[B ₁ R ₁₋₂ R ₂₋₁ PR ₃₋₂ D + H] ⁺	PE _(O-X:Y)
[B ₁ R ₁₋₃ R ₂₋₁ PR ₃₋₂ D + H] ⁺	PE _(P-X:Y)
[B ₁ R ₁₋₁ R ₂₋₄ PR ₃₋₂ D + H] ⁺	LPE(X:Y)
[B ₁ R ₁₋₂ R ₂₋₄ PR ₃₋₂ D + H] ⁺	LPE _(O-X:Y)
$[B_1R_{1-3}R_{2-4}PR_{3-2}D + H]^{+}$	LPE(P-X:Y)
[B ₁ R ₁₋₁ R ₂₋₁ PR ₃₋₃ D + H] ⁺	PS _(X:Y)
[B ₁ R ₁₋₂ R ₂₋₁ PR ₃₋₃ D + H] ⁺	PS _(O-X:Y)
[B ₁ R ₁₋₃ R ₂₋₁ PR ₃₋₃ D + H] ⁺	PS _(P-X:Y)
[B ₁ R ₁₋₁ R ₂₋₄ PR ₃₋₃ D + H] ⁺	LPS _(X:Y)
$[B_1R_{1-2}R_{2-4}PR_{3-3}D + H]^{+}$	LPS _(O-X:Y)

Table B.6 (Cont'd)

Table B.6 (Cont'd)	
[B ₁ R ₁₋₃ R ₂₋₄ PR ₃₋₃ D + H] ⁺	LPS _(P-X:Y)
[B ₁ R ₁₋₁ R ₂₋₁ PR ₃₋₄ + NH ₄] ⁺	PI(X:Y)
[B ₁ R ₁₋₂ R ₂₋₁ PR ₃₋₄ + NH ₄] ⁺	PI _(O-X:Y)
[B ₁ R ₁₋₃ R ₂₋₁ PR ₃₋₄ + NH ₄] ⁺	PI(P- X :Y)
[B ₁ R ₁₋₁ R ₂₋₄ PR ₃₋₄ + NH ₄] ⁺	LPI(X:Y)
[B ₁ R ₁₋₂ R ₂₋₄ PR ₃₋₄ + NH ₄] ⁺	LPI _(O-X:Y)
[B ₁ R ₁₋₃ R ₂₋₄ PR ₃₋₄ + NH ₄] ⁺	LPI _(P-X:Y)
[B ₁ R ₁₋₁ R ₂₋₁ PR ₃₋₅ + NH ₄] ⁺	PG(x : y)
[B ₁ R ₁₋₂ R ₂₋₁ PR ₃₋₅ + NH ₄] ⁺	PG _(O-X:Y)
[B ₁ R ₁₋₃ R ₂₋₁ PR ₃₋₅ + NH ₄] ⁺	PG(P- X:Y)
[B ₁ R ₁₋₁ R ₂₋₄ PR ₃₋₅ + NH ₄] ⁺	LPG _(X:Y)
[B ₁ R ₁₋₂ R ₂₋₄ PR ₃₋₅ + NH ₄] ⁺	LPG _(O-X:Y)
[B ₁ R ₁₋₃ R ₂₋₄ PR ₃₋₅ + NH ₄] ⁺	LPG _(P-X:Y)
[B ₁ R ₁₋₁ R ₂₋₁ PR ₃₋₆ + NH ₄] ⁺	PA(x : y)
[B ₁ R ₁₋₂ R ₂₋₁ PR ₃₋₆ + NH ₄] ⁺	PA _(O-X:Y)
[B ₁ R ₁₋₃ R ₂₋₁ PR ₃₋₆ + NH ₄] ⁺	PA(P- X:Y)
[B ₁ R ₁₋₁ R ₂₋₄ PR ₃₋₆ + NH ₄] ⁺	LPA(x : y)
$[B_1R_{1-2}R_{2-4}PR_{3-6} + NH_4]^+$	LPA _(O-X:Y)
[B ₁ R ₁₋₃ R ₂₋₄ PR ₃₋₆ + NH ₄] ⁺	LPA(P- X:Y)
[B ₁ R ₁₋₁ R ₂₋₁ R ₃₋₁ + NH ₄] ⁺	TG(X:Y)
$[B_1R_{1-2}R_{2-1}R_{3-1} + NH_4]^{+}$	TG _(O-X:Y)
[B ₁ R ₁₋₃ R ₂₋₁ R ₃₋₁ + NH ₄] ⁺	TG _(P-X:Y)
[B ₁ R ₁₋₁ R ₂₋₁ R ₃₋₆ + NH ₄] ⁺	$DG_{(\mathbf{X}:\mathbf{Y})}$
[B ₁ R ₁₋₂ R ₂₋₁ R ₃₋₆ + NH ₄] ⁺	DG _(O-X:Y)
[B ₁ R ₁₋₃ R ₂₋₁ R ₃₋₆ + NH ₄] ⁺	DG _(P-X:Y)
[B ₁ R ₁₋₁ R ₂₋₄ R ₃₋₆ + NH ₄] ⁺	$MG_{(X:Y)}$
[B ₁ R ₁₋₂ R ₂₋₄ R ₃₋₆ + NH ₄] ⁺	MG _(O-X:Y)
[B ₁ R ₁₋₃ R ₂₋₄ R ₃₋₆ + NH ₄] ⁺	MG _(P-X:Y)
[B ₂ R ₁₋₂ R ₂₋₁ PR ₃₋₁ + H] ⁺	SM(X +2: Y)
[B ₂ R ₁₋₂ R ₂₋₁ R ₃₋₆ + H] ⁺	Cer _(X+2:Y)
[B ₂ R ₁₋₂ R ₂₋₁ R ₃₋₄ + H] [†]	Hex-Cer(x +2: Y)
$[B_3R_{1-4} + NH_4]^{+}$	Chol
$[B_3R_{1-1} + NH_4]^+$	Chol Ester(X:Y)

Table B.7 Codes and Lipid Sum Composition readout for negative ionization mode MS analysis. (Note: E, F, G and X = number of C where E + F + G = X. T, U, V and Y = number of double bonds where T + U + V = Y).

lon Observed ([M +/- adduct])	Readout
[B ₁ R ₁₋₁ R ₂₋₁ PR ₃₋₁ + HCO ₂]	PC(X:Y)
[B ₁ R ₁₋₂ R ₂₋₁ PR ₃₋₁ + HCO ₂]	PC _(O-X:Y)
[B ₁ R ₁₋₃ R ₂₋₁ PR ₃₋₁ + HCO ₂]	PC _(P-X:Y)
[B ₁ R ₁₋₁ R ₂₋₄ PR ₃₋₁ + HCO ₂]	LPC(X:Y)
[B ₁ R ₁₋₂ R ₂₋₄ PR ₃₋₁ + HCO ₂]	LPC _(O-X:Y)
[B ₁ R ₁₋₃ R ₂₋₄ PR ₃₋₁ + HCO ₂]	LPC _(P-X:Y)
[B ₁ R ₁₋₁ R ₂₋₁ PR ₃₋₂ - H] ⁺	PE(X:Y)
[B ₁ R ₁₋₂ R ₂₋₁ PR ₃₋₂ - H] ⁺	PE(O- X:Y)
[B ₁ R ₁₋₃ R ₂₋₁ PR ₃₋₂ - H] [†]	PE(P-X:Y)
[B ₁ R ₁₋₁ R ₂₋₄ PR ₃₋₂ - H] ⁺	LPE(X:Y)
[B ₁ R ₁₋₂ R ₂₋₄ PR ₃₋₂ - H] ⁺	LPE _(O-X:Y)
[B ₁ R ₁₋₃ R ₂₋₄ PR ₃₋₂ - H] ⁺	LPE(P-X:Y)
[B ₁ R ₁₋₁ R ₂₋₁ PR ₃₋₃ - H] ⁺	PS(x : y)
[B ₁ R ₁₋₂ R ₂₋₁ PR ₃₋₃ - H] ⁺	PS _(O-X:Y)
[B ₁ R ₁₋₃ R ₂₋₁ PR ₃₋₃ - H] [†]	PS _(P-X:Y)
[B ₁ R ₁₋₁ R ₂₋₄ PR ₃₋₃ - H] [†]	LPS(x:y)
[B ₁ R ₁₋₂ R ₂₋₄ PR ₃₋₃ - H] ⁺	LPS _(O-X:Y)
[B ₁ R ₁₋₃ R ₂₋₄ PR ₃₋₃ - H] ⁺	LPS _(P-X:Y)
[B ₁ R ₁₋₁ R ₂₋₁ PR ₃₋₄ - H] ⁺	PI(X:Y)
[B ₁ R ₁₋₂ R ₂₋₁ PR ₃₋₄ - H] ⁺	PI(O-X:Y)
[B ₁ R ₁₋₃ R ₂₋₁ PR ₃₋₄ - H] ⁺	PI(P-X:Y)
[B ₁ R ₁₋₁ R ₂₋₄ PR ₃₋₄ - H] ⁺	LPI(X:Y)
[B ₁ R ₁₋₂ R ₂₋₄ PR ₃₋₄ - H] [†]	LPI _(O-X:Y)
[B ₁ R ₁₋₃ R ₂₋₄ PR ₃₋₄ - H] ⁺	LPI(P-X:Y)
[B ₁ R ₁₋₁ R ₂₋₁ PR ₃₋₅ - H] ⁺	PG(X:Y)
[B ₁ R ₁₋₂ R ₂₋₁ PR ₃₋₅ - H] ⁺	PG _(O-X:Y)
[B ₁ R ₁₋₃ R ₂₋₁ PR ₃₋₅ - H] ⁺	PG _(P-X:Y)
[B ₁ R ₁₋₁ R ₂₋₄ PR ₃₋₅ - H] ⁺	LPG _(X:Y)
[B ₁ R ₁₋₂ R ₂₋₄ PR ₃₋₅ - H] ⁺	LPG _(O-X:Y)
[B ₁ R ₁₋₃ R ₂₋₄ PR ₃₋₅ - H] [†]	LPG _(P-X:Y)

Table B.7 (Cont'd)

Table Bit (Some a)	
[B ₁ R ₁₋₁ R ₂₋₁ PR ₃₋₆ - H] ⁺	PA(X:Y)
[B ₁ R ₁₋₂ R ₂₋₁ PR ₃₋₆ - H] ⁺	PA(O- X:Y)
[B ₁ R ₁₋₃ R ₂₋₁ PR ₃₋₆ - H] ⁺	PA(P- X:Y)
[B ₁ R ₁₋₁ R ₂₋₄ PR ₃₋₆ - H] ⁺	LPA(X:Y)
[B ₁ R ₁₋₂ R ₂₋₄ PR ₃₋₆ - H] ⁺	LPA(O-X:Y)
[B ₁ R ₁₋₃ R ₂₋₄ PR ₃₋₆ - H] ⁺	LPA(P- X:Y)
[B ₂ R ₁₋₂ R ₂₋₁ PR ₃₋₁ + HCO ₂]	SM _(X+2:Y)
[B ₂ R ₁₋₂ R ₂₋₁ R ₃₋₆ - H] [†]	Cer(X +2: Y)
[B ₂ R ₁₋₂ R ₂₋₁ R ₃₋₄ - H] ⁺	Hex-Cer(X+2:Y)

Table B.8 Codes and Readout for the confirmation and acyl/alkyl/alkenyl chain identification of PC lipids via MS/MS analysis. (Note: E, F and X = number of C where E + F = X. T, U and Y = number of double bonds where T + U = Y).

If	Then (Readout)
+MS or -MS Ion Observed includes B ₁ R ₁₋₁ R ₂₋₁ PR ₃₋₁ <i>AND</i>	PC _(E:T/F:U) AND
-MS/MS of [M + HCO ₂] yields [B ₁ R ₁₋₁ R ₂₋₁ PR ₃₋₁ – CH ₃]	PC(F:U/E:T)
and [B ₁ R ₁₋₁ R ₂₋₄ PR ₃₋₁ – CH ₃] and	
[B ₁ R ₁₋₄ R ₂₋₁ PR ₃₋₁ – CH ₃] AND	
[B ₁ R ₁₋₁ R ₂₋₄ PR ₃₋₁ - CH ₃] * 0.6 <	
[B ₁ R ₁₋₄ R ₂₋₁ PR ₃₋₁ – CH ₃] AND	
E + F = X and T + U = Y	
+MS or -MS Ion Observed includes B ₁ R ₁₋₁ R ₂₋₁ PR ₃₋₁ <i>AND</i>	PC _(E:T/F:U)
-MS/MS of [M + HCO ₂] yields [B ₁ R ₁₋₁ R ₂₋₁ PR ₃₋₁ – CH ₃]	
and [B ₁ R ₁₋₁ R ₂₋₄ PR ₃₋₁ – CH ₃] and	
[B ₁ R ₁₋₄ R ₂₋₁ PR ₃₋₁ – CH ₃] AND	
$[B_1R_{1-1}R_{2-4}PR_{3-1} - CH_3]^{-*} 0.6 \ge$	
[B ₁ R ₁₋₄ R ₂₋₁ PR ₃₋₁ – CH ₃] AND	
E + F = X and $T + U = Y$	
+MS or -MS Ion Observed includes B ₁ R ₁₋₁ R ₂₋₁ PR ₃₋₁ AND	PC _(E:T/F:U)
-MS/MS of [M + HCO ₂] yields [B ₁ R ₁₋₁ R ₂₋₁ PR ₃₋₁ – CH ₃]	
and [B ₁ R ₁₋₁ R ₂₋₄ PR ₃₋₁ – CH ₃] and [R ₂₋₁ + O] AND	
$\mathbf{E} + \mathbf{F} = \mathbf{X}$ and $\mathbf{T} + \mathbf{U} = \mathbf{Y}$	
+MS or -MS Ion Observed includes B ₁ R ₁₋₁ R ₂₋₁ PR ₃₋₁ AND	PC(E:T_F:U)
-MS/MS of [M + HCO ₂] yields [B ₁ R ₁₋₁ R ₂₋₁ PR ₃₋₁ - CH ₃]	
and [R ₁₋₁ + O] and [R ₂₋₁ + O] AND	
$\mathbf{E} + \mathbf{F} = \mathbf{X}$ and $\mathbf{T} + \mathbf{U} = \mathbf{Y}$	

Table B.8 (Cont'd)

+MS or -MS Ion Observed includes B ₁ R ₁₋₁ R ₂₋₁ PR ₃₋₁ <i>AND</i>	PC _(X:Y)
-MS/MS of [M + HCO ₂] yields [B ₁ R ₁₋₁ R ₂₋₁ PR ₃₋₁ - CH ₃]	
+MS or -MS Ion Observed includes B ₁ R ₁₋₂ R ₂₋₁ PR ₃₋₁ <i>AND</i>	PC _(O-E:T/F:U)
-MS/MS of [M + HCO ₂] yields [B ₁ R ₁₋₂ R ₂₋₁ PR ₃₋₁ - CH ₃]	
and [B ₁ R ₁₋₂ R ₂₋₄ PR ₃₋₁ – CH ₃] and [R ₂₋₁ + O] AND	
$\mathbf{E} + \mathbf{F} = \mathbf{X}$ and $\mathbf{T} + \mathbf{U} = \mathbf{Y}$	
+MS or -MS Ion Observed includes B ₁ R ₁₋₂ R ₂₋₁ PR ₃₋₁ <i>AND</i>	PC _(O-X:Y)
-MS/MS of [M + HCO ₂] yields [B ₁ R ₁₋₂ R ₂₋₁ PR ₃₋₁ - CH ₃]	
+MS or -MS Ion Observed includes B ₁ R ₁₋₃ R ₂₋₁ PR ₃₋₁	PC _{(P-(X-F):(Y-}
AND +MS/MS of [M + H] ⁺ yields [PR₃₋₁ + OH] ⁺ and	U)/F:U)
[B ₁ R ₁₋₄ R ₂₋₁ PR ₃₋₁ + H] ⁺	
+MS or -MS Ion Observed includes B ₁ PR ₃₋₁ <i>AND</i>	Will Include "PC" (PC, O-PC, P-PC,
+MS/MS of [M + H] ⁺ yields [PR ₃₋₁ + OH] ⁺	LPC, O-LPC, P- LPC)

Table B.9 Codes and Readout for the confirmation and acyl/alkyl/alkenyl chain identification of PE lipids via MS/MS analysis. (Note: E, F and X = number of C where E + F = X. T, U and Y = number of double bonds where T + U = Y).

If	Then (Readout)
+MS or -MS Ion Observed includes B ₁ R ₁₋₁ R ₂₋₁ PR ₃₋₂ <i>AND</i>	PE _(E:T/F:U) AND
-MS/MS of [M - H] yields [B ₁ R ₁₋₁ R ₂₋₄ PR ₃₋₂ - H] and	PE(F:U/E:T)
[B ₁ R ₁₋₄ R ₂₋₁ PR ₃₋₂ – H] AND	
[B ₁ R ₁₋₁ R ₂₋₄ PR ₃₋₂ - H] * 0.6 < [B ₁ R ₁₋₄ R ₂₋₁ PR ₃₋₂ - H] AND	
E+ F = X and T + U = Y	
+MS or -MS Ion Observed includes B ₁ R ₁₋₁ R ₂₋₁ PR ₃₋₂ <i>AND</i>	PE(E:T/F:U)
-MS/MS of [M - H] yields [B ₁ R ₁₋₁ R ₂₋₄ PR ₃₋₂ - H] and	
[B ₁ R ₁₋₄ R ₂₋₁ PR ₃₋₂ – H] AND	
$[B_1R_{1-1}R_{2-4}PR_{3-2} - H]^{-*} 0.6 \ge [B_1R_{1-4}R_{2-1}PR_{3-2} - H]^{-*}$ AND	
E+ F = X and T + U = Y	
+MS or -MS Ion Observed includes B ₁ R ₁₋₁ R ₂₋₁ PR ₃₋₂ <i>AND</i>	PE(E:T/F:U)
-MS/MS of [M - H] yields [B ₁ R ₁₋₁ R ₂₋₄ PR ₃₋₂ - H] and	
[R ₂₋₁ + O] AND	
E+ F = X and T + U = Y	
+MS or -MS Ion Observed includes B ₁ R ₁₋₁ R ₂₋₁ PR ₃₋₂ AND	PE _(E:T_F:U)
-MS/MS of [M - H] yields [R ₁₋₁ + O] and [R ₂₋₁ + O]	
AND E+ F = X and T + U = Y	
+MS or -MS Ion Observed includes B ₁ R ₁₋₁ R ₂₋₁ PR ₃₋₂ AND	PE(X:Y)
+MS/MS of [M - H] yields [B ₁ PR ₃₋₂ -H]	

Table B.9 (Cont'd)

+MS or –MS Ion Observed includes B ₁ R ₁₋₂ R ₂₋₁ PR ₃₋₂ AND	PE _(O-E:T/F:U)
-MS/MS of [M - H] yields [B ₁ R ₁₋₂ R ₂₋₄ PR ₃₋₂ – H] and	
[R ₂₋₁ + O] ⁻	
AND E+ F = X and T + U = Y	
+MS or -MS Ion Observed includes B ₁ R ₁₋₂ R ₂₋₁ PR ₃₋₂	PE _(O-X:Y)
AND	
+MS/MS of [M - H] yields [B ₁ PR ₃₋₂ -H]	
+MS or -MS Ion Observed includes B ₁ R ₁₋₃ R ₂₋₁ PR ₃₋₂	PE(P-(X-F):(Y-
AND	U)/F:U)
$+MS/MS \text{ of } [\mathbf{M} + H]^{+} \text{ yields } [\mathbf{B_1R_{1-4} R_{2-1}PR_{3-2}} + O_2C_3H_6]^{+}$	- , ,
+MS or -MS Ion Observed includes B ₁ PR ₃₋₂ D	Will Include "PE"
AND	(PE, O-PE, P-PE,
$+MS/MS$ of $[M + H]^{+}$ yields $[PR_{3-2} + O_2C_3H_6]^{+}$	LPE, O-LPE, P-
1100/100 01 [m 1 11] y10103 [1 113-2 + 02031 16]	LPE)

Table B.10 Codes and Readout for the confirmation and acyl/alkyl/alkenyl chain identification of PS lipids via MS/MS analysis. (Note: E, F and X = number of C where E + F = X. T, U and Y = number of double bonds where T + U = Y).

If	Then (Readout)
+MS or -MS Ion Observed includes B ₁ R ₁₋₁ R ₂₋₁ PR ₃₋₃ AND	PS _(E:T/F:U) AND
-MS/MS of [M - H] yields [B ₁ R ₁₋₁ R ₂₋₁ P] and [B ₁ R ₁₋₁ P - H]	PS(F:U/E:T)
and [B ₁ R ₂₋₁ P – H] AND	
[B ₁ R ₁₋₁ P- H] * 0.6 < [B ₁ R ₂₋₁ P - H] AND	
E+ F = X and T + U = Y	
+MS or -MS Ion Observed includes B ₁ R ₁₋₁ R ₂₋₁ PR ₃₋₃ <i>AND</i>	PS(E:T/F:U)
-MS/MS of [M - H] yields [B ₁ R ₁₋₁ R ₂₋₁ P] and [B ₁ R ₁₋₁ P – H]	
and [B ₁ R ₂₋₁ P – H] AND	
$[B_1R_{1-1}P - H]^{-*} 0.6 \ge [B_1R_{2-1}P - H]^{-*}$ AND	
E+ F = X and T + U = Y	
+MS or -MS Ion Observed includes B ₁ R ₁₋₁ R ₂₋₁ PR ₃₋₃ AND	PS(E:T/F:U)
-MS/MS of [M - H] yields [B ₁ R ₁₋₁ R ₂₋₁ P] and	
[B ₁ R ₁₋₁ P– H] and [R ₂₋₁ + O] AND	
E+ F = X and T + U = Y	
+MS or -MS Ion Observed includes B ₁ R ₁₋₁ R ₂₋₁ PR ₃₋₃ AND	PS(E:T_F:U)
-MS/MS of [M - H] yields [B ₁ R ₁₋₁ R ₂₋₁ P] and [R ₁₋₁ + O]	
and [R ₂₋₁ + O]	
AND	
E+ F = X and T + U = Y	
+MS or –MS Ion Observed includes B ₁ R ₁₋₁ R ₂₋₁ PR ₃₋₃ AND	PS _(X:Y)
+MS/MS of [M - H] yields [B ₁ R ₁₋₁ R ₂₋₁ P]	

Table B.10 (Cont'd)

+MS or -MS Ion Observed includes B ₁ R ₁₋₂ R ₂₋₁ PR ₃₋₃ AND	PS _(O-E:T/F:U)
-MS/MS of [M - H] yields [B ₁ R ₁₋₁ R ₂₋₁ P] and	
[B ₁ R ₁₋₁ P- H] and [R ₂₋₁ + O] AND	
E+ F = X and T + U = Y	
+MS or -MS Ion Observed includes B ₁ R ₁₋₂ R ₂₋₁ PR ₃₋₃ <i>AND</i>	PS _(O-X:Y)
+MS/MS of [M - H] yields [B ₁ R ₁₋₁ R ₂₋₁ P]	
+MS or -MS Ion Observed includes B ₁ R ₁₋₃ R ₂₋₁ PR ₃₋₃	PS(P-(X-F):(Y-
AND +MS/MS of $[M + H]^{+}$ yields $[B_{1}R_{1-4} R_{2-1}PR_{3-3} + O_{2}C_{3}H_{6}]^{+}$	U)/F:U)
+MS or –MS Ion Observed includes B ₁ PR ₃₋₃ D	Will Include "PS" (PS, O-PS, P-PS,
AND +MS/MS of $[M + H]^{+}$ yields $[PR_{3-3} + O_2C_3H_6]^{+}$	LPS, O-LPS, P- LPS)

Table B.11 Codes and Readout for the confirmation and acyl/alkyl/alkenyl chain identification of PI lipids via MS/MS analysis. (Note: E, F and X = number of C where E + F = X. T, U and Y = number of double bonds where T + U = Y).

If	Then (Readout)
+MS or -MS Ion Observed includes B ₁ R ₁₋₁ R ₂₋₁ PR ₃₋₄ AND	PI(E:T/F:U) AND
-MS/MS of [M - H] yields [PR₃₋₄ – 2H] and	PI(F:U/E:T)
[B ₁ R ₁₋₁ PR ₃₋₄ – H] and [B ₁ R ₂₋₁ PR ₃₋₄ – H] AND	
[B ₁ R ₁₋₁ PR ₃₋₄ - H] * 0.6 < [B ₁ R ₂₋₁ PR ₃₋₄ - H] AND	
E+ F = X and T + U = Y	
+MS or -MS Ion Observed includes B ₁ R ₁₋₁ R ₂₋₁ PR ₃₋₄ <i>AND</i>	PI(E:T/F:U)
-MS/MS of [M - H] yields [PR₃₋₄ – 2H] and	
[B ₁ R ₁₋₁ PR ₃₋₄ – H] and [B ₁ R ₂₋₁ PR ₃₋₄ – H] AND	
$[B_1R_{1-1}PR_{3-4} - H]^{-*} 0.6 \ge [B_1R_{2-1}PR_{3-4} - H]^{-*}$ AND	
E+ F = X and T + U = Y	
+MS or -MS Ion Observed includes B ₁ R ₁₋₁ R ₂₋₁ PR ₃₋₄ <i>AND</i>	PI(E:T/F:U)
-MS/MS of [M - H] yields [PR₃₋₄ – 2H] and	
[B ₁ R ₁₋₁ PR ₃₋₄ – H] and [R ₂₋₁ + O]	
<i>AND</i> E + F = X and T + U = Y	
+MS or -MS Ion Observed includes B ₁ R ₁₋₁ R ₂₋₁ PR ₃₋₄ AND	PI(E:T_F:U)
-MS/MS of [M - H] yields [PR₃₋₄ – 2H] and [R₁₋₁ + O] and	
$[R_{2-1} + O]^{-}$	
AND	
E+ F = X and T + U = Y	
+MS or -MS Ion Observed includes B ₁ R ₁₋₁ R ₂₋₁ PR ₃₋₄ AND	PI(X:Y)
+MS/MS of [M - H] yields [PR₃₋₄ – 2H]	

Table B.11 (Cont'd)

+MS or -MS Ion Observed includes B ₁ R ₁₋₂ R ₂₋₁ PR ₃₋₄ AND	PI(O-E:T/F:U)
-MS/MS of [M - H] yields [PR₃₋₄ – 2H] and	
[B ₁ R ₁₋₁ PR ₃₋₄ - H] and [R ₂₋₁ + O]	
AND	
E+ F = X and T + U = Y	
+MS or -MS Ion Observed includes B ₁ R ₁₋₂ R ₂₋₁ PR ₃₋₄	PI _(O-X:Y)
AND	
+MS/MS of [M - H] yields [PR₃₋₄ – 2H]	
+MS or -MS Ion Observed includes B ₁ PR ₃₋₄	Will Include "PI"
AND	(PI, O-PI, P-PI,
+MS/MS of $[\mathbf{M} + \mathbf{H}]^{+}$ yields $[\mathbf{BR_1R_2} - \mathbf{O}]^{+}$	LPI, O-LPI, P-LPI)

Table B.12 Codes and Readout for the confirmation and acyl/alkyl/alkenyl chain identification of PG lipids via MS/MS analysis. (Note: E, F and X = number of C where E + F = X. T, U and Y = number of double bonds where T + U = Y).

If	Then (Readout)
+MS or -MS Ion Observed includes B ₁ R ₁₋₁ R ₂₋₁ PR ₃₋₅ <i>AND</i>	PG(E:T/F:U) AND
-MS/MS of [M - H] yields [PR₃₋₅ – 2H] and	PG(F:U/E:T)
[B ₁ R ₁₋₁ PR ₃₋₅ – H] and [B ₁ R ₂₋₁ PR ₃₋₅ – H] AND	
[B ₁ R ₁₋₁ PR ₃₋₅ - H] * 0.6 < [B ₁ R ₂₋₁ PR ₃₋₅ - H] AND	
E+ F = X and T + U = Y	
+MS or -MS Ion Observed includes B ₁ R ₁₋₁ R ₂₋₁ PR ₃₋₅ <i>AND</i>	PG(E:T/F:U)
-MS/MS of [M - H] yields [PR₃₋₅ – 2H] and	
[B ₁ R ₁₋₁ PR ₃₋₅ – H] and [B ₁ R ₂₋₁ PR ₃₋₅ – H] AND	
$[B_1R_{1-1}PR_{3-5} - H]^{-*} 0.6 \ge [B_1R_{2-1}PR_{3-5} - H]^{-*}$ AND	
E+F=X and $T+U=Y$	
+MS or -MS Ion Observed includes B ₁ R ₁₋₁ R ₂₋₁ PR ₃₋₅ AND	PG(E:T/F:U)
-MS/MS of [M - H] yields [PR₃₋₅ – 2H] and	
[B ₁ R ₁₋₁ PR ₃₋₅ – H] and [R ₂₋₁ + O] AND	
E+ F = X and T + U = Y	
+MS or -MS Ion Observed includes B ₁ R ₁₋₁ R ₂₋₁ PR ₃₋₅ <i>AND</i>	PG(E : T _ F : U)
-MS/MS of [M - H] yields [PR₃₋₅ – 2H] and [R₁₋₁ + O] and	
$\begin{bmatrix} R_{2-1} + O \end{bmatrix}^{-}$ AND	
E+ F = X and T + U = Y	
+MS or –MS Ion Observed includes B ₁ R ₁₋₁ R ₂₋₁ PR ₃₋₄	PG _(X:Y)
<i>AND</i> +MS/MS of [M - H] vields [PR₃₋₅ – 2H]	
+MS or –MS Ion Observed includes B ₁ PR ₃₋₅	Will Include "PG"
AND	(PG, O-PG, P-PG,
+MS/MS of [M + H] ⁺ yields [BR ₁ R ₂ - O] ⁺	LPG, O-LPG, P- LPG)

Table B.13 Codes and Readout for the confirmation and acyl/alkyl/alkenyl chain identification of PA lipids via MS/MS analysis. (Note: E, F and X = number of C where E + F = X. T, U and Y = number of double bonds where T + U = Y).

+MS or –MS Ion Observed includes B_1R_{1-1} $R_{2-1}PR_{3-6}$ AND PA(E:T/F:U) AND PA(F:U/E:T)
MS/MS of $[M - H]$ vields $[B_1R_1, P H]$ and $PA(E, U/E, T)$
$\begin{bmatrix} \mathbf{B_1R_{2-1}P} - \mathbf{H} \end{bmatrix}^{T}$
$[\mathbf{B_1R_{1-1}P} - \mathbf{H}]^{-*} 0.6 < [\mathbf{B_1R_{2-1}P} - \mathbf{H}]^{-*}$
E+ F = X and T + U = Y
+MS or -MS Ion Observed includes B₁R₁₋₁ R₂₋₁PR₃₋₆ PA(E : T / F : U)
MS/MS of [M - H] yields [B ₁ R ₁₋₁ P – H] and
[B ₁ R ₂₋₁ P – H]
AND
$[\mathbf{B}_1 \mathbf{R}_{1-1} \mathbf{P} - \mathbf{H}]^{-*} \cdot 0.6 \ge [\mathbf{B}_1 \mathbf{R}_{2-1} \mathbf{P} - \mathbf{H}]^{-*}$
AND
E+ F = X and T + U = Y
+MS or –MS Ion Observed includes B ₁ R ₁₋₁ R ₂₋₁ PR ₃₋₆ PA(E:T/F:U)
·MS/MS of [M - H] yields [B ₁ R ₁₋₁ P – H] and [R ₂₋₁ + O]
AND
E+ F = X and T + U = Y
+MS or –MS Ion Observed includes B ₁ R ₁₋₁ R ₂₋₁ PR ₃₋₃ PA(E:T_F:U)
-MS/MS of [M - H] yields [R ₁₋₁ + O] and [R ₂₋₁ + O]
AND
E+ F = X and T + U = Y
+MS or –MS Ion Observed includes B_1R_{1-2} $R_{2-1}PR_{3-6}$ $PA(O-E:T/F:U)$
MS/MS of [M - H] yields [B ₁ R ₁₋₁ P - H] and [R ₂₋₁ + O]
AND E+ F = X and T + U = Y

Table B.14 Codes and Readout for the confirmation and acyl chain identification of TG lipids via MS/MS analysis. (Note: E, F and X = number of C where E + F = X. T, U and Y = number of double bonds where T + U = Y).

If	Then (Readout)
+MS or -MS Ion Observed includes B ₁ R ₁₋₁ R ₂₋₁ R ₃₋₇ AND	TG _(E:T_F:U_G:V)
+MS/MS of $[\mathbf{M} + NH_4]^{\dagger}$ yields $[\mathbf{BR}_{2-1}\mathbf{R}_{3-7} - O]^{\dagger}$ and	
[BR ₁₋₁ R ₃₋₇ - O] ⁺ and [BR ₁₋₁ R ₂₋₁ - O] ⁺	
E + F = X and $T + U = Y$	

Table B.15 Codes and Readout for the confirmation and acyl chain identification of SM lipids via MS/MS analysis. (Note: E, F and X = number of C where E + F = X. T, U and Y = number of double bonds where T + U = Y).

If	Then (Readout)
+MS or -MS Ion Observed includes B ₂ R ₁₋₂ R ₂₋₁ PR ₃₋₁ AND	SM(dE:T/X-E:Y-T)
+MS/MS of [M + H] ⁺ yields [R ₂₋₁ + N - H] ⁺	
E + F = X and $T + U = Y$	
+MS or -MS Ion Observed includes B ₂ R ₁₋₂ R ₂₋₁ PR ₃₋₁	SM _(X:Y)
AND	
-MS/MS of [M + HCO ₂] yields [B₂R₁₋₂R₂₋₁PR₃₋₁ - CH ₃]	
+MS or -MS Ion Observed includes B ₂ PR ₃₋₁	SM _(X:Y)
AND	, ,
+MS/MS of $[\mathbf{M} + \mathbf{H}]^{+}$ yields $[\mathbf{PR}_{3-1} + \mathbf{OH}]^{+}$	

Table B.16 Codes and Readout for the confirmation and acyl chain identification of Cer lipids via MS/MS analysis. (Note: E, F and X = number of C where E + F = X. T, U and Y = number of double bonds where T + U = Y).

If	Then (Readout)
+MS or -MS Ion Observed includes B ₂ R ₁₋₂ R ₂₋₁ R ₃₋₆ <i>AND</i>	Cer(dE:T/X-E:Y-T)
+MS/MS of [M + H] ⁺ yields [R ₂₋₁ + N - H] ⁺ E + F = X and T + U = Y	

APPENDIX C

This appendix contains figures and tables to support Chapter 4.

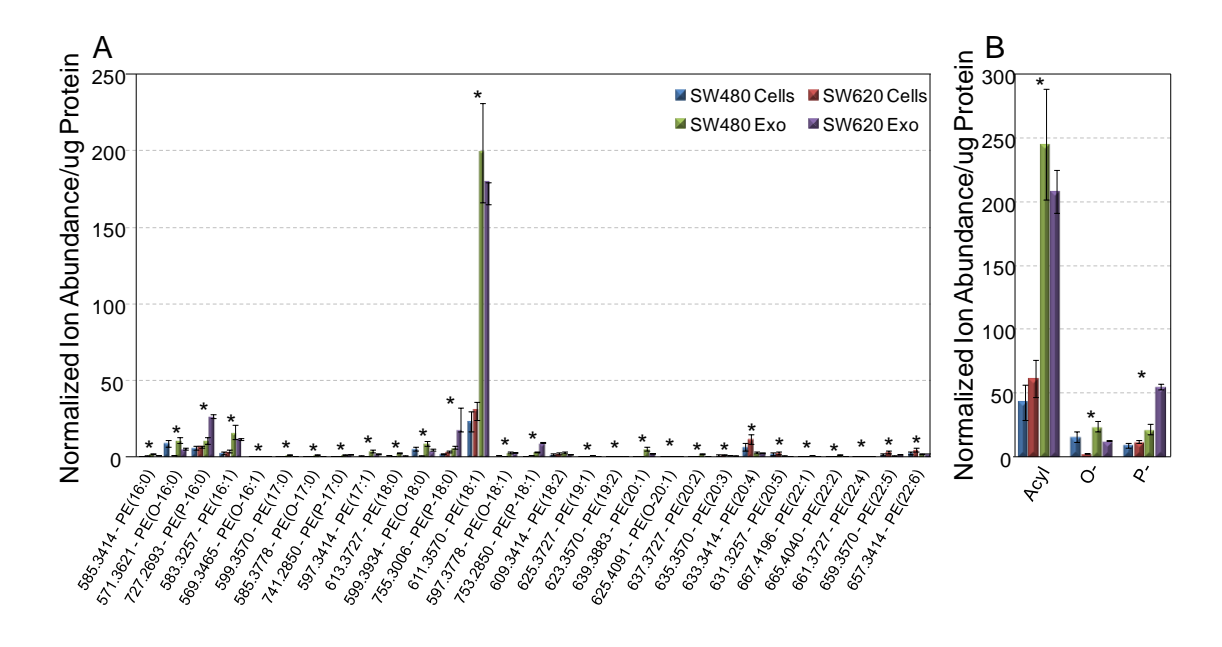


Figure C.1 Quantification of Lyso PE (LPE) lipids from the 13 C₁-DMBNHS derivatized SW480 and SW620 cell and exosome crude lipid extracts. (A) Individual normalized lipid sum composition abundances/µg protein and (B) acyl, O- and P- distribution of LPE species. * = p < 0.01.

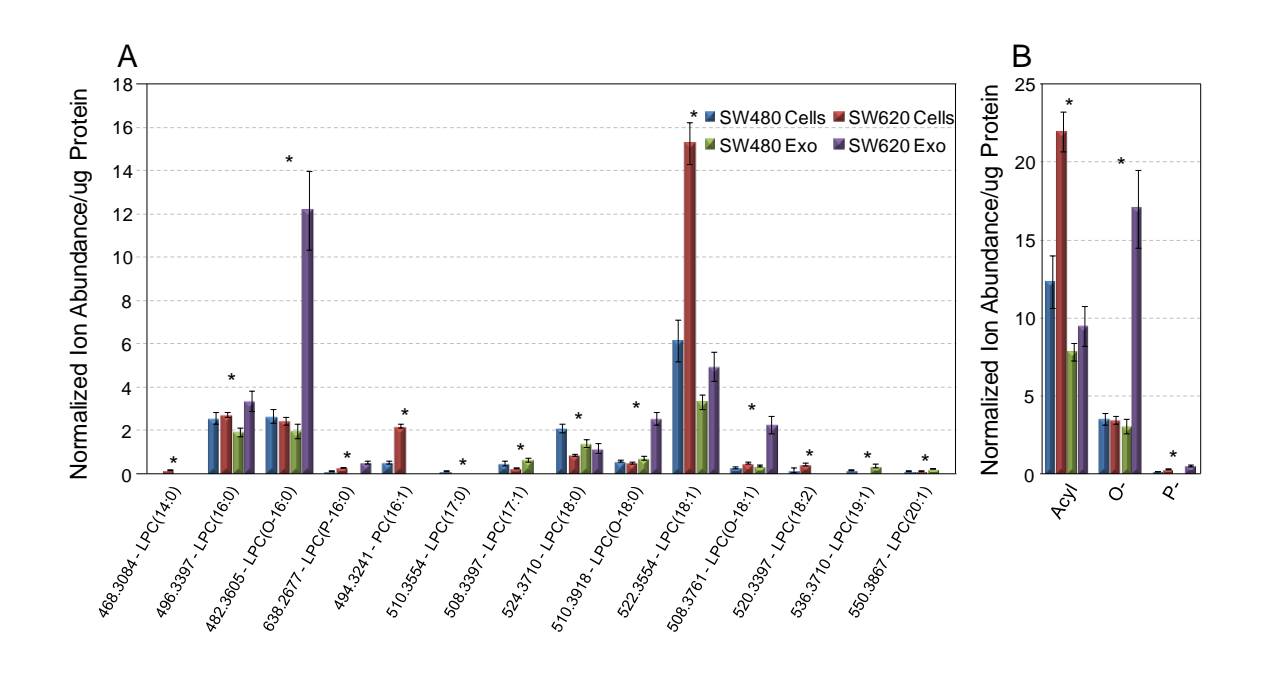


Figure C.2 Quantification of LPC lipids from the 13 C₁-DMBNHS derivatized SW480 and SW620 cell and exosome crude lipid extracts. (A) Individual normalized lipid sum composition abundances/µg protein and (B) acyl, O- and P-distribution of LPC species. * = p < 0.01.

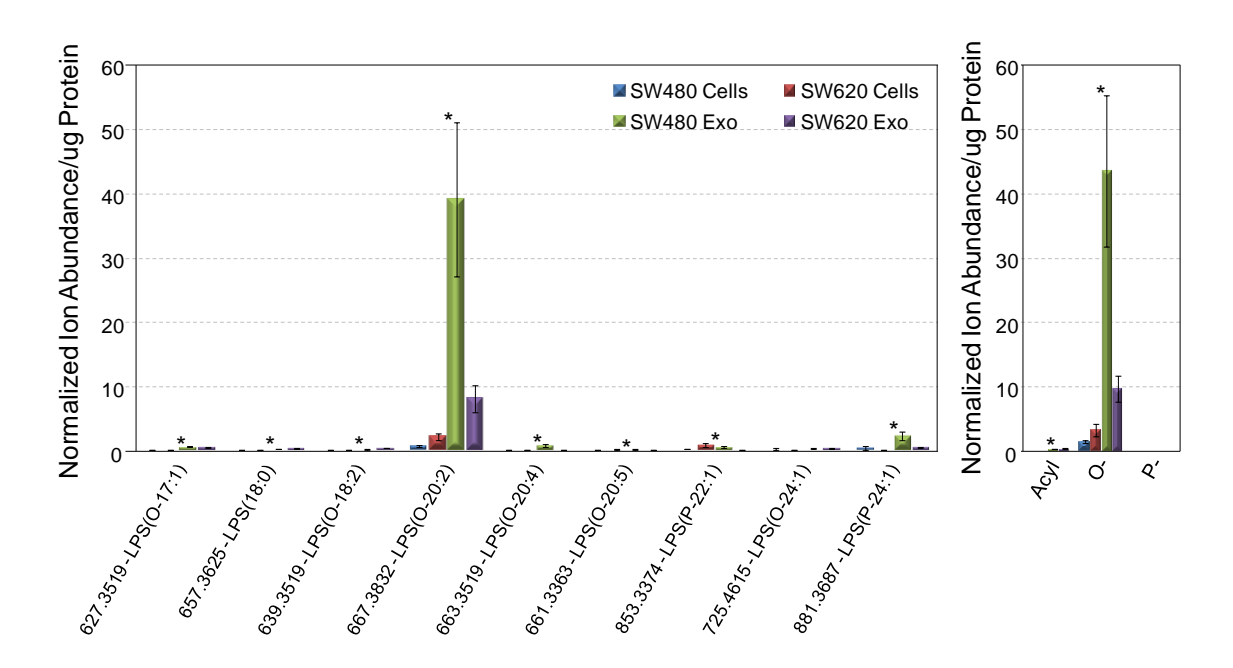


Figure C.3 Quantification of Lyso PS (LPS) lipids from the 13 C₁-DMBNHS derivatized SW480 and SW620 cell and exosome crude lipid extracts. (A) Individual normalized lipid sum composition abundances/µg protein and (B) acyl, O- and P- distribution of LPS species. * = p < 0.01.

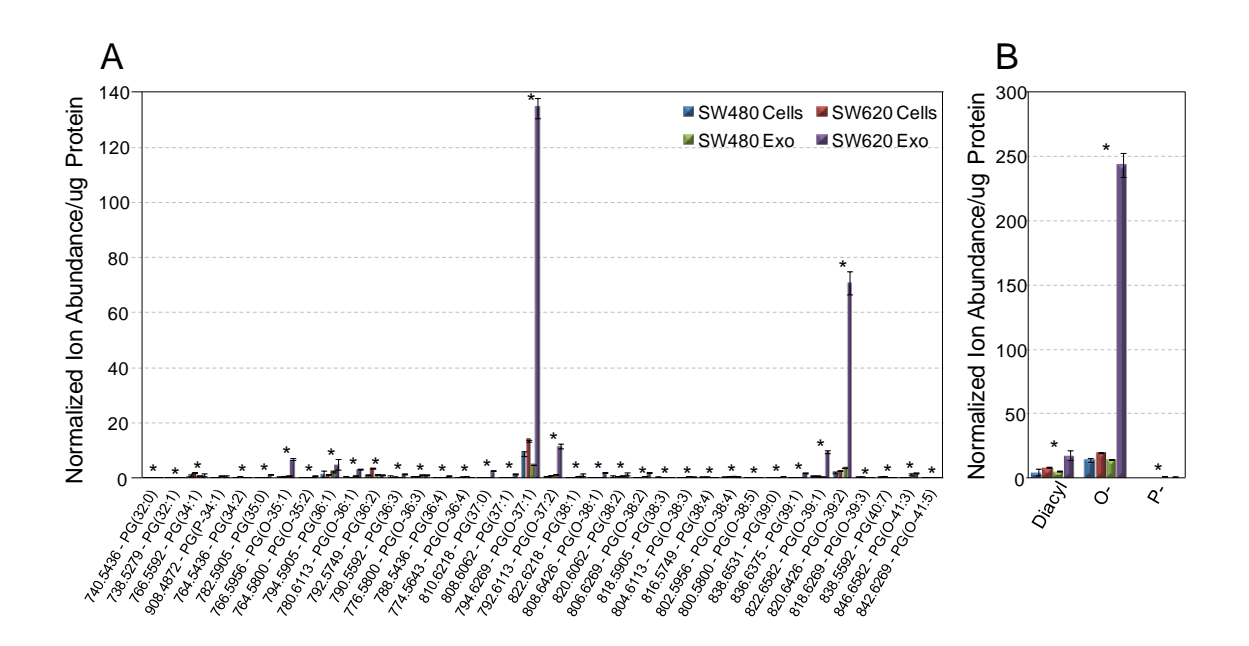


Figure C.4 Quantification of PG lipids from the 13 C₁-DMBNHS derivatized SW480 and SW620 cell and exosome crude lipid extracts. (A) Individual normalized lipid sum composition abundances/µg protein and (B) acyl, O- and P-distribution. * = p < 0.01.

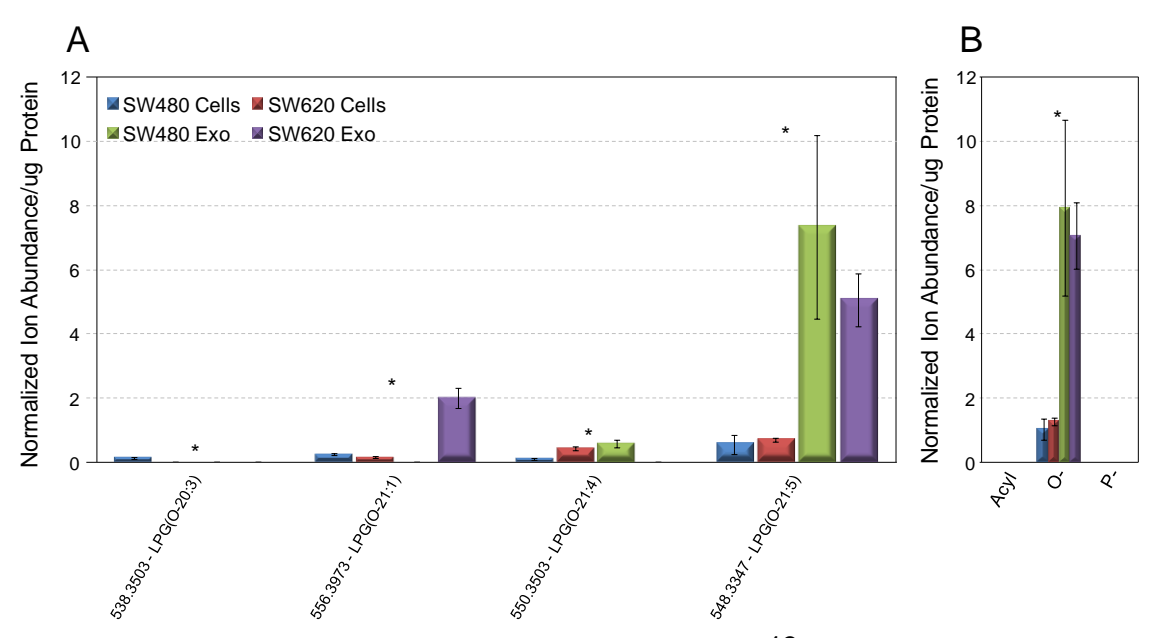


Figure C.5 Quantification of LPG lipids from the 13 C₁-DMBNHS derivatized SW480 and SW620 cell and exosome crude lipid extracts. (A) Individual normalized lipid sum composition abundances/µg protein and (B) acyl, O- and P-distribution. * = p < 0.01.

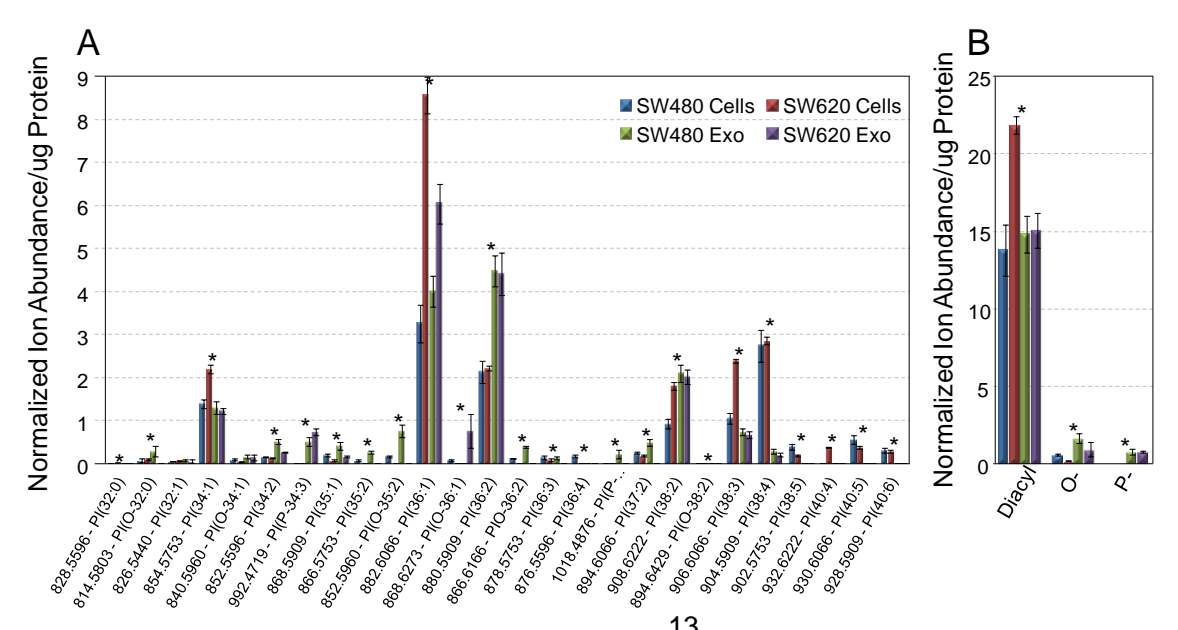


Figure C.6 Quantification of PI lipids from the 13 C₁-DMBNHS derivatized SW480 and SW620 cell and exosome crude lipid extracts. (A) Individual normalized lipid sum composition abundances/µg protein and (B) acyl, O- and P- distribution of PI species. * = p < 0.01.

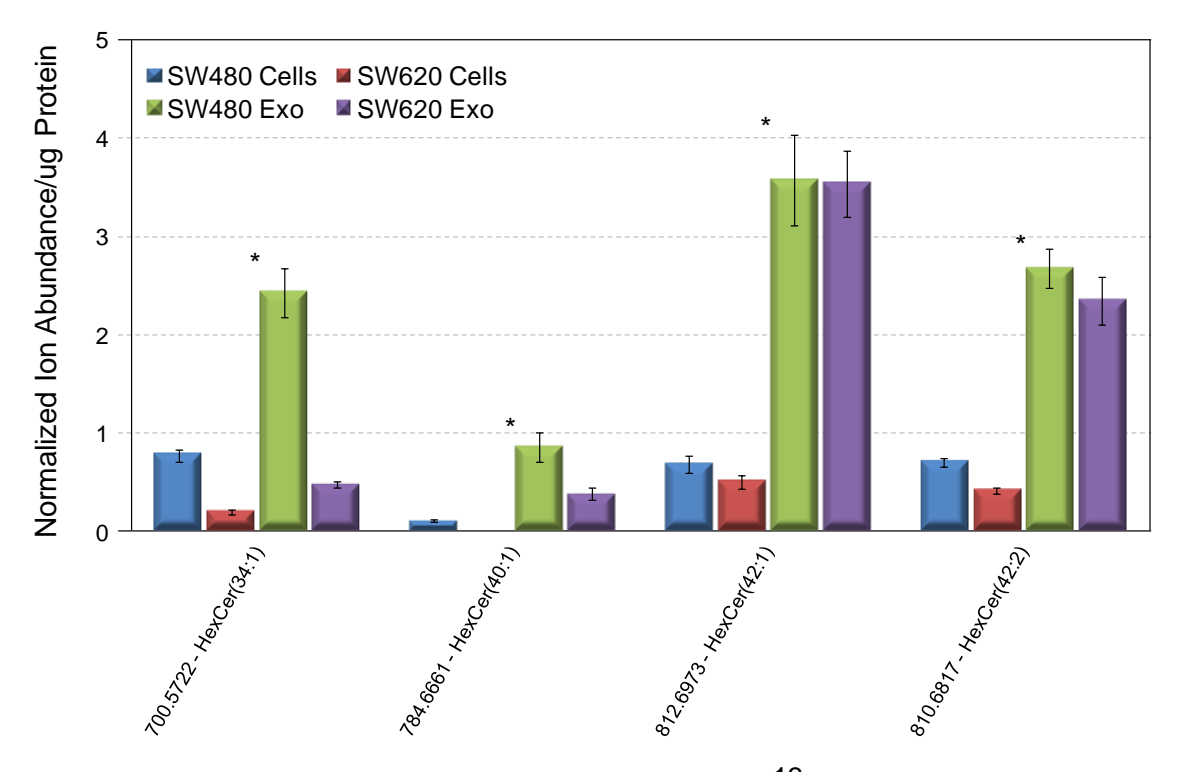


Figure C.7 Quantification of Hex-Cer from the 13 C₁-DMBNHS derivatized SW480 and SW620 cell and exosome crude lipid extracts. Individual normalized lipid sum composition abundances/µg protein. * = p < 0.01.

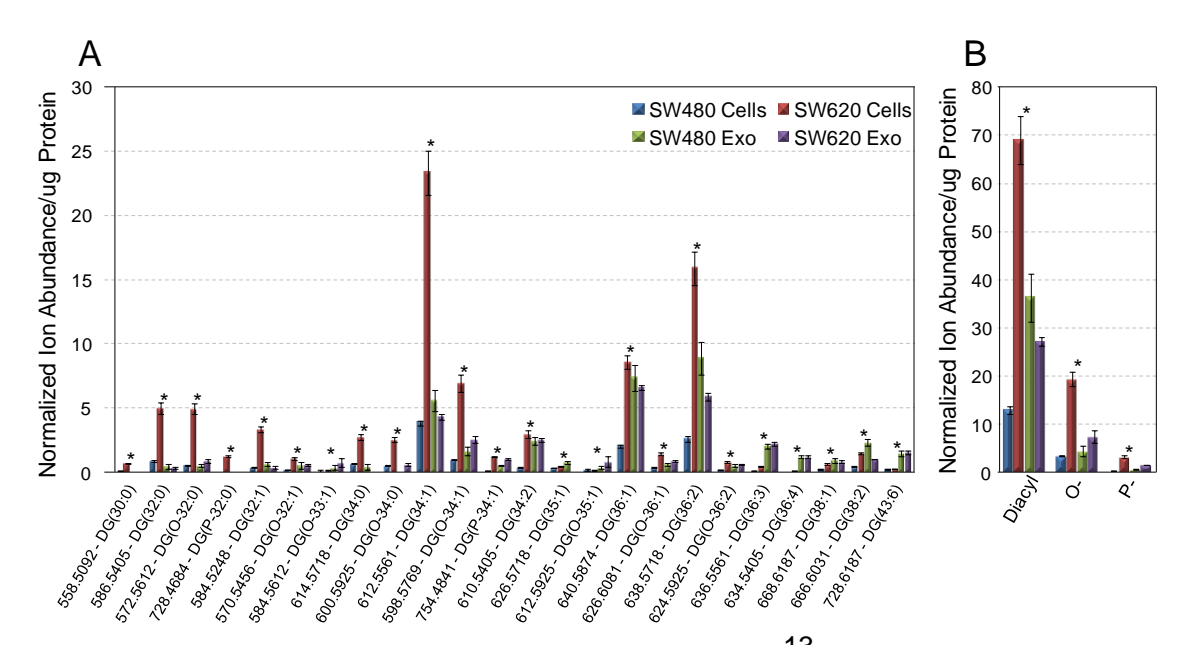


Figure C.8 Quantification of DG lipids from the 13 C₁-DMBNHS derivatized SW480 and SW620 cell and exosome crude lipid extracts. (A) Individual normalized lipid sum composition abundances/µg protein and (B) diacyl, O- and P- distribution. * = p < 0.01.

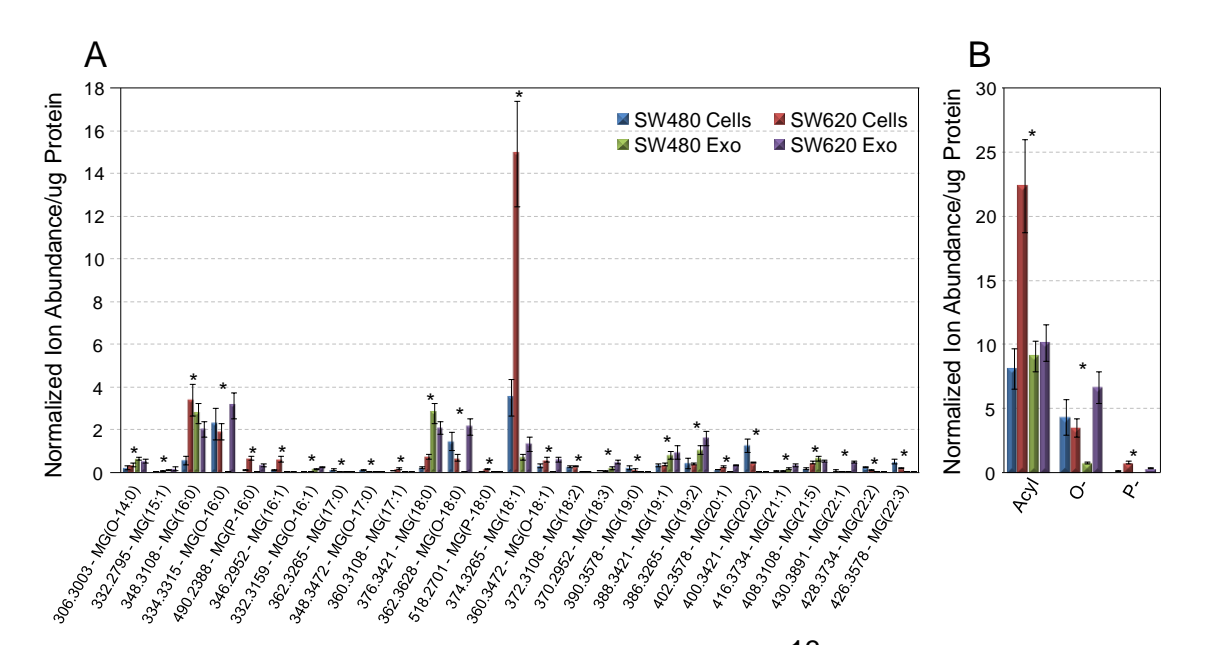


Figure C.9 Quantification of MG lipids from the 13 C₁-DMBNHS derivatized SW480 and SW620 cell and exosome crude lipid extracts. (A) Individual normalized lipid sum composition abundances/µg protein and (B) acyl, O- and P-distribution. * = p < 0.01.

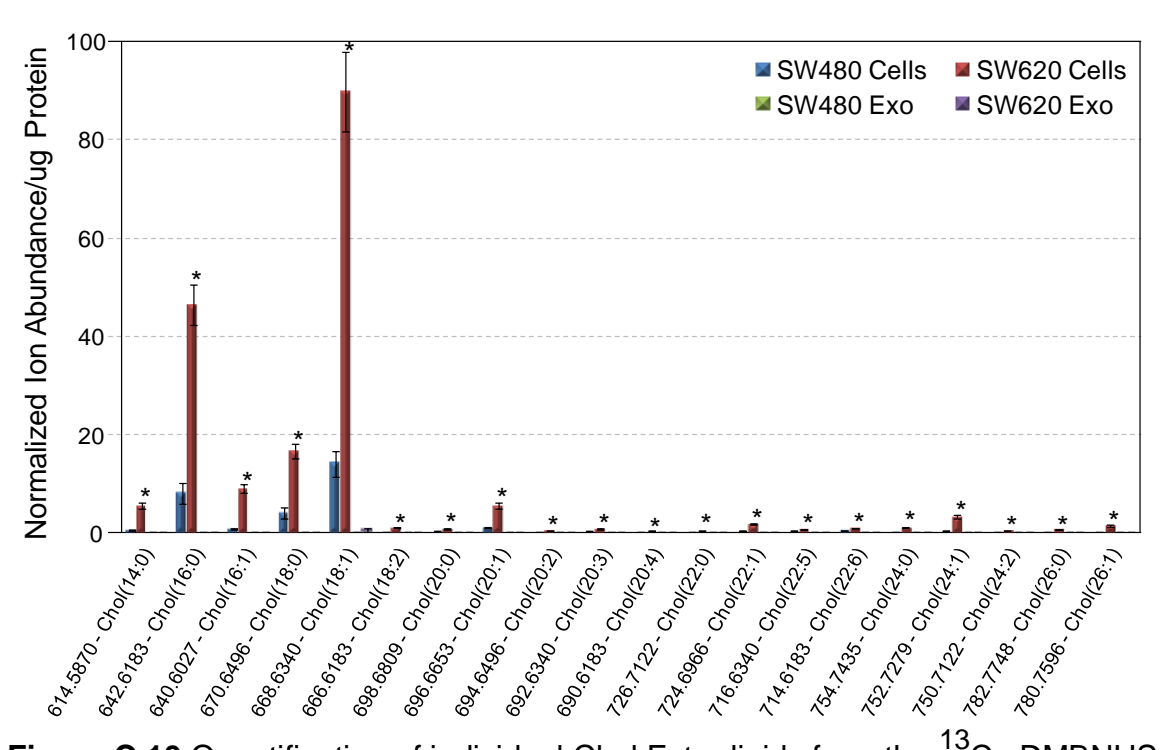


Figure C.10 Quantification of individual Chol Ester lipids from the 13 C₁-DMBNHS derivatized SW480 and SW620 cell and exosome crude lipid extracts as normalized lipid sum composition abundances/µg protein. * = p < 0.01.

Table C.1 PE sum compositions, their positive ionization mode m/z for MS analysis and molecular lipids identified for SW480 cells, SW620 cells, SW480 exosomes and SW620 exosomes.

		SW480 Cells	SW620 Cells	SW480 Exo	SW620 Exo
Sum Comp	(+) Mass	Molecular Lipid	Molecular Lipid	Molecular Lipid	Molecular Lipid
	m/z				
PE(29:1)	779.5084			15:0/14:1	
PE(30:0)	795.5397			16:0/14:0	
PE(P-30:0)	937.4677			P-30:0	
PE(30:1)	793.5241			14:0/16:1	
PE(O-30:1)	779.5448			O-30:1	
PE(P-30:1)	935.4520			P-12:0/18:1	P-12:0/18:1
PE(31:0)	809.5554	15:0/16:0	15:0/16:0	15:0/16:0	15:0/16:0
PE(O-31:0)	795.5761	O-16:0/15:0		O-16:0/15:0	O-16:0/15:0
		O-18:0/13:0		O-18:0/13:0	O-18:0/13:0
PE(P-31:0)	951.4833	P-31:0	P-31:0	P-31:0	P-31:0
PE(31:1)	807.5397			31:1	
PE(O-31:1)	793.5605			O-31:1	
PE(P-31:1)	949.4677	P-31:1	P-31:1	P-31:1	
PE(32:0)	823.5710	16:0/16:0	16:0/16:0	16:0/16:0	16:0/16:0
		18:0/14:0	18:0/14:0	18:0/14:0	18:0/14:0
PE(O-32:0)	809.5918	O-18:0/14:0		O-18:0/14:0	O-18:0/14:0
PE(P-32:0)	965.4990			P-16:0/16:0	P-16:0/16:0
PE(32:1)	821.5554	16:0/16:1	16:0/16:1	16:0/16:1	16:0/16:1
		14:0/18:1	14:0/18:1	14:0/18:1	14:0/18:1
PE(O-32:1)	807.5761	O-16:0/16:1	O-16:0/16:1	O-16:0/16:1	O-16:0/16:1
PE(P-32:1)	963.4833	P-16:0/16:1	P-16:0/16:1	P-16:0/16:1	P-16:0/16:1
		P-14:0/18:1			P-14:0/18:1
PE(32:2)	819.5397	16:1/16:1	16:1/16:1	16:1/16:1	16:1/16:1
		14:0/18:2	14:1/18:1		
PE(P-32:2)	961.4677	P-32:2	P-32:2	P-32:2	
PE(O-32:3)	803.5448	O-32:3	O-32:3	O-32:3	O-32:3
PE(33:0)	837.5867	18:0/15:0	18:0/15:0	18:0/15:0	18:0/15:0
		17:0/16:0	17:0/16:0	17:0/16:0	17:0/16:0
PE(O-33:0)	823.6074	O-18:0/15:0	O-18:0/15:0	O-18:0/15:0	O-18:0/15:0
		O-16:0/17:0	O-16:0/17:0	O-16:0/17:0	O-16:0/17:0

Table C.1 (Cont'd)

PE(P-33:0)	979.5146	P-16:0/17:0		P-16:0/17:0	P-33:0
PE(33:1)	835.5710	17:0/16:1	15:0/18:1	15:0/18:1	15:0/18:1
		17:1/16:0	17:1/16:0	17:0/16:1	17:1/16:0
		15:0/18:1	17:0/16:1	17:1/16:0	17:0/16:1
			15:1/18:0		
PE(O-33:1)	821.5918	O-15:0/18:1	O-15:0/18:1	O-15:0/18:1	O-15:0/18:1
		O-16:0/17:1	O-16:0/17:1	O-16:0/17:1	O-16:0/17:1
		O-18:0/15:1	O-18:0/15:1		
		O-18:1/15:0			
PE(P-33:1)	977.4990	P-16:0/17:1	P-16:0/17:1	P-16:0/17:1	P-16:0/17:1
		P-17:0/16:1	P-17:0/16:1	P-17:0/16:1	P-17:0/16:1
		P-15:0/18:1	P-15:0/18:1	P-15:0/18:1	P-15:0/18:1
PE(33:2)	833.5554	17:1/16:1	17:1/16:1	17:1/16:1	17:1/16:1
				15:0/18:2	
PE(O-33:2)	819.5761			O-16:1/17:1	
PE(P-33:2)	975.4833	P-33:2	P-33:2	P-33:2	P-33:2
PE(34:0)	851.6023	18:0/16:0	18:0/16:0	18:0/16:0	18:0/16:0
PE(O-34:0)	837.6231	O-18:0/16:0	O-18:0/16:0	O-18:0/16:0	O-18:0/16:0
			O-20:0/14:0		
PE(34:1)	849.5867	18:0/16:1	18:0/16:1	16:0/18:1	16:0/18:1
		16:0/18:1	16:0/18:1	18:0/16:1	18:0/16:1
		20:1/14:0	20:1/14:0		
PE(O-34:1)	835.6074	O-16:0/18:1	O-18:0/16:1	O-16:0/18:1	O-16:0/18:1
		O-18:0/16:1	O-16:0/18:1	O-18:0/16:1	O-18:0/16:1
		O-18:1/16:0	O-18:1/16:0		O-18:1/16:0
			O-20:1/14:0		
PE(P-34:1)	991.5146	P-16:0/18:1	P-16:0/18:1	P-16:0/18:1	P-16:0/18:1
		P-18:0/16:1	P-18:0/16:1	P-18:0/16:1	P-18:0/16:1
			P-18:1/16:0	P-18:1/16:0	P-18:1/16:0
PE(34:2)	847.5710	18:1/16:1	18:1/16:1	18:1/16:1	18:1/16:1
		16:0/18:2	16:0/18:2	16:1/18:1	16:0/18:2
PE(O-34:2)	833.5918	O-16:0/18:2	O-16:1/18:1	O-16:1/18:1	O-16:1/18:1
		O-18:1/16:1	O-18:1/16:1	O-18:1/16:1	O-18:1/16:1
		O-16:1/18:1	O-16:0/18:2		
PE(P-34:2)	989.4990	P-16:0/18:2	P-16:0/18:2	P-16:0/18:2	P-16:0/18:2
		P-18:1/16:1	P-18:1/16:1	P-18:1/16:1	P-18:1/16:1
				-	
		P-18:0/16:2	P-18:0/16:2	P-18:0/16:2	P-18:0/16:2

Table C.1 (Cont'd)

PE(34:3)	845.5554	16:1/18:2	16:1/18:2	16:1/18:2	16:1/18:2
		16:0/18:3	16:2/18:1		
			16:0/18:3		
PE(O-34:3)	831.5761	O-16:0/18:3		O-18:2/16:1	
		O-18:2/16:1		O-16:1/18:2	
		O-16:2/18:1			
		O-16:1/18:2			
PE(P-34:3)	987.4833	P-16:0/18:3	P-16:0/18:3	P-34:3	P-34:3
PE(P-34:4)	985.4677	P-16:0/18:4	P-16:0/18:4	P-16:0/18:4	P-16:0/18:4
PE(O-35:0)	851.6364	O-18:0/17:0			O-18:0/17:0
		O-16:0/19:0			
PE(35:1)	863.6023	18:0/17:1	18:0/17:1	18:0/17:1	17:0/18:1
		17:0/18:1	17:0/18:1	18:1/17:0	18:0/17:1
		20:1/15:0	20:1/15:0	15:0/20:1	15:0/20:1
PE(O-35:1)	849.6231	O-18:0/17:1	O-18:0/17:1	O-18:0/17:1	O-18:0/17:1
		O-18:1/17:0	O-20:1/15:0	O-18:1/17:0	O-18:1/17:0
		O-16:0/19:1		O-16:0/19:1	O-20:1/15:0
		O-20:1/15:0			O-16:0/19:1
PE(P-35:1)	1005.5303	P-19:0/16:1	P-19:0/16:1	P-19:0/16:1	P-19:0/16:1
		P-18:0/17:1	P-19:1/16:0	P-19:1/16:0	P-18:0/17:1
		P-18:1/17:0	P-18:0/17:1	P-18:0/17:1	P-18:1/17:0
		P-17:0/18:1	P-18:1/17:0	P-18:1/17:0	P-17:0/18:1
		P-16:0/19:1	P-17:0/18:1	P-17:0/18:1	P-16:0/19:1
		P-15:0/20:1	P-16:0/19:1	P-16:0/19:1	P-15:0/20:1
			P-15:0/20:1	P-15:0/20:1	
PE(35:2)	861.5867	18:1/17:1	17:1/18:1	17:1/18:1	17:1/18:1
		17:0/18:2			
		15:0/20:2			
PE(O-35:2)	847.6074	O-18:1/17:1	O-17:1/18:1	O-17:1/18:1	O-17:1/18:1
		O-17:0/18:2	O-18:1/17:1	O-18:1/17:1	O-18:1/17:1
		O-16:0/19:2		O-16:0/19:2	O-16:0/19:2
PE(P-35:2)	1003.5146	P-19:1/16:1	P-19:1/16:1	P-19:1/16:1	P-19:1/16:1
		P-18:0/17:2	P-18:0/17:2	P-18:0/17:2	P-18:0/17:2
		P-18:1/17:1	P-18:1/17:1	P-18:1/17:1	P-18:1/17:1
		P-17:0/18:2	P-17:0/18:2	P-17:0/18:2	P-17:0/18:2
		P-17:1/18:1	P-17:1/18:1	P-17:1/18:1	P-17:1/18:1
		P-16:0/19:2	P-16:0/19:2	P-16:0/19:2	P-16:0/19:2
					P-15:0/20:2

Table C.1 (Cont'd)

PE(35:3)	859.5710	17:1/18:2	17:2/18:1	35:3	17:1/18:2
			17:1/18:2		
PE(O-35:3)	845.5910	O-16:0/19:3		O-16:0/19:3	
PE(P-35:3)	1001.4990	P-17:0/18:3	P-17:0/18:3	P-35:3	P-35:3
		P-16:0/19:3	P-16:0/19:3		
PE(P-35:4)	999.4833	P-17:0/18:4	P-17:0/18:4	P-17:0/18:4	
		P-16:0/19:4	P-16:0/19:4	P-16:0/19:4	
		P-15:0/20:4	P-15:0/20:4	P-15:0/20:4	
PE(36:0)	879.6336	20:0/16:0	20:0/16:0	36:0	20:0/16:0
		18:0/18:0	18:0/18:0		18:0/18:0
PE(O-36:0)	865.6544	O-18:0/18:0	O-18:0/18:0	O-18:0/18:0	O-18:0/18:0
		O-20:0/16:0	O-20:0/16:0		O-20:0/16:0
PE(36:1)	877.6180	18:0/18:1	18:0/18:1	18:0/18:1	18:0/18:1
		18:1/18:0	18:1/18:0	18:1/18:0	18:1/18:0
		20:1/16:0	20:1/16:0	20:1/16:0	20:1/16:0
		20:0/16:1	20:0/16:1	20:0/16:1	20:0/16:1
PE(O-36:1)	863.6387	O-18:0/18:1	O-18:0/18:1	O-18:0/18:1	O-18:0/18:1
		O-20:0/16:1	O-20:0/16:1	O-16:0/20:1	O-20:1/16:0
		O-20:1/16:0	O-20:1/16:0		O-20:0/16:1
		O-16:0/20:1	O-16:0/20:1		O-16:0/20:1
PE(P-36:1)	1019.5459	P-18:0/18:1	P-18:0/18:1	P-18:0/18:1	P-18:0/18:1
		P-16:0/20:1	P-16:0/20:1	P-16:0/20:1	P-18:1/18:0
		P-18:1/18:0	P-18:1/18:0	P-18:1/18:0	P-16:0/20:1
PE(36:2)	875.6023	18:1/18:1	18:1/18:1	18:1/18:1	18:1/18:1
		18:0/18:2	18:0/18:2	20:1/16:1	20:1/16:1
		20:1/16:1	20:1/16:1	18:0/18:2	18:0/18:2
		20:2/16:0	20:2/16:0	20:2/16:0	20:2/16:0
PE(O-36:2)	861.6231	O-18:1/18:1	O-18:1/18:1	O-18:1/18:1	O-18:1/18:1
		O-18:0/18:2	O-18:0/18:2	O-16:0/20:2	O-20:1/16:1
		O-20:1/16:1	O-20:1/16:1	O-16:1/20:1	O-18:0/18:2
		O-16:0/20:2	O-16:0/20:2	O-18:0/18:2	O-16:1/20:1
			O-16:1/20:1		O-16:0/20:2
PE(P-36:2)	1017.5303	P-18:1/18:1	P-18:1/18:1	P-18:1/18:1	P-18:1/18:1
		P-18:0/18:2	P-18:0/18:2	P-18:0/18:2	P-18:0/18:2
		P-16:0/20:2	P-16:0/20:2	P-16:0/20:2	P-16:0/20:2
PE(36:3)	873.5867	18:1/18:2	18:1/18:2	18:1/18:2	18:1/18:2
		18:0/18:3	18:0/18:3	16:0/20:3	
		16:0/20:3	16:0/20:3		
		16:1/20:2			

Table C.1 (Cont'd)

PE(O-36:3)	859.6074	O-16:0/20:3	O-18:2/18:1	O-18:2/18:1	O-18:2/18:1
		O-18:1/18:2	O-18:1/18:2	O-18:1/18:2	O-18:1/18:2
		O-18:0/18:3	O-16:0/20:3	O-16:0/20:3	O-16:0/20:3
		O-18:2/18:1	O-18:0/18:3	O-16:1/20:2	
		O-16:1/20:2	O-16:1/20:2		
PE(P-36:3)	1015.5146	P-18:0/18:3	P-18:0/18:3	P-18:0/18:3	P-18:0/18:3
		P-18:1/18:2	P-18:1/18:2	P-18:1/18:2	P-18:1/18:2
		P-16:0/20:3	P-18:2/18:1	P-18:2/18:1	P-18:2/18:1
			P-16:0/20:3	P-16:0/20:3	P-16:0/20:3
PE(36:4)	871.5710	16:0/20:4	16:0/20:4	16:0/20:4	18:2/18:2
		18:1/18:3	18:1/18:3	18:2/18:2	16:0/20:4
		16:1/20:3	16:1/20:3		
		18:2/18:2	18:2/18:2		
PE(O-36:4)	857.5918	O-16:0/20:4	O-16:0/20:4	O-16:0/20:4	O-16:0/20:4
			O-16:1/20:3	O-16:1/20:3	
PE(P-36:4)	1013.4990	P-16:0/20:4	P-16:0/20:4	P-16:0/20:4	P-16:0/20:4
		P-18:0/18:4	P-18:0/18:4	P-18:0/18:4	P-18:0/18:4
PE(36:5)	869.5554	16:0/20:5	16:0/20:5	16:1/20:4	16:1/20:4
		16:1/20:4	16:1/20:4		
		14:0/22:5			
PE(O-36:5)	855.5761	O-16:0/20:5	O-16:1/20:4	O-16:1/20:4	O-16:0/20:5
		O-16:1/20:4	O-16:0/20:5	O-16:0/20:5	O-16:1/20:4
PE(P-36:5)	1011.4833	P-18:1/18:4	P-16:0/20:5	P-18:1/18:4	P-18:1/18:4
		P-16:0/20:5		P-16:0/20:5	P-16:0/20:5
PE(37:1)	891.6336	20:1/17:0	19:0/18:1	19:0/18:1	19:0/18:1
		18:0/19:1	17:0/20:1	17:0/20:1	18:1/19:0
		19:0/18:1			19:1/18:0
		15:0/22:1			
PE(O-37:1)	877.6544	O-19:0/18:1		O-19:0/18:1	O-19:0/18:1
		O-20:0/17:1		O-18:0/19:1	O-18:0/19:1
		O-18:0/19:1		O-20:0/17:1	O-20:0/17:1
		O-20:1/17:0		O-20:1/17:0	O-20:1/17:0
PE(P-37:1)	1033.5616	P-19:0/18:1	P-19:0/18:1	P-19:0/18:1	P-19:0/18:1
				P-17:0/20:1	
PE(37:2)	889.6180	19:1/18:1	18:1/19:1	19:1/18:1	19:1/18:1
		20:1/17:1	20:1/17:1	17:1/20:1	18:1/19:1
		18:0/19:2	18:0/19:2		17:1/20:1
		17:0/20:2			
		15:0/22:2			

Table C.1 (Cont'd)

PE(O-37:2)	875.6387	O-20:1/17:1	O-20:1/17:1	O-16:0/21:2	O-20:1/17:1
		O-18:0/19:2	O-18:0/19:2	O-18:0/19:2	O-18:1/19:1
		O-18:1/19:1		O-18:1/19:1	
				O-20:1/17:1	
PE(P-37:2)	1031.5459	P-19:0/18:2	P-19:0/18:2	P-19:0/18:2	P-19:0/18:2
		P-19:1/18:1	P-19:1/18:1	P-19:1/18:1	P-19:1/18:1
				P-18:0/19:2	
				P-18:1/19:1	
				P-17:0/20:2	
PE(37:3)	887.6023	18:0/19:3	18:1/19:2	37:3	
		18:1/19:2	19:3/18:0		
		17:1/20:2	15:0/22:3		
		17:0/20:3	17:1/20:2		
		19:1/18:2	18:2/19:1		
		15:0/22:3			
PE(O-37:3)	873.6231	O-18:0/19:3		O-18:1/19:2	
		O-16:0/21:3			
		O-18:1/19:2			
PE(P-37:3)	1029.5303	P-19:1/18:2	P-19:1/18:2	P-18:1/19:2	P-18:1/19:2
		P-17:0/20:3	P-17:0/20:3	P-17:0/20:3	P-17:0/20:3
PE(37:4)	885.5867	17:0/20:4	17:0/20:4	37:4	
		18:1/19:3	18:1/19:3		
		15:0/22:4	15:0/22:4		
PE(O-37:4)	871.6074	O-17:0/20:4	O-17:0/20:4	O-37:4	
		O-16:0/21:4			
PE(P-37:4)	1027.5146	P-18:0/19:4	P-17:0/20:4	P-18:0/19:4	P-17:0/20:4
		P-17:0/20:4		P-17:0/20:4	
PE(37:5)	883.5710	37:5			
PE(O-37:5)	869.5918	O-17:0/20:5			
		O-16:0/21:5			
PE(P-37:5)	1025.4990	P-18:1/19:4	P-17:0/20:5	P-18:1/19:4	P-17:0/20:5
		P-17:0/20:5		P-17:0/20:5	
				P-17:1/20:4	
PE(P-37:6)	1023.4833	P-37:6			
PE(38:1)	905.6493	20:0/18:1	20:0/18:1	20:0/18:1	20:0/18:1
		20:1/18:0	20:1/18:0	20:1_18:0	20:1/18:0
			22:1/16:0	22:1_16:0	22:1/16:0

Table C.1 (Cont'd)

O-18:0/20:1 O-18:0/20:1 O-18:0/20:1 O-18:0/ O-16:0/22:1 O-16:0/	18:1
	20:1
PE(P. 0.4) 10.17 F770 P. 0.0 (10.4 P. 0.4 P. 0.4 P. 0.0 (10.4 P. 0.4 P. 0.4 P. 0.0 (10.4 P. 0.4 P. 0.4 P. 0.4 P. 0.0 (10.4 P. 0.4 P. 0.4 P. 0.0 (10.4 P. 0.4 P. 0.4 P. 0.4 P. 0.0 (10.4 P. 0.4 P. 0.4 P. 0.0 (10.4 P. 0.4 P. 0.4 P. 0.4 P. 0.0 (10.4 P. 0.4 P. 0.4 P. 0.4 P. 0.4 P.	22:1
PE(P-38:1) 1047.5772 P-20:0/18:1 P-20:0/18:1 P-20:0/18:1 P-20:0/	18:1
P-18:0/20:1 P-18:0/20:1 P-18:0/	20:1
P-16:0/22:1 P-16:0/	22:1
PE(38:2) 903.6336 20:1/18:1 20:1/18:1 20:1/18:1 20:1/1	8:1
18:0/20:2 22:1/16:0 18:0/20:2 18:0/2	0:2
20:0/18:2 20:0/18:2 16:0/22:2 16:0/2	2:2
22:1/16:0 18:0/20:2	
PE(O-38:2) 889.6544 O-20:1/18:1 O-20:1/18:1 O-18:0/20:2 O-20:1/	18:1
O-20:0/18:2 O-20:0/18:2 O-16:0/22:2 O-18:0/	20:2
O-18:0/20:2 O-18:0/20:2 O-16:1/22:1 O-18:1/	20:1
O-16:0/22:2	
PE(P-38:2) 1045.5616 P-20:1/18:1 P-20:1/18:1 P-20:1/18:1 P-20:0/	18:2
P-18:1/20:1 P-18:0/20:2 P-18:0/20:2 P-20:1/	18:1
P-18:1/20:1 P-18:1/20:1 P-18:0/	20:2
P-16:0/22:2 P-18:1/.	20:1
P-16:0/	22:2
PE(38:3) 901.6180 18:0/20:3 18:0/20:3 20:2/18:1 20:2/1	8:1
20:2/18:1 20:2/18:1 18:0/20:3 20:1/1	8:2
20:1/18:2 20:1/18:2 18:0/2	0:3
PE(O-38:3) 887.6387 O-18:0/20:3 O-18:0/20:3 O-18:0/20:3	20:3
O-20:1/18:2 O-20:1/18:2 O-18:2/20:1 O-20:2/	18:1
O-16:1/22:2 O-20:2/18:1 O-20:1/	18:2
O-20:0/18:3 O-18:1/20:2 O-18:2/	20:1
O-16:0/22:3 O-18:1/	20:2
O-16:1/22:2	
	20:3
PE(P-38:3) 1043.5459 P-18:0/20:3 P-18:0/20:3 P-18:0/20:3 P-18:0/20:3	aa a
PE(P-38:3) 1043.5459 P-18:0/20:3	20:2
	20:2
P-18:1/20:2 P-18:1/20:2 P-18:1/	
P-18:1/20:2 P-18:1/20:2 P-18:1/. P-16:0/22:3 P-16:0/22:3	0:3
P-18:1/20:2 P-18:1/20:2 P-18:1/20:2 P-18:1/20:2 P-16:0/22:3 P-16:0/22:3 P-16:0/22:3 PE(38:4) 899.6023 18:0/20:4 18:0/20:4 18:1/20:3 18:1/2	0:3
P-18:1/20:2 P-18:1/20:2 P-18:1/20:2 P-18:1/20:2 P-16:0/22:3 P-16:0/22:3 P-16:0/22:3 PE(38:4) 899.6023 18:0/20:4 18:0/20:4 18:1/20:3 18:1/20:3 18:0/20:4 18:1/20:3 18:1/20:3 18:0/20:4 18:0/20:4 18:0/20:4	0:3
P-18:1/20:2 P-18:1/20:2 P-18:1/20:2 P-18:1/20:2 P-16:0/22:3 P-16:0/22:3 P-16:0/22:3 PE(38:4) 899.6023 18:0/20:4 18:0/20:4 18:1/20:3 18:1/20:3 18:0/20:4 18	0:3 0:4 20:4

Table C.1(Cont'd)

PE(P-38:4)	1041.5303	P-18:0/20:4	P-18:0/20:4	P-18:0/20:4	P-18:0/20:4
		P-18:1/20:3	P-16:0/22:4	P-18:1/20:3	P-18:1/20:3
		P-16:0/22:4	P-18:1/20:3		P-16:0/22:4
PE(38:5)	897.5867	18:1/20:4	18:1/20:4	18:1/20:4	18:1/20:4
		18:0/20:5	18:0/20:5	18:0/20:5	18:0/20:5
		16:0/22:5	16:0/22:5		16:0/22:5
			18:2/20:3		
PE(O-38:5)	883.6074	O-16:0/22:5	O-16:0/22:5	O-16:0/22:5	O-16:0/22:5
		O-18:0/20:5	O-18:1/20:4	O-18:0/20:5	O-18:0/20:5
		O-18:1/20:4	O-18:0/20:5	O-18:1/20:4	O-18:1/20:4
PE(P-38:5)	1039.5146	P-16:0/22:5	P-16:0/22:5	P-18:1/20:4	P-18:1/20:4
		P-18:0/20:5	P-18:0/20:5	P-16:0/22:5	P-16:0/22:5
		P-18:1/20:4	P-18:1/20:4	P-18:0/20:5	P-18:0/20:5
PE(38:6)	895.5710	18:1/20:5	18:1/20:5	16:0/22:6	16:0/22:6
		16:0/22:6	16:0/22:6		16:1/22:5
		18:2/20:4	18:2/20:4		
			16:1/22:5		
PE(O-38:6)	881.5918	O-16:0/22:6	O-16:0/22:6	O-16:0/22:6	O-16:0/22:6
		O-18:1/20:5	O-16:1/22:5	O-16:1/22:5	O-16:1/22:5
		O-16:1/22:5	O-18:1/20:5		O-18:1/20:5
			O-18:2/20:4		
PE(P-38:6)	1037.4990	P-18:1/20:5	P-18:1/20:5	P-18:1/20:5	P-16:0/22:6
		P-16:0/22:6	P-16:0/22:6	P-16:0/22:6	
PE(P-38:7)	1035.4833	P-38:7	P-38:7		
PE(39:1)	919.6649	21:0/18:1	19:0/20:1	39:1	
		18:0/21:1			
PE(O-39:1)	905.6857			O-39:1	
PE(P-39:1)	1061.5929			P-19:0/20:1	
				P-17:0/22:1	
PE(39:2)	917.6493	21:1/18:1	21:1/18:1	20:1/19:1	19:1/20:1
		20:1/19:1	18:1/21:1	17:1/22:1	17:1/22:1
		22:1/17:1	18:0/21:2		
		17:0/22:2			
		18:0/21:2			
		20:0/19:2			
PE(O-39:2)	903.6700			O-20:1/19:1	

Table C.1 (Cont'd)

PE(P-39:2)	1059.5772			P-19:0/20:2	P-17:0/22:2
, , , , , , , , , , , , , , , , , , , ,				P-19:1/20:1	
				P-17:0/22:2	
PE(39:3)	915.6336	18:0/21:3		39:3	
		18:1/21:2			
PE(P-39:3)	1057.5616		P-19:0/20:3	P-39:3	
PE(39:4)	913.6180	18:1/21:3	18:1/21:3		
		18:0/21:4	18:0/21:4		
PE(P-39:4)	1055.5459	P-39:4	P-39:4	P-39:4	P-39:4
PE(39:5)	911.6023	18:0/21:5	20:4/19:1		
PE(O-39:5)	897.6231	O-17:0/22:5		O-39:5	
		O-18:0/21:5			
PE(P-39:5)	1053.5303	P-19:0/20:5	P-19:0/20:5	P-19:0/20:5	P-19:1/20:4
		P-19:1/20:4	P-19:1/20:4	P-19:1/20:4	P-17:0/22:5
		P-17:0/22:5	P-17:0/22:5	P-17:0/22:5	
PE(39:6)	909.5867	39:6			
PE(O-39:6)	895.6074	O-17:0/22:6		O-39:6	
		O-17:1/22:5			
PE(P-39:6)	1051.5146	P-17:0/22:6	P-19:1/20:5	P-17:0/22:6	P-17:0/22:6
			P-17:0/22:6		
PE(40:1)	933.6806	22:0/18:1	22:0/18:1	40:1	
		18:0/22:1	18:1/22:0		
			18:0/22:1		
PE(O-40:1)	919.7013	O-18:0/22:1	O-18:0/22:1	O-18:0/22:1	O-18:0/22:1
PE(P-40:1)	1075.6085	P-40:1		P-18:0/22:1	P-40:1
PE(40:2)	931.6649	22:1/18:1	22:1/18:1	22:1/18:1	22:1/18:1
		20:1/20:1	20:1/20:1	20:1/20:1	20:1/20:1
PE(O-40:2)	917.6857	O-18:0/22:2		O-18:0/22:2	O-18:0/22:2
PE(P-40:2)	1073.5929	P-40:2	P-18:0/22:2	P-18:0/22:2	P-18:0/22:2
				P-18:1/22:1	P-18:1/22:1
PE(40:3)	929.6493	18:0/22:3	18:0/22:3	18:1/22:2	
		20:0/20:3	20:1/20:2		
		20:1/20:2	20:0/20:3		
			18:1/22:2		

Table C.1 (Cont'd)

PE(O-40:3)	915.6700		O-20:0/20:3	O-18:1/22:2	O-18:1/22:2
FE(O-40.3)	915.0700				
			O-18:0/22:3	O-18:0/22:3	O-20:0/20:3
			O-20:1/20:2		
77/7 (2.2)			O-18:1/22:2	D 00 0/00 0	5 40 0
PE(P-40:3)	1071.5772		P-20:0/20:3	P-20:0/20:3	P-40:3
			P-20:1/20:2	P-20:1/20:2	
PE(40:4)	927.6336	18:0/22:4	18:0/22:4	20:1/20:3	20:1/20:3
		20:1/20:3	20:1/20:3		
		20:0/20:4	20:0/20:4		
		18:1/22:3	18:1/22:3		
PE(O-40:4)	913.6544	O-20:0/20:4		O-18:0/22:4	O-18:0/22:4
		O-18:0/22:4			O-20:0/20:4
		O-20:1/20:3			
PE(P-40:4)	1069.5616	P-40:4	P-20:0/20:4	P-40:4	P-40:4
			P-18:0/22:4		
PE(40:5)	925.6180	18:0/22:5	20:1/20:4	18:0/22:5	20:1/20:4
		20:1/20:4	18:0/22:5		18:0/22:5
		18:1/22:4	18:1/22:4		
		20:0/20:5	20:0/20:5		
PE(O-40:5)	911.6387	O-18:0/22:5	O-18:0/22:5	O-18:0/22:5	O-18:0/22:5
		O-20:1/20:4	O-20:1/20:4		O-20:1/20:4
		O-20:0/20:5	O-20:0/20:5		O-18:1/22:4
		O-18:1/22:4	O-18:1/22:4		
		O-16:0/24:5	O-16:0/24:5		
PE(P-40:5)	1067.5459	P-18:0/22:5	P-18:0/22:5	P-18:0/22:5	P-18:0/22:5
			P-18:1/22:4	P-18:1/22:4	
PE(40:6)	923.6023	18:1/22:5	18:1/22:5	18:1/22:5	18:1/22:5
		18:0/22:6	18:0/22:6		18:0/22:6
		20:1/20:4	20:1/20:4		
			20:0/20:5		
PE(O-40:6)	909.6231	O-18:0/22:6	O-18:0/22:6	O-18:0/22:6	O-18:0/22:6
		O-18:1/22:5	O-18:1/22:5	O-18:1/22:5	O-18:1/22:5
PE(P-40:6)	1065.5303	P-18:0/22:6	P-18:0/22:6	P-20:5/18:1	P-20:5/18:1
		P-18:1/22:5	P-18:1/22:5	P-18:0/22:6	P-18:0/22:6
				P-18:1/22:5	P-18:1/22:5
PE(40:7)	921.5867	18:1/22:6	18:1/22:6		18:1/22:6
PE(O-40:7)	907.6074	O-18:1/22:6	O-18:1/22:6	O-18:1/22:6	O-18:1/22:6
			O-18:2/22:5		
PE(P-40:7)	1063.5146	P-18:1/22:6	P-18:1/22:6	P-18:1/22:6	P-18:1/22:6
·	1		1	1	1

Table C.1 (Cont'd)

PE(41:2)	945.6806			41:2	
PE(P-41:6)	1079.5459	P-41:6	P-19:0/22:6		
			P-19:1/22:5		
PE(42:1)	961.7119	24:0/18:1	24:0/18:1	24:0/18:1	
				24:1/18:0	
PE(P-42:1)	1103.6398				P-24:0/18:1
PE(42:2)	959.6962	20:1/22:1	20:1/22:1	20:1/22:1	
		18:1/24:1	18:1/24:1	18:1/24:1	
PE(P-42:2)	1101.6242			P-42:2	P-42:2
PE(42:3)	957.6806			42:3	
PE(42:4)	955.6649	20:0/22:4	20:0/22:4		
		22:0/20:4	22:0/20:4		
PE(42:5)	953.6493	20:1/22:4	20:1/22:4		
		20:0/22:5	22:1/20:4		
		22:1/20:4	20:0/22:5		
PE(42:6)	951.6336	22:1/20:5	20:0/22:6	20:1/22:5	20:1/22:5
		20:0/22:6	20:1/22:5		
PE(P-42:6)	1093.5616	P-42:6			
PE(44:2)	987.7275			20:1/24:1	
				18:1/26:1	
PE(44:4)	983.6962	24:0/20:4	24:0/20:4		
PE(44:5)	981.6806	24:1/20:4	24:1/20:4		
		24:0/20:5	24:0/20:5		

Table C.2 LPE sum compositions, their positive ionization mode m/z for MS analysis and molecular lipids identified for SW480 cells, SW620 cells, SW480 exosomes and SW620 exosomes.

		SW480 Cells	SW620 Cells	SW480 Exo	SW620 Exo
Sum Comp	(+) Mass	Molecular Lipid	Molecular Lipid	Molecular Lipid	Molecular Lipid
	m/z				
PE(16:0)	585.3414	16:0	16:0	16:0	16:0
PE(O-16:0)	571.3621	O-16:0	O-16:0	O-16:0	O-16:0
PE(P-16:0)	727.2693	P-16:0	P-16:0	P-16:0	P-16:0
PE(16:1)	583.3257	16:1	16:1	16:1	16:1
PE(O-16:1)	569.3465				O-16:1
PE(17:0)	599.3570	17:0		17:0	17:0
PE(O-17:0)	585.3778	O-17:0		O-17:0	

Table C.2 (Cont'd)

PE(P-17:0)	741.2850	P-17:0	P-17:0	P-17:0	P-17:0
PE(17:1)	597.3414	17:1	17:1	17:1	17:1
PE(18:0)	613.3727	18:0	18:0	18:0	18:0
PE(O-18:0)	599.3934	O-18:0	O-18:0	O-18:0	O-18:0
PE(P-18:0)	755.3006	P-18:0	P-18:0	P-18:0	P-18:0
PE(18:1)	611.3570	18:1	18:1	18:1	18:1
PE(O-18:1)	597.3778	O-18:1	O-18:1	O-18:1	O-18:1
PE(P-18:1)	753.2850	P-18:1	P-18:1	P-18:1	P-18:1
PE(18:2)	609.3414	18:2	18:2	18:2	18:2
PE(19:1)	625.3727			19:1	19:1
PE(19:2)	623.3570			19:2	
PE(20:1)	639.3883	20:1	20:1	20:1	20:1
PE(O-20:1)	625.4091	O-20:1	O-20:1		
PE(20:2)	637.3727	20:2		20:2	20:2
PE(20:3)	635.3570	20:3	20:3	20:3	20:3
PE(20:4)	633.3414	20:4	20:4	20:4	20:4
PE(20:5)	631.3257	20:5	20:5	20:5	20:5
PE(22:1)	667.4196			22:1	22:1
PE(22:2)	665.4040			22:2	
PE(22:4)	661.3727	22:4	22:4		
PE(22:5)	659.3570	22:5	22:5	22:5	22:5
PE(22:6)	657.3414	22:6	22:6	22:6	22:6

Table C.3 PC sum compositions, their positive ionization mode m/z for MS analysis and molecular lipids identified for SW480 cells, SW620 cells, SW480 exosomes and SW620 exosomes.

		SW480 Cells	SW620 Cells	SW480 Exo	SW620 Exo
Sum Comp	(+) Mass	Molecular Lipid	Molecular Lipid	Molecular Lipid	Molecular Lipid
	m/z				
PC(O-28:0)	664.5275			O-28:0	O-28:0
PC(29:0)	692.5224	15:0/14:0	15:0/14:0	15:0/14:0	15:0/14:0
		13:0/16:0			
PCO-29:0)	678.5432	O-15:0/14:0	O-15:0/14:0	O-15:0/14:0	O-15:0/14:0
		O-16:0/13:0	O-16:0/13:0		O-16:0/13:0
PC(29:1)	690.5068	15:0/14:1	15:0/14:1	29:1	15:0/14:1
PC(30:0)	706.5381	14:0/16:0	14:0/16:0	16:0/14:0	14:0/16:0
		16:0/14:0	16:0/14:0		
PC(O-30:0)	692.5588	O-16:0/14:0	O-16:0/14:0	O-16:0/14:0	O-16:0/14:0

Table C.3 (Cont'd)

PC(P-30:0)	848.4660	P-30:0	P-30:0	P-30:0	P-30:0
PC(30:1)	704.5224	14:0/16:1	14:0/16:1	14:0/16:1	14:0/16:1
PC(0-30:1)	690.5432	O-16:0/16:1	O-16:0/16:1	O-30:1	O-16:0/16:1
PC(31:0)	720.5537	16:0/15:0	16:0/15:0	16:0/15:0	16:0/15:0
FC(31.0)	120.5551	14:0/17:0	14:0/17:0	14:0/17:0	14:0/17:0
DC(O 24-0)	700 5745				
PC(O-31:0)	706.5745	O-16:0/15:0	O-16:0/15:0	O-16:0/15:0	O-16:0/15:0
DO(D 04 0)	000 1017	O-14:0/17:0	D 40 0/45 0	D 04 0	D 04 0
PC(P-31:0)	862.4817	P-16:0/15:0	P-16:0/15:0	P-31:0	P-31:0
PC(31:1)	718.5381	15:0/16:1	16:0/15:1	14:0/17:1	14:0/17:1
		14:0/17:1	14:0/17:1		
		16:0/15:1			
PC(O-31:1)	704.5588	O-31:1	O-31:1	O-31:1	O-31:1
PC(P-31:1)	860.4660	P-31:1	P-31:1	P-31:1	P-31:1
PC(32:0)	734.5694	16:0/16:0	16:0/16:0	16:0/16:0	16:0/16:0
		18:0/14:0	18:0/14:0	18:0/14:0	18:0/14:0
PC(O-32:0)	720.5901	O-16:0/16:0	O-16:0/16:0	O-16:0/16:0	O-16:0/16:0
		O-18:0/14:0			O-18:0/14:0
PC(P-32:0)	876.4973	P-16:0/16:0	P-16:0/16:0	P-16:0/16:0	P-16:0/16:0
PC(32:1)	732.5537	16:0/16:1	16:0/16:1	14:0/18:1	16:0/16:1
		14:0/18:1	14:0/18:1	16:0/16:1	14:0/18:1
PC(O-32:1)	718.5745	O-16:0/16:1	O-16:0/16:1	O-16:0/16:1	O-16:0/16:1
PC(P-32:1)	874.4817	P-16:0/16:1	P-16:0/16:1	P-16:0/16:1	P-16:0/16:1
PC(32:2)	730.5381	16:1/16:1	16:1/16:1	16:1/16:1	16:1/16:1
PC(O-32:2)	716.5588	O-16:1/16:1	O-16:0/16:2	O-16:1/16:1	O-16:1/16:1
		O-16:0/16:2			
PC(32:3)	728.5224			32:3	
PC(33:0)	748.5850	16:0/17:0	16:0/17:0	15:0/18:0	15:0/18:0
		15:0/18:0	15:0/18:0	16:0/17:0	16:0/17:0
PC(O-33:0)	734.6058	O-16:0/17:0	O-16:0/17:0	O-16:0/17:0	O-16:0/17:0
		O-18:0/15:0	O-18:0/15:0	O-18:0/15:0	O-18:0/15:0
PC(P-33:0)	890.5130	P-33:0	P-33:0	P-33:0	P-33:0
PC(33:1)	746.5694	16:0/17:1	16:0/17:1	15:0/18:1	17:1/16:0
		17:0/16:1	17:0/16:1	17:0/16:1	15:0/18:1
		15:0/18:1	15:0/18:1	16:0/17:1	17:0/16:1
PC(O-33:1)	732.5901	O-16:0/17:1	O-16:0/17:1	O-16:0/17:1	O-16:0/17:1
~		O-16:1/17:0	O-16:1/17:0		
PC(P-33:1)	888.4973	P-15:0/18:1	P-15:0/18:1	P-33:1	P-33:1
PC(O-33:2)	730.5745	O-33:2	O-33:2	O-33:2	
PC(P-33:2)	886.4817	P-33:2	P-33:2	P-33:2	P-33:2
<u>,</u>	1	1	1	ı	1

Table C.3 (Cont'd)

PC(34:0)	762.6007	16:0/18:0	16:0/18:0	18:0/16:0	16:0/18:0
PC(0-34:0)					
PC(O-34:0)	748.6214	O-18:0/16:0	O-18:0/16:0	O-18:0/16:0	O-18:0/16:0
DO(0.4.4)	700 5050	10.0/10.1	O-16:0/18:0	10.0/10.1	O-16:0/18:0
PC(34:1)	760.5850	16:0/18:1	16:0/18:1	16:0/18:1	16:0/18:1
		18:0/16:1	18:0/16:1	_	18:0/16:1
PC(O-34:1)	746.6058	O-16:0/18:1	O-16:0/18:1	O-16:0/18:1	O-16:0/18:1
		O-18:1/16:0	O-18:1/16:0	O-18:1/16:0	O-18:1/16:0
		O-18:0/16:1	O-18:0/16:1	O-18:0/16:1	O-18:0/16:1
PC(P-34:1)	902.5130	P-16:0/18:1	P-16:0/18:1	P-16:0/18:1	P-16:0/18:1
		P-18:0/16:1			
PC(34:2)	758.569392	16:1/18:1	16:1/18:1	16:1/18:1	16:1/18:1
		18:1/16:1	18:1/16:1	18:1/16:1	18:1/16:1
		16:0/18:2	16:0/18:2		
PC(O-34:2)	744.590127	O-16:0/18:2	O-16:0/18:2	O-16:0/18:2	O-16:0/18:2
		O-18:1/16:1	O-18:1/16:1		
			O-16:1/18:1		
PC(P-34:2)	900.497339	P-16:0/18:2	P-16:0/18:2	P-34:2	P-34:2
		P-18:1/16:1	P-18:1/16:1		
PC(34:3)	756.553743	16:0/18:3	16:1/18:2	34:3	16:1/18:2
		16:1/18:2	16:0/18:3		
PC(O-34:3)	742.574478	O-34:3	O-34:3	O-34:3	O-34:3
PC(O-34:4)	740.558829	O-34:4	O-34:4	O-34:4	O-34:4
PC(35:0)	776.61634	18:0/17:0		18:0/17:0	
		16:0/19:0		16:0/19:0	
PC(O-35:0)	762.637075	O-18:0/17:0	O-18:0/17:0	O-18:0/17:0	O-18:0/17:0
		O-16:0/19:0			
PC(P-35:0)	918.544286	P-35:0			
PC(35:1)	774.60069	17:0/18:1	18:1/17:0	17:0/18:1	17:0/18:1
		18:0/17:1	17:0/18:1	15:0/20:1	15:0/20:1
		16:0/19:1	18:0/17:1		
		15:0/20:1	16:0/19:1		
			15:0/20:1		
PC(O-35:1)	760.621426	O-18:0/17:1	O-18:0/17:1	O-18:0/17:1	O-18:0/17:1
PC(P-35:1)	916.528637	P-15:0/20:1	P-15:0/20:1	P-17:0/18:1	P-17:0/18:1
-		P-17:0/18:1	P-17:0/18:1		
		P-18:0/17:1			
PC(35:2)	772.585041	18:1/17:1	18:1/17:1	18:1/17:1	18:1/17:1
		16:0/19:2	16:0/19:2		
l	ı		l .	I.	1

Table C.3 (Cont'd)

DO(O 05-0)	750 005770	0.40:0/47:4	0.40:0/47:4	0.40.0/47.4	0.05:0
PC(O-35:2)	758.605776	O-18:0/17:1	O-18:0/17:1	O-18:0/17:1	O-35:2
PC(P-35:2)	914.512988	P-35:2	P-35:2	P-35:2	
PC(35:3)	770.569392	35:3	35:3	35:3	
PC(O-35:3)	756.590127	O-35:3		O-35:3	
PC(P-35:3)	912.497339	P-35:3	P-35:3		
PC(35:4)	768.553743	35:4	35:4	35:4	
PC(P-35:4)	910.48169	P-16:0/19:4			
PC(36:1)	788.61634	18:0/18:1	18:0/18:1	18:0/18:1	18:0/18:1
		16:0/20:1	16:0/20:1	20:1/16:0	20:1/16:0
			16:1/20:0		
PC(O-36:1)	774.637075	O-18:0/18:1	O-18:0/18:1	O-18:0/18:1	O-18:0/18:1
		O-16:0/20:1	O-16:0/20:1	O-16:0/20:1	O-16:0/20:1
			O-18:1/18:0		
PC(P-36:1)	930.544286	P-18:0/18:1	P-18:0/18:1		
		P-16:0/20:1	P-16:0/20:1		
PC(36:2)	786.60069	18:1/18:1	18:1/18:1	18:1/18:1	18:1/18:1
		18:0/18:2	20:1/16:1		
		20:1/16:1	18:0/18:2		
PC(O-36:2)	772.621426	O-18:1/18:1	O-18:1/18:1	O-18:1/18:1	O-18:1/18:1
		O-18:0/18:2	O-18:0/18:2		
		O-16:0/20:2	O-16:0/20:2		
PC(P-36:2)	928.528637	P-18:1/18:1	P-18:1/18:1	P-18:1/18:1	P-18:1/18:1
		P-18:0/18:2	P-18:0/18:2		P-18:0/18:2
PC(36:3)	784.585041	18:1/18:2	18:1/18:2	18:1/18:2	18:1/18:2
		18:2/18:1	16:0/20:3		
		16:0/20:3			
PC(O-36:3)	770.605776	O-16:0/20:3	O-16:0/20:3	O-36:3	O-36:3
		O-18:1/18:2	O-18:1/18:2		
PC(P-36:3)	926.512988	P-20:2/16:0	P-16:0/20:3		
		P-18:2/18:1			
		P-16:0/20:3			
PC(36:4)	782.569392	16:0/20:4	16:0/20:4	16:0/20:4	16:0/20:4
		16:1/20:3	16:1/20:3	16:1/20:3	18:2/18:2
		18:3/18:1	18:3/18:1	18:2/18:2	
		18:2/18:2	18:2/18:2		
PC(O-36:4)	768.590127	O-16:0/20:4	O-16:0/20:4	O-16:0/20:4	O-16:0/20:4
PC(P-36:4)	924.497339	P-17:0/19:4	P-17:0/19:4	P-17:0/19:4	P-17:0/19:4
		P-16:0/20:4	P-16:0/20:4	P-15:0/21:4	
		P-18:3/18:1	P-18:3/18:1		
	1			1	1

Table C.3 (Cont'd)

PC(36:5)	780.553743	16:0/20:5	16:0/20:5		16:1/20:4
		16:1/20:4	16:1/20:4		
PC(O-36:5)	766.574478	O-16:0/20:5	O-16:0/20:5		
PC(P-36:5)	922.48169	P-17:1/19:4	P-17:1/19:4		P-17:1/19:4
		P-17:0/19:5	P-17:0/19:5		
PC(36:6)	778.538094	16:1/20:5	16:1/20:5	36:6	36:6
PC(37:1)	802.631989	17:0/20:1	17:0/20:1	17:0/20:1	17:0/20:1
		19:0/18:1	19:0/18:1	18:1/19:0	18:1/19:0
		18:0/19:1	18:0/19:1	18:0/19:1	
				15:0/22:1	
PC(O-37:1)	788.652724	O-37:1	O-37:1	O-37:1	O-37:1
PC(P-37:1)	944.559936	P-37:1	P-37:1		
PC(37:2)	800.61634	19:1/18:1	19:1/18:1	19:1/18:1	19:1/18:1
PC(O-37:2)	786.637075	O-37:2	O-37:2	O-37:2	O-37:2
PC(37:3)	798.60069	37:3			
PC(O-37:3)	784.621426	O-37:3			
PC(37:4)	796.585041	37:4		37:4	
PC(O-37:4)	782.605776	O-37:4			
PC(P-37:4)	938.512988	P-37:4	P-37:4		
PC(P-37:5)	936.497339	P-37:5	P-37:5		
PC(38:1)	816.647638	16:0/22:1	16:0/22:1	16:0/22:1	38:1
		20:0/18:1	20:0/18:1	20:0/18:1	
		18:0/20:1	18:0/20:1	18:0/20:1	
PC(O-38:1)	802.668373	O-38:1	O-16:0/22:1	O-16:0/22:1	O-16:0/22:1
PC(P-38:1)	958.575585	P-18:0/20:1	P-38:1		
		P-20:0/18:1			
PC(38:2)	814.631989	20:1/18:1	20:1/18:1	20:1/18:1	20:1/18:1
			16:0/22:2		
PC(O-38:2)	800.652724	O-16:0/22:2	O-16:0/22:2	O-16:0/22:2	O-16:0/22:2
PC(P-38:2)	956.559936	P-18:1/20:1	P-18:1/20:1		P-18:1/20:1
		P-20:1/18:1			
PC(38:3)	812.61634	18:0/20:3	18:0/20:3	18:0/20:3	20:2/18:1
		18:1/20:2	20:2/18:1	20:2/18:1	
		20:2/18:1	20:1/18:2	20:1/18:2	
		20:1/18:2			
PC(O-38:3)	798.637075	O-18:0/20:3	O-18:0/20:3		
PC(P-38:3)	954.544286	P-18:0/20:3	P-18:0/20:3		

Table C.3 (Cont'd)

PC(38:4)	810.60069	18:1/20:3	18:1/20:3	18:1/20:3	18:1/20:3
		18:0/20:4	18:0/20:4		
PC(O-38:4)	796.621426	O-18:0/20:4	O-18:0/20:4	O-38:4	O-38:4
		O-18:1/20:3	O-18:1/20:3		
PC(P-38:4)	952.528637	P-18:0/20:4	P-18:0/20:4		
PC(38:5)	808.585041	16:0/22:5	16:0/22:5		18:1/20:4
		18:1/20:4	18:1/20:4		
		18:0/20:5			
PC(O-38:5)	794.605776	O-18:1/20:4	O-18:1/20:4	O-38:5	O-38:5
		O-18:0/20:5			
PC(P-38:5)	950.512988	P-38:5	P-38:5		
PC(38:6)	806.569392	16:0/22:6	16:0/22:6	38:6	
			16:1/22:5		
PC(O-38:6)	792.590127	O-38:6	O-38:6		
PC(P-38:6)	948.497339	P-16:0/22:6	P-16:0/22:6		
PC(39:1)	830.663287	39:1		39:1	
PC(39:2)	828.647638	39:2		39:2	
PC(P-39:5)	964.528637		P-39:5		
PC(39:6)	820.585041	39:6		39:6	
PC(40:0)	846.694586	18:0_22:0		40:0	
PC(O-40:0)	832.715321	O-40:0	O-40:0	O-40:0	O-40:0
PC(40:1)	844.678936	18:0_22:1	18:0_22:1	18:0_22:1	18:0_22:1
				24:1_16:0	24:1_16:0
PC(O-40:1)	830.699672	O-40:1	O-40:1	O-40:1	O-40:1
PC(40:2)	842.663287	40:2	20:1/20:1	20:1/20:1	20:1/20:1
PC(40:3)	840.647638	18:1_22:2	18:1_22:2		
PC(40:4)	838.631989	20:1/20:3	20:1/20:3		
		18:0/22:4	18:0/22:4		
PC(O-40:4)	824.652724				
PC(O-40:5)	822.637075	O-40:5	O-40:5		
PC(40:6)	834.60069	18:1_22:5	18:1_22:5	18:1_22:5	18:1_22:5
		18:0_22:6	18:0_22:6		
		20:1_20:5			
PC(O-40:6)	820.621426	O-40:6	O-40:6		
PC(P-40:6)	976.528637	P-40:6	P-40:6		
PC(40:7)	832.585041	18:1_22:6	18:1_22:6	40:7	
PC(O-40:7)	818.605776	O-40:7			

Table C.3 (Cont'd)

PC(42:1)	872.710235	24:0_18:1	24:0_18:1	24:0_18:1	24:0_18:1
		24:1_18:0		26:1_16:0	26:1_16:0
PC(42:2)	870.694586	42:2	24:1_18:1	24:1_18:1	24:1_18:1
PC(42:7)	860.61634			42:7	42:7
PC(P-43:3)	1024.62253	P-43:3	P-43:3		
PC(44:1)	900.741533		18:1_26:0	18:1_26:0	18:0_26:1
PC(44:2)	898.725884			18:1_26:1	18:1_26:1
PC(O-44:4)	880.715321	O-44:4	O-44:4		

Table C.4 LPC sum compositions, their positive ionization mode m/z for MS analysis and molecular lipids identified for SW480 cells, SW620 cells, SW480 exosomes and SW620 exosomes.

		SW480 Cells	SW620 Cells	SW480 Exo	SW620 Exo
Sum Comp	(+) Mass	Molecular Lipid	Molecular Lipid	Molecular Lipid	Molecular Lipid
	m/z				
LPC(14:0)	468.3084		14:0		
LPC(16:0)	496.3397	16:0	16:0	16:0	16:0
LPC(O-16:0)	482.3605	O-16:0	O-16:0	O-16:0	O-16:0
LPC(P-16:0)	638.2677	P-16:0	P-16:0		P-16:0
PC(16:1)	494.3241	16:1	16:1		
LPC(17:0)	510.3554	17:0			
LPC(17:1)	508.3397	17:1	17:1	17:1	
LPC(18:0)	524.3710	18:0	18:0	18:0	18:0
LPC(O-18:0)	510.3918	O-18:0	O-18:0	O-18:0	O-18:0
LPC(18:1)	522.3554	18:1	18:1	18:1	18:1
LPC(O-18:1)	508.3761	O-18:1	O-18:1	O-18:1	O-18:1
LPC(18:2)	520.3397	18:2	18:2		
LPC(19:1)	536.3710	19:1		19:1	
LPC(20:1)	550.3867	20:1	20:1	20:1	

Table C.5 PS sum compositions, their positive ionization mode m/z for MS analysis and molecular lipids identified for SW480 cells, SW620 cells, SW480 exosomes and SW620 exosomes.

		SW480 Cells	SW620 Cells	SW480 Exo	SW620 Exo
Sum Comp	(+) Mass	Molecular Lipid	Molecular Lipid	Molecular Lipid	Molecular Lipid
	m/z				
PS(32:1)	865.5452		32:1	32:1	32:1
PS(O-32:1)	851.5659	O-16:0/16:1	O-16:0/16:1	O-16:0/16:1	O-16:0/16:1
PS(P-33:0)	1023.5045				P-33:0
PS(33:1)	879.5609	17:0/16:1		16:1/17:0	17:0/16:1
PS(O-33:1)	865.5816	O-16:0/17:1	O-16:1/17:0	O-33:1	O-16:1/17:0
PS(O-33:2)	863.5659	O-33:2	O-33:2	O-33:2	O-33:2
PS(O-34:0)	881.6129	O-16:0/18:0	O-16:0/18:0	O-16:0/18:0	O-16:0/18:0
PS(34:1)	893.5765	18:0/16:1	18:0/16:1	18:0/16:1	18:0/16:1
		16:0/18:1	16:0/18:1	16:0/18:1	16:0/18:1
PS(O-34:1)	879.5972	O-16:0/18:1	O-16:0/18:1	O-16:0/18:1	O-16:0/18:1
		O-18:0/16:1	O-18:0/16:1	O-18:0/16:1	O-18:0/16:1
PS(P-34:1)	1035.5045	P-16:0/18:1	P-16:0/18:1	P-16:0/18:1	P-16:0/18:1
PS(34:2)	891.5609	18:1/16:1	18:1/16:1	18:1/16:1	18:1/16:1
		16:0/18:2	16:0/18:2		16:0/18:2
PS(35:0)	909.6078	17:0/18:0		18:0/17:0	18:0/17:0
		18:0/17:0			
		16:0/19:0			
PS(O-35:0)	895.6285	O-16:0/17:0		O-16:0/17:0	O-16:0/17:0
PS(P-35:0)	1051.5358				P-35:0
PS(35:1)	907.5922	17:0/18:1	18:1/17:0	17:0/18:1	17:0/18:1
		18:0/17:1	18:0/17:1	18:0/17:1	18:0/17:1
		19:0/16:1	16:0/19:1	19:0/16:1	16:0/19:1
			16:1/19:0		19:0/16:1
PS(O-35:1)	893.6129	O-18:0/17:1	O-16:0/19:1	O-18:1/17:0	O-17:0/18:1
		O-16:0/19:1	O-17:0/18:1	O-17:0/18:1	O-18:0/17:1
		O-17:0/18:1		O-18:0/17:1	O-16:0/19:1
		O-18:1/17:0			
PS(P-35:1)	1049.5201		P-35:1	P-35:1	P-35:1
PS(35:2)	905.5765	18:1/17:1	18:1/17:1	18:1/17:1	18:1/17:1
		17:0/18:2	18:2/17:0		
			17:0/18:2		
			16:0/19:2		
			16:1/19:1		

Table C.5 (Cont'd)

PS(O-36:0) 909.6442 O-18:0/18:0 O-18:0/18:1 D-18:0/18:1 18:0/18:1 18:0/18:1 18:0/18:1 18:0/18:1 18:0/18:1 18:0/18:1 18:0/18:1 18:0/18:1 O-18:0/18:1 P-18:0/18:1 P-18:0/18:1 </th <th>PS(O-35:2)</th> <th>891.5972</th> <th>O-18:1/17:1</th> <th>O-16:1/19:1</th> <th>O-16:0/19:1</th> <th>O-18:1/17:1</th>	PS(O-35:2)	891.5972	O-18:1/17:1	O-16:1/19:1	O-16:0/19:1	O-18:1/17:1
PS(36:1) 921.6078 18:0/18:1 18:0/18:1 18:0/18:1 18:0/18:1 18:0/18:1 18:0/18:1 20:0/16:1 20:0/16:1 20:0/16:1 20:0/16:1 20:0/16:1 20:0/16:1 20:0/16:1 20:0/16:1 20:0/16:1 20:0/16:1 20:0/16:1 20:0/16:1 20:0/16:1 20:0/16:1 20:0/16:1 20:0/16:1 20:0/16:1 20:0/16:1 20:0/18:1 0-18:0/18:1 0-18:0/18:1 0-18:0/18:1 0-18:0/18:1 0-18:0/18:1 0-18:0/18:1 0-18:0/18:1 0-18:0/18:1 0-18:0/18:1 0-18:0/18:1 0-18:0/18:1 0-18:0/18:1 0-18:0/18:1 0-18:0/18:1 0-18:0/18:1 0-18:0/18:1 18:0/18:1				O-18:1/17:1	O-18:1/17:1	
20:0/16:1 20:0/16:1 20:0/16:1 20:0/16:1	PS(O-36:0)	909.6442	O-18:0/18:0	O-18:0/18:0	O-18:0/18:0	O-18:0/18:0
Tein	PS(36:1)	921.6078	18:0/18:1	18:0/18:1	18:0/18:1	18:0/18:1
PS(0-36:1) 907.6285 O-18:0/18:1 O-18:0/18:1 O-18:0/18:1 O-18:0/18:1 O-16:0/20:1 PS(P-36:1) 1063.5358 P-18:0/18:1 18:1/18:1 18:1/18:1 18:1/18:1 18:1/18:1 18:1/18:1 18:0/18:2 18:0/18:2 18:0/18:2 18:0/18:2 18:0/18:2 18:0/18:2 18:0/18:2 18:0/18:2 18:0/18:2 18:0/18:2 18:0/18:2 18:0/18:2 18:0/18:1 0-18:0/18:2 0-18:1/18:1 0-18:0/18:2 0-18:1/18:1 0-18:0/18:2 0-18:0/18:2 0-18:0/18:2 0-18:0/18:2 0-18:0/18:2 0-18:0/18:2 0-18:0/18:2 0-18:0/18:2 0-18:0/18:2 0-18:0/18:2 0-18:0/18:2 0-18:0/18:2 0-18:0/18:2 0-18:0/18:2 0-18:0/18:2 0-18:0/18:2 0-18:0/18:2 0-18:0/18:2			20:0/16:1	20:0/16:1	20:0/16:1	20:0/16:1
O-16:0/20:1 O-16:0/20:1 O-16:0/20:1				16:0/20:1	16:0/20:1	
PS(P-36:1) 1063.5358 P-18:0/18:1 18:1/18:1 18:1/18:1 18:1/18:1 18:0/18:2 18:0/18:2 18:0/18:2 18:0/18:2 18:0/18:2 18:0/18:2 18:0/18:2 18:0/18:2 18:0/18:2 0-18:1/18:1 0-18:1/18:1 0-18:1/18:1 0-18:0/18:2 0-18:0/18:1 18:0/18:1 18:0/18:1 18:0/18:1 18:0/19:1 18:0/19:1 19:0/18:1 18:	PS(O-36:1)	907.6285	O-18:0/18:1	O-18:0/18:1	O-18:0/18:1	O-18:0/18:1
PS(P-36:1) 1063.5358 P-18:0/18:1 18:1/18:1 18:1/18:1 18:1/18:1 18:1/18:1 18:1/18:1 20:1/16:1 20:1/16:1 20:1/16:1 20:1/16:1 20:1/16:1 20:1/16:1 20:1/16:1 20:1/16:1 20:1/16:1 20:1/16:1 20:1/18:2 18:0/18:2 20:1/18:1 20:18:1/18:1 20:18:1/18:1 20:18:1/18:1 20:18:1/18:1 20:18:1/18:1 20:18:1/18:1 20:18:1/18:1 20:18:1/18:1 20:18:1/18:1 20:18:1/18:1 20:18:1/18:1 20:18:1/18:1 20:18:1/18:1 20:18:1/18:1 20:18:1/18:1 20:18:1/18:1 20:18:1/18:1 20:18:1/18:1 18:1/18:2 18:1/18:2 18:1/18:2 18:1/18:2 18:1/18:2 18:1/18:1 18:1/18:2 18:1/18:1 18:1/18:1 18:1/18:1 20:3/16:0 20:3/16:0 20:3/16:0 18:2/18:1 18:2/18:1 18:2/18:1 18:2/18:1 18:2/18:1 18:2/18:1 18:2/18:1 18:2/18:1 18:2/18:1 18:2/18:1 20			O-16:0/20:1	O-16:0/20:1		O-16:0/20:1
PS(36:2) 919.5922 18:1/18:1 18:1/18:1 18:1/18:1 18:1/18:1 18:1/18:1 18:1/18:1 18:1/18:1 18:1/18:1 18:1/18:1 20:1/16:1 20:1/16:1 20:1/16:1 20:1/16:1 20:1/16:1 20:1/16:1 20:1/16:1 20:1/16:1 20:1/16:1 20:1/16:1 20:1/16:1 20:1/16:1 20:1/18:1 0-18:0/18:2 0-18:0/18:1 0-18:1/18:1 0-18:1/18:1 0-18:0/18:2 0-18:0/18:2 0-18:0/18:2 0-18:0/18:2 0-18:0/18:2 0-18:0/18:2 0-18:0/20:2 0-18:0/18:2 0-18:0/18:2 0-18:0/18:2 0-18:0/18:2 0-18:0/20:2 PS(9:0.20:2 0-18:0/18:2 0-18:0/18:2 0-18:0/20:2 PS(9:0.20:2 0-18:0/18:2 0-18:0/18:2 0-18:0/18:2 0-18:0/18:2 0-18:0/18:2 0-18:0/18:2 0-18:0/18:2 0-18:0/18:2 0-18:0/18:2 0-18:0/18:2 0-18:0/18:2 18:1/18:2 18:1/18:2 18:1/18:1 18:1/18:2 18:1/18:1 18:1/18:2 18:1/18:1 18:1/18:1 18:1/18:1 18:1/18:1 0-18:0/18:1 18:0/18:1 18:0/18:1 18:0/19:1 19:0/18:1 18:0/19:1 19:0/18:1				O-18:1/18:0		O-18:1/18:0
18:0/18:2 18:0/18:2 20:1/16:1 20:1/16:1 20:1/16:1 16:0/20:2 18:0/18:2 18:0/18:2 16:0/20:2 16:1/20:1 20:1/16:1 20:1/16:1 20:1/16:1 20:1/16:1 20:1/16:1 20:1/16:1 20:1/16:1 PS(0-36:2) 905.6129 O-18:1/18:1 O-16:0/20:2 O-18:1/18:1 O-18:0/18:2 O-18:0/18:2 O-18:1/18:1 O-18:0/18:2 O-16:0/20:2 O-18:0/18:2 O-16:0/20:2 PS(P-36:2) 1061.5201 P-18:1/18:1 PS(36:3) 917.5765 18:1/18:2 18:1/18:2 18:2/18:1 18:1/18:2 18:0/18:3 20:3/16:0 18:2/18:1 18:1/18:2 20:3/16:0 20:2/16:1 20:3/16:0 20:2/16:1 PS(0-37:0) 923.6598 O-37:0 PS(37:1) 935.6235 19:0/18:1 18:0/19:1 19:0/18:1 18:0/19:1 18:0/19:1 18:1/19:0 18:0/19:1 19:0/18:1 20:0/17:1 20:0/17:1 20:0/17:1 18:1/19:0 PS(0-37:1) 921.6442 O-18:0/19:1 O-18:0/19:1 O-18:0/19:1 PS(37:2) 933.6078 19:1/18:1 18:1/19:1 19:1/18:1 19:1/18:1 17:0/20:2 18:2/19:0 20:1/17:1 18:1/19:1 17:0/20:2 20:1/17:1 18:1/19:1	PS(P-36:1)	1063.5358	P-18:0/18:1	P-18:0/18:1	P-18:0/18:1	P-18:0/18:1
20:1/16:1 16:0/20:2 18:0/18:2 18:0/18:2 16:0/20:2 16:1/20:1 20:1/16:1 20:1/16:1 PS(0-36:2) 905.6129 O-18:1/18:1 O-16:0/20:2 O-18:1/18:1 O-18:0/18:2 O-18:0/18:2 O-18:1/18:1 O-18:0/18:2 O-16:0/20:2 PS(P-36:2) 1061.5201 P-18:1/18:1 PS(36:3) 917.5765 18:1/18:2 18:1/18:2 18:2/18:1 18:1/18:2 18:0/18:3 20:3/16:0 18:2/18:1 18:1/18:2 20:3/16:0 20:2/16:1 20:2/16:1 18:0/18:3 PS(0-37:0) 923.6598 O-37:0 PS(37:1) 935.6235 19:0/18:1 18:0/19:1 19:0/18:1 18:0/19:1 18:0/19:1 18:1/19:0 18:0/19:1 19:0/18:1 20:0/17:1 20:0/17:1 20:0/17:1 18:1/19:0 PS(0-37:1) 921.6442 O-18:0/19:1 O-18:0/19:1 O-18:0/19:1 PS(37:2) 933.6078 19:1/18:1 18:1/19:1 19:1/18:1 19:1/18:1 17:0/20:2 18:2/19:0 20:1/17:1 18:1/19:1	PS(36:2)	919.5922	18:1/18:1	18:1/18:1	18:1/18:1	18:1/18:1
16:0/20:2 16:1/20:1 20:1/16:1			18:0/18:2	18:0/18:2	20:1/16:1	20:1/16:1
PS(O-36:2) 905.6129 O-18:1/18:1 O-16:0/20:2 O-18:1/18:1 O-18:1/18:1 PS(O-36:2) 905.6129 O-18:1/18:1 O-16:0/20:2 O-18:1/18:1 O-18:0/18:2 O-16:0/20:2 O-18:0/18:2 O-16:0/20:2 PS(P-36:2) 1061.5201 P-18:1/18:1 PS(36:3) 917.5765 18:1/18:2 18:1/18:2 18:2/18:1 18:1/18:2 18:0/18:3 20:3/16:0 18:2/18:1 18:2/18:1 20:3/16:0 20:2/16:1 20:3/16:0 20:2/16:1 PS(O-37:0) 923.6598 O-37:0 PS(37:1) 935.6235 19:0/18:1 18:0/19:1 19:0/18:1 18:0/19:1 18:0/19:1 18:1/19:0 18:0/19:1 19:0/18:1 20:0/17:1 20:0/17:1 20:0/17:1 20:0/17:1 18:1/19:0 20:1/17:0 20:0/17:1 19:1/18:1 19:1/18:1 PS(O-37:1) 921.6442 O-18:0/19:1 0-18:0/19:1 0-18:0/19:1 PS(37:2) 933.6078 19:1/18:1 18:1/19:1 19:1/18:1 19:1/18:1 19:1/18:1 19:1/18:1 17:0/20:2 18:2/19:0 20:1/17:1			20:1/16:1	16:0/20:2	18:0/18:2	18:0/18:2
PS(O-36:2) 905.6129 O-18:1/18:1 O-16:0/20:2 O-18:1/18:1 O-18:1/18:1 O-18:0/18:2 O-18:0/18:2 O-18:0/18:2 O-16:0/20:2 PS(P-36:2) 1061.5201 P-18:1/18:2 P-18:1/18:1 PS(36:3) 917.5765 18:1/18:2 18:1/18:2 18:2/18:1 18:1/18:2 PS(36:3) 917.5765 18:1/18:2 18:0/18:1 18:2/18:1 18:1/18:2 PS(37:1) 923.6598 0-37:0 0-37:0 0-37:0 0-37:0 PS(37:1) 935.6235 19:0/18:1 18:0/19:1 19:0/18:1 18:0/19:1 19:0/18:1 PS(0-37:1) 921.6442 0-18:0/19:1 20:0/17:1 20:0/17:1 20:0/17:1 0-18:0/19:1 0-18:0/19:1 0-18:0/19:1 19:1/18:1			16:0/20:2	16:1/20:1		
O-18:0/18:2 O-18:1/18:1 O-18:0/18:2 PS(P-36:2) 1061.5201 P-18:1/18:1 PS(36:3) 917.5765 18:1/18:2 18:1/18:2 18:2/18:1 18:1/18:2 18:0/18:3 20:3/16:0 18:2/18:1 20:3/16:0 20:2/16:1 20:2/16:1 18:0/18:3 PS(0-37:0) 923.6598 O-37:0 PS(37:1) 935.6235 19:0/18:1 18:0/19:1 19:0/18:1 18:0/19:1 18:0/19:1 18:1/19:0 18:0/19:1 19:0/18:1 20:0/17:1 20:0/17:1 20:0/17:1 20:0/17:1 PS(0-37:1) 921.6442 O-18:0/19:1 0-18:0/19:1 19:1/18:1 PS(37:2) 933.6078 19:1/18:1 18:1/19:1 19:1/18:1 19:1/18:1 20:1/17:1 18:0/19:2 20:1/17:1 18:1/19:1 17:0/20:2 18:2/19:0 20:1/17:1				20:1/16:1		
PS(P-36:2) 1061.5201 P-18:0/18:2 P-18:1/18:1 PS(36:3) 917.5765 18:1/18:2 18:1/18:2 18:2/18:1 18:1/18:2 PS(36:3) 917.5765 18:1/18:2 18:1/18:2 18:2/18:1 18:1/18:2 PS(37:1) 20:3/16:0 20:2/16:1 20:2/16:1 18:0/18:3 7.3 PS(0-37:0) 923.6598 O-37:0 O-37:0 PS(37:1) 935.6235 19:0/18:1 18:0/19:1 19:0/18:1 18:0/19:1 19:0/18:1	PS(O-36:2)	905.6129	O-18:1/18:1	O-16:0/20:2	O-18:1/18:1	O-18:1/18:1
PS(P-36:2) 1061.5201 P-18:1/18:1 PS(36:3) 917.5765 18:1/18:2 18:1/18:2 18:2/18:1 18:1/18:2 PS(0-37:0) 923.6598 20:2/16:1 32:2/18:1 32:2/18:1 32:2/18:1 PS(37:1) 935.6235 19:0/18:1 18:0/19:1 19:0/18:1 18:0/19:1 18:0/19:1 19:0/18:1 PS(0-37:1) 935.6235 19:0/18:1 18:0/19:1 19:0/18:1 19:0/18:1 PS(07:1) 935.6235 19:0/18:1 18:0/19:1 19:0/18:1 19:0/18:1 PS(37:1) 935.6235 19:0/18:1 18:0/19:0 19:0/18:1 19:0/18:1 PS(37:2) 933.6038 19:1/17:0 20:0/17:1 0-18:0/19:1 0-18:0/19:1 0-18:0/19:1 PS(37:2) 933.6078 19:1/18:1 18:0/19:1 19:1/18:1 19:1/18:1 PS(37:2) 933.6078 19:1/18:1 18:0/19:1 20:1/17:1 18:1/19:1 PS(37:2) 933.6078 19:1/18:1 18:0/19:2 20:1/17:1 18:1/19:1 PS(37:2) 933.6078			O-18:0/18:2	O-18:1/18:1		O-18:0/18:2
PS(36:3) 917.5765 18:1/18:2 18:1/18:2 18:2/18:1 18:1/18:2 18:0/18:3 20:3/16:0 18:2/18:1 18:2/18:1 20:3/16:0 20:2/16:1 18:2/18:1 PS(0-37:0) 923.6598 0-37:0 PS(37:1) 935.6235 19:0/18:1 18:0/19:1 19:0/18:1 18:0/19:1 18:0/19:1 18:0/19:1 19:0/18:1 20:0/17:1 20:0/17:1 20:0/17:1 18:1/19:0 PS(0-37:1) 921.6442 0-18:0/19:1 0-18:0/19:1 0-18:0/19:1 PS(37:2) 933.6078 19:1/18:1 18:1/19:1 19:1/18:1 19:1/18:1 17:0/20:2 18:2/19:0 20:1/17:1 18:1/19:1 17:0/20:2 20:1/17:1 17:0/20:2			O-16:0/20:2	O-18:0/18:2		O-16:0/20:2
18:0/18:3 20:3/16:0 18:2/18:1 20:3/16:0 20:2/16:1 20:2/16:1 18:0/18:3 PS(0-37:0) 923.6598 O-37:0 PS(37:1) 935.6235 19:0/18:1 18:0/19:1 19:0/18:1 18:0/19:1 18:0/19:1 19:0/18:1 19:0/18:1 20:0/17:1 20:0/17:1 20:0/17:1 18:1/19:0 PS(0-37:1) 921.6442 O-18:0/19:1 O-18:0/19:1 O-18:0/19:1 PS(37:2) 933.6078 19:1/18:1 18:1/19:1 19:1/18:1 19:1/18:1 17:0/20:2 18:2/19:0 20:1/17:1 18:1/19:1 17:0/20:2 18:2/19:0 20:1/17:1	PS(P-36:2)	1061.5201				P-18:1/18:1
20:3/16:0 20:2/16:1	PS(36:3)	917.5765	18:1/18:2	18:1/18:2	18:2/18:1	18:1/18:2
PS(0-37:0) 923.6598 O-37:0 PS(37:1) 935.6235 19:0/18:1 18:0/19:1 19:0/18:1 18:0/19:1 18:0/19:1 18:1/19:0 18:0/19:1 19:0/18:1 20:0/17:1 20:0/17:1 20:0/17:1 18:1/19:0 20:1/17:0 C-18:0/19:1 O-18:0/19:1 O-18:0/19:1 PS(37:2) 933.6078 19:1/18:1 18:1/19:1 19:1/18:1 19:1/18:1 20:1/17:1 18:0/19:2 20:1/17:1 18:1/19:1 17:0/20:2 18:2/19:0 20:1/17:1			18:0/18:3	20:3/16:0		18:2/18:1
PS(0-37:0) 923.6598 O-37:0 PS(37:1) 935.6235 19:0/18:1 18:0/19:1 19:0/18:1 18:0/19:1 18:0/19:1 18:0/19:1 18:0/19:1 19:0/18:1 20:0/17:1 20:0/17:1 20:0/17:1 18:1/19:0 PS(0-37:1) 921.6442 O-18:0/19:1 O-18:0/19:1 O-18:0/19:1 PS(37:2) 933.6078 19:1/18:1 18:1/19:1 19:1/18:1 19:1/18:1 17:0/20:2 18:2/19:0 20:1/17:1 18:1/19:1 17:0/20:2 20:1/17:1 20:1/17:1			20:3/16:0	20:2/16:1		
PS(37:1) 935.6235 19:0/18:1 18:0/19:1 19:0/18:1 18:0/19:1 18:0/19:1 19:0/18:1 18:0/19:1 18:0/19:1 18:0/19:1 19:0/18:1 19:0/18:1 20:0/17:1 20:0/17:1 20:0/17:1 18:1/19:0 PS(0-37:1) 921.6442 0-18:0/19:1 0-18:0/19:1 0-18:0/19:1 PS(37:2) 933.6078 19:1/18:1 18:1/19:1 19:1/18:1 19:1/18:1 20:1/17:1 18:0/19:2 20:1/17:1 18:1/19:1 17:0/20:2 18:2/19:0 20:1/17:1 20:1/17:1 20:1/17:1			20:2/16:1	18:0/18:3		
18:0/19:1 18:1/19:0 18:0/19:1 19:0/18:1 20:0/17:1 20:0/17:1 20:0/17:1 18:1/19:0 20:1/17:0 20:0/17:1 20:0/17:1 PS(0-37:1) 921.6442 0-18:0/19:1 0-18:0/19:1 0-18:0/19:1 PS(37:2) 933.6078 19:1/18:1 18:1/19:1 19:1/18:1 19:1/18:1 20:1/17:1 18:0/19:2 20:1/17:1 18:1/19:1 17:0/20:2 18:2/19:0 20:1/17:1 20:1/17:1 20:1/17:1	PS(O-37:0)	923.6598				O-37:0
20:0/17:1 20:0/17:1 20:0/17:1 18:1/19:0 20:1/17:0 20:0/17:1 20:0/17:1 PS(0-37:1) 921.6442 O-18:0/19:1 O-18:0/19:1 O-18:0/19:1 PS(37:2) 933.6078 19:1/18:1 18:1/19:1 19:1/18:1 19:1/18:1 20:1/17:1 18:0/19:2 20:1/17:1 18:1/19:1 17:0/20:2 18:2/19:0 20:1/17:1 17:0/20:2 20:1/17:1	PS(37:1)	935.6235	19:0/18:1	18:0/19:1	19:0/18:1	18:0/19:1
20:1/17:0 20:0/17:1 PS(0-37:1) 921.6442 O-18:0/19:1 O-18:0/19:1 O-18:0/19:1 O-18:0/19:1 PS(37:2) 933.6078 19:1/18:1 18:1/19:1 19:1/18:1 19:1/18:1 19:1/18:1 20:1/17:1 18:0/19:2 20:1/17:1 18:1/19:1 17:0/20:2 18:2/19:0 20:1/17:1 20:1/17:1 20:1/17:1			18:0/19:1	18:1/19:0	18:0/19:1	19:0/18:1
PS(0-37:1) 921.6442 O-18:0/19:1 O-18:0/19:1 O-18:0/19:1 PS(37:2) 933.6078 19:1/18:1 18:1/19:1 19:1/18:1 19:1/18:1 20:1/17:1 18:0/19:2 20:1/17:1 18:1/19:1 17:0/20:2 18:2/19:0 20:1/17:1 17:0/20:2 20:1/17:1			20:0/17:1	20:0/17:1	20:0/17:1	18:1/19:0
PS(37:2) 933.6078 19:1/18:1 18:1/19:1 19:1/18:1 19:1/18:1 20:1/17:1 18:0/19:2 20:1/17:1 18:1/19:1 17:0/20:2 18:2/19:0 20:1/17:1 17:0/20:2 20:1/17:1			20:1/17:0			20:0/17:1
20:1/17:1 18:0/19:2 20:1/17:1 18:1/19:1 17:0/20:2 18:2/19:0 20:1/17:1 20:1/17:1 20:1/17:1 20:1/17:1	PS(O-37:1)	921.6442		O-18:0/19:1	O-18:0/19:1	O-18:0/19:1
17:0/20:2 18:2/19:0 20:1/17:1 17:0/20:2 20:1/17:1	PS(37:2)	933.6078	19:1/18:1	18:1/19:1	19:1/18:1	19:1/18:1
17:0/20:2 20:1/17:1			20:1/17:1	18:0/19:2	20:1/17:1	18:1/19:1
20:1/17:1			17:0/20:2	18:2/19:0		20:1/17:1
				17:0/20:2		
PS(O-38:0) 937.6755 O-38:0 O-38:0 O-38:0				20:1/17:1		
	PS(O-38:0)	937.6755	O-38:0		O-38:0	O-38:0

Table C.5 (Cont'd)

PS(38:1)	949.6391	20:0/18:1	20:0/18:1	20:0/18:1	20:0/18:1
		18:0/20:1	18:0/20:1	18:0/20:1	18:0/20:1
		22:0/16:1	22:0/16:1	20:1/18:0	20:1/18:0
				22:0/16:1	22:0/16:1
					22:1/16:0
PS(O-38:1)	935.6598	O-18:0/20:1		O-18:0/20:1	O-18:0/20:1
<u> </u>		O-18:1/20:0			
PS(38:2)	947.6235	20:1/18:1	20:1/18:1	20:1/18:1	20:1/18:1
		18:0/20:2	18:1/20:1	18:0/20:2	22:1/16:1
		22:1/16:1	18:0/20:2	20:2/18:0	18:0/20:2
		20:0/18:2	22:1/16:1	22:1/16:1	
			20:0/18:2	20:0/18:2	
PS(O-38:2)	933.6442	O-18:0/20:2	O-18:0/20:2		O-16:0/22:2
					O-18:0/20:2
PS(38:3)	945.6078	18:0/20:3	18:0/20:3	20:2/18:1	18:0/20:3
		20:2/18:1	18:1/20:2	18:0/20:3	20:2/18:1
		18:1/20:2	20:1/18:2	20:1/18:2	20:1/18:2
		20:1/18:2	18:2/20:1		
PS(O-38:3)	931.6285	O-18:0/20:3	O-18:0/20:3		O-38:3
			O-18:1/20:2		
PS(38:4)	943.5922	18:0/20:4	18:0/20:4	18:0/20:4	18:0/20:4
		18:1/20:3	18:1/20:3	18:1/20:3	18:1/20:3
		16:0/22:4	16:0/22:4		
PS(O-38:4)	929.6129	O-18:0/20:4	O-18:0/20:4	O-38:4	O-18:0/20:4
		O-16:0/22:4	O-16:0/22:4		
			O-18:1/20:3		
PS(P-38:4)	1085.5201	P-38:4	P-18:0/20:4		
			P-18:1/20:3		
PS(38:5)	941.5765	18:0/20:5	18:1/20:1	18:1/20:4	18:1/20:1
		18:1/20:1	18:0/20:5		18:0/20:5
		16:0/22:5	16:0/22:5		
PS(39:1)	963.6548	18:1/21:0	18:1/21:0	21:0/18:1	21:0/18:1
		21:0/18:1	20:0/19:1	22:0/17:1	18:1/21:0
		22:0/17:1	18:0/21:1	22:1/17:0	22:1/17:0
			22:0/17:1	20:0/19:1	22:0/17:1
				21:1/18:1	20:0/19:1
PS(39:2)	961.6391	21:1/18:1	21:1/18:1	22:1/17:1	21:1/18:1
			18:1/21:1		
PS(39:4)	957.6078	39:4	39:4		39:4

Table C.5 (Cont'd)

PS(O-40:0)	965.7068				O-40:0
PS(40:1)	977.6704	22:0/18:1	22:0/18:1	22:0/18:1	22:0/18:1
		22:1/18:0	22:1/18:0	22:1/18:0	22:1/18:0
		18:0/22:1	24:0/16:1	18:0/22:1	24:0/16:1
		24:0/16:1		24:0/16:1	
PS(40:2)	975.6548	22:1/18:1	22:1/18:1	22:1/18:1	22:1/18:1
		22:0/18:2	22:0/18:2	18:0/22:2	24:1/16:1
		18:0/22:2	20:0/20:2	24:1/16:1	18:0/22:2
		24:1/16:1	24:1/16:1	20:1/20:1	22:2/18:0
			18:0/22:2	22:0/18:2	20:1/20:1
					20:0/20:2
PS(40:3)	973.6391	18:0/22:3	18:0/22:3	22:2/18:1	22:2/18:1
		22:2/18:1	22:2/18:1	18:0/22:3	22:1/18:2
		22:1/18:2	18:1/22:2	22:1/18:2	20:0/20:3
		20:0/20:3	22:1/18:2	20:0/20:3	
			20:0/20:3		
			20:1/20:2		
PS(40:4)	971.6235	18:0/22:4	18:0/22:4	20:0/20:4	20:0/20:4
		20:0/20:4	20:0/20:4	20:1/20:3	20:1/20:3
		20:1/20:3	20:1/20:3	18:0/22:4	18:0/22:4
		18:1/22:3		18:1/22:3	18:1/22:3
PS(O-40:4)	957.6442	O-18:0/22:4	O-18:0/22:4		
PS(40:5)	969.6078	18:0/22:5	18:0/22:5	20:1/20:4	20:1/20:4
		18:1/22:4	18:1/22:4	18:1/22:4	18:1/22:4
		20:1/20:4	20:1/20:4	18:0/22:5	18:0/22:5
PS(O-40:5)	955.6285	O-18:0/22:5	O-18:0/22:5	O-40:5	O-18:0/22:5
			O-18:1/22:4		
PS(40:6)	967.5922	18:0/22:6	18:0/22:6	18:0/22:6	18:0/22:6
		18:1/22:5	18:1/22:5	18:1/22:5	18:1/22:5
PS(O-40:6)	953.6129	O-18:0/22:6	O-18:0/22:6		
			O-18:1/22:5		
PS(41:1)	991.6861	23:0/18:1		23:0/18:1	23:0/18:1
		24:0/17:1		24:0/17:1	18:1/23:0
					24:0/17:1
PS(41:2)	989.6704	23:1/18:1		23:1/18:1	23:1/18:1
				24:1/17:1	24:1/17:1
PS(O-42:0)	993.7381				O-42:0
PS(42:1)	1005.7017	24:0/18:1	24:0/18:1	24:0/18:1	24:0/18:1
			18:0/24:1		

Table C.5 (Cont'd)

PS(42:2)	1003.6861	24:1/18:1	24:1/18:1	24:1/18:1	24:1/18:1
		24:0/18:2	24:0/18:2		
PS(42:3)	1001.6704			24:2/18:1	24:2/18:1

Table C.6 LPS sum compositions, their positive ionization mode m/z for MS analysis and molecular lipids identified for SW480 cells, SW620 cells, SW480 exosomes and SW620 exosomes.

		SW480 Cells	SW620 Cells	SW480 Exo	SW620 Exo
Sum Comp	(+) Mass	Molecular Lipid	Molecular Lipid	Molecular Lipid	Molecular Lipid
	m/z				
PS(O-17:1)	627.3519		O-17:1	O-17:1	O-17:1
PS(18:0)	657.3625			18:0	18:0
PS(O-18:2)	639.3519	O-18:2	O-18:2	O-18:2	O-18:2
PS(O-20:2)	667.3832			O-20:2	
PS(O-20:4)	663.3519	O-20:4	O-20:4	O-20:4	
PS(O-20:5)	661.3363	O-20:5	O-20:5	O-20:5	O-20:5
PS(P-22:1)	853.3374	P-22:1	P-22:1	P-22:1	P-22:1
PS(O-24:1)	725.4615	O-24:1		O-24:1	O-24:1
PS(P-24:1)	881.3687	P-24:1	P-24:1	P-24:1	P-24:1

Table C.7 PG sum compositions, their positive ionization mode m/z for MS analysis and molecular lipids identified for SW480 cells, SW620 cells, SW480 exosomes and SW620 exosomes.

		SW480 Cells	SW620 Cells	SW480 Exo	SW620 Exo
Sum Comp	(+) Mass	Molecular Lipid	Molecular Lipid	Molecular Lipid	Molecular Lipid
	m/z			•	
PG(32:0)	740.5436	32:0	32:0		
PG(32:1)	738.5279		32:1		32:1
PG(34:1)	766.5592	16:0/18:1	16:0/18:1	16:0/18:1	16:0/18:1
		16:1/18:0	18:1/16:0	18:1/16:0	18:1/16:0
			16:1/18:0		
PG(P-34:1)	908.4872	P-34:1		P-34:1	P-34:1
PG(34:2)	764.5436		16:1/18:1		
			18:1/16:1		
PG(35:0)	782.5905				35:0
PG(O-35:1)	766.5956	O-35:1	O-35:1	O-35:1	O-35:1
PG(O-35:2)	764.5800				O-35:2
PG(36:1)	794.5905	18:0/18:1	18:0/18:1	18:0_18:1	18:0/18:1
		18:1/18:0	18:1/18:0		18:1/18:0
			16:0/20:1		
PG(O-36:1)	780.6113	O-36:1	O-36:1	O-36:1	O-18:0/18:1
PG(36:2)	792.5749	18:1/18:1	18:1/18:1	18:1/18:1	18:1/18:1
PG(36:3)	790.5592	18:1_18:2	18:1/18:2		18:1_18:2
			18:2/18:1		
PG(O-36:3)	776.5800	O-36:3	O-36:3	O-36:3	O-36:3
PG(36:4)	788.5436		36:4		36:4
PG(O-36:4)	774.5643	O-36:4	O-36:4	O-36:4	O-36:4
PG(37:0)	810.6218				37:0
PG(37:1)	808.6062				37:1
PG(O-37:1)	794.6269	O-37:1	O-37:1	O-37:1	O-37:1
PG(O-37:2)	792.6113	O-37:2	O-37:2	O-37:2	O-37:2
PG(38:1)	822.6218			38:1	38:1
PG(O-38:1)	808.6426	O-38:1			O-38:1
820.6062 - PG(38:2)	820.6062	18:1/20:1	18:1/20:1	38:2	38:2
		20:1/18:1	20:1/18:1		
PG(O-38:2)	806.6269	O-38:2	O-38:2	O-38:2	O-38:2
PG(38:3)	818.5905	18:1_20:2	18:1_20:2		

Table C.8 LPG sum compositions, their positive ionization mode m/z for MS analysis and molecular lipids identified for SW480 cells, SW620 cells, SW480 exosomes and SW620 exosomes.

		SW480 Cells	SW620 Cells	SW480 Exo	SW620 Exo
Sum Comp	(+) Mass	Molecular Lipid	Molecular Lipid	Molecular Lipid	Molecular Lipid
	m/z				
LPG(O-20:3)	538.3503	O-20:3			
LPG(O-21:1)	556.3973	O-21:1	O-21:1		O-21:1
LPG(O-21:4)	550.3503	O-21:4	O-21:4	O-21:4	
LPG(O-21:5)	548.3347	O-21:5	O-21:5	O-21:5	O-21:5

Table C.9 PI sum compositions, their positive ionization mode m/z for MS analysis and molecular lipids identified for SW480 cells, SW620 cells, SW480 exosomes and SW620 exosomes.

		SW480 Cells	SW620 Cells	SW480 Exo	SW620 Exo
Sum Comp	(+) Mass	Molecular Lipid	Molecular Lipid	Molecular Lipid	Molecular Lipid
	m/z				
PI(32:0)	828.5596		32:0		
PI(O-32:0)	814.5803	O-32:0	O-32:0	O-16:0/16:0	
PI(32:1)	826.5440	32:1	32:1	32:1	32:1
PI(34:1)	854.5753	16:0/18:1	16:0/18:1	16:0/18:1	16:0/18:1
		18:0/16:1	18:0/16:1	18:0/16:1	18:0/16:1
PI(O-34:1)	840.5960	O-16:0/18:1	O-16:0/18:1	O-16:0/18:1	O-16:0/18:1
			O-18:1/16:0		
PI(34:2)	852.5596	18:1/16:1	18:1/16:1	18:1/16:1	18:1/16:1
		16:0/18:2	16:0/18:2	16:0/18:2	16:0/18:2
PI(P-34:3)	992.4719			P-34:3	P-34:3
PI(35:1)	868.5909	17:0/18:1	17:0/18:1	17:0/18:1	17:0/18:1
		18:0/17:1	18:0/17:1	18:0/17:1	
		16:0/19:1	16:0/19:1		
PI(35:2)	866.5753	18:1/17:1	18:1/17:1	18:1/17:1	
PI(O-35:2)	852.5960	O-35:2		O-35:2	
PI(36:1)	882.6066	18:0/18:1	18:0/18:1	18:0/18:1	18:0/18:1
		16:0/20:1	16:0/20:1	16:0/20:1	
PI(O-36:1)	868.6273	O-18:0/18:1			O-18:0/18:1
		O-16:0/20:1			

Table C.9 (Cont'd)

PI(36:2)	880.5909	18:1/18:1	18:1/18:1	18:1/18:1	18:1/18:1
		18:0/18:2	18:0/18:2	18:0/18:2	18:0/18:2
		16:0/20:2	16:0/20:2	16:0/20:2	
PI(O-36:2)	866.6166	O-18:1/18:1		O-18:1/18:1	
		O-16:0/20:1			
PI(36:3)	878.5753	16:0/20:3	16:0/20:3	18:1/18:2	
		18:1/18:2	18:1/18:2	18:2/18:1	
		18:0/18:3	18:0/18:3		
PI(36:4)	876.5596	16:0/20:4			
PI(P-36:4)	1018.4876			P-36:4	
PI(37:2)	894.6066	18:0/19:2	18:0/19:2	18:0/19:2	
		19:1/18:1	19:1/18:1	19:1/18:1	
PI(38:2)	908.6222	18:0/20:2	18:0/20:2	18:0/20:2	18:0/20:2
		18:1/20:1	18:1/20:1	18:1/20:1	18:1/20:1
			20:1/18:1	20:1/18:1	20:1/18:1
PI(O-38:2)	894.6429	O-18:0/20:2			
		O-18:1/20:1			
PI(38:3)	906.6066	18:1/20:2	18:1/20:2	18:1/20:2	18:1/20:2
		18:0/20:3	18:0/20:3	18:0/20:3	18:0/20:3
PI(38:4)	904.5909	18:0/20:4	18:0/20:4	18:0/20:4	18:0/20:4
		18:1/20:3	18:1/20:3	18:1/20:3	18:1/20:3
PI(38:5)	902.5753	18:1/20:4	18:1/20:4		
		16:0/22:5	16:0/22:5		
		18:0/20:5	18:0/20:5		
PI(40:4)	932.6222		18:0/22:4		
PI(40:5)	930.6066	40:5	18:0/22:5		
			18:1/22:4		
PI(40:6)	928.5909	40:6	18:0/22:6		
			18:1/22:5		

Table C.10 SM sum compositions, their positive ionization mode m/z for MS analysis and molecular lipids identified for SW480 cells, SW620 cells, SW480 exosomes and SW620 exosomes.

		SW480 Cells	SW620 Cells	SW480 Exo	SW620 Exo
Sum Comp	(+) Mass	Molecular Lipid	Molecular Lipid	Molecular Lipid	Molecular Lipid
	m/z				
SM(32:1)	675.5435	32:1	32:1	32:1	32:1
SM(33:1)	689.5592	33:1	33:1	33:1	33:1
SM(34:1)	703.5748	d18:1/16:0	d18:1/16:0	d18:1/16:0	d18:1/16:0
SM(34:2)	701.5592	d18:2/16:0	d18:2/16:0	d18:2/16:0	d18:2/16:0
		d18:1/16:1			
SM(35:1)	717.5905	35:1		35:1	35:1
SM(36:1)	731.6061	36:1	36:1	d18:1/18:0	d18:1/18:0
SM(36:2)	729.5905	36:2	36:2	36:2	36:2
SM(38:1)	759.6374	38:1	38:1	38:1	38:1
SM(38:2)	757.6218			38:2	
SM(39:1)	773.6531	39:1		39:1	
SM(40:1)	787.6687	40:1	40:1	40:1	40:1
SM(40:2)	785.6531	40:2	40:2	40:2	40:2
SM(41:1)	801.6844	41:1	41:1	41:1	41:1
SM(41:2)	799.6687	41:2	41:2	41:2	41:2
SM(42:1)	815.7000	d18:1/24:0	d18:1/24:0	d18:1/24:0	d18:1/24:0
SM(42:2)	813.6844	d18:1/24:1	d18:1/24:1	d18:1/24:1	d18:1/24:1
SM(42:3)	811.6687	d18:1/24:2	d18:1/24:2	d18:1/24:2	d18:1/24:2
			d18:0/24:3		d18:0/24:3
SM(43:1)	829.7157	43:1		43:1	d18:1/25:0
SM(43:2)	827.7000			43:2	d18:1/25:1
SM(44:1)	843.7313			44:1	44:1
SM(44:2)	841.7157			44:2	44:2
SM(44:3)	839.7000			44:3	44:3
SM(44:5)	835.6687			44:5	44:5

Table C.11 Cer sum compositions, their positive ionization mode m/z for MS analysis and molecular lipids identified for SW480 cells, SW620 cells, SW480 exosomes and SW620 exosomes.

		SW480 Cells	SW620 Cells	SW480 Exo	SW620 Exo
Sum Comp	(+) Mass	Molecular Lipid	Molecular Lipid	Molecular Lipid	Molecular Lipid
	m/z				
Cer(32:0)	512.5037	d18:0/14:0			d18:0/14:0
Cer(34:0)	540.5350	d18:0/16:0	d18:0/16:0	d18:0/16:0	d18:0/16:0
Cer(34:1)	538.5193	d18:1/16:0	d18:1/16:0	d18:1/16:0	d18:1/16:0
		d16:1/18:0			
Cer(34:2)	536.5037			d18:2/16:0	d18:2/16:0
				d18:1/16:1	d18:1/16:1
Cer(36:0)	568.5660		d18:0/18:0	d18:0/18:0	
Cer(36:1)	566.5502	d18:1/18:0		d18:1/18:0	d18:1/18:0
Cer(36:2)	564.5350	d18:2/18:0	d18:2/18:0		
		d18:1/18:1			
Cer(40:1)	622.6132	d18:1/22:0	d18:1/22:0	d18:1/22:0	d18:1/22:0
		d18:0/22:1	d18:0/22:1	d18:0/22:1	d18:0/22:1
		d16:1/24:0	d16:1/24:0		d16:1/24:0
Cer(41:1)	636.6289	41:1	41:1	41:1	
Cer(42:0)	652.6602		d18:0/24:0	d18:0/24:0	d18:0/24:0
Cer(42:1)	650.6445	d18:1/24:0	d18:1/24:0	d18:1/24:0	d18:1/24:0
		d18:0/24:1	d18:0/24:1	d18:0/24:1	d18:0/24:1
		d20:1/22:0		d20:1/22:0	
Cer(42:2)	648.6289	d18:1/24:1	d18:1/24:1	d18:1/24:1	d18:1/24:1
		d18:2/24:0	d18:2/24:0	d18:2/24:0	d18:2/24:0
		d18:0/24:2	d18:0/24:2	d18:0/24:2	d18:0/24:2
Cer(42:3)	646.6132	d18:2/24:1	d18:2/24:1	d18:2/24:1	d18:2/24:1
		d18:1/24:2	d18:1/24:2	d18:1/24:2	d18:1/24:2
				d18:0/24:3	d18:0/24:3

Table C.12 Hex-Cer sum compositions, their positive ionization mode m/z for MS analysis and molecular lipids identified for SW480 cells, SW620 cells, SW480 exosomes and SW620 exosomes.

		SW480 Cells	SW620 Cells	SW480 Exo	SW620 Exo
Sum Comp	(+) Mass	Molecular Lipid	Molecular Lipid	Molecular Lipid	Molecular Lipid
	m/z				
Hex- Cer(34:1)	700.5722	34:1	34:1	34:1	34:1
Hex- Cer(40:1)	784.6661	40:1		40:1	40:1
Hex- Cer(42:1)	812.6973	42:1	42:1	42:1	42:1
Hex- Cer(42:2)	810.6817	42:2	42:2	42:2	42:2

Table C.13 TG sum compositions, their positive ionization mode m/z for MS analysis and molecular lipids identified for SW480 cells, SW620 cells, SW480 exosomes and SW620 exosomes.

		SW480 Cells	SW620 Cells	SW480 Exo	SW620 Exo
Sum Comp	(+) Mass	Molecular Lipid	Molecular Lipid	Molecular Lipid	Molecular Lipid
	m/z				
TG(44:0)	768.7075	12:0_14:0_18:0	12:0_14:0_18:0	12:0_16:0_16:0	12:0_14:0_18:0
		12:0_16:0_16:0	12:0_16:0_16:0	14:0_14:0_16:0	12:0_16:0_16:0
		14:0_14:0_16:0	14:0_14:0_16:0	15:0_15:0_14:0	14:0_14:0_16:0
		13:0_13:0_18:0	15:0_15:0_14:0		13:0_13:0_18:0
		13:0_15:0_16:0			13:0_15:0_18:0
		15:0_15:0_14:0			15:0_15:0_14:0
TG(O-44:0)	754.7283		O-44:0		
TG(44:1)	766.6919		12:0_14:0_18:1		12:0_14:0_18:1
			12:0_16:0_16:1		12:0_16:0_16:1
			14:0_14:0_16:1		14:0_14:0_16:1
			14:0_14:1_16:0		14:0_14:1_16:0
TG(O-44:1)	752.7126		O-44:1		
TG(44:4)	760.6449		44:4	44:4	
TG(45:0)	782.7232	12:0_16:0_17:0	13:0_16:0_16:0	13:0_16:0_16:0	13:0_16:0_16:0
		13:0_16:0_16:0	14:0_15:0_16:0	14:0_15:0_16:0	14:0_15:0_16:0
		14:0_15:0_16:0	14:0_14:0_17:0	14:0_14:0_17:0	14:0_14:0_17:0
		14:0_14:0_17:0			
TG(45:1)	780.7075		12:0_15:0_18:1	14:0_15:0_16:1	14:0_15:0_16:1
			12:0_16:0_17:1	14:0_15:1_16:1	14:1_15:0_16:0
			13:0_14:0_18:1	14:1_15:0_16:0	
			13:0_16:0_16:0		
			14:0_14:0_17:1		
			14:0_15:0_16:1		
			14:1_15:0_16:0		
TG(46:0)	796.7388	12:0_14:0_20:0	12:0_16:0_18:0	12:0_14:0_20:0	14:0_14:0_18:0
		12:0_16:0_18:0	14:0_14:0_18:0	12:0_16:0_18:0	14:0_16:0_16:0
		12:0_17:0_17:0	14:0_16:0_16:0	12:0_17:0_17:0	14:0_15:0_17:0
		14:0_14:0_18:0	15:0_15:0_16:0	14:0_14:0_18:0	15:0_15:0_16:0
		14:0_16:0_16:0		14:0_16:0_16:0	
		14:0_15:0_17:0		14:0_15:0_17:0	
		15:0_15:0_16:0		15:0_15:0_16:0	
TG(O-46:0)	782.7596	TG(O-46:0)	TG(O-46:0)		

Table C.13 (Cont'd)

	ı				
TG(46:1)	794.7232	14:0_14:0_18:1	12:0_16:0_18:1	12:0_16:0_18:1	14:0_14:0_18:1
		14:0_16:0_16:1	14:0_14:0_18:1	14:0_14:0_18:1	14:0_16:0_16:1
			14:0_16:0_16:1	14:0_16:0_16:1	
			14:1_16:0_16:0	14:1_16:0_16:0	
TG(O-46:1)	780.7439		TG(O-46:1)		
TG(46:2)	792.7075		14:0_14:0_18:2		14:0_14:1_18:1
			14:0_14:1_18:1		14:0_16:1_16:1
			14:0_16:1_16:1		14:1_16:0_16:1
			14:1_16:0_16:1		
TG(47:0)	810.7545	13:0_16:0_18:0	13:0_16:0_18:0	14:0_15:0_18:0	14:0_15:0_18:0
		14:0_15:0_18:0	14:0_15:0_18:0	14:0_16:0_17:0	14:0_16:0_17:0
		14:0_16:0_17:0	14:0_16:0_17:0	15:0_16:0_16:0	15:0_16:0_16:0
		15:0_16:0_16:0	15:0_16:0_16:0		
TG(O-47:0)	796.7752		TG(O-47:0)		
TG(47:1)	808.7388	13:0_16:0_18:1	13:0_16:0_18:1	13:0_16:0_18:1	13:0_16:0_18:1
		14:0_15:0_18:1	14:0_15:0_18:1	14:0_15:0_18:1	14:0_15:0_18:1
		15:0_16:0_16:1	14:0_16:0_17:1	14:0_16:1_17:0	14:0_16:0_17:1
			14:0_16:1_17:0	15:0_16:0_16:1	14:0_16:1_17:0
			15:0_16:0_16:1		15:0_16:0_16:1
			15:1_16:0_16:0		15:1_16:0_16:0
TG(47:2)	806.7232		13:0_16:1_18:1		13:0_16:1_18:1
			13:1_16:0_18:1		14:0_15:1_18:1
			14:0_15:1_18:1		14:0_16:1_17:1
			14:0_16:1_17:1		14:1_15:0_18:1
			14:1_15:0_18:1		14:1_16:0_17:1
			14:1_16:0_17:1		15:0_16:1_16:1
			15:0_16:1_16:1		15:1_16:0_16:1
			15:1_16:0_16:1		
TG(48:0)	824.7701	16:0_16:0_16:0	16:0_16:0_16:0	16:0_16:0_16:0	16:0_16:0_16:0
		14:0_16:0_18:0	14:0_16:0_18:0	14:0_16:0_18:0	14:0_16:0_18:0
		15:0_16:0_17:0	15:0_16:0_17:0	15:0_16:0_17:0	15:0_16:0_17:0
TG(O-48:0)	810.7909	TG(O-48:0)	TG(O-48:0)		
TG(P-48:0)	966.6981		TG(P-48:0)		

Table C.13 (Cont'd)

14:0_16:0_18:1 12:0_18:0_18:1 14:0_16:1_18:0 14:0_16:1_18:0 14:0_16:0_18:1 14:0_16:0_18:1 14:0_16:0_18:1 14:0_16:0_18:1 15:0_15:0_18:1 15:0_15:0_18:1 15:0_15:0_18:1 15:0_15:0_18:1 15:0_15:0_18:1 15:0_15:0_18:1 15:0_15:0_18:1 15:0_15:0_18:1 15:0_15:0_18:1 15:0_15:0_18:1 15:0_15:0_16:1 15:0_17:0_16:1 15:0_17:0_16:1 15:0_17:0_16:1 15:0_17:0_16:1 15:0_17:0_16:1 16:0_16:0_16:1 16:0_16:0_16:1 16:0_16:0_16:1 16:0_16:0_16:1 16:0_16:0_16:1 16:0_16:0_16:1 16:0_16:0_16:1 16:0_16:0_16:1 16:0_16:0_16:1 16:0_16:0_18:2 14:0_16:0_18:2 14:0_16:0_18:2 14:0_16:0_18:2 14:0_16:1_18:1 14:0_16:1_18:1 14:0_16:1_18:1 14:0_16:1_18:1 14:0_16:1_18:1 14:0_16:1_18:1 14:0_16:1_18:1 14:0_16:1_18:1 14:0_16:1_18:1 14:0_16:1_16:1 16:0_16:0_16:0_16:0_16:0 16:0_16:0_16:0_16:0_16:0_16:0_16:0_16:0_	TC(40.4)	000 7545	12.0 10.0 10.1	12:0 16:0 20:1	12:0 10:0 10:1	10.0 10.0 10.1
14:0_16:1_18:0	TG(48:1)	822.7545	12:0_18:0_18:1	12:0_16:0_20:1	12:0_18:0_18:1	12:0_18:0_18:1
15:0_15:0_18:1			 			
16:0_16:0_16:1						
15:0_15:0_18:1 16:0_16:0_16:1 16:0_16:0_16:1 TG(0-48:1) 808.7752 TG(0-48:1) TG(0-48:1) TG(0-48:1) TG(48:2) 820.7388 14:0_16:0_18:2 12:0_18:1_18:1 12:0_18:1_18:1 12:0_18:1_18:1 14:0_16:1_18:1 14:0_16:0_18:2 14:0_16:0_18:2 14:0_16:0_18:2 14:0_16:0_18:2 14:1_16:0_18:1 14:0_16:1_18:1 14:0_16:1_18:1 14:0_16:1_18:1 14:0_16:1_18:1 16:0_16:1_16:1 14:1_16:0_18:1 14:1_16:0_18:1 14:1_16:0_18:1 TG(0-48:2) 806.7596 TG(0-48:2) TG(48:3) 818.7232 14:0_16:1_18:2 14:1_16:1_18:1 14:0_16:1_18:1 14:0_16:2_18:1 16:1_16:1 14:1_16:1_18:1 14:0_16:1_18:1 14:1_16:0_18:2 14:1_16:1_16:1 14:1_16:1_18:1 TG(49:0) 838.7858 14:0_16:0_19:0 14:0_16:0_19:0 15:0_16:0_18:0 16:0_16:0_17:0 TG(0-49:0) 824.8065 TG(0-49:0) TG(0-49:0) TG(49:1) 836.7701 13:0_18:0_18:1 13:0_18:0_18:1 15:0_16:0_18:1 15:0_16:0_18:1 TG(0-49:0) 824.8065 TG(0-49:0) TG(0-49:0) TG(0-49:0) TG(49:1) 836.7701 13:0_18:0_18:1 13:0_18:0_18:1 15:0_16:0_18:1 15:0_16:0_18:1 15:0_16:0_17:0 TG(0-49:0) TG(0-49:0) TG(0-49:0) TG(0-49:0) TG(0-49:0) 15:0_16:0_18:1 14:0_17:0_18:1 15:0_16:0_18:1 15:0_16:0_17:0 TG(0-49:0) 13:0_18:0_18:1 13:0_18:0_18:1 15:0_16:0_18:1 15:0_16:0_17:0 TG(0-49:0) 13:0_18:0_18:1 13:0_18:0_18:1 15:0_16:0_18:1 15:0_16:0_18:1 TG(0-16:0_17:1 15:0_16:0_18:1 15:0_16:0_18:1 15:0_16:0_17:0 TG(0-16:0_17:1 15:0_16:0_18:1 15:0_16:0_18:1 15:0_16:0_18:1 TG(0-16:0_17:1						
TG(0-48:1) 808.7752 TG(0-48:1) TG(0-48:1) TG(0-48:1) TG(48:2) 820.7388 14:0_16:0_18:2 12:0_18:1_18:1 12:0_18:1_18:1 12:0_18:1_18:1 TG(48:2) 820.7388 14:0_16:0_18:2 12:0_18:1_18:1 14:0_16:0_18:2 14:0_16:0_18:2 14:0_16:0_18:2 14:1_16:0_18:1 14:0_16:1_18:1 14:0_16:1_18:1 14:0_16:1_18:1 14:0_16:1_18:1 14:0_16:1_18:1 16:0_16:1_16:1 16:0_16:1_16:1 16:0_16:1_16:1 16:0_16:1_16:1 16:0_16:1_16:1 16:0_16:1_16:1 TG(0-48:2) TG(0-48:2) TG(0-48:2) TG(0-48:2) TG(0-48:2) TG(0-48:2) TG(0-48:2) TG(0-16:1_16:1 14:0_16:1_18:1 <th></th> <th></th> <th>16:0_16:0_16:1</th> <th>14:1_16:0_18:0</th> <th>15:0_17:0_16:1</th> <th>15:0_17:0_16:1</th>			16:0_16:0_16:1	14:1_16:0_18:0	15:0_17:0_16:1	15:0_17:0_16:1
TG(O-48:1) TG(O-48:1) TG(O-48:1) TG(O-48:1) TG(48:2) 820.7388 14:0_16:0_18:2 12:0_18:1_18:1 12:0_18:1_18:1 12:0_18:1_18:1 TG(48:2) 820.7388 14:0_16:0_18:2 12:0_18:1_18:1 12:0_16:0_18:2 14:0_16:0_18:2 14:0_16:0_18:2 14:0_16:0_18:1 14:0_16:0_18:1 14:0_16:1_18:1 14:0_16:1_18:1 14:0_16:1_18:1 14:0_16:1_18:1 14:0_16:1_18:1 14:0_16:0_18:1 14:1_16:0_18:1 14:1_16:0_18:1 14:1_16:0_18:1 16:0_16:1_16:1 16:0_16:0_16:0 16:0_16:0_16:0 16:0_16:0_16:0 16:0_16:0_16:0 16:0_16:0_16:0 16:0_16:0_16:0 16:0_16:0_16:0 16:0_16:0_16:0 16:0_16:0_16:0 16:0_16:0_16:0 16:0_16:0_17:0 16:0_16:0_17:0 16:0_16:0				15:0_15:0_18:1	16:0_16:0_16:1	16:0_16:0_16:1
TG(48:2) 820.7388 14:0_16:0_18:2 12:0_18:1_18:1 12:0_18:1_18:1 12:0_18:1_18:1 12:0_18:1_18:1 12:0_18:1_18:1 12:0_18:1_18:1 12:0_18:1_18:1 12:0_18:1_18:1 14:0_16:0_18:2 14:0_16:0_18:2 14:0_16:0_18:2 14:0_16:0_18:2 14:0_16:0_18:2 14:0_16:1_18:1 14:0_16:1_18:1 14:0_16:1_18:1 14:0_16:1_18:1 14:0_16:1_18:1 14:0_16:1_18:1 14:1_16:0_18:1 14:1_16:0_18:1 14:1_16:0_18:1 14:1_16:0_18:1 14:1_16:0_18:1 14:1_16:0_18:1 14:1_16:0_18:1 14:1_16:1_18:1 14:0_16:1_18:1 14:0_16:1_18:1 14:0_16:1_18:1 14:0_16:1_18:1 14:0_16:1_18:1 14:0_16:1_18:1 14:1_16:1_18:1				16:0_16:0_16:1		
14:0_16:1_18:1	TG(O-48:1)	808.7752	TG(O-48:1)	TG(O-48:1)		
14:1_16:0_18:1	TG(48:2)	820.7388	14:0_16:0_18:2	12:0_18:1_18:1	12:0_18:1_18:1	12:0_18:1_18:1
16:0_16:1_16:1			14:0_16:1_18:1	14:0_16:0_18:2	14:0_16:0_18:2	14:0_16:0_18:2
TG(O-48:2) 806.7596 TG(O-48:2) 16:0_16:1_16:1 16:0_16:1_16:1 16:0_16:1_16:1 16:0_16:1_16:1 16:0_16:1_16:1 16:0_16:1_16:1 14:0_16:1_18:2 14:1_16:1_18:1 14:0_16:1_18:1 14:0_16:1_18:1 14:1_16:1_16:1 14:1_16:1_18:1 16:1_16:1_16:1 16:1_16:1_16:1 16:1_16:1_16:1 16:1_16:1_16:1 16:0_16:1_16:2 16:0_16:1_16:2 16:0_16:1_16:2 16:0_16:1_16:1 16:0_16:0_17:0 15:0_16:0_18:0 14:0_17:0_18:0 14:0_17:0_18:0 15:0_16:0_18:0 14:0_17:0_18:0 16:0_16:0_17:0 15:0_16:0_18:0 16:0_16:0_17:1 16:0_16:0_17:1 16:0_16:0_17:1 16:0_16:0_17:1			14:1_16:0_18:1	14:0_16:1_18:1	14:0_16:1_18:1	14:0_16:1_18:1
TG(O-48:2) B06.7596 TG(O-48:2) 14:0_16:1_18:2 14:1_16:1_18:1 14:0_16:1_18:2 14:0_16:2_18:1 16:1_16:1_16:1 14:1_16:1_18:1 14:1_16:0_18:2 16:1_16:1_16:1 14:1_16:1_18:1 16:0_16:1_16:2 16:0_16:1_16:2 16:1_16:1_16:1 TG(49:0) 838.7858 14:0_16:0_19:0 15:0_16:0_18:0 14:0_17:0_18:0 15:0_16:0_18:0 14:0_17:0_18:0 16:0_16:0_17:0 15:0_16:0_18:0 16:0_16:0_17:0 TG(O-49:0) 824.8065 TG(O-49:0) TG(O-49:0) TG(O-49:0) 15:0_16:0_18:1 15:0_16:0_18:1 15:0_16:0_18:1 15:0_16:0_18:1 16:0_16:0_17:0 16:0_16:0_17:1 <td< th=""><th></th><th></th><th>16:0_16:1_16:1</th><th>14:1_16:0_18:1</th><th>14:1_16:0_18:1</th><th>14:1_16:0_18:1</th></td<>			16:0_16:1_16:1	14:1_16:0_18:1	14:1_16:0_18:1	14:1_16:0_18:1
TG(48:3) 818.7232 14:0_16:1_18:2 14:1_16:1_18:1 14:0_16:1_18:1 14:0_16:1_18:1 14:0_16:1_18:1 14:0_16:1_18:1 14:1_16:1_18:1 16:1_16:1_16:1 16:1_16:1_16:1 TG(49:0) 838.7858 14:0_16:0_19:0 14:0_16:0_19:0 15:0_16:0_18:0 14:0_17:0_18:0 16:0_16:0_17:0 15:0_16:0_18:0 16:0_16:0_17:0 15:0_16:0_18:0 16:0_16:0_17:1 16:0_16:0_17:1 16:0_16:0_17:1 16:0_16:0_17:1 16:0_16:0_17:1 16:0_16:0_17:1 16:0_16:0_17:1				16:0_16:1_16:1	16:0_16:1_16:1	16:0_16:1_16:1
14:0_16:2_18:1 16:1_16:1_16:1 14:1_16:1_18:1 14:1_16:0_18:2 16:1_16:1_16:1 14:1_16:1_18:1 16:0_16:1_16:2 16:0_16:1_16:2 16:1_16:1_16:1 TG(49:0) 838.7858 14:0_16:0_19:0 14:0_16:0_19:0 15:0_16:0_18:0 14:0_17:0_18:0 14:0_17:0_18:0 14:0_17:0_18:0 16:0_16:0_17:0 15:0_16:0_18:0 16:0_16:0_17:0 TG(0-49:0) 16:0_16:0_17:0 16:0_16:0_17:0 16:0_16:0_18:1 15:0_16:0_18:1 TG(49:1) 836.7701 13:0_18:0_18:1 13:0_18:0_18:1 15:0_16:0_18:1 15:0_16:0_18:1 14:0_17:0_18:1 14:0_17:0_18:1 16:0_16:1_17:0 16:0_16:1_17:0 16:0_16:1_17:0 15:0_16:0_18:1 14:0_17:1_18:0 16:0_16:1_17:0 16:0_16:1_17:0 15:0_16:0_18:1 15:0_16:0_18:1 16:0_16:1_17:0	TG(O-48:2)	806.7596		TG(O-48:2)		
14:1_16:0_18:2	TG(48:3)	818.7232		14:0_16:1_18:2	14:1_16:1_18:1	14:0_16:1_18:2
14:1_16:1_18:1				14:0_16:2_18:1	16:1_16:1_16:1	14:1_16:1_18:1
TG(49:0) 838.7858 14:0_16:0_19:0 14:0_16:0_19:0 15:0_16:0_18:0 14:0_17:0_18:0 14:0_17:0_18:0 14:0_17:0_18:0 16:0_16:0_17:0 15:0_16:0_18:0 15:0_16:0_18:0 15:0_16:0_18:0 15:0_16:0_18:0 16:0_16:0_17:0 16:0_16:0_17:0 TG(0-49:0) 824.8065 TG(0-49:0) TG(0-49:0) TG(0-49:0) TG(49:1) 836.7701 13:0_18:0_18:1 13:0_18:0_18:1 15:0_16:0_18:1 15:0_16:0_18:1 14:0_17:0_18:1 14:0_17:0_18:1 14:0_17:0_18:1 16:0_16:1_17:0 16:0_16:1_17:0 15:0_16:0_18:1 14:0_17:1_18:0 14:0_17:1_18:0 16:0_16:1_17:0 15:0_16:0_18:1 14:0_17:1_18:0 15:0_16:0_18:1 15:0_16:0_17:1 15:0_16:0_18:1 15:0_16:0_18:1 16:0_16:0_17:1 15:0_16:0_17:1 16:0_16:0_17:1 16:0_16:1_17:0 16:0_16:0_17:1 16:0_16:0_17:1				14:1_16:0_18:2		16:1_16:1_16:1
TG(49:0) 838.7858 14:0_16:0_19:0 14:0_16:0_19:0 15:0_16:0_18:0 14:0_17:0_18:0 14:0_17:0_18:0 14:0_17:0_18:0 14:0_17:0_18:0 16:0_16:0_17:0 15:0_16:0_18:0 15:0_16:0_18:0 15:0_16:0_18:0 16:0_16:0_17:0 16:0_16:0_17:0 TG(0-49:0) 824.8065 TG(0-49:0) TG(0-49:0) TG(0-49:0) TG(49:1) 836.7701 13:0_18:0_18:1 13:0_18:0_18:1 15:0_16:0_18:1 15:0_16:0_18:1 14:0_17:0_18:1 14:0_16:0_19:1 16:0_16:1_17:0 16:0_16:1_17:0 15:0_16:0_18:1 14:0_17:1_18:0 14:0_17:1_18:0 15:0_16:0_18:1 14:0_17:1_18:0 16:0_16:1_17:0 15:0_16:1_18:0 15:0_16:0_18:1 15:0_16:0_18:1 16:0_16:1_17:0 16:0_16:0_17:1 15:0_16:0_17:1 16:0_16:1_17:0 16:0_16:0_17:1 16:0_16:0_17:1				14:1_16:1_18:1		
TG(49:0) 838.7858 14:0_16:0_19:0 14:0_16:0_19:0 15:0_16:0_18:0 14:0_17:0_18:0 14:0_17:0_18:0 14:0_17:0_18:0 16:0_16:0_17:0 15:0_16:0_18:0 15:0_16:0_18:0 15:0_16:0_18:0 16:0_16:0_17:0 16:0_16:0_17:0 16:0_16:0_17:0 TG(0-49:0) TG(0-49:0) TG(0-49:0) TG(49:1) 836.7701 13:0_18:0_18:1 13:0_18:0_18:1 15:0_16:0_18:1 15:0_16:0_18:1 14:0_17:0_18:1 14:0_17:0_18:1 14:0_17:0_18:1 16:0_16:1_17:0 16:0_16:1_17:0 15:0_16:0_18:1 14:0_17:1_18:0 14:0_17:1_18:0 16:0_16:1_17:0 15:0_16:1_18:0 15:0_16:0_18:1 15:0_16:0_18:1 16:0_16:1_17:0 16:0_16:1_17:0 16:0_16:1_17:0				16:0_16:1_16:2		
14:0_17:0_18:0 14:0_17:0_18:0 16:0_16:0_17:0 15:0_16:0_18:0 15:0_16:0_18:0 15:0_16:0_18:0 16:0_16:0_17:0 16:0_16:0_17:0 16:0_16:0_17:0 16:0_16:0_17:0 TG(0-49:0) TG(0-49:0) TG(0-49:0) TG(49:1) 836.7701 13:0_18:0_18:1 13:0_18:0_18:1 15:0_16:0_18:1 15:0_16:0_18:1 14:0_17:0_18:1 14:0_16:0_19:1 16:0_16:1_17:0 16:0_16:0_17:1 14:0_17:1_18:0 14:0_17:0_18:1 16:0_16:1_17:0 15:0_16:0_18:1 14:0_17:1_18:0 15:0_16:0_18:1 15:0_16:1_18:0 15:0_16:0_18:1 15:0_16:0_18:1 16:0_16:0_17:1 15:0_16:0_17:1 15:0_16:0_17:1 16:0_16:1_17:0 16:0_16:0_17:1 16:0_16:0_17:1				16:1_16:1_16:1		
15:0_16:0_18:0 15:0_16:0_18:0 16:0_16:0_17:0 16:0_16:0_17:0 16:0_16:0_17:0 16:0_16:0_17:0 TG(0-49:0) TG(O-49:0) TG(O-49:0) TG(49:1) 836.7701 13:0_18:0_18:1 13:0_18:0_18:1 15:0_16:0_18:1 15:0_16:0_18:1 14:0_17:0_18:1 14:0_16:0_19:1 16:0_16:1_17:0 16:0_16:0_17:1 15:0_16:0_18:1 14:0_17:0_18:1 16:0_16:1_17:0 15:0_16:1_18:0 15:0_16:0_18:1 15:0_16:0_18:1 16:0_16:1_17:0 16:0_16:0_17:1 15:0_16:0_17:1 16:0_16:1_17:0 16:0_16:0_17:1 16:0_16:0_17:1	TG(49:0)	838.7858	14:0_16:0_19:0	14:0_16:0_19:0	15:0_16:0_18:0	14:0_17:0_18:0
TG(0-49:0) 824.8065 TG(O-49:0) TG(O-49:0) TG(49:1) 836.7701 13:0_18:0_18:1 13:0_18:0_18:1 15:0_16:0_18:1 15:0_16:0_18:1 14:0_17:0_18:1 14:0_16:0_19:1 16:0_16:1_17:0 16:0_16:0_17:1 14:0_17:1_18:0 14:0_17:0_18:1 16:0_16:1_17:0 15:0_16:0_18:1 14:0_17:1_18:0 15:0_16:0_18:1 15:0_16:1_18:0 15:0_16:0_18:1 15:0_16:0_18:1 16:0_16:0_17:1 15:0_16:1_18:0 16:0_16:0_17:1 16:0_16:1_17:0 16:0_16:0_17:1 16:0_16:0_17:1			14:0_17:0_18:0	14:0_17:0_18:0	16:0_16:0_17:0	15:0_16:0_18:0
TG(O-49:0) 824.8065 TG(O-49:0) TG(O-49:0) TG(O-49:0) TG(49:1) 836.7701 13:0_18:0_18:1 13:0_18:0_18:1 15:0_16:0_18:1 15:0_16:0_18:1 15:0_16:0_18:1 16:0_16:1_17:0 16:0_16:0_17:1 14:0_17:1_18:0 14:0_17:0_18:1 16:0_16:1_17:0 16:0_16:1_17:0 16:0_16:1_17:0 15:0_16:1_18:0 15:0_16:0_18:1 15:0_16:1_18:0 16:0_16:1_17:0 16:0_16:1_17:0 16:0_16:1_17:0 16:0_16:0_17:1 16:0_16:1_17:0 16:0_16:1_17:0 16:0_16:1_17:0			15:0_16:0_18:0	15:0_16:0_18:0		16:0_16:0_17:0
TG(49:1) 836.7701 13:0_18:0_18:1 13:0_18:0_18:1 15:0_16:0_18:1 15:0_16:0_18:1 14:0_17:0_18:1 14:0_16:0_19:1 16:0_16:1_17:0 16:0_16:0_17:1 14:0_17:1_18:0 14:0_17:0_18:1 16:0_16:1_17:0 15:0_16:0_18:1 14:0_17:1_18:0 15:0_16:0_18:1 15:0_16:1_18:0 15:0_16:0_18:1 15:0_16:0_18:1 16:0_16:0_17:1 15:0_16:1_18:0 16:0_16:1_17:0 16:0_16:1_17:0 16:0_16:0_17:1 16:0_16:1_17:0			16:0_16:0_17:0	16:0_16:0_17:0		
14:0_17:0_18:1 14:0_16:0_19:1 16:0_16:1_17:0 16:0_16:0_17:1 14:0_17:1_18:0 14:0_17:0_18:1 16:0_16:1_17:0 15:0_16:0_18:1 14:0_17:1_18:0 15:0_16:0_18:1 16:0_16:1_18:0 15:0_16:0_18:1 16:0_16:0_17:1 16:0_16:1_17:0 16:0_16:0_17:1 16:0_16:0_17:1 16:0_16:1_17:0 16:0_16:1_17:0	TG(O-49:0)	824.8065	TG(O-49:0)	TG(O-49:0)		
14:0_17:1_18:0 14:0_17:0_18:1 16:0_16:1_17:0 15:0_16:0_18:1 14:0_17:1_18:0 15:0_16:0_18:1 15:0_16:1_18:0 15:0_16:0_18:1 15:0_16:1_18:0 16:0_16:0_17:1 15:0_16:1_18:0 16:0_16:1_17:0 16:0_16:1_17:0 16:0_16:1_17:0 16:0_16:1_17:0	TG(49:1)	836.7701	13:0_18:0_18:1	13:0_18:0_18:1	15:0_16:0_18:1	15:0_16:0_18:1
15:0_16:0_18:1			14:0_17:0_18:1	14:0_16:0_19:1	16:0_16:1_17:0	16:0_16:0_17:1
15:0_16:1_18:0			14:0_17:1_18:0	14:0_17:0_18:1		16:0_16:1_17:0
16:0_16:0_17:1			15:0_16:0_18:1	14:0_17:1_18:0		
16:0_16:1_17:0			15:0_16:1_18:0	15:0_16:0_18:1		
16:0_16:1_17:0			16:0_16:0_17:1	15:0_16:1_18:0		
			16:0_16:1_17:0	16:0_16:0_17:1		
TC(0.40.4) 922.7000 TC(0.40.4) TC(0.40.4)				16:0_16:1_17:0		
16(0-49:1) 822.7909 16(0-49:1) 16(0-49:1)	TG(O-49:1)	822.7909	TG(O-49:1)	TG(O-49:1)		

Table C.13 (Cont'd)

	004		100 101 101	100 151 151	100 15 : :5 :
TG(49:2)	834.7545		13:0_18:1_18:1	13:0_18:1_18:1	13:0_18:1_18:1
			14:0_17:1_18:1	15:0_16:0_18:2	15:0_16:0_18:2
			15:0_16:0_18:2	15:0_16:1_18:1	15:0_16:1_18:1
			15:0_16:1_18:1	16:0_16:1_17:1	15:1_16:0_18:1
			15:1_16:0_18:1		16:0_16:1_17:1
			16:0_16:1_17:1		
TG(50:0)	852.8014	14:0_16:0_20:0	14:0_16:0_20:0	14:0_18:0_18:0	14:0_18:0_18:0
		14:0_18:0_18:0	14:0_18:0_18:0	16:0_16:0_18:0	16:0_16:0_18:0
		16:0_16:0_18:0	16:0_16:0_18:0	17:0_17:0_16:0	15:0_17:0_18:0
		15:0_17:0_18:0	17:0_17:0_16:0		17:0_17:0_16:0
		17:0_17:0_16:0			
TG(O-50:0)	838.8222	TG(O-50:0)	TG(O-50:0)		
TG(P-50:0)	994.7294		TG(P-50:0)		
TG(50:1)	850.7858	14:0_16:0_20:1	14:0_16:0_20:1	14:0_18:0_18:1	14:0_18:0_18:1
		14:0_18:0_18:1	14:0_18:0_18:1	16:0_16:0_18:1	16:0_16:0_18:1
		16:0_16:0_18:1	16:0_16:0_18:1	16:0_16:1_18:0	16:0_16:1_18:0
		16:0_16:1_18:0	16:0_16:1_18:0		17:0_17:0_16:1
		15:0_17:0_18:1	17:0_17:0_16:1		
		15:0_17:1_18:0			
		17:0_17:0_16:1			
		17:0_17:1_16:0			
TG(O-50:1)	836.8065	TG(O-50:1)	TG(O-50:1)		
TG(P-50:1)	992.7137		TG(P-50:1)		
TG(50:2)	848.7701	14:0_18:0_18:2	14:0_16:0_20:2	14:0_18:0_18:2	14:0_18:0_18:2
		14:0_18:1_18:1	14:0_16:1_20:1	14:0_18:1_18:1	14:0_18:1_18:1
		16:0_16:0_18:2	14:0_18:0_18:2	16:0_16:0_18:2	16:0_16:0_18:2
		16:0_16:1_18:1	14:0_18:1_18:1	16:0_16:1_18:1	16:0_16:1_18:1
		16:1_16:1_18:0	14:1_16:0_20:1	16:1_16:1_18:0	16:1_16:1_18:0
		16:0_17:1_17:1	14:1_18:0_18:1		
			16:0_16:0_18:2		
	1		16:0_16:1_18:1		
			10.0_10.1_10.1		
			16:0_16:2_18:0		
			<u> </u>		
			16:0_16:2_18:0		

Table C.13 (Cont'd)

TG(50:3)	846.7545	16:0_16:0_18:3	14:0_16:0_20:3	14:0_18:1_18:2	14:0_18:1_18:2
,		16:0_16:1_18:2	14:0_18:1_18:2	14:1_18:1_18:1	14:1_18:1_18:1
		16:0_16:2_18:1	14:1_18:1_18:1	16:0_16:1_18:2	16:0_16:0_18:3
		16:1_16:1_18:1	16:0_16:0_18:3	16:0_16:2_18:1	16:0_16:1_18:2
			16:0_16:1_18:2	16:1_16:1_18:1	16:0_16:2_18:1
			16:0_16:2_18:1		16:1_16:1_18:1
			16:1_16:1_18:1		
TG(O-50:3)	832.7752		TG(O-50:3)		
TG(51:0)	866.8171	14:0_16:0_21:0	14:0_16:0_21:0		14:0_18:0_19:0
		14:0_17:0_20:0	14:0_17:0_20:0		15:0_18:0_18:0
		14:0_18:0_19:0	14:0_18:0_19:0		16:0_16:0_19:0
		15:0_16:0_20:0	15:0_16:0_20:0		16:0:17:0_18:0
		15:0_18:0_18:0	15:0_18:0_18:0		10.0.17.0_10.0
		16:0_16:0_19:0	16:0_16:0_19:0		
		16:0_17:0_18:0	16:0_17:0_18:0		
TG(O-51:0)	852.8378	TG(O-51:0)	TG(O-51:0)		
TG(51:1)	864.8014	14:0_17:0_20:1	14:0_17:0_20:1	16:0_17:0_18:1	15:0_18:0_18:1
10(31.1)	004.0014	14:0_17:0_20:1	14:0_17:0_20:1	10.0_17.0_10.1	16:0_17:0_18:1
					10.0_17.0_18.1
		14:0_18:1_19:0	14:0_18:1_19:0		
		15:0_16:0_20:1	15:0_16:0_20:1		
		15:0_18:0_18:1	15:0_18:0_18:1		
		16:0_16:0_19:1	16:0_16:0_19:1		
		16:0_16:1_19:0	16:0_16:1_19:0		
		16:0_17:0_18:1	16:0_17:0_18:1		
		16:0_17:1_18:0	16:0_17:1_18:0		
		16:1_17:0_18:0	16:1_17:0_18:0		
TG(O-51:1)	850.8222	TG(O-51:1)	TG(O-51:1)		
TG(P-51:1)	1006.7294		TG(P-51:1)		
TG(51:2)	862.7858		15:0_16:1_20:1		
		15:0_18:0_18:2	15:0_18:1_18:1	16:0_17:1_18:1	16:0_17:0_18:2
		16:0_17:0_18:2	15:0_18:0_18:2	16:1_17:0_18:1	16:0_17:1_18:1
		16:0_17:1_18:1	15:1_16:0_20:1		16:1_17:0_18:1
		16:0_16:0_19:2	15:1_18:0_18:1		
		16:0_16:1_19:1	16:0_17:0_18:2		
		16:1_17:0_18:1	16:0_17:1_18:1		
		16:1_17:1_18:0	16:0_16:0_19:2		
			16:0_16:1_19:1		
			16:1_17:0_18:1		
			16:1_17:1_18:0		

Table C.13 (Cont'd)

TG(O-51:2)	848.8065		TG(O-51:2)		
TG(P-51:2)	1004.7137		TG(P-51:2)		
TG(51:3)	860.7701		15:0_18:1_18:2		15:0_18:1_18:2
			16:0_17:1_18:2		16:0_17:1_18:2
			16:0_17:2_18:1		16:0_17:2_18:1
			16:1_17:1_18:1		16:1_17:0_18:2
					16:1_17:1_18:1
TG(52:0)	880.8327	15:0_15:0_22:0	16:0_16:0_20:0	16:0_16:0_20:0	14:0_18:0_20:0
		15:0_17:0_20:0	16:0_18:0_18:0	16:0_18:0_18:0	16:0_16:0_20:0
		16:0_16:0_20:0			16:0_18:0_18:0
		16:0_17:0_19:0			17:0_17:0_18:0
		16:0_18:0_18:0			
		17:0_17:0_18:0			
TG(O-52:0)	866.8535	TG(O-52:0)	TG(O-52:0)		
TG(52:1)	878.8171	14:0_18:0_20:1	14:0_16:0_22:1	16:0_16:0_20:1	16:0_16:0_20:1
		14:0_18:1_20:0	14:0_18:0_20:1	16:0_18:0_18:1	16:0_18:0_18:1
		16:0_16:0_20:1	14:0_18:1_20:0	16:1_18:0_18:0	16:1_18:0_18:0
		16:0_16:1_20:0	16:0_16:0_20:1		
		16:0_18:0_18:1	16:0_16:1_20:0		
		16:1_18:0_18:0	16:0_18:0_18:1		
		17:0_17:0_18:1	16:1_18:0_18:0		
		17:0_16:0_19:1	17:0_17:0_18:1		
TG(O-52:1)	864.8378	TG(O-52:1)	TG(O-52:1)		
TG(P-52:1)	1020.7450		TG(P-52:1)		
TG(52:2)	876.8014	14:0_18:1_20:1	14:0_18:1_20:1	16:0_16:1_20:1	16:0_16:1_20:1
		14:0_18:2_20:0	14:0_18:2_20:0	16:1_18:0_18:1	16:1_18:0_18:1
		16:0_16:1_20:1	16:0_16:1_20:1	16:0_18:1_18:1	16:0_18:1_18:1
		16:1_16:1_20:0	16:1_16:1_20:0	16:0_18:0_18:2	16:0_18:0_18:2
		16:1_18:0_18:1	16:1_18:0_18:1		
		16:0_18:1_18:1	16:0_18:1_18:1		
		16:0_18:0_18:2	16:0_18:0_18:2		
TG(O-52:2)	862.8222	TG(O-52:2)	TG(O-52:2)		

Table C.13 (Cont'd)

TG(52:3)	874.7858	16:0_16:0_20:3	14:0_18:0_20:3	16:0_18:1_18:2	16:0_18:1_18:2
		16:0_16:1_20:2	16:0_16:0_20:3	16:0_18:0_18:3	16:0_18:0_18:3
		16:0_18:1_18:2	16:0_16:1_20:2	16:1_18:1_18:1	16:1_18:1_18:1
		16:0_18:0_18:3	16:1_16:1_20:1	16:1_18:0_18:2	16:1_18:0_18:2
		16:1_18:1_18:1	16:0_16:2_20:1		
		16:1_18:0_18:2	16:0_18:1_18:2		
			16:0_18:0_18:3		
			16:1_18:1_18:1		
			16:1_18:0_18:2		
TG(O-52:3)	860.8065		TG(O-52:3)		
TG(52:4)	872.7701		14:0_16:0_22:4	16:0_18:1_18:3	16:0_18:1_18:3
			14:0_18:0_20:4	16:0_18:2_18:2	16:0_18:2_18:2
			14:0_18:1_20:3	16:1_18:1_18:2	16:1_18:1_18:2
			16:0_16:0_20:4	16:2_18:1_18:1	16:2_18:1_18:1
			16:0_16:1_20:3		
			16:0_18:1_18:3		
			16:0_18:2_18:2		
			16:1_18:0_18:3		
			16:1_18:1_18:2		
			16:2_18:0_18:2		
			16:2_18:1_18:1		
TG(O-52:4)	858.7909		TG(O-52:4)		
TG(52:5)	870.7545		14:0_16:0_22:5	16:0_16:0_20:5	16:0_16:0_20:5
			14:0_18:1_20:4	16:0_18:2_18:3	16:0_18:2_18:3
			16:0_16:0_20:5	16:1_18:1_18:3	16:1_18:1_18:3
			16:0_16:1_20:4	16:1_18:2_18:2	16:1_18:2_18:2
			16:0_18:2_18:3		
			16:1_18:1_18:3		
			16:1_18:2_18:2		
TG(O-52:5)	856.7752		TG(O-52:5)		
TG(53:0)	894.8484	14:0_18:0_21:0	14:0_18:0_21:0		16:0_18:0_19:0
		14:0_19:0_20:0	14:0_19:0_20:0		17:0_18:0_18:0
		15:0_18:0_20:0	16:0_17:0_20:0		
		16:0_17:0_20:0	16:0_18:0_19:0		
		16:0_18:0_19:0	17:0_18:0_18:0		
		17:0_18:0_18:0			

Table C.13 (Cont'd)

TG(53:1)	892.8327	15:0_18:0_20:1	14:0_18:0_21:1	16:0_18:1_19:0	16:0_18:1_19:0
		15:0_18:1_20:0	14:0_19:0_20:1	17:0_18:0_18:1	16:1_18:0_19:0
		16:0_16:0_21:1	14:0_19:1_20:0		17:0_18:0_18:1
		16:0_17:0_20:1	15:0_18:0_20:1		
		16:0_17:1_20:0	15:0_18:1_20:0		
		16:0_18:0_19:1	16:0_16:0_21:1		
		16:0_18:1_19:0	16:0_17:0_20:1		
		16:1_18:0_19:0	16:0_17:1_20:0		
		17:0_18:0_18:1	16:0_18:0_19:1		
		17:1_18:0_18:0	16:0_18:1_19:0		
			16:1_18:0_19:0		
			17:0_18:0_18:1		
			17:1_18:0_18:0		
TG(O-53:1)	878.8535		TG(O-53:1)		
TG(53:2)	890.8171	15:0_18:0_20:2	15:0_18:0_20:2	16:0_18:1_19:1	16:0_18:1_19:1
		15:0_18:1_20:1	15:0_18:1_20:1	16:1_18:0_19:1	16:1_18:0_19:1
		16:0_17:0_20:2	16:0_16:1_21:1	16:1_18:1_19:0	16:1_18:1_19:0
		16:0_17:1_20:1	16:0_17:0_20:2	17:0_18:1_18:1	17:0_18:1_18:1
		16:0_18:0_19:2	16:0_17:1_20:1	17:1_18:0_18:1	17:1_18:0_18:1
		16:0_18:1_19:1	16:0_18:0_19:2		
		16:0_18:2_19:0	16:0_18:1_19:1		
		16:1_18:0_19:1	16:0_18:2_19:0		
		16:1_18:1_19:0	16:1_18:0_19:1		
		17:0_18:0_18:2	16:1_18:1_19:0		
		17:0_18:1_18:1	17:0_18:0_18:2		
		17:1_18:0_18:1	17:0_18:1_18:1		
			17:1_18:0_18:1		
TG(53:3)	888.8014	16:0_18:1_19:2	16:0_17:2_20:1	17:0_18:1_18:2	16:1_18:1_19:1
		16:0_18:2_19:1	16:0_18:1_19:2	17:1_18:1_18:1	17:0_18:1_18:2
		16:1_18:1_19:1	16:0_18:2_19:1		17:1_18:1_18:1
		17:0_18:1_18:2	16:1_17:1_20:1		
		17:1_18:1_18:1	16:1_18:0_19:2		
			16:1_18:1_19:1		
			17:0_18:1_18:2		
			17:1_18:0_18:2		
			17:1_18:1_18:1		
			17:2_18:0_18:1		
TG(O-53:3)	874.8222		TG(O-53:3)		

Table C.13 (Cont'd)

TG(54:0)	908.8640	14:0_16:0_24:0	16:0_16:0_22:0		14:0_16:0_24:0
		14:0_18:0_22:0	16:0_18:0_20:0		18:0_18:0_18:0
		14:0_20:0_20:0	18:0_18:0_18:0		
		15:0_15:0_24:0			
		15:0_17:0_22:0			
		15:0_19:0_20:0			
		16:0_16:0_22:0			
		16:0_18:0_20:0			
		17:0_17:0_20:0			
		17:0_18:0_19:0			
		18:0_18:0_18:0			
TG(O-54:0)	894.8847	TG(O-54:0)	TG(O-54:0)		
TG(54:1)	906.8484	14:0_16:0_24:1	14:0_16:0_24:1	16:0_18:1_20:0	16:0_18:1_20:0
		14:0_18:0_22:1	14:0_18:0_22:1	18:0_18:0_18:1	18:0_18:0_18:1
		14:0_20:0_20:1	14:0_20:0_20:1		
		16:0_16:0_22:1	14:0_18:1_22:0		
		16:0_18:0_20:1	16:0_16:0_22:1		
		16:0_18:1_20:0	16:0_16:1_22:0		
		16:1_18:0_20:0	16:0_18:0_20:1		
		17:0_17:0_20:1	16:0_18:1_20:0		
		17:0_18:1_19:0	16:1_18:0_20:0		
		18:0_18:0_18:1	18:0_18:0_18:1		
TG(O-54:1)	892.8691	TG(O-54:1)	TG(O-54:1)		
TG(54:2)	904.8327	14:0_18:0_22:2	14:0_18:0_22:2	16:0_18:1_20:1	16:0_18:1_20:1
		14:0_18:1_22:1	14:0_18:1_22:1	16:0_18:2_20:0	16:0_18:2_20:0
		14:0_16:0_20:2	14:0_16:0_20:2	16:1_18:0_20:1	16:1_18:0_20:1
		14:0_16:1_20:1	14:0_16:1_20:1	16:1_18:1_20:0	16:1_18:1_20:0
		16:0_16:0_22:2	16:0_16:0_22:2	18:0_18:0_18:2	18:0_18:0_18:2
		16:0_16:1_22:1	16:0_16:1_22:1	18:0_18:1_18:1	18:0_18:1_18:1
		16:0_18:0_20:2	16:0_18:0_20:2		
		16:0_18:1_20:1	16:0_18:1_20:1		
		16:0_18:2_20:0	16:0_18:2_20:0		
		16:1_18:0_20:1	16:1_18:0_20:1		
		16:1_18:1_20:0	16:1_18:1_20:0		
		17:0_18:1_19:1	17:0_17:0_20:2		
		18:0_18:0_18:2	17:0_18:1_19:1		
		18:0_18:1_18:1	18:0_18:0_18:2		
			18:0_18:1_18:1		
TG(O-54:2)	890.8535	TG(O-54:2)	TG(O-54:2)		

Table C.13 (Cont'd)

TG(54:3)	902.8171	18:1_18:1_18:1	18:1_18:1_18:1	18:1_18:1_18:1	18:1_18:1_18:1
10(04.0)	002.0171	16:0_18:0_20:3	16:0_18:0_20:3	16:0_18:1_20:2	16:0_18:1_20:2
		16:0_18:1_20:2	16:0_18:1_20:2	16:0_18:2_20:1	16:0_18:2_20:1
		16:0_18:2_20:1	16:0_18:2_20:1	16:1_18:1_20:1	16:1_18:1_20:1
		16:1_18:1_20:1	16:1_18:1_20:1	16:1_18:0_20:2	16:1_18:0_20:2
		16:1_18:0_20:2	16:1_18:0_20:2	18:0_18:1_18:2	18:0_18:1_18:2
		18:0_18:1_18:2	18:0_18:1_18:2	10.0_10.1_10.2	10.0_10.1_10.2
TG(O-54:3)	888.8378	TG(O-54:3)	TG(O-54:3)		
TG(54:4)	900.8014	16:0_18:0_20:4	16:0_16:0_22:4	16:0_18:1_20:3	16:0_18:2_20:2
	000.0011	16:0_18:1_20:3	16:0_18:0_20:4	16:0_18:2_20:2	16:1_18:1_20:2
		16:1_18:0_20:3	16:0_18:1_20:3	16:1_18:0_20:3	18:0_18:1_18:3
		18:0_18:1_18:3	16:0_18:2_20:2	16:1_18:1_20:2	18:0_18:2_18:2
		18:0_18:2_18:2	16:0_18:3_20:1	18:0_18:1_18:3	18:1_18:1_18:2
		18:1_18:1_18:2	16:1_18:0_20:3	18:0_18:2_18:2	10.1_10.1_10.2
		10.1_10.1_10.2	16:1_18:1_20:2	18:1_18:1_18:2	
			16:1_18:2_20:1	10.1_10.1_10.2	
			18:0_18:1_18:3		
			18:0_18:2_18:2		
			18:1_18:1_18:2		
TG(P-54:4)	1042.7294		TG(P-54:4)		
TG(54:5)	898.7858	16:0_16:0_22:5	16:0_16:0_22:5	16:0_16:0_22:5	18:0_18:2_18:3
, ,		16:0_18:1_20:4	16:0_16:1_22:4	16:0_18:0_20:5	18:1_18:1_18:3
		18:1_18:1_18:3	16:0_18:0_20:5	18:0_18:2_18:3	18:1_18:2_18:2
		18:1_18:2_18:2	16:0_18:1_20:4	18:1_18:1_18:3	
			16:0_18:2_20:3	18:1_18:2_18:2	
			16:0_18:2_20:3 16:1_18:0_20:4	18:1_18:2_18:2	
				18:1_18:2_18:2	
			16:1_18:0_20:4	18:1_18:2_18:2	
			16:1_18:0_20:4 16:1_18:1_20:3	18:1_18:2_18:2	
			16:1_18:0_20:4 16:1_18:1_20:3 18:0_18:2_18:3	18:1_18:2_18:2	
TG(0-54:5)	884.8065	TG(O-54:5)	16:1_18:0_20:4 16:1_18:1_20:3 18:0_18:2_18:3 18:1_18:1_18:3	18:1_18:2_18:2	
TG(O-54:5) TG(54:6)	884.8065 896.7701	TG(O-54:5)	16:1_18:0_20:4 16:1_18:1_20:3 18:0_18:2_18:3 18:1_18:1_18:3 18:1_18:2_18:2	18:1_18:2_18:2	18:1_18:2_18:3
		TG(O-54:5)	16:1_18:0_20:4 16:1_18:1_20:3 18:0_18:2_18:3 18:1_18:1_18:3 18:1_18:2_18:2 TG(O-54:5)		18:1_18:2_18:3 18:2_18:2_18:2
		TG(O-54:5)	16:1_18:0_20:4 16:1_18:1_20:3 18:0_18:2_18:3 18:1_18:1_18:3 18:1_18:2_18:2 TG(O-54:5) 16:0_18:1_20:5	18:1_18:2_18:3	
		TG(O-54:5)	16:1_18:0_20:4 16:1_18:1_20:3 18:0_18:2_18:3 18:1_18:1_18:3 18:1_18:2_18:2 TG(O-54:5) 16:0_18:1_20:5 16:0_18:2_20:4	18:1_18:2_18:3	
		TG(O-54:5)	16:1_18:0_20:4 16:1_18:1_20:3 18:0_18:2_18:3 18:1_18:1_18:3 18:1_18:2_18:2 TG(O-54:5) 16:0_18:1_20:5 16:0_18:2_20:4 16:1_18:1_20:4	18:1_18:2_18:3	
-		TG(O-54:5)	16:1_18:0_20:4 16:1_18:1_20:3 18:0_18:2_18:3 18:1_18:1_18:3 18:1_18:2_18:2 TG(O-54:5) 16:0_18:1_20:5 16:0_18:2_20:4 16:1_18:1_20:4 18:1_18:2_18:3	18:1_18:2_18:3	

Table C.13 (Cont'd)

TG(55:1)	920.8640	14:0_17:0_24:1	14:0_17:0_24:1	
		14:0_19:0_22:1	14:0_19:0_22:1	
		14:0_20:0_21:1	14:0_19:1_22:0	
		14:0_20:1_21:0	14:0_20:1_21:0	
		15:0_16:0_24:1	15:0_16:0_24:1	
		15:0_18:0_22:1	15:0_18:0_22:1	
		15:0_20:0_20:1	15:0_18:1_22:0	
		16:0_17:0_22:1	15:0_20:0_20:1	
		16:0_18:0_19:1	16:0_17:0_22:1	
		16:0_18:1_19:0	16:0_17:1_22:0	
		17:0_18:0_20:1	16:0_18:0_19:1	
		17:0_18:1_20:0	16:0_18:1_19:0	
		17:1_18:0_20:0	17:0_18:0_20:1	
		18:0_18:0_19:1	17:0_18:1_20:0	
		18:0_18:1_19:0	17:1_18:0_20:0	
			18:0_18:0_19:1	
			18:0_18:1_19:0	
TG(O-55:1)	906.8847		TG(O-55:1)	
TG(55:2)	918.8484	16:0_17:1_22:1	16:0_17:1_22:1	
		16:0_18:0_21:2	16:0_18:1_21:1	
		16:0_18:1_21:1	16:0_19:1_20:1	
		16:0_19:0_20:2	16:1_17:0_22:1	
		16:0_19:1_20:1	16:1_18:0_21:1	
		16:1_17:0_22:1	16:1_19:0_20:1	
		16:1_18:0_21:1	17:0_18:1_20:1	
		16:1_19:0_20:1	17:1_18:0_20:1	
		17:0_18:0_20:2	17:1_18:1_20:0	
		17:0_18:1_20:1	18:0_18:1_19:1	
		17:1_18:0_20:1	18:1_18:1_19:0	
		17:1_18:1_20:0		
		18:0_18:1_19:1		
		18:1_18:1_19:0		
TG(O-55:2)	904.8691		TG(O-55:2)	

Table C.13 (Cont'd)

TG(55:3)	916.8327	16:0_18:1_21:2	16:0_18:1_21:2	18:1_18:1_19:1
		16:0_19:1_20:2	16:0_19:1_20:2	
		16:0_19:2_20:1	16:0_19:2_20:1	
		17:0_18:1_20:2	16:1_18:0_21:2	
		17:0_18:2_20:1	16:1_19:0_20:2	
		17:1_18:0_20:2	16:1_19:1_20:1	
		17:1_18:1_20:1	17:0_18:1_20:2	
		18:0_18:1_19:2	17:0_18:2_20:1	
		18:0_18:2_19:1	17:1_18:0_20:2	
		18:1_18:1_19:1	17:1_18:1_20:1	
		18:1_18:2_19:0	18:0_18:1_19:2	
			18:0_18:2_19:1	
			18:1_18:1_19:1	
			18:1_18:2_19:0	
TG(55:4)	914.8171		16:0_18:1_21:3	
			16:0_19:1_20:3	
			16:0_19:2_20:2	
			17:0_18:1_20:3	
			17:0_18:2_20:2	
			18:1_18:1_19:2	
			18:1_18:2_19:1	
TG(56:0)	936.8953	TG(56:0)	14:0_16:0_26:0	
			14:0_18:0_24:0	
			14:0_20:0_22:0	
			16:0_16:0_24:0	
			16:0_18:0_22:0	
			16:0_20:0_20:0	
			18:0_18:0_20:0	

Table C.13 (Cont'd)

TG(56:1)	934.8797	14:0_16:0_26:1	14:0_16:0_26:1	16:0_18:1_22:0	16:0_18:1_22:0
		14:0_18:0_24:1	14:0_18:0_24:1	18:0_18:1_20:0	18:0_18:1_20:0
	_	14:0_18:1_24:0	14:0_18:1_24:0		
		14:0_20:0_22:1	14:0_20:0_22:1		
		14:0_20:1_22:0	14:0_20:1_22:0		
		16:0_16:0_24:1	16:0_16:0_24:1		
		16:0_16:1_24:0	16:0_16:1_24:0		
		16:0_18:0_22:1	16:0_18:0_22:1		
		16:0_18:1_22:0	16:0_18:1_22:0		
		16:0_20:0_20:1	16:0_20:0_20:1		
		16:1_18:0_22:0	16:1_18:0_22:0		
		16:1_20:0_20:0	16:1_20:0_20:0		
		18:0_18:0_20:1	18:0_18:0_20:1		
		18:0_18:1_20:0	18:0_18:1_20:0		
TG(O-56:1)	920.9004		TG(O-56:1)		
TG(56:2)	932.8640	14:0_18:0_24:2	14:0_18:0_24:2	16:0_18:1_22:1	16:0_18:1_22:1
		14:0_18:1_24:1	14:0_18:1_24:1	16:0_18:2_22:0	16:0_18:2_22:0
		14:0_20:0_22:2	14:0_18:2_24:0	16:0_20:1_20:1	16:0_20:1_20:1
		14:0_20:1_22:1	14:0_20:0_22:2	16:1_18:0_22:1	16:1_18:0_22:1
		14:0_20:2_22:0	14:0_20:1_22:1	16:1_18:1_22:0	16:1_18:1_22:0
		16:0_16:0_24:2	14:0_20:2_22:0	16:1_20:0_20:1	16:1_20:0_20:1
		16:0_16:1_24:1	16:0_16:0_24:2	18:0_18:1_20:1	18:0_18:1_20:1
		16:0_18:0_22:2	16:0_16:1_24:1	18:0_18:2_20:0	18:0_18:2_20:0
		16:0_18:1_22:1	16:0_18:0_22:2	18:1_18:1_20:0	18:1_18:1_20:0
		16:0_18:2_22:0	16:0_18:1_22:1		
		16:0_20:0_20:2	16:0_18:2_22:0		
		16:0_20:1_20:1	16:0_20:0_20:2		
		16:1_18:0_22:1	16:0_20:1_20:1		
		16:1_18:1_22:0	16:1_16:1_24:0		
		16:1_20:0_20:1	16:1_18:0_22:1		
		18:0_18:0_20:2	16:1_18:1_22:0		
		18:0_18:1_20:1	16:1_20:0_20:1		
		18:0_18:2_20:0	18:0_18:0_20:2		
		18:1_18:1_20:0	18:0_18:1_20:1		
			18:0_18:2_20:0		
			18:1_18:1_20:0		
TG(O-56:2)	918.8847		TG(O-56:2)		

Table C.13 (Cont'd)

TG(56:3)	930.8484	16:0_18:0_22:3	16:0_18:0_22:3	16:0_20:1_20:2	16:1_20:1_20:1
, ,		16:0_18:1_22:2	16:0_18:1_22:2	16:1_20:0_20:2	18:1_18:1_20:1
		16:0_18:2_22:1	16:0_18:2_22:1	16:1_20:1_20:1	18:1_18:2_20:0
		16:0_20:0_20:3	16:0_20:0_20:3	18:1_18:1_20:1	
		16:0_20:1_20:2	16:0_20:1_20:2	18:1_18:2_20:0	
		16:1_18:0_22:2	16:1_18:0_22:2		
		16:1_18:1_22:1	16:1_18:1_22:1		
		16:1_20:0_20:2	16:1_20:0_20:2		
		16:1_20:1_20:1	16:1_20:1_20:1		
		18:0_18:0_20:3	18:0_18:0_20:3		
		18:0_18:1_20:2	18:0_18:1_20:2		
		18:0_18:2_20:1	18:0_18:2_20:1		
		18:1_18:1_20:1	18:1_18:1_20:1		
		18:1_18:2_20:0	18:1_18:2_20:0		
TG(O-56:3)	916.8691		TG(O-56:3)		
TG(56:4)	928.8327	16:0_20:1_20:3	16:0_18:0_22:4	18:1_18:1_20:2	18:1_18:1_20:2
		16:0_20:2_20:2	16:0_18:1_22:3	18:1_18:2_20:1	18:1_18:2_20:1
		18:0_18:1_20:3	16:0_18:2_22:2	18:2_18:2_20:0	18:2_18:2_20:0
		18:0_18:2_20:2	16:0_20:1_20:3		
		18:1_18:1_20:2	16:0_20:2_20:2		
		18:1_18:2_20:1	16:1_18:0_22:3		
			16:1_18:1_22:2		
			16:1_20:0_20:3		
			16:1_20:1_20:2		
			18:0_18:1_20:3		
			18:0_18:2_20:2		
			18:1_18:1_20:2		
			18:1_18:2_20:1		
			18:2_18:2_20:0		
TG(O-56:4)	914.8535		TG(O-56:4)		

Table C.13 (Cont'd)

		I		
TG(56:5)	926.8171	16:0_18:0_22:5	16:0_18:0_22:5	
		16:0_18:1_22:4	16:0_18:1_22:4	
		16:0_20:1_20:4	16:0_20:1_20:4	
		16:1_18:0_22:4	16:0_20:2_20:3	
		16:1_20:1_20:3	16:1_18:0_22:4	
		18:0_18:1_20:4	16:1_20:1_20:3	
		18:0_18:2_20:3	16:1_20:2_20:2	
		18:1_18:1_20:3	18:0_18:1_20:4	
		18:2_18:2_20:1	18:0_18:2_20:3	
			18:0_18:3_20:2	
			18:1_18:1_20:3	
			18:1_18:2_20:2	
			18:1_18:3_20:1	
			18:2_18:2_20:1	
TG(O-56:5)	912.8378	TG(O-56:5)	TG(O-56:5)	
TG(P-56:5)	1068.7450		TG(P-56:5)	
TG(56:6)	924.8014	16:0_18:0_22:6	16:0_18:0_22:6	
		16:0_18:1_22:5	16:0_18:1_22:5	
		16:1_18:0_22:5	16:1_18:0_22:5	
		18:0_18:1_20:5	18:0_18:1_20:5	
		18:1_18:1_20:4	18:1_18:1_20:4	
TG(O-56:6)	910.8222		TG(O-56:6)	
TG(P-56:6)	1066.7294		TG(P-56:6)	
TG(O-56:7)	908.8065	TG(O-56:7)	TG(O-56:7)	
TG(P-56:7)	1064.7137		TG(P-56:7)	

Table C.13 (Cont'd)

TG(57:1)	948.8953	16:0_16:0_25:1	16:0_16:0_25:1	
		16:0_17:0_24:1	16:0_16:1_25:0	
		16:0_18:0_23:1	16:0_17:0_24:1	
		16:0_18:1_23:0	16:0_17:1_24:0	
		16:0_19:0_22:1	16:0_18:0_23:1	
		16:0_19:1_22:0	16:0_18:1_23:0	
		16:0_20:0_21:1	16:1_17:0_24:0	
		16:0_20:1_21:0	16:1_18:0_23:0	
		16:1_17:0_24:0	16:1_19:0_22:0	
		16:1_18:0_23:0	16:1_20:0_21:0	
		16:1_19:0_22:0	17:0_18:1_22:0	
		16:1_20:0_21:0	17:1_18:0_22:0	
		17:0_18:0_22:1	17:1_20:0_20:0	
		17:0_18:1_22:0	18:1_19:0_20:0	
		17:0_20:0_20:1		
		18:0_19:0_20:1		
		18:0_19:1_20:0		
		18:1_19:0_20:0		
TG(O-57:1)	934.9160		TG(O-57:1)	
TG(57:2)	946.8797	16:0_17:1_24:1	16:0_16:1_25:1	
		16:0_18:1_23:1	16:0_17:1_24:1	
		16:0_19:1_22:1	16:0_18:1_23:1	
		16:0_20:1_21:1	16:0_19:1_22:1	
		16:1_17:0_24:1	16:0_20:1_21:1	
		16:1_18:0_23:1	16:1_17:0_24:1	
		16:1_19:0_22:1	16:1_18:0_23:1	
		16:0_20:0_21:1	16:1_19:0_22:1	
		16:0_20:1_21:0	16:0_20:0_21:1	
		17:0_18:1_22:1	16:0_20:1_21:0	
		17:0_20:1_20:1	17:0_18:1_22:1	
		17:1_18:0_22:1	17:0_20:1_20:1	
		17:1_20:0_20:1	17:1_18:0_22:1	
		18:0_18:1_21:1	17:1_20:0_20:1	
		18:0_19:1_20:1	18:0_18:1_21:1	
		18:1_18:1_21:0	18:0_19:1_20:1	
		18:1_19:0_20:1	18:1_18:1_21:0	
		18:1_19:1_20:0	18:1_19:0_20:1	
			18:1_19:1_20:0	

Table C.13 (Cont'd)

TG(57:3)	944.8640		16:1_19:1_22:1	
1.0(01.10)	011.0010		18:1_19:1_20:1	
TG(58:0)	964.9266	16:0_16:0_26:0	16:0_16:0_26:0	
10(38.0)	904.9200			
		16:0_18:0_24:0	16:0_18:0_24:0	
		16:0_20:0_22:0	18:0_18:0_22:0	
		18:0_18:0_22:0		
		18:0_20:0_20:0		
TG(O-58:0)	950.9473		TG(O-58:0)	
TG(58:1)	962.9110	14:0_18:0_26:1	14:0_18:0_26:1	16:0_18:1_24:0
		14:0_18:1_26:0	14:0_18:1_26:0	18:0_18:1_22:0
		14:0_20:0_24:1	14:0_20:0_24:1	
		14:0_20:1_24:0	14:0_20:1_24:0	
		14:0_22:0_22:1	14:0_22:0_22:1	
		16:0_16:0_26:1	16:0_16:0_26:1	
		16:0_16:1_26:0	16:0_16:1_26:0	
		16:0_18:0_24:1	16:0_18:0_24:1	
		16:0_18:1_24:0	16:0_18:1_24:0	
		16:0_20:0_22:1	16:0_20:0_22:1	
		16:0_20:1_22:0	16:0_20:1_22:0	
		16:1_18:0_24:0	16:1_18:0_24:0	
		16:1_20:0_22:0	16:1_20:0_22:0	
		18:0_18:0_22:1	18:0_18:0_22:1	
		18:0_18:1_22:0	18:0_18:1_22:0	
		18:0_20:0_20:1	18:0_20:0_20:1	
		18:1_20:0_20:0	18:1_20:0_20:0	
TG(O-58:1)	948.9317		TG(O-58:1)	

Table C.13 (Cont'd)

TG(58:2)	960.8953	14:0_18:0_26:2	14:0_18:0_26:2	18:1_18:1_22:0	16:0_18:1_24:1
		14:0_18:1_26:1	14:0_18:1_26:1		16:0_18:2_24:0
		14:0_20:0_24:2	14:0_20:0_24:2		16:1_18:0_24:1
		14:0_20:1_24:1	14:0_20:1_24:1		16:1_18:1_24:0
		14:0_20:2_24:2	14:0_22:0_22:2		18:0_18:2_22:0
		14:0_22:0_22:2	14:0_22:1_22:1		18:1_18:1_22:0
		14:0_22:1_22:1	16:0_16:0_26:2		
		16:0_16:0_26:2	16:0_16:1_26:1		
		16:0_16:1_26:1	16:0_18:0_24:2		
		16:0_18:0_24:2	16:0_18:1_24:1		
		16:0_18:1_24:1	16:0_18:2_24:0		
		16:0_18:2_24:0	16:0_20:0_22:2		
		16:0_20:0_22:2	16:0_20:1_22:1		
		16:0_20:1_22:1	16:1_18:0_24:1		
		16:0_20:2_22:0	16:1_18:1_24:0		
		16:1_18:0_24:1	16:1_20:0_22:1		
		16:1_18:1_24:0	18:0_18:0_22:2		
		16:1_20:0_22:1	18:0_18:1_22:1		
		18:0_18:0_22:2	18:0_18:2_22:0		
		18:0_18:1_22:1	18:0_20:1_20:1		
		18:0_18:2_22:0	18:1_18:1_22:0		
		18:0_20:0_20:2	18:1_20:0_20:1		
		18:0_20:1_20:1	18:2_20:0_20:0		
		18:1_18:1_22:0			
		18:1_20:0_20:1			
		18:2_20:0_20:0			
TG(O-58:2)	946.9160		TG(O-58:2)		

Table C.13 (Cont'd)

TG(58:3)	958.8797	16:0_18:1_24:2	16:0_16:1_26:2	18:1_18:1_22:1	18:1_18:1_22:1
		16:0_18:2_24:1	16:0_18:1_24:2	18:1_18:2_22:0	18:1_18:2_22:0
		16:0_20:1_22:2	16:0_18:2_24:1		
		16:0_20:2_22:1	16:0_20:1_22:2		
		16:1_18:0_24:2	16:0_20:2_22:1		
		16:1_18:1_24:1	16:1_18:0_24:2		
		16:1_20:0_22:2	16:1_18:1_24:1		
		16:1_20:1_22:1	16:1_20:0_22:2		
		16:1_20:2_22:0	16:1_20:1_22:1		
		18:0_18:1_22:2	16:1_20:2_22:0		
		18:0_18:2_22:1	18:0_18:1_22:2		
		18:0_20:1_20:2	18:0_18:2_22:1		
		18:1_18:1_22:1	18:0_20:1_20:2		
		18:1_18:2_22:0	18:1_18:1_22:1		
		18:1_20:0_20:2	18:1_18:2_22:0		
		18:1_20:1_20:1	18:1_20:0_20:2		
		18:2_20:0_20:1	18:1_20:1_20:1		
			18:2_20:0_20:1		
TG(O-58:3)	944.9004		TG(O-58:3)		
TG(58:4)	956.8640		16:0_18:1_24:3	18:2_18:2_22:0	18:2_18:2_22:0
			16:0_20:1_22:3		
			16:0_20:2_22:2		
			16:0_20:3_22:1		
			16:1_18:0_24:3		
			16:1_20:0_22:3		
			16:1_20:1_22:2		
			16:1_20:2_22:1		
			18:0_18:1_22:3		
			18:0_18:2_22:2		
			18:0_20:1_20:3		
			18:0_20:2_20:2		
			18:1_18:1_22:2		
			18:1_18:2_22:1		
			18:1_20:0_20:3		
			18:1_20:1_20:2		
			18:2_20:0_20:2		
			18:2_20:1_20:1		

Table C.13 (Cont'd)

TG(58:5)	954.8484	16:0_18:1_24:4
		16:0_20:1_22:4
		16:1_18:0_24:4
		16:1_20:1_22:3
		18:0_18:0_22:5
		18:0_18:1_22:4
		18:0_20:1_20:4
		18:1_18:1_22:3
		18:1_20:1_20:3
TG(O-58:5)	940.8691	TG(O-58:5)
TG(58:6)	952.8327	16:0_18:1_24:5
		16:0_20:1_22:5
		18:0_18:0_22:6
		18:0_18:1_22:5
		18:1_18:1_22:4
		18:1_20:1_20:4
TG(O-58:6)	938.8535	TG(O-58:6)
TG(O-58:7)	936.8378	TG(O-58:7)
TG(59:1)	976.9266	16:0_18:0_25:1
		16:0_18:1_25:0
		17:0_18:1_24:0
		18:0_18:1_23:0

Table C.13 (Cont'd)

TG(59:2)	974.9110	16:0_17:1_26:1	16:0_17:1_26:1	
,		16:0_18:1_25:1	16:0_18:1_25:1	
		16:0_19:1_24:1	16:0_19:1_24:1	
		16:0_20:1_23:1	16:0_20:1_23:1	
		16:1_17:0_26:1	16:1_17:0_26:1	
		16:1_18:0_25:1	16:1_18:0_25:1	
		16:1_19:0_24:1	16:1_18:1_25:0	
		16:1_19:1_24:0	16:1_19:0_24:1	
		16:1_20:1_23:0	16:1_19:1_24:0	
		17:0_18:1_24:1	16:1_20:1_23:0	
		17:0_20:1_22:1	17:0_18:1_24:1	
		17:1_18:0_24:1	17:1_18:0_24:1	
		17:1_18:1_24:0	17:1_18:1_24:0	
		17:1_20:1_22:0	18:0_18:1_23:1	
		18:0_18:1_23:1	18:1_18:1_23:0	
		18:0_19:1_22:1	19:0_20:1_20:1	
		18:1_18:1_23:0		
		18:1_19:0_22:1		
		18:1_19:1_22:0		
		19:0_20:1_20:1		
TG(59:3)	972.8953		16:0_18:2_25:1	
			17:1_18:1_24:1	
			17:1_20:1_22:1	
			18:1_18:1_23:1	
			18:1_19:1_22:1	
			19:1_20:1_20:1	
TG(O-60:0)	978.9786		TG(O-60:0)	
TG(60:1)	990.9423	TG(60:1)	TG(60:1)	
TG(O-60:1)	976.9630		TG(O-60:1)	

Table C.13 (Cont'd)

TG(60:2)	988.9266	TG(60:2)	16:0_18:0_26:2	
			16:0_18:1_26:1	
			16:0_18:2_26:0	
			16:0_20:1_24:1	
			16:0_22:1_22:1	
			16:1_18:0_26:1	
			16:1_18:1_26:0	
			16:1_20:0_24:1	
			16:1_20:1_24:0	
			16:1_22:0_22:1	
			18:0_18:1_24:1	
			18:0_18:2_24:0	
			18:0_20:1_22:1	
			18:1_18:1_24:0	
			18:1_20:0_22:1	
			18:1_20:1_22:0	
			18:2_20:0_22:0	
			20:0_20:1_20:1	
TG(O-60:2)	974.9473		TG(O-60:2)	
TG(60:3)	986.9110	16:0_18:1_26:2	16:0_18:1_26:2	18:1_18:1_24:1
		16:0_18:2_26:1	16:0_18:2_26:1	18:1_18:2_24:0
		16:0_20:1_24:2	16:0_20:1_24:2	
		16:0_20:2_24:1	16:0_20:2_24:1	
		16:0_22:1_22:2	16:0_22:1_22:2	
		16:1_18:0_26:2	16:1_18:0_26:2	
		16:1_18:1_26:1	16:1_18:1_26:1	
		16:1_20:1_24:1	16:1_20:1_24:1	
		16:1_20:2_24:0	16:1_20:2_24:0	
		16:1_22:1_22:1	16:1_22:1_22:1	
		18:0_18:1_24:2	18:0_18:1_24:2	
		18:0_18:2_24:1	18:0_18:2_24:1	
		18:0_20:1_22:2	18:0_20:1_22:2	
		18:0_20:2_22:1	18:0_20:2_22:1	
		18:1_18:1_24:1	18:1_18:1_24:1	
		18:1_18:2_24:0	18:1_18:2_24:0	
		18:1_20:1_22:1	18:1_20:1_22:1	
TG(O-60:3)	972.9317		TG(O-60:3)	

Table C.13 (Cont'd)

TG(60:4)	984.8953	16:0_18:1_26:3	
<u> </u>		16:0_18:2_26:2	
		16:0_20:2_24:2	
		16:0_20:3_24:1	
		16:0_20:4_24:0	
		16:0_22:2_22:2	
		16:1_18:0_26:3	
		16:1_18:1_26:2	
		16:1_20:1_24:2	
		16:1_20:2_24:1	
		16:1_20:3_24:0	
		16:1_22:1_22:2	
		18:0_18:2_24:2	
		18:0_20:2_22:2	
		18:0_20:3_22:1	
		18:1_18:1_24:2	
		18:1_18:2_24:1	
		18:1_20:1_22:2	
		18:1_20:2_22:1	
		18:2_18:2_24:0	
		18:2_20:1_22:1	
		20:1_20:1_20:2	
TG(61:2)	1002.9423	16:0_18:1_27:1	
		16:0_19:1_26:1	
		16:0_20:1_25:1	
		17:0_18:1_26:1	
		17:0_20:1_24:1	
		17:1_18:0_26:1	
		17:1_18:1_26:0	
		17:1_20:1_24:0	
		18:0_18:1_25:1	
		18:0_19:1_24:1	
		18:1_18:1_25:0	
		18:1_19:0_24:1	
		18:1_19:1_24:0	

Table C.13 (Cont'd)

TG(61:3)	1000.9266	17:1_18:1_26:1	
10(01.3)	1000.9200	17:1_20:1_24:1	
		18:1_18:1_25:1	
TO(04 - 4)	000 0440	18:1_19:1_24:1	
TG(61:4)	998.9110	TG(61:4)	
TG(62:1)	1018.9736	16:0_18:1_28:0	
		18:0_18:1_26:0	
		18:1_20:0_24:0	
TG(62:2)	1016.9579	16:0_18:1_28:1	
		16:0_20:1_26:1	
		16:0_22:1_24:1	
		16:1_18:0_28:1	
		16:1_18:1_28:0	
		16:1_20:0_26:1	
		16:1_20:1_26:0	
		16:1_22:0_24:1	
		16:1_22:1_24:0	
		18:0_18:1_26:1	
		18:0_20:1_24:1	
		18:0_22:1_22:1	
		18:1_18:1_26:0	
		18:1_20:0_24:1	
		18:1_20:1_24:0	
		18:1_22:0_22:1	
		20:0_20:1_22:1	
TG(62:3)	1014.9423	16:0_20:1_26:2	
		16:0_20:2_26:1	
		18:0_20:2_26:1	
		18:0_18:2_26:2	
		18:0_20:2_24:1	
		18:1_18:1_26:1	
		18:1_18:2_26:0	
		18:1_20:1_24:1	
		18:1_20:2_24:0	
		18:1_22:1_22:1	
		18:2_20:1_24:0	

Table C.13 (Cont'd)

TG(62:4)	1012.9266		18:0_18:2_26:2	
			18:0_20:2_24:2	
			18:0_20:3_24:1	
			18:0_20:4_24:0	
			18:1_18:1_26:2	
			18:1_18:2_26:1	
			18:1_20:1_24:2	
			18:1_20:2_24:1	
			28:1_20:3_24:0	
			18:2_20:1_24:1	
			18:2_20:2_24:0	
TG(62:5)	1010.9110	TG(62:5)	18:0_20:4_24:1	
			18:1_20:3_24:1	
			18:1_20:4_24:0	
TG(62:8)	1004.8640		TG(62:8)	
TG(63:5)	1024.9266		TG(63:5)	
TG(64:0)	1049.0205		TG(64:0)	
TG(64:2)	1044.9892		16:0_22:1_26:1	
			16:0_24:1_24:1	
			18:0_20:1_26:1	
			18:0_22:1_24:1	
			18:1_18:1_28:0	
			18:1_20:0_26:1	
			18:1_20:1_26:0	
			20:0_20:1_24:1	
			20:0_22:1_22:1	
TG(64:3)	1042.9736		18:1_18:1_28:1	
			18:1_20:1_26:1	
			18:1_22:1_24:1	
			20:1_20:1_24:1	
			20:1_22:1_22:1	
TG(64:6)	1036.9266		18:0_22:6_24:0	
			18:1_22:5_24:0	
TG(64:8)	1032.8953	TG(64:8)	TG(64:8)	
TG(64:9)	1030.8797		TG(64:9)	
TG(66:8)	1060.9266	TG(66:8)	TG(66:8)	
TG(66:9)	1058.9110	TG(66:9)	TG(66:9)	
TG(68:1)	1103.0675		TG(68:1)	
TG(68:2)	1101.0518		TG(68:2)	

Table C.13 (Cont'd)

TG(68:9)	1086.9423	TG(68:9)	
TG(70:1)	1131.0988	TG(70:1)	
TG(70:2)	1129.0831	TG(70:2)	
TG(72:1)	1159.1301	TG(72:1)	
TG(72:2)	1157.1144	TG(72:2)	

Table C.14 DG sum compositions and their positive ionization mode m/z for MS analysis for SW480 cells, SW620 cells, SW480 exosomes and SW620 exosomes.

		SW480 Cells	SW620 Cells	SW480 Exo	SW620 Exo
Sum Comp	(+) Mass	Molecular Lipid	Molecular Lipid	Molecular Lipid	Molecular Lipid
	m/z				
DG(28:0)	530.4779	28:0	28:0	28:0	28:0
DG(30:0)	558.5092	30:0	30:0		
DG(O-30:0)	544.5299		O-30:0		
DG(32:0)	586.5405	32:0	32:0	32:0	32:0
DG(O-32:0)	572.5612	O-32:0	O-32:0	O-32:0	O-32:0
DG(P-32:0)	728.4684		P-32:0		
DG(32:1)	584.5248	32:1	32:1	32:1	32:1
DG(O-32:1)	570.5456	O-32:1	O-32:1	O-32:1	O-32:1
DG(P-32:1)	726.4528		P-32:1		
DG(32:2)	582.5092		32:2		
DG(33:0)	600.5561	33:0	33:0		
DG(O-33:0)	586.5769	O-33:0	O-33:0		
DG(33:1)	598.5405	33:1	33:1	33:1	
DG(O-33:1)	584.5612	O-33:1	O-33:1	O-33:1	O-33:1
DG(34:0)	614.5718	34:0	34:0	34:0	
DG(O-34:0)	600.5925	O-34:0	O-34:0		O-34:0
DG(P-34:0)	756.4997		P-34:0		
DG(34:1)	612.5561	34:1	34:1	34:1	34:1
DG(O-34:1)	598.5769	O-34:1	O-34:1	O-34:1	O-34:1
DG(P-34:1)	754.4841	P-34:1	P-34:1	P-34:1	P-34:1
DG(34:2)	610.5405	34:2	34:2	34:2	34:2
DG(O-34:2)	596.5612		O-34:2		
DG(35:1)	626.5718	35:1	35:1	35:1	
DG(O-35:1)	612.5925	O-35:1	O-35:1	O-35:1	O-35:1
DG(35:2)	624.5561	35:2	35:2	35:2	

Table C.14 (Cont'd)

DC(26.0)	642.6031	36:0	36:0		
DG(36:0)					
DG(O-36:0)	628.6238	O-36:0	O-36:0		
DG(36:1)	640.5874	36:1	36:1	36:1	36:1
DG(O-36:1)	626.6081	O-36:1	O-36:1	O-36:1	O-36:1
DG(P-36:1)	782.5154		P-36:1		P-36:1
DG(36:2)	638.5718	36:2	36:2	36:2	36:2
DG(O-36:2)	624.5925	O-36:2	O-36:2	O-36:2	O-36:2
DG(36:3)	636.5561	36:3	36:3	36:3	36:3
DG(36:4)	634.5405		36:4	36:4	36:4
DG(37:2)	652.5874	37:2	37:2	37:2	
DG(38:1)	668.6187	38:1	38:1	38:1	38:1
DG(O-38:1)	654.6394	O-38:1	O-38:1		
DG(38:2)	666.6031	38:2	38:2	38:2	38:2
DG(38:3)	664.5874	38:3	38:3	38:3	
DG(38:4)	662.5718	38:4	38:4		
DG(38:5)	660.5561		38:5		
DG(O-38:5)	646.5769	O-38:5	O-38:5		
DG(O-38:6)	644.5612	O-38:6	O-38:6		
DG(O-39:1)	668.6551		O-39:1		
DG(40:1)	696.6500	40:1	40:1		40:1
DG(40:2)	694.6344	40:2	40:2	40:2	
DG(42:1)	724.6813		42:1		
DG(42:2)	722.6657		42:2		
DG(43:6)	728.6187	43:6	43:6	43:6	43:6

Table C.15 MG sum compositions, their positive ionization mode m/z for MS analysis and molecular lipid identities for SW480 cells, SW620 cells, SW480 exosomes and SW620 exosomes.

		SW480 Cells	SW620 Cells	SW480 Exo	SW620 Exo
Sum Comp	(+) Mass	Molecular Lipid	Molecular Lipid	Molecular Lipid	Molecular Lipid
	m/z				
MG(O-14:0)	306.3003	O-14:0	O-14:0	O-14:0	O-14:0
MG(15:1)	332.2795	15:1	15:1	15:1	15:1
MG(16:0)	348.3108	16:0	16:0	16:0	16:0
MG(O-16:0)	334.3315	O-16:0	O-16:0		O-16:0
MG(P-16:0)	490.2388	P-16:0	P-16:0		P-16:0
MG(16:1)	346.2952	16:1	16:1		
MG(O-16:1)	332.3159	O-16:1	O-16:1	O-16:1	O-16:1
MG(17:0)	362.3265	17:0			
MG(O-17:0)	348.3472	O-17:0			
MG(17:1)	360.3108	17:1	17:1		
MG(18:0)	376.3421	18:0	18:0	18:0	18:0
MG(O-18:0)	362.3628	O-18:0	O-18:0		O-18:0
MG(P-18:0)	518.2701		P-18:0		
MG(18:1)	374.3265	18:1	18:1	18:1	18:1
MG(O-18:1)	360.3472	O-18:1	O-18:1		O-18:1
MG(18:2)	372.3108	18:2	18:2		
MG(18:3)	370.2952	18:3	18:3	18:3	18:3
MG(19:0)	390.3578	19:0			
MG(19:1)	388.3421	19:1	19:1	19:1	19:1
MG(19:2)	386.3265	19:2	19:2	19:2	19:2
MG(20:1)	402.3578	20:1	20:1		20:1
MG(20:2)	400.3421	20:2	20:2		
MG(21:1)	416.3734	21:1	21:1	21:1	21:1
MG(21:5)	408.3108	21:5	21:5	21:5	21:5
MG(22:1)	430.3891	22:1			22:1
MG(22:2)	428.3734	22:2	22:2		
MG(22:3)	426.3578	22:3	22:3		

Table C.16 Chol Ester sum compositions, their positive ionization mode m/z for MS analysis and molecular lipid identities for SW480 cells, SW620 cells, SW480 exosomes and SW620 exosomes.

		SW480 Cells	SW620 Cells	SW480 Exo	SW620 Exo
Sum Comp	(+) Mass	Molecular Lipid	Molecular Lipid	Molecular Lipid	Molecular Lipid
	m/z		_		
Chol(14:0)	614.5870	14:0	14:0		
Chol(16:0)	642.6183	16:0	16:0		
Chol(16:1)	640.6027	16:1	16:1		
Chol(18:0)	670.6496	18:0	18:0		
Chol(18:1)	668.6340	18:1	18:1		18:1
Chol(18:2)	666.6183	18:2	18:2		
Chol(20:0)	698.6809	20:0	20:0		
Chol(20:1)	696.6653	20:1	20:1		
Chol(20:2)	694.6496	20:2	20:2		
Chol(20:3)	692.6340	20:3	20:3		
Chol(20:4)	690.6183		20:4		
Chol(22:0)	726.7122		22:0		
Chol(22:1)	724.6966	22:1	22:1		
Chol(22:5)	716.6340	22:5	22:5		
Chol(22:6)	714.6183	22:6	22:6		
Chol(24:0)	754.7435	24:0	24:0		
Chol(24:1)	752.7279	24:1	24:1		
Chol(24:2)	750.7122		24:2		
Chol(26:0)	782.7748		26:0		
Chol(26:1)	780.7592	26:1	26:1		

BIBLIOGRAPHY

BIBLIOGRAPHY

- 1. Fahy, E., Subramaniam, S., Brown, H. A., Glass, C. K., Merrill Jr., A. H., Murphy, R. C., Raetz, C. R. H., Russell, D. W., Seyama, Y., Shaw, W., Shimizu, T., Spener, F., van Meer, G., VanNieuwenhze, M. S., White, S. H., Witztum, J. L., Dennis, E. A., A comprehensive classification system for lipids. *J. Lipid Res.* **2005**, *46*, 839.
- 2. Fahy, E., Subramaniam, S., Murphy, R., Nishijima, M., Raetz, C., Shimizu, T., Spener, F., van Meer, G., Wakelam, M., Dennis, E. A., Update of the LIPID MAPS comprehensive classification system for lipids. *J. Lipid Res.* **2009**, *50*, S9.
- 3. Lipidomics Perspective: From Molecular Lipidomics to Validated Clinical Diagnostics; First ed.; Ekroos, K., Ed.; Wiley-VCH Verlag GmbH & Co. KGaA., 2012.
- 4. Liebisch, G., Vizcaino, J. A., Kofeler, H., Trotzmuller, M., Griffiths, W. J., Schmitz, G., Spener, F., Wakelam, M. J. O., Shorthand notation for lipid structures derived from mass spectrometry. *J. Lipid Res.* **2013**, *54*, 1523.
- 5. Zhang, X., Fhaner, C.J., Ferguson-Miller, S.M., Reid, G.E., Evaluation of ion activation strategies and mechanisms for the gas-phase fragmentation of sulfoquinovosyldiacylglycerol lipids from *Rhodobacter sphaeroides*. *Int. J. Mass Spectrom.* **2012**, *316-318*, 100.
- 6. van Meer, G., Voelker, D. R., Feigenson, G. W., Membrane Lipids: where they are and how they behave. *Nature Rev. Mol. Cell Biol.* **2008**, *9*, 112.
- 7. Marsh, D., Lateral pressure profile, spontaneous curvature frustration, and the incorporation and conformation of proteins in membranes. *Biophys. J.* **2007**, 93, 3884.
- 8. de Almeida, R. F. M., Fedorov, A., Prieto, M., Sphingomyelin/phosphatidylcholine/cholesterol phase diagram: boundaries and composition of lipid rafts. *Biophys. J.* **2003**, *85*, 2406.
- 9. Brown, D. A., London, E., Functions of lipid rafts in biological membranes. *Annu. Rev. Cell Dev. Biol.* **1998**, *14*, 111.
- 10. Simons, K., Ehehalt, R., Cholesterol, lipid rafts, and disease. *J. Clin. Invest.* **2002**, *110*, 597.
- 11. Escriba, P. V., Gonzalez-Ros, J. M., Goni, F. M., Kinnunen, P. K. J., Vigh, L., Sanchez-Magraner, L., Fernandez, A. M., Busquets, X., Horvath, I., Barcelo-

- Coblijn, G.,, Membranes: a meeting point for lipids, proteins and therapies. *J. Cell. Mol. Med.* **2008**, *12*, 829.
- 12. Clarke, S. D., Jump, D. B., Dietary polyunsaturated fatty acid regulation of gene transcription. *Annu. Rev. Nutr.* **1994**, *14*, 83.
- 13. Nolan, C. J., Madiraju, M. S. R., Delghingaro-Augusto, V., Peyot, M., Prentki, M., Fatty acid signaling in the B-cell and insulin secretion. *Diabetes* **2006**, *55*, S16.
- 14. Davies, P., Bailey, P. J., Goldenberg, M. M., Ford-Hutchinson, A. W., The role of arachidonic acid oxygenation products in pain and inflammation. *Ann. Rev. Immunol.* **1984**, *2*, 335.
- 15. Needleman, P., Turk, J., Jakschik, B. A., Morrison, A. R., Lefkowith, J. B., Arachidonic Acid Metabolism. *Ann. Rev. Biochem.* **1986**, *55*, 69.
- 16. Kennedy, A., Martinez, K., Chuang, C., LaPoint, K., McIntosh, M., Saturated fatty acid-mediated inflammation and insulin resistance in adipose tissue: mechanisms of action and implications. *J. Nutr.* **2009**, *139*, 1.
- 17. Guilherme, A., Virbasius, J. V., Puri, v., Czech, M. P., Adipocyte dysfunctions linking obesity to insulin resistance and type 2 diabetes. *Nat. Rev. Molec. Cell Biol.* **2008**, *9*, 367.
- 18. Kim, M., Linardic, C., Obeid, L., Hannun, Y., Identification of sphingomyelin turnover as an effector mechanism for the action of tumor necrosis factor a and g-interferon specific role in cell differentiation. *J. Biol. Chem.* **1991**, *266*, 484.
- 19. Haimovitz-Friedman, A., Kolesnick, R. N., Fuks, Z., Ceramide signaling in apoptosis. *Br. Med. Bull.* **1997**, *53*, 539.
- 20. Annapurna, A., Kumar, K. V., Kumar, V. K., Rambabu, G., Nammi, S., Ceramide: a novel second messenger. *Proc. Indian natn. Sci. Acad.* **2001**, *B67*, 97.
- 21. Kolesnick, R., Golde, D. W., The sphingomyelin pathway in tumor necrosis factor and interleukin-1 signaling. *Cell* **1994**, *77*, 325.
- 22. Gomez-Munoz, A., Modulation of cell signalling by ceramides. *Biochim. Biophys. Acta* **1998**, *1391*, 92.
- 23. Gomez-Munoz, A., Ceramide-1-phosphate: a novel regulator of cell activation. *FEBS Lett.* **2004**, *562*, 5.
- 24. Gomez-Munoz, A., Kong, J. Y., Parhar, K., Wang, S. W., Gangoiti, P., Gonzalez, M., Eivemark, S., Salh, B., Duronio, V., Steinbrecher, U. P., Ceramide-1-

- phosphate promotes cell survival through activation of the phosphatidylinositol 3-kinase/protein kinase B pathway. *FEBS Lett.* **2005**, *579*, 3744.
- 25. Zhang, G., Contos, J. J. A., Weiner, J. A., Fukushima, N., Chun, J., Comparative analysis of three murine G-protein coupled receptors activated by sphingosine-1-phosphate. *Gene* **1999**, *227*, 89.
- 26. Lee, M. J., Van Brocklyn, J., R., Thangada, S., Liu, C. H., Hand, A. R., Menzeleev, R., Spiegel, S., Hla, T., Sphingosine-1-phosphate as a ligand for the G protein-coupled receptor EDG-1. *Science* **1998**, *279*, 1552.
- 27. Nishizuka, Y., Protein kinase C and lipid signaling for sustained cellular responses. *FASEB J.* **1995**, *9*, 484.
- 28. Divecha, N., Irvine, R. F., Phospholipid signaling. *Cell* **1995**, *80*, 269.
- 29. Takenawa, T., Itoh, T., Phosphoinositides, key molecules for regulation of actin cytoskeletal organization and membrane traffic from the plasma membrane. *Biochim. Biophys. Acta* **2001**, *1552*, 190.
- 30. Stokoe, D., Stephens, L. R., Copeland, T., Gaffney, P. R. J., Reese, C. B., Painter, G. F., Holmes, A. B., McCormick, F., Hawkins, P. T., Dual role of phosphatidylinositol-3,4,5-triphosphate in the activation of protein kinase B. *Science* **1997**, *277*, 567.
- 31. Ishii, I., Fukushima, N., Ye, X., Chun, J., Lysophospholipid receptors: signaling and biology. *Annu. Rev. Biochem.* **2004**, *73*, 321.
- 32. Lin, P., Ye, R. D., The lysophospholipid receptor G2A activates a specific combination of G proteins and promotes apoptosis. *J. Biol. Chem.* **2003**, *278*, 14379.
- 33. Brasaemle, D. L., The perilipin family of structural lipid droplet proteins: stabilization of lipid droplets and control of lipolysis. *J. Lipid Res.* **2007**, *48*, 2547.
- 34. Owen, O. E., Smalley, K. J., D'Alessio, D. A., Mozzoli, M. A., Kawson, E. K., Protein, fat, and carbohydrate requirements during starvation: anaplerosis and cataplerosis. *Am. J. Clin. Nutr.* **1998**, *68*, 12.
- 35. Han, X., Yang, J., Cheng, H., Yang, K., Abendschein, D. R., Gross, R. W., Shotgun Lipidomics Identifies Cardiolipin Depletion in Diabetic Myocardium Linking Altered Substrate Utilization with Mitochondrial Dysfunction. *Biochemistry* **2005**, *44*, 16684.
- 36. Gross, R. W., Han, X., Lipidomics in diabetes and the metabolic syndrome. *Meth. Enzymol.* **2007**, *433*, 73.

- 37. Han, X., Yang, J., Yang, K., Zhao, Z., Abendschein, D. R., Gross, R. W., Alterations in Myocardial Cardiolipin Content and Composition Occur at the Very Earliest Stages of Diabetes: A Shotgun Lipidomics Study. *Biochemistry* **2007**, *46*, 6417.
- 38. Lydic, T. A., Renis, R., Busik, J. V., Reid, G. E., Analysis of Retina and Erythrocyte Glycerophospholipid Alterations in a Rat Model of Type 1 Diabetes. *J. Lab. Autom.* **2009**, *14*, 383.
- 39. Shi, Y., Emerging roles of cardiolipin remodeling in mitochondrial dysfunction associated with diabetes, obesity, and cardiovascular diseases. *J. Biomed. Res.* **2010**, *24*, 6.
- 40. Tikhonenko, M., Lydic, T. A., Wang, Y., Chen, W., Opreanu, M., Sochacki, A., McSorley, K. M., Renis, R. L., Kern, T., Jump, D. B., Reid, G. E., Busik, J. V., Remodeling of retinal fatty acids in an animal model of diabetes: a decrease in long-chain polyunsaturated fatty acids is associated with a decrease in fatty acid eslongases Elovl2 adn Elovl4. *Diabetes* **2010**, *59*, 219.
- 41. Wells, K., Farooqui, A. A., Liss, L., Horrocks, L. A., Neural membrane phospholipids in Alzheimer disease. *Neurochem. Res.* **1995**, *20*, 1329.
- 42. Guan, Z., Wang, Y., Cairns, N. J., Lantos, P. L., Dallner, G., Sindelar, P. J., Decrease and structural modifications of phosphatidylethanolamine plasmalogen in the brain with Alzheimer disease. *J. Neuropathol. Exp. Neurol.* **1999**, *58*, 740.
- 43. Farooqui, A. A., Rapoport, S. I., Horrocks, L. A., Membrane phospholipid alterations in Alzheimer's disease: deficiency of ethanolamine plasmalogens. *Neurochem. Res.* **1997**, *22*, 523.
- 44. Han, X., Holtzman, D. M., McKeel Jr., D. W., Plasmalogen deficiency in early Alzheimer's disease subjects and in animal models: molecular characterization using electrospray ionization mass spectrometry. *J. Neurochem.* **2001**, *77*, 1168.
- 45. Grimm, M. O. W., Kuchenbecker, J., Rothhaar, T. L., Grosgen, S.. Hundsdorfer, B., Burg, V. K., Friess, P., Muller, U., Grimm, H. S., Riemenschneider, M., Hartmann, T., Plasmalogen synthesis is regulated via alkyl-dihydroxyacetonephosphate-synthase by amyloid precursor protein processing and is affected in Alzheimer's disease. *J. Neurochem.* **2011**, *116*, 916.
- 46. Brites, P., Waterham, H. R., Wanders, R. J. A., Functions and biosynthesis of plasmalogens in health and disease. *Biochim. Biophys. Acta* **2004**, *1636*, 219.
- 47. Braverman, N. E., Moser, A. B., Functions of plasmalogen lipids in health and disease. *Biochim. Biophys. Acta* **2012**, *1822*, 1442.

- 48. Ginsbrerg, L., Rafique, S., Xuereb, J. H., Rapoport, S. I., Gershfeld, N. L., Disease and anatomic specificity of ethanolamine plasmalogen deficiency in Alzheimer's disease brain. *Brain Res.* **1995**, *698*, 223.
- 49. Heymans, H. S. A., Schutgens, R. B. H., Tan, R., van den Bosch, H., Borst, P., Severe plasmalogen deficiency in tissues of infants without peroxisomes (Zellweger syndrome). *Nature* **1983**, *306*, 69.
- 50. Fernandis, A. Z., Wenk, M. R., Lipid-based biomarkers for cancer. *J. Chromatogr. B* **2009**, *877*, 2830.
- 51. Griffitts, J., Tesiram, Y., Reid, G. E., Saunders, D., Floyd, R. A., Towner, R. A., In vivo MRS assessment of altered fatty acyl unsaturation in liver tumor formation of a TGF a/c-myc transgenic mouse model. *J. Lipid Res.* **2009**, *50*, 611.
- 52. Azordegan, N., Fraser, V., Le, K., Hillyer, L. M., Ma, D. W. L., Fischer, G., Moghadasian, M. H., Carcinogenesis alters fatty acid profile in breast tissue. *Mol. Cell. Biochem.* **2013**, *374*, 223.
- 53. Maillard, V., Bougnous, P., Ferrari, P., Jourdan, M., Pinault, M., Lavillonniere, F., Body, G., Fe Floch, O., Chajes, V., N-3 and N-6 Fatty Acids in Breast Adipose Tissue and Relative Risk of Breast Cancer in a Case-Control Study in Tours, France. *Int. J. Cancer* **2002**, *98*, 78.
- 54. Griffitts, J., Saunders, D., Tesiram, Y. A., Reid, G. E., Salih, A., Liu, S., Lydic, T. A., Busik, J. V., Non-mammalian *fat-1* gene prevents neoplasia when introduced to a mouse hepatocarcinogenesis medol Omega-3 fatty acids prevent liver neoplasia. *Biochim. Biophys. Acta* **2010**, *1801*, 1133.
- 55. Menendez, J. A., Lupu, R., Fatty acid synthase and the lipogenic phenotype in cancer pathogenesis. *Nat. Rev. Cancer* **2007**, *7*, 763.
- 56. Kuhajda, F. P., Fatty-acid synthase and human cancer: new perspectives on its role in tumor biology. *Nutrition* **2000**, *16*, 202.
- 57. Roos, D. S., Choppin, P. W., Tumorigenicity of cell lines with altered lipid composition. *Proc. Natl. Acad. Sci. USA* **1984**, *81*, 7622.
- 58. Howard, B. V., Morris, H. P., Bailey, J. M., Ether-lipids, a-glycerol phosphate dehydrogenase, and growth rate in tumore and cultured cells. *Cancer Res.* **1972**, 32, 1533.
- 59. Snyder, F., Wood, R., The occurrence and metabolism of alkyl and alk-1-enyl ethers of glycerol in transplantable rat and mouse tumors. *Cancer Res.* **1968**, *28*, 972.

- 60. Ruggieri, S., Mugnai, G., Mannini, A., Calorini, L., Fallani, A., Barletta, E., Mannori, G., Cecconi, O., Lipid Characteristics in Metastatic Cells. *Clin. Exp. Metastasis* **1999**, *17*, 271.
- 61. Chabot, M. C., Wykle, R. L., Modest, E. J., Daniel, L. W., Correlation of ether lipid content of human leukemia cell lines and their susceptibility to 1-o-octadecyl-2-methyl-*rac*-glycero-3-phosphocholine. *Cancer Res.* **1989**, *49*, 4441.
- 62. Katz-Brull, R., Seger, D., Rivenson-Segal, D., Rushkin, E., Degani, H., Metabolic markers of breast cancer: enhanced choline metabolism and reduced choline-ether-phospholipid synthesis. *Cancer Res.* **2002**, *62*, 1966.
- 63. Smith, R. E., Lespi, P., Di Luca, M., Busos, C., Marra, F. A., de Alaniz, M. J. T., Marra, C. A., A Reliable Biomarker Derived from Plasmalogens to Evaluate Malignancy and Metastatic Capacity of Human Cancers. *Lipids* **2008**, *43*, 79.
- 64. Dueck, D., Chan, M., Tran, K., Wong, J. T., Jay, F. T., Littman, C., Stimpson, R., Choy, P. C., The modulation of choline phosphoglyceride metabolism in human colon cancer. *Mol. Cell. Biochem.* **1996**, *162*, 97.
- 65. Xu, Y., Fang, X., Casey, G., Mills, G. B., Lysophospholipids activate ovarian and breast cancer cells. *Biochem. J.* **1995**, *309*, 933.
- 66. Murph, M., Tanaka, T., Pang, J., Felix, E., Liu, S., Trost, R., Godwin, A. K., Newman, R., Mills, G., Liquid chromatography mass spectrometry for quantifying plasma lysophospholipids: potential biomarkers for cancer diagnosis. *Methods Enzymol.* **2007**, *433*, 1.
- 67. Sutphen, R., Xu, Y., Wilbanks, G. D., Fiorica, J., Grendys Jr., E. C., LaPolla, J. P., Arango, H., Hoffman, M. S., Martino, M., Wakeley, K., Griffin, D., Blanco, R. W., Cantor, A. B., Xiao, Y., Krischer, J. P., Lysophospholipids are potential biomarkers of ovarian cancer. *Cancer Epidemiol. Biomarkers Prev.* **2004**, *13*, 1185.
- 68. Dória, M. L., Cotrim, Z., Macedo, B., Simões, C., Domingues, P., Helguero, L., Domingues, M. R., Lipidomic appreach to identify patterns in phospholipid profiles and define class differences in mammary epithelial and breast cancer cells. *Breast Cancer Res. Treat.* **2012**, *133*, 635.
- 69. Zhao, Z., Xiao, Y., Elson, P., Tan, H., Plummer, S. J., Berk, M., Aung, P. P., Lavery, I. C., Achkar, J. P., Li, L., Casey, G., Xu, Y., Plasma Lysophosphatidylcholine Levels: Potential Biomarker for Colorectal Cancer. *J. Clin. Oncol.* **2007**, *25*, 2696.

- 70. Xiao, Y., Chen, Y., Kennedy, A. W., Belinson, J., Xu, Y., Diagnostic significance using electrospray ionization mass spectrometry (ESI-MS) analyses. *Ann. NY Acad. Sci.* **2000**, *905*, 242.
- 71. Merchant, T. E., Kasimos, J. N., de Graaf, P. W., Minsky, B. D., Gierke, L. W., Glonek, T., Phospholipid profiles of human colon cancer using ³¹P magnetic resonance spectroscopy. *Int. J. Colorectal Dis.* **1991**, *6*, 121.
- 72. Min, H. K., Lim, S., Chung, B. C., Moon, M. H., Shotgun lipidomics for candidate biomarkers of urinary phospholipids in prostate cancer. *Anal. Bioanal. Chem.* **2011**, 399, 823.
- 73. Friedberg, S. J., Smajdek, J., Anderson, K., Surface Membrane O-Alkyl Lipid Concentration and Metastasizing Behavior in Transplantable Rat Mammary Carcinomas. *Cancer Res.* **1986**, *46*, 845.
- 74. Snyder, F., Wood., R., Alkyl and alk-1-enyl ethers of glycerol in lipids from normal and neoplastic human tissues. *Cancer Res.* **1969**, *29*, 251.
- 75. Benjamin, D. I., Cozzo, A., Ji, X., Roberts, L. S., Louie, S. M., Mulvihill, M. M., Luo, K., Nomura, D. K., Ether lipid generating enzyme AGPS alters the balance of structural and signaling lipids to fuel cancer pathogenicity. *Proc. Natl. Acad. Sci. USA* **2013**, 1.
- 76. Snyder, F., Blank, M. L., Morris, H. P., Occurrence and nature of O-alkyl and O-alkyl-1-enyl moieties of glycerol in lipids of morris transplanted hepatomas and normal rat liver. *Biochim. Biophys. Acta* **1969**, *176*, 502.
- 77. Lin, H. J., Wu, P. C., Ho, J. C. I., The Ether Lipid Tumour Marker in Human Liver with Hepatocellular Carcinoma. *Brit. J. Cancer* **1980**, *41*, 320.
- 78. Lin, H. J., Ho, F. C. S., Lee, C. L. H., Abnormal distribution of O-alkyl groups in the neutral glycerolipids from human hepatocellular carcinomas. *Cancer Res.* **1978**, *38*, 946.
- 79. Smith, R. R., White, H. B., Neutral Lipid Patterns of Normal and Pathologic Nervous Tissue. *Arch. Neurol.* **1968**, *19*, 54.
- 80. Ogretmen, B., Sphingolipids in cancer: regulation of pathogenesis and therapy. *FEBS Lett.* **2006**, *580*, 5467.
- 81. Ryland, L. K., Fox, T. E., Liu, X., Loughran, T. P., Kester, M., Dysregulation of sphingolipid metabolism in cancer. *Cancer Biol. Ther.* **2011**, *11*, 138.

- 82. Nava, V. E., Hobson, J. P., Murthy, S., Milstien, S., Spiegel, S., Sphingosine kinase type 1 promotes estrogen-dependent tumorigenesis of breast cancer MCF-7 cells. *Exp. Cell Res.* **2002**, *281*, 115.
- 83. Sarkar, S., Maceyka, M., Hait, N. C., Paugh, S. W., Sankala, H., Milstien, S., Spiegel, S., Sphingosine kinase 1 is required for migration, proliferation and survival of MCF-7 human breast cancer cells. *FEBS Lett.* **2005**, *579*, 5313.
- 84. Mathivanan, S., Ji, H., Simpson, R. J., Exosomes: Extracellular organelles important in intercellular communication. *Journal of Proteomics* **2010**, *73*, 1907.
- 85. Mathivanan, S., Fhaner, C.J., Reid, G.E., Simpson, R.J., ExoCarta 2012: database of exosomal proteins, RNA and lipids. *Nucl. Acids Res.* **2012**, *40*, D1241.
- 86. Banigan, M. G., Kao, P. F., Kozubek, J. A., Winslow, A. R., Medina, J., Costa, J., Schmitt, A., Schneider, A., Cabral, H., Cagsal-Getkin, O., Vanderburg, C. R., Delalle, I., Differential expression of exosomal microRNAs in prefrontal cortices of schizophrenia and bipolar disorder patients. *PLoS ONE* **2013**, *8*, e48814.
- 87. Delabranche, X., Berger, A., Boisrame-Helms, J., Meziani, F., Microparticles and infectious diseases. *Med. Maladies Infect.* **2012**, *42*, 335.
- 88. Lee, T. H., D'Asti, E., Magnus, N., Al-Nedawi, K., Meehan, B., Rak, J., Microvesicles as mediators of intercellular communication in cancer-the emerging science of cellular 'debris'. *Semin Immunopathol.* **2011**, 33, 455.
- 89. Camussi, G., Deregibus, M., Bruno, S., Grange, C., Valentina, F., Tetta, C., Exosome/microvesicle-mediated epigenetic reprogramming of cells. *Am. J. Cancer Res.* **2011**, *1*, 98.
- 90. Valadi, H., Ekstrom, K., Bossios, A., Sjostrand, M., Lee, J. J., Lotvall, J. O., Exosome-mediated transfer of mRNAs and microRNAs is a novel mechanism of genetic exchange between cells. *Nat. Cell Biol.* **2007**, *9*, 654.
- 91. Skog, J., Wurdinger, T., van Rijn, S., Meijer, D. H., Gainche, L., Sena-Esteves, M., Curry Jr., W. T., Carter, B. S., Krichevsky, A. M., Breakefield, X. O., Glioblastoma microvesicles transport RNA and proteins that promote tumour growth and provide diagnostic biomarkers. *Nat. Cell Biol.* **2008**, *10*, 1470.
- 92. Yu, S., Liu, C., Su, K., Wang, J., Liu, Y., Zhang, L., Li, C., Cong, Y., Kimberly, R., Grizzle, W. E., Falkson, C., Zhang, H., Tumor Exosomes Inhibit Differentiation of Bone Marrow Dendritic Cells. *J Immunol* **2007**, *178*, 6867.
- 93. Peinado, H., Aleckovic, M., Lavotshkin, S., Matei, I., Costa-Silva, B., Moreno-Bueno, G., Hergueta-Redondo, M., Williams, C., Garcia-Santos, G., Ghajar, C.

- M., Nitadori-Hoshino, A., Hoffman, C., Badal, K., Garcia, B. A., Callahan, M. K., Yuan, J., Martins, V. R., Skog, J., Kaplan, R. N., Brady, M. S., Wolchok, J. D., Chapman, P. B., Kang, Y., Bromberg, J., Lyden, D., Melanoma Exosomes Educate Bone Marrow Progenitor Cells Toward a Pro-Metastatic Phenotype Through MET. *Nat. Med.* **2012**, *18*, 883.
- 94. Clayton, A., Mitchell, J. P., Court, J., Mason, M. D., Tabi, Z., Human tumor-derived exosomes selectively impair lymphocyte responses to interleukin-2. *Cancer Res.* **2007**, *67*, 7458.
- 95. Webber, J., Steadman, R., Mason, M. D., Tabi, Z., Clayton, A., Cancer Exosomes Trigger Fibroblast to Myofibroblast Differentiation. *Cancer Res.* **2010**, *70*, 9621.
- 96. Rabinowits, G., Gercel-Taylor, C., Day, J. M., Taylor, D. D., Kloecker, G. H., Exosomal microRNA: a diagnostic marker for lung cancer. *Clin. Lung Cancer* **2009**, *10*, 42.
- 97. Taylor, D. D., Gercel-Taylor, C., MicroRNA signatures of tumor-derived exosomes as diagnostic biomarkers for ovarian cancer. *Gynecol. Oncol.* **2008**, *110*, 2008.
- 98. Trajkovic, K., Hsu, C., Chiantia, S., Rajendran, L., Wenzel, D., Wieland, F., Schwille, P., Brugger, B., Simons, M., Ceramide Triggers Budding of Exosome Vesicles into Multivesicular Endosomes. *Science* **2008**, *319*, 1244.
- 99. Subra, C., Laulagnier, K., Perret, B., Record, M., Exosome lipidomics unravels lipid sorting at the level of multivesicular bodies. *Biochimie* **2007**, *89*, 205.
- 100. Thery, C., Zitvogel, L., Amigorena, S., Exosomes: composition, biogenesis and function. *Nat. Rev. Immun.* **2002**, *2*, 569.
- Llorente, A., Skotland, T., Sylvanne, T., Kauhanen, D., Rog, T., Orlowski, A., Vattulainen, I., Ekroos, K., Sandvig, K., Molecular Lipidomics of Exosomes Released by PC-3 Prostate Cancer Cells. *Biochim. Biophys. Acta* 2013, 1831, 1302.
- 102. de Gassart, A., Geminard, C., Fevrier, B., Raposo, G., Vidal, M., Lipid raft-associated protein sorting in exosomes. *Blood* **2003**, *102*, 4336.
- 103. Beloribi, S., Ristorcelli, e., Breuzard, G., Silvy, F., Betrand-Michel, J., Beraud, E., Verine, A., Lombardo, D., Exosomal Lipids Impact Notch Signaling and Induce Death of Human Pancreatic Tumoral SOJ-6 Cells. *PLoS ONE* 2012, 7, e47480.
- 104. Christie, W. W. In *Advances in Lipid Methodology*; Christie, W. W., Ed.; Oily Press: Invergowrie, Dundee, Scotland, 1993; Vol. 2, p 195.

- 105. Moscatelli, E. A., Duff, J. A., Effects of storage conditions on rat brain ethanolamine glycerophospholipids, cerebrosides, and cholesterol. *Lipids* **1978**, *13*, 294.
- 106. Ellis, S. R., Ferris, C. J., Gilmore, K. J., Mitchell, T. W., Blanksby, S. J., Panhuis, M., Direct lipid profiling of single cells from inkjet printed microarrays. *Anal. Chem.* **2012**, *84*, 9679.
- 107. Jackson, S. N., Ugarov, M., Egan, T., Post, J. D., Langlais, D., Schultz, J. A., Woods, A. S., MALDI-ion mobility-TOFMS imaging of lipids in rat brain tissue. *J. Mass Spectrom.* **2007**, *42*, 1093.
- 108. Folch, J., Lees, M., Sloane Stanley, G. H., A Simple Method for the Isolation and Purification of Total Lipides from Animal Tissues. *J. Biol. Chem.* **1956**, *226*, 497.
- 109. Toschi, T. G., Bendini, A., Ricci, A., Lercker, G., Pressurized solvent extraction of total lipids in poultry meat. *Food Chem.* **2003**, *83*, 551.
- 110. Lydic, T. A., Busik, J. V., Esselman, W. J., Reid, G. E., Complementary precursor ion and neutral loss scan mode tandem mass spectrometry for the analysis of glycerophosphatidylethanolamine lipids from whole rat retina. *Anal. Bioanal. Chem.* 2009, 394, 267.
- 111. Ekroos, K., Chernushevich, I. V., Simons, K., Shevchenko, A., Quantitative profiling of phospholipids by multiple percursor ion scanning on a hybrid quadrupole time-of-flight mass spectrometer. *Anal. Chem.* **2002**, *74*, 941.
- 112. Westrick, M. A., Lee, W. M. F., Macher, B. A., Isolation and characterization of gangliosides from chronic myelogenous leukemia cells. *Cancer Res.* **1983**, *43*, 5890.
- 113. Bligh, E. G., Dyer, W. J., A rapid method of total lipid extraction and purification. *Can. J. Biochem. Physiol.* **1959**, *37*, 911.
- 114. Fang, J., Barcelona, M. J., Structural determination and quantitative analysis of bacterial phospholpids using liquid chromatography/electrospray ionization/mass spectrometry. *J. Microbiol. Methods* **1998**, 33, 23.
- 115. Ivanova, P. T., Milne, S. B., Brown, H. A., Identification of atypical ether-linked glycerophospholipid species in microphages by mass spectrometry. *J. Lipid Res.* **2010**, *51*, 1581.
- 116. Matyash, V., Lievisch, G., Kurzchalia, T. V., Shevchenko, A., Schwudke, D., Lipid extraction by methyl-*tert*-butyl ether for high-throughput lipidomics. *J. Lipid Res.* **2008**, *49*, 1137.

- 117. Merrill Jr., A. H., Sullards, M. C., Allegood, J. C., Kelly, S., Wang, E., Sphingolipidomics: High-throughput, structure-specific and quantitative analysis of sphingolipids by liquid chromatography tandem mass spectrometry. *Methods* **2005**, *36*, 207.
- 118. Svennerholm, L., Fredman, P., A procedure for the quantitative isolation of brain gangliosides. *Biochim. Biophys. Acta* **1980**, *617*, 97.
- 119. Ejsing, C. S., Sampaio, J. L., Surendranath, V., Duchoslav, E., Ekroos, K., Klemm, R. W., Simons, K., Shevchenko, A., Global analysis of the yeast lipidome by quantitative shotgun mass spectrometry. *Proc. Natl. Acad. Sci.USA* **2009**, *106*, 2136.
- 120. Fuchs, B., Suss, R., Teuber, K., Eibisch, M., Schiller, J., Lipid analysis by thin-layer chromatography-A review of the current state. *J. Chromatogr. A* **2011**, *1218*, 2754.
- 121. Dobson, G., Christie, W. W., Nikolova-Damyanova, B., Silver ion chromatography of lipids and fatty acids. *J. Chromatogr. B* **1995**, *671*, 197.
- 122. Skipski, V. P., Peterson, R. F., Barclay, M., Quantitative Analysis of Phospholipids by Thin-Layer Chromatography. *Biochem. J.* **1964**, *90*, 374.
- 123. Aloisi, J., Fried, B., Sherma, J., Comparison of mobile phases for separation of phospholipids by one-dimensional TLC on preadsorbent high performance silica gel plates. *J. Liq. Chromatogr.* **1991**, *14*, 3269.
- 124. Mangold, H. K., Malins, D. C., Fractionation of fats, oils, and waxes on thin layers of silicic acid. *J. Am. Oil Chem. Soc.* **1960**, *37*, 383.
- 125. Kishimoto, K., Urade, R., Ogawa, T., Moriyama, T., Nondestructive Quantification of Neutral Lipids by Thin-Layer Chromatography and Laser-Fluorescent Scanning: Suitable Methods for "Lipidome" Analysis. *Biochem. Biophys. Res. Commun.* **2001**, *281*, 657.
- 126. Pelick, N., Wilson, T. L., Miller, M. E., Angeloni, F. M., Steim, J. M., Some practical aspects of thin-layer chromatography of lipids. *J. Am. Oil Chem. Soc.* **1965**, *42*, 393.
- 127. Malins, D. C., Mangold, H. K., Analysis of complex lipid mixtures by thin-layer chromatography and complementary methods. *J. Am. Oil Chem. Soc.* **1960**, *37*, 576.
- 128. Wolfman, L., Sachs, B. A., Separation of cholesterol and demosterol by thin-layer chromatography. *J. Lipid Res.* **1964**, *5*, 127.

- 129. Domnas, A. J., Warner, S. A., Johnson, S. L., Reversed-phase thin layer chromatography of some common sterols. *Lipids* **1983**, *18*, 87.
- 130. Rouser, G., Siakotos, A. N., Fleischer, S., Quantitative analysis of phospholipids by thin-layer chromatography and phosphorus analysis of spots. *Lipids* **1966**, *1*, 85.
- 131. Rouser, G., Fleischer, S., Yamamoto, A., Two dimensional thin layer chromatographic separation of polar lipids and determination of phospholipids by phosphorus analysis of spots. *Lipids* **1969**, *5*, 494.
- 132. Galli, C., White, H. B., Paoletti, R., Brain lipid modifications induced by essential fatty acid deficiency in growing male and female rats. *J. Neurochem.* **1970**, *17*, 347.
- 133. Shantha, N. C., Napolitano, G. E., Gas chromatography of fatty acids. *J. Chromatogr.* **1992**, *624*, 37.
- 134. Morrison, W. R., Smith, L. M., Preparation of fatty acid methyl esters and dimethylacetals from lipids wiht boron fluoride-methanol. *J. Lipid Res.* **1964**, *5*, 600.
- 135. Hullin, F., Bossant, M., Salem, N., Aminophospholipid molecular species asymmetry in the human erythrocyte plasma membrane. *Biochim. Biophys. Acta* **1991**, *1061*, 15.
- 136. Reynier, M., Sari, H., d'Anglebermes, M., Kye, E. A., Pasero, L., Differences in Lipid Characteristics of Undifferentiated and Enterocytic differentiated HT29 Human Colonie Cells. *Cancer Res.* **1991**, *51*, 1270.
- 137. Lin, H. J., Lie, M. S. F., Lee, C. L. H., Lee, D. H. S., Composition of O-alkyl and O-alk-1-enyl moieties in the glycerolipids of the human adrenal. *Lipids* **1977**, *12*, 620.
- 138. Albro, P. W., Dittmer, J. C., Determination of the distribution of the aliphatic groups of glyceryl ethers by gas-liquid chromatography of the diacetyl derivatives. *J. Chromatogr.* **1968**, *38*, 230.
- 139. Dodds, E. D., McCoy, M. R., Rea, L. D., Kennish, J. M., Gas chromatographic quantification of fatty acid methyl esters: flame ionization detection vs. electrom impact mass spectrometry. *Lipids* **2005**, *40*, 419.
- 140. Snyder, L. R., Kirkland, J. J., Dolan, W. *Introduction to Modern Liquid Chromatography*; 3 ed.; John Wiley & Sons, Inc.: Hoboken, NJ, 2011.

- Christie, W. W. Detectors for high-performance liquid chromatography of lipids with special references to evaporative light-scattering detection; Oily Press: Ayr, 1992.
- 142. Jungalwala, F. B., Turel, R. J., Evans, J. E., McCluer, R. H., Sensitive analysis of ethanolamine- and serine-containing phosphoglycerides by high-performance liquid chromatography. *Biochem. J.* **1975**, *145*, 517.
- 143. Sokol, E., Almeida, R., Hannibal-Bach, H. K., Kotowska, D., Vogt, J., Baumgart, J., Kristiansen, K., Nitsch, R., Knudsen, J., Ejsing, C. S., Profiling of lipid species by normal-phase liquid chromatography nanoelectrospray ionization, and ion trap-orbitrap mass spectrometry. *Anal. Biochem.* **2013**, *443*, 88.
- 144. McLaren, D. G., Miller, P. L., Lassman, M. E., Castro-Perez, J. M., Hubbard, B. K., Roddy, T. P., An ultraperformance liquid chromatography method for the normal-phase separation of lipids. *Anal. Biochem.* **2011**, *414*, 266.
- 145. Brouwers, J. F., Liquid chromatographic-mass spectrometric analysis of phospholipids. Chromatography, ionization and quantification. *Biochim. Biophys. Acta* **2011**, *1811*, 763.
- 146. Wang, Y., Krull, I. S., Liu, C., Orr, J. D., Derivatization of phospholipids. *J. Chromatogr. B* **2003**, 793, 3.
- 147. Cooper, M. J., Anders, M. W., Determination of long chain fatty acids as 2-naphthacyl esters by high pressure liquid chromatography and mass spectrometry. *Anal. Chem.* **1974**, *46*, 1849.
- 148. Grelard, A., Couvreux, A., Loudet, C., Dufourc, E. J. In *Lipid Signaling Protocols*; Larijani, B., Ed.; Humana Press: Totowa, NJ, 2009, p 111.
- 149. Natarajan, K., Mori, N., Artemov, D., Aboagye, E. O., Chacko, V. P., Bhujwalla, Z. M., Phospholipid profiles of invasive human breast cancer cells are altered towards a less invasive phospholipid profile by the anti-inflammatory agent indomethacin. *Advan. Enzyme Regul.* **2000**, *40*, 271.
- 150. Tugnoli, V., Bottura, G., Fini, G., Reggiani, A., Tinti, A., Trinchero, A., Tosi, M. R.,

 ¹H-NMR and ¹³C-NMR lipid profiles of human renal tissues. *Biopolymers* **2003**,
 72, 86.
- 151. Ritchie, S. A., Ahiahonu, P. W. K., Jayasinghe, D., Heath, D., Liu, J., Lu, Y., Jin, W., Kavianpour, A., Yamazaki, Y., Khan, A. M., Hossain, M., Su-Myat, K. K., Wood, P. L., Krenitsky, K., Takemasa, I., Miyake, M., Sekimoto, M., Monden, M., Matsubara, H., Nomura, F., Goodenowe, D. B., Reduced levels of hydroxylated, polyunsaturated ultra long-chain fatty acids in the serum of colorectal cancer patients: implications for early screening and detection. *BMC Med.* **2010**, *8*, 1.

- 152. Greiner, J. V., Kopp, S. J, Sanders, D. R., Glonek, T., Organophosphates of the crystalline lens: a nuclear magnetic resonance spectroscopic study. *Invest. Ophthalmol. Vis. Sci.* **1981**, *21*, 700.
- 153. Wenk, M. R., The Emerging Field of Lipidomics. *Nat. Rev. Drug Discovery* **2005**, *4*, 594.
- 154. Mannina, L., Segre, A., High resolution nuclear magnetic resonance: from chemical structure to food authenticity. *Grasas Aceites* **2002**, *53*, 22.
- 155. Han, X., Yang, K., Gross, R. W., Multi-dimensional mass spectrometry-based shotgun lipidomics and novel strategies for lipidomic analyses. *Mass Spectrom. Rev.* **2012**, *31*, 134.
- 156. Blanksby, S. J., Mitchell, T. W., Advances in mass spectrometry for lipidomics. *Annu. Rev. Anal. Chem.* **2010**, *3*, 433.
- 157. Curstedt, T., Analysis of molecular species of ether analogues of phosphatidylcholines from biological samples. *Biochim. Biophys. Acta* **1977**, *489*, 79.
- 158. Andersson, B. A., Holman, R. T., Pyrrolidides for mass spectrometric determination of the position of the double bond in monounsaturated fatty acids. *Lipids* **1974**, *9*, 185.
- 159. Fay, L., Richli, U., Location of double bonds in polyunsaturated fatty acids by gas chromatography-mass spectrometry after 4,4-dimethyloxazoline derivatization. *J. Chromatogr.* **1991**, *541*, 89.
- 160. Yamamoto, K., Shibahara, A., Nakayama, T., Kajimoto, G., Determination of double-bond positions in methylene-interrupted dienoic fatty acids by GC-MS as their dimethyl disulfide adducts. *Chem. Phys. Lipids* **1991**, *60*, 39.
- 161. Dunkelblum, E., Tan, S. H., Silk, P. J., Double-bond location in monounsaturated fatty acids by dimethyl disulfide derivatization and mass spectrometry: application to analysis of fatty acids in pheromone glands of four lepidoptera. *J. Chem. Ecol.* **1985**, *11*, 265.
- 162. Vincenti, M., Guglielmetti, G., Cassani, G., Tonini, C., Determination of double bond position in diunsaturated compounds by mass spectrometry of dimethyl disulfide derivatives. *Anal. Chem.* **1987**, *59*, 694.
- 163. Buser, H., Arn, H., Guerin, P., Rauscher, S., Determination of double bond position in mono-unsaturated acetates by mass spectrometry of dimethyl disulfide adducts. *Anal. Chem.* **1983**, *55*.

- 164. Shibahara, A., Yamamoto, K., Kinoshita, A., Anderson, B. L., An improved method for preparing dimethyl disulfide adducts for GC/MS analysis. *J. Am. Oil Chem. Soc.* **2008**, *85*, 93.
- 165. Francis, G. W., Alkylthiolation for the determination of double-bond position in unsaturated fatty acid esters. *Chem. Phys. Lipids* **1981**, *29*, 369.
- 166. Hejazi, L., Ebrahimi, D., Guilhaus, M., Hibbert, D. B., Discrimination among geometrical isomers of a-linolenic acid methyl ester using low energy electron ionization mass spectrometry. *J. Am. Soc. Mass Spectrom.* **2009**, *20*, 1272.
- 167. Kim, H., Want, T. L., Ma, Y., Liquid chromatography/mass spectrometry of phospholipids using electrospray ionization. *Anal. Chem.* **1994**, *66*, 3977.
- 168. Jungalwala, F. B., Evans, J. E., McCluer, R. H., High-performance liquid chromatography of phosphatidylcholine and sphingomyelin with detection in the region of 200nm. *Biochem. J.* **1976**, *155*, 55.
- 169. Houjou, T., Yamatani, K., Imagawa, M., Shimizu, T., Taguchi, R., A shotgun tandem mass spectrometric analysis of phospholipids with normal-phase and/or reverse-phase liquid chromatography/electrospray ionization mass spectrometry. *Rapid Commun. Mass Spectrom.* **2005**, *19*, 654.
- 170. Han, X., Gross, R. W., Electrospray ionization mass spectrscopic analysis of human erythrocyte plasma membrane phospholipids. *Proc. Natl. Acad. Sci. USA* **1994**, *91*, 10635.
- 171. Ivanova, P. T., Milne, S. B., Myers, D. S., Brown, H. A., Lipidomics: a mass spectrometry based systems level analysis of cellular lipids. *Curr. Opin. Chem. Biol.* **2009**, *13*, 526.
- 172. Harkewicz, R., Dennis E. A., Applications of mass spectrometry to lipids and membranes. *Annu. Rev. Biochem.* **2011**, *80*, 301.
- 173. Hsu, F., Turk, J., Electrospray ionization with low-energy collisionally activated dissociation tandem mass spectrometry of glycerophospholipids: Mechanisms of fragmentation and structural characterization. J. Chromatogr. B 2009, 877, 2673.
- 174. Hsu, F., Turk, J., Electrospray Ionization/Tandem Quadrupole Mass Spectrometric Studies on Phosphatidylcholines: The Fragmentation Process. *J. Am. Soc. Mass Spectrom.* **2003**, *14*, 352.
- 175. McLafferty, F. W., Billionfold data increase from mass spectrometry instrumentation. *J. Am. Soc. Mass Spectrom.* **1997**, *8*, 1.

- 176. Zubarev, R. A., Makarov, A., Orbitrap Mass Spectrometry. *Anal. Chem.* **2013**, *85*, 5288.
- 177. Verentchikov, A. N., Yavor, M. I., Hasin, Y. I., Gavrik, M. A., multireflection planar time-of-flight mass analyzer. II: the high-resolution mode. *Tech. Phys.* **2005**, *50*, 82.
- 178. Watson, J. T., Sparkman, O. D. *Introduction to Mass Spectrometry*; Fourth ed. West Sussex, England, 2007.
- 179. Yost, R. A., Enke, C. G., Triple quadrupole mass spectrometry. *Anal. Chem.* **1979**, *51*, 1251.
- 180. Brugger, B., Erben, G., Sandhoff, R., Wieland, F. T., Lehmann, W. D., Quantitative analysis of biological membrane lipids at the low picomole level by nano-electrospray ionization tandem mass spectrometry. *Proc. Natl. Acad. Sci. USA* **1997**, *94*, 2339.
- 181. Pulfer, M., Murphy, R. C., Electrospray Mass Spectrometry of Phospholipids. *Mass Spectrom. Rev.* **2003**, *22*, 332.
- 182. Busik, J. V., Reid, G. E., Lydic, T. A., Global Analysis of Retina Lipids by Complementary Precursor Ion and Neutral Loss Mode Tandem Mass Spectrometry. *Meth. Mol. Biol* **2009**, *579*, 33.
- 183. Houjou, T., Yamatani, K., Nakanishi, H., Imagawa, M., Shimizu, T., Taguchi, R., Rapid and selective identification of molecular species in phosphatidylcholine and sphingomyelin by conditional neutral loss scanning and MS³. *Rapid Commun. Mass Spectrom.* **2004**, *18*, 3123.
- 184. Han, X., Gross, R. W., Structural Determination of Picomole Amounts of Phospholipids Via Electrospray Ionization Tandem Mass Spectrometry. *J. Am. Soc. Mass Spectrom.* **1995**, *6*, 1202.
- 185. Han, X., Gross, R. W., Shotgun lipidomics: electrospray ionization mass spectrometric analysis and quantitation of cellular lipidomes directly from crude extracts of biological samples. *Mass Spectrom. Rev.* **2005**, *24*, 367.
- 186. Zhang, X., Reid, G. E., Multistage Tandem Mass Spectrometry of Anionic Phosphatidylcholine Lipid Adducts Reveals Novel Dissociation Pathways. *Int. J. Mass Spectrom.* **2006**, *252*, 242.
- 187. Zemski Berry, K. A., Murphy, R. C., Electrospray Ionization Tandem Mass Spectrometry of Glycerophosphoethanolamine Plasmalogen Phospholipids. *J. Am. Soc. Mass Spectrom.* **2004**, *15*, 1499.

- 188. Hsu, F., Turk, J., Characterization of phosphatidylethanolamine as a lithiated adduct by triple quadrupole tandem mass spectrometry with electrospray ionization. *J. Mass Spectrom.* **2000**, *35*, 596.
- 189. Hsu, F., Turk, J., Studies on phosphatidylserine by tandem quadrupole and multiple stage quadrupole ion-trap mass spectrometry with electrospray ionization: structural characterization and the fragmentation process. *J. Am. Soc. Mass Spectrom.* **2005**, *16*, 1510.
- 190. Kerwin, J. L., Tuininga, A. R., Ericsson, L. H., Identification of molecular species of glycerophospholipids and sphingomyelin using electrospray mass spectrometry. *J. Lipid Res.* **1994**, *35*, 1102.
- 191. Hsu, F., Turk, J., Characterization of phosphatidylinositol, phosphatidylinositol-4-phosphate, and phosphatidylinositol-4,5-biphosphate by electrospray ionization tandem mass spectrometry: a mechanistic study. *J. Am. Soc. Mass Spectrom.* **2000**, *11*, 986.
- 192. Taguchi, R., Houjou, T., Nakanishi, H., Yamazaki, T., Ishida, M., Imagawa, M., Shimizu, T., Focused lipidomics by tandem mass spectrometry. *J. chromatogr. B* **2005**, *8*23, 26.
- 193. Hsu, F., Turk, J., Studies on phosphatidylglycerol with triple quadrupole tandem mass spectrometry with electrospray ionization: fragmentation processes and structural characterization. *J. Am. Soc. Mass Spectrom.* **2001**, *12*, 1036.
- 194. Hsu, F., Turk, J., Charge-driven fragmentation processes in diacyl glycerophosphatidic acids upon low-energy collisional activation. A mechanistic proposal. *J. Am. Soc. Mass Spectrom.* **2000**, *11*, 797.
- 195. Hsu, F., Turk, J., Structural determination of sphingomyelin by tandem mass spectrometry with electrospray ionization. *J. Am. Soc. Mass Spectrom.* **2000**, *11*, 437.
- 196. Duffin, K., Obukowicz, M., Raz, A., Shieh, J. J., Electrospray/tandem mass spectrometry for quantitative analysis of lipid remodeling in essential fatty acid deficient mice. *Anal. Biochem.* **2000**, *279*, 179.
- 197. Liebsch, G., Binder, M., Schifferer, R., Langmann, T., Schulz, B., Schmitz, G., High throughput quantification of cholesterol and cholesteryl ester by electrospray ionization tandem mass spectrometry (ESI-MS/MS). *Biochim. Biophys. Acta* **2006**, *1761*, 121.
- 198. Marzilli, L. A., Fay, Laurent B., Fabiola, Dionisi, Vouros, Paul, Structural Characterization of Triglycerols Using Electrospray Ionization-MSⁿ Ion-Trap MS. *J. Am. Oil Chem. Soc.* **2003**, *80*, 195.

- 199. Han, X., Gross, R. W., Quantitative analysis and molecular species fingerprinting of triacylglyceride molecular species directly from lipid extracts of biological samples by electrospray ionization tandem mass spectrometry. *Anal. Biochem.* **2001**, *295*, 88.
- 200. McAnoy, A. M., Wu, C. C., Murphy R. C., Direct qualitative analysis of triacylglycerols by electrospray mass spectrometry using a linear ion trap. *J. Am. Soc. Mass Spectrom.* **2005**, *16*, 1498.
- 201. Gross, R. W., Han, X., Shotgun lipidomics of neutral lipids as an enabling technology for elucidation of lipid-related diseases. *Am. J. Physiol. Endocrinol. Metab.* **2009**, 297, E297.
- 202. Cheng, C., Gross, M. L., Complete structural elucidation of triacylglycerols by tandem sector mass spectrometry. *Anal. Chem.* **1998**, *70*, 4417.
- 203. Mu, H., Sillen, H., Hiy, C., Identification of diacylglycerols and triacylglycerols in a structured lipid sample by atmospheric pressure chemical ionization liquid chromatography/mass spectrometry. *J. Am. Oil Chem. Soc.* **2000**, *77*, 1049.
- 204. Haynes, C. A., Allegood, J. C., Park, H., Sullards, M. C., Sphingolipidomics: Methods for the comprehensive analysis of sphingolipids. *J. Chromatogr. B* **2009**, *877*, 2696.
- 205. Gu, M., Kerwin, J. L., Watts, J. D., Aebersold, R., Ceramide profiling of complex lipid mixtures by electrospray ionization mass spectrometry. *Anal. Biochem.* **1997**, *244*, 347.
- 206. Hsu, F., Turk, J., Stewart, M. E., Downing, D. T., Structural studies on ceramides as lithiated adducts by low energy collisional-activated dissociation tandem mass spectrometry with electrospray ionization. *J. Am. Soc. Mass Spectrom.* **2002**, *13*, 690.
- 207. Karlsson, A. A., Michelsen, P., Odham, G., Molecular species of sphingomyelin: determination by high-performance liquid chromatography/mass spectrometry with electrospray and high-performance liquid chromatography/tandem mass spectrometry with atmospheric pressure chemical ionization. *J. Mass Spectrom.* **1998**, 33, 1192.
- 208. Hsu, F., Turk, J., Differentiation of 1-O-alk-1'-enyl-2-acyl and 1-O-alkyl-2-acyl Glycerophospholipids by Multiple-Stage Linear Ion-Trap Mass Spectrometry with Electrospray Ionization. *J. Am. Soc. Mass Spectrom.* **2007**, *18*, 2065.
- 209. Raith, K., Neubert, R. H. H., Structural studies on ceramides by electrospray tandem mass spectrometry. *Rapid Commun. Mass Spectrom.* **1998**, *12*, 935.

- 210. Raith, K., Neubert, R. H. H., Liquid chromatography-electrospray mass spectrometry and tandem mass spectrometry of ceramides. *Anal. Chim. Acta* **2000**, *403*, 295.
- 211. Hsu, F., Turk, J., Characterization of ceramides by low energy collisional-activated dissociation tandem mass spectrometry with negative-ion electrospray ionization. *J. Am. Soc. Mass Spectrom.* **2002**, *13*, 558.
- 212. Valsecchi, M., Mauri, L., Casellato, R., Prioni, S., Loberto, N., Prinetti, A., Chigorno, V., Sonnino, S., Ceramide and sphingomyelin species of fibroblasts and neurons in culture. *J. Lipid Res.* **2007**, *48*, 417.
- 213. Yang, W., Adamec, J., Regnier, F. E., Enhancement of the LC/MS analysis of fatty acids through derivatization and stable isotope coding. *Anal. Chem.* **2007**, 79, 5150.
- 214. Woo, H., Go, E. P., Hoang, L., Trauger, S. A., Bowen, B., Siuzdak, G., Northen, T. R., Phosphonium labeling for increasing metabolomic coverage of neutral lipids using electrospray ionization mass spectrometry. *Rapid Commun. Mass Spectrom.* **2009**, *23*, 1849.
- 215. Li, Y. L., Su, X., Stahl, P. D., Gross, M. L., Quantification of diacylglycerol molecular species in biological samples by electrospray ionization mass spectrometry after one-step derivatization. *Anal. Chem.* 2007, 79, 1569.
- 216. Han, X., Yang, K., Cheng, H., Fikes, K. N., Gross, R. W., Shotgun lipidomics of phosphatidylethanolamine-containing lipids in biologial samples after one-step in situ derivatization. *J. Lipid Res.* **2005**, *46*, 1548.
- 217. Sandhoff, R., Brügger, B., Jeckel, D., Lehmann, W. D., Wieland, F. T., Determination of cholesterol at the low picomole level by nano-electrospray ionization tandem mass spectrometry. *J. Lipid Res.* **1999**, *40*, 126.
- 218. Horning, M. G., Martin, D. B., Karmen, A., Vagelos, P. R., Fatty acid synthesis in adipose tissue. *J. Biol. Chem.* **1961**, *236*, 669.
- 219. Wendel, U., Abnormality of odd-numbered long-chain fatty acids in erythrocyte membrane lipids from patients with disorders of propionate metabolism. *Pediatr. Res.* **1989**, *25*, 147.
- 220. Ståhlman, M., Ejsing, C. S., Tarasov, K., Perman, J., Borén, J., Ekroos, K., Highthroughput shotgun lipidomics by quadrupole time-of-flight mass spectrometry. *J. Chromatogr. B Analyt. Technol. Biomed. Life Sci.* **2009**, *877*, 2664.

- 221. Fauland, A., Kofeler, H., Trotzmuller, M., Knopf, A., Hartler, J., Eberl, A., Chitraju, C., Lankmayr, E., Spener, F., A comprehensive method for lipid profiling by liquid chromatography-ion cyclotron resonance mass spectrometry. *J. Lipid Res.* **2011**, *52*, 2314.
- 222. Schuhmann, K., Herzog, R., Schudke, D., Metelmann-strupat, W., Bornstein, S. R., Shevchenko, A., Bottom-up shotgun lipidomics by higher energy collisional dissociation on LTQ orbitrap mass spectrometers. *Anal. Chem.* **2011**, *83*, 5480.
- 223. Schuhmann, K., Almeida, R., Baumert, M., Herzog, R., Bornstein, S. R., Shevchenko, A., Shotgun Lipidomics on a LTQ Orbitrap Mass Spectrometer by Successive Switching Between Acquisition Polarity Modes. *J. Mass Spectrom.* **2012**, *47*, 96.
- 224. Ejsing, C. S., Duchoslav, E., Sampaio, J., Simons, K., Bonner, R., Thiele, C., Ekroos, K., Shevchenko, A., Automated identification and quantification of glycerophospholipid molecular species by multiple precursor ion scanning. *Anal. Chem.* **2006**, *78*, 6202.
- 225. Koivusalo, M., Haimi, P., Heikinheimo, L., Kostiainen, R., Somerharju, P., Quantitative determination of phospholipid compositions by ESI-MS: effects of acyl chain length, unsaturation, and lipid concentration on instrument response. *J. Lipid Res.* **2001**, *42*, 663.
- 226. Zemski Berry, K. A., Murphy, R. C., Analysis of cell membrane aminophospholipids as isotope-tagged derivatives. *J. Lipid Res.* **2005**, *46*, 1038.
- 227. Zemski Berry, K. A., Murphy, R. C., Analysis of polyunsaturated aminophospholipid molecular species using isotope-tagged derivatives and tandem mass spectrometry/mass spectrometry/mass spectrometry. *Anal. Biochem.* **2006**, *349*, 118.
- 228. Zemski Berry, K. A., Turner, W. W., VanNieuwenhze, M. S., Murphy, R. C., Stable iostope labeled 4-(dimethylamino)benzoic acid derivatives of glycerophosphoethanolamine lipids. *Anal. Chem.* 2009, 81, 6633.
- 229. Zemski Berry, K. A., Turner, W. W., VanNieuwenhze, M. S., Murphy, R. C., Characterization of oxidized phosphatidylethanolamine derived from RAW 264.7 cells using 4-(dimethylamino)benzoic acid derivatives. *Eur. J. Mass Spectrom.* **2010**, *16*, 463.
- 230. Leavell, M. D., Leary, J. A., Fatty Acid Analysis Tool (FAAT): An FT-ICR MS Lipid Analysis Algorithm. *Anal. Chem.* **2006**, *78*, 5497.
- 231. Hubner, G., Crone, C., Lindner, B., LipID a software tool for automated assignment of lipids in mass spectra. *J. Mass Spectrom.* **2009**, *44*, 1676.

- 232. Taguchi, R., Ishikawa, M., Precise and global identification of phospholipid molecular species by an orbitrap mass spectrometer and automated search engine lipid search. *J. Chromatogr. A* **2010**, *1217*, 4229.
- 233. Haimi, P., Uphoff, A., Hermansson, M., Somerharju, P., Software tools for analysis of mass spectrometric lipidome data. *Anal. Chem.* **2006**, *78*, 8324.
- 234. Herzog, R., Schwudke, D., Schuhmann, K., Sampaio, J. L., Bornstein, S. R., Schroeder, M., Shevchenko, A., A Novel Informatics Concept for High-Throughput Shotgun Lipidomics Based on the Molecular Fragmentation Query Language. *Genome Biol.* **2011**, *12*.
- 235. Herzog, R., Schuhmann, K., Schwudke, D., Sampaio, J. L., Bornstein, S. R., Schroeder, M., Shevchenko, A., LipidXplorer: a software for consensual cross-platform lipidomics. *PLoS ONE* **2012**, *7*, e29851.
- 236. Song, H., Hsu, F., Ladenson, J., Turk, J., Algorithm for processing raw mass spectrometric data to identify and quantitate complex lipid molecular species in mixtures by data-dependent scanning and fragment ion database searching. *J. Am. Soc. Mass Spectrom.* **2007**, *18*, 1848.
- 237. Yang, K., Cheng, H., Gross, R. W., Han, X., Automated Lipid Identification and Quantification by Multidimensional Mass Spectrometry-Based Shotgun Lipidomics. *Anal. Chem.* **2009**, *81*, 4356.
- 238. Taguchi, R., Hayakawa, J., Takeuchi, Y., Ishida, M., Two-dimensional analysis of phospholipids by capillary liquid chromatography/electrospray ionization mass spectrometry. *J. Mass Spectrom.* **2000**, *35*, 953.
- 239. Schwudke, D., Schuhmann, K., Herzog, R., Bornstein, S. R., Shevchenko, A., Shotgun Lipidomics on High Resolution Mass Spectrometers. *Cold Spring Harb. Perspect. Biol.* **2011**, *3*.
- 240. Zhou, X., Lu, Y., Wang, W., Borhan, B., Reid, G. E., 'Fixed Charge' Chemical Derivatization and Data Dependant Multistage Tandem Mass Spectrometry for Mapping Protein Surface Residue Accessibility. *J. Am. Soc. Mass Spectrom.* **2010**, *21*, 1339.
- 241. Lu, Y., Zhou, X., Stemmer, P. M., Reid, G. E., Sulfonium ion derivatization, isobaric stable isotope labeling and data dependent CID- and ETD-MS/MS for enhanced phosphopeptide quantitation, identification and phosphorylation site characterization. *J. Am. Soc. Mass Spectrom.* **2012**, 23, 577.

- 242. Murphy, E. J., Stephens, R., Jurkowitz-Alexander, M., Horrocks, L. A.and, Acidic hydrolysis of plasmalogens followed by high-perfomance liquid chromatography. *Lipids* **1993**, *28*, 565.
- 243. Siggia, S., Edsberg, R. L., Iodometric Determination of Vinyl Alkyl Ethers. *Anal. Chem.* **1948**, *20*, 762.
- 244. Rapport, M. M., Lerner, B., The structure of plasmalogens. *Biochim. Biophys. Acta* **1959**, 33, 319.
- 245. Norton, W. T., Potentiometric iodometric determination of plasmalogen. *Biochim. Biophys. Acta* **1960**, *38*, 340.
- 246. Liu, S., Michigan State University, 2010.
- 247. Hui, S., Chiba, H., Kurosawa, T., Liquid chromatography-mass spectrometric determination of plasmalogens in human plasma. *Anal. Bioanal. Chem.* **2011**, *400*, 1923.
- 248. Hannun, Y. A., Obeid, L. M., Principles of bioactive lipid signalling: lessons from sphingolipids. *Nature Rev. Mol. Cell Biol.* **2008**, *9*, 139.
- 249. Green, D. E., Tzagoloff, A., Role of lipids in the structure and function of biological membranes. *J. Lipid Res.* **1966**, *7*, 587.
- 250. Opreanu, M., Lydic, T. A., Reid, G. E., McSorley, K. M., Esselman, W. J., Busik, J. V., Inhibition of cytokine signaling in human retinal endothelial cells through downregulation of sphingomyelinases by docosahexaenoic acid. *Invest. Ophthalmol. Vis. Sci.* **2010**, *51*, 3253.
- 251. Opreanu, M., Tikhonenko, M., Bozack, S., Lydic, T. A., Reid, G. E., McSorley, K. M., Sochacki, A., Perez, G. I., Esselman, W. J., Kern, T., Kolesnick, R., Grant, M. B., Busik, J. V., The unconventional role of acid sphingomyelinase in regulation of retinal microangiopathy in diabetic human and animal models. *Diabetes* 2011, 60, 2370.
- 252. O'Donnell, J. M., Fielda, A. D., Sorokina, N., Lewandowski, E. D., The absence of endogenous lipid oxidation in early stage heart failure exposes limits in lipid storage and turnover. *J. Mol. Cell. Cardiol.* **2008**, *44*, 315.
- 253. Slagel, D. E., Dittmer, J. C., Wilson, C. B., Lipid composition of human glial tumour and adjacent brain. *J. Neurochem.* **1967**, *14*, 789.
- 254. White-Gilbertson, S., Mullen, T., Senkal, C., Lu, P., Ogretmen, B., Obeid, L., Voelkel-Johnson, C., Ceramide synthase 6 modulates TRAIL sensitivity and

- nuclear translocation of active caspase-3 in colon cancer cells. *Oncogene* **2009**, 28, 1132.
- 255. Schonberg, S. A., Lundemo, A. G., Fladvad, T., Holmgren, K., Bremseth, H., Nilsen, A., Gederaas, O., Tvedt, K. E., Egeberg, K. W., Krokan, H. E., Closely related colon cancer cell lines display different sensitivity to polyunsaturated fatty acids, accumulate different lipid classes and downregulate sterol regulatory element-binding protein 1. *FEBS J.* **2006**, *273*, 2749.
- 256. Siegel, R., Jemal, A. Colorectal Cancer Facts & Figures 2011-2013, American Cancer Society, 2011.
- 257. Lu, J., Xiao, Y., Baudhuin, L. M., Hong, G., Xu, Y., Role of ether-linked lysophosphatidic acids in ovarian cancer cells. *J. Lipid Res.* **2002**, *43*.
- 258. Lee, T. C., Fitzgerald, V., Phase transitions of alkyl ether analogs of phosphatidylcholine. *Biochim. Biophys. Acta* **1980**, *598*, 189.
- 259. Spector, A. A., Yorek, M. A., Membrane lipid composition and cellular function. *J. Lipid Res.* **1985**, *26*, 1015.
- 260. Paltauf, F., Ether lipids in biomembranes. Chem. Phys. Lipids 1994, 74, 101.
- 261. Lessig, J., Fuchs, B., Plasmalogens in biological systems: their role in oxidative processes in biological membranes, their contribution to pathological processes and aging and plasmalogen analysis. *Curr. Med. Chem.* **2009**, *16*, 2021.
- 262. Spector, A. A., Burns, C. P., Biological and therapeutic potential of membrane lipid modification in tumors. *Cancer Res.* **1987**, *47*, 4529.
- 263. Deeley, J. M., Mitchell, T. W., Wei, X., Korth, J., Nealon, J. R., Blanksby, S. J., Truscott, R. J. W., Human lens lipids differ markedly from those of commonly used experimental animals. *Biochim. Biophys. Acta* **2008**, *1781*, 288.
- 264. Deeley, J. M., Thomas, M. C., Truscott, R. J. W., Mitchell, T. W., Blanksby, S. J., Identification of abundant alkyl ether glycerophospholipids in the human lens by tandem mass spectrometry techniques. *Anal. Chem.* **2009**, *81*, 1920.
- 265. Ookhtens, M., Kannan, R., Lyon, I., Baker, N., Liver and adipose tissue contributions to newly formed fatty acids in an ascites tumor. *Am. J. Physiol.* **1984**, *247*, R146.
- 266. Thomas, R. L. J., Matsko, C. M., Lotze, M. T. Amoscato, A. A., Mass spectrometric identification of increased C16 ceramide levels during apoptosis. *J. Biol. Chem.* **1999**, *274*, 30580.

- 267. Voelkel-Johnson, C., Hannun, Y. A., El-Zawahry, A., Resistance to TRAIL is associated with defects in ceramide signaling that can be overcome by exogenous C₆-ceramide without requiring down-regulation of cellular FLICE inhibitory protein. *Mol. Cancer Ther.* **2005**, *4*, 1320.
- 268. Mankidy, R., Ahiahonu, P. W. K., Ma, H., Jayasinghe, D., Ritchie, S. A., Khan, M. A., Su-Myat, K. K., Wood, P. L., Goodenowe, D. B., Membrane plasmalogen composition and cellular cholesterol regulation: a structure activity study. *Lipids Health Dis.* **2010**, *9*, 62.
- 269. Fhaner, C. J., Liu, S., Ji, H., Simpson, R. J., Reid, G. E., Comprehensive Lipidome Profiling of Isogenic Primary and Metastatic Colon Adenocarcinoma Cell Lines. *Anal. Chem.* **2012**, *84*, 8917.
- 270. Parolini, I., Federici, C., Raggi, C., Lugini, L., Palleschi, S., De Milito, A., Coscia, C., Iessi, E., Logozzi, M., Moliarni, A., Colone, M., Tatti, M., Sargiacomo, M., Fais, S., Microenvironmental pH is a key factor for exosome traffic in tumor cells. *J. Biol. Chem.* **2009**, *284*, 34211.
- 271. Hannafon, B. N., Ding, W., Intercellular communication by exosome-derived microRNAs in cancer. *Int. J. Mol. Sci.* **2013**, *14*, 14240.
- 272. Thery, C., Ostrowski, M., Segura, E., Membrane vesicles as conveyors of immune responses. *Nat. Rev. Immun.* **2009**, *9*, 581.
- 273. Record, M. In *Emerging concepts of tumor exosome mediated cell-cell communication*; Zhang, H., Ed.; Springer: New York, NY, 2013, p 47.
- 274. Van Niel, G., Raposo, G., Candalh, C., Boussac, M., Hershberg, R., Cerf-Bensussan, N., Heyman, M., Intestinal Epithelial Cells Secrete Exosome-like Vesicles. *Gastroenterology* **2001**, *121*, 337.
- 275. Steinberg, T. H., Lauber, W. M., Berggren, K., Kemper, C., Yue, S., Patton, W. F., Fluorescence detection of proteins in sodium dodecyl sulfate-polyacrylamide gels using environmentally benign, nonfixative, saline solution. *Electrophoresis* **2000**, *21*, 497.
- 276. Glaser, P. E., Gross, R. W., Plasmenylethanolamine facilitates rapid membrane fusion: a stopped-flow kinetic investigation correlating the propensity of a major plasma membrane constituent to adopt an HII phase with its ability to promote membrane fusion. *Biochemistry* **1994**, 33, 5805.
- 277. Murphy, R. C., Free-Radical-Induced Oxidation of Arachidonoyl Plasmalogen Phospholipids: Antioxidant Mechanism and Precursor pathway for Bioactive Eicosanoids. *Chem. Res. Toxicol.* **2001**, *14*, 463.

- 278. Fan, D., Bucana, C. D., O'Brian, C. A., Zwelling, L. A., Seid, C., Fidler, I. J., Enhancement of murine tumor cell sensitivity to adriamycin by presentation of the drug in phosphatidylcholine-phosphatidylserine liposomes. *Cancer Res.* **1990**, *50*, 3619.
- 279. Laulagnier, K., Motta, C., Hamdi, S., Roy, S., Fauvelle, F., Pageaux, J., Kobayashi, T., Salles, J., Perret, B., Bonnerot, C., Record, M., Mast cell- and dendritic cell-derived exosomes display a specific lipid composition and an unusual membrane organization. *Biochem. J.* **2004**, *380*, 161.
- 280. Karahatay, S., Thomas, K., Koybasi, S., Senkal, C. E., ElOjeimy, S., Liu, X, Bielawski, J., Day, T. A., Gillespie, M. B., Sinha, D., Norris, J. S., Hannun, Y. A., Ogretmen, B., Clinical relevance of ceramide metabolism in the pathogenesis of human head and neck squamous cell carcinoma (HNSCC): attenuation of C₁₈-ceramide in HNSCC tumors correlates with lymphovascular invasion and nodal metastasis. *Cancer Lett.* **2007**, *256*, 101.
- 281. Simons, M., Raposo, G., Exosomes-vesicular carriers for intercellular communication. *Curr. Opin. Cell Biol.* **2009**, *21*, 1.
- 282. Fhaner, C. J., Liu, S., Zhou, X., Reid, G. E., Functional Group Selective Derivatization and Gas-Phase Fragmentation Reactions of Plasmalogen Glycerophospholipids. *Mass Spectrom.* **2013**, *2*, S0015.